



NTNU – Trondheim
Norwegian University of
Science and Technology

Transition metal catalyzed cyclotrimerization to new pyridine ligands for asymmetric hydrogenation

Vegard Torp Lien

Chemistry

Submission date: August 2013

Supervisor: Odd Reidar Gautun, IKJ

Norwegian University of Science and Technology
Department of Chemistry

Acknowledgments

This master thesis, “Transition metal catalyzed cyclotrimerization to new pyridine ligands for asymmetric hydrogenation”, is conducted in collaboration with my supervisor, associate professor Odd Reidar Gautun. It is also a collaboration with professor Pher Andersson at the Department of Organic Chemistry, Arrhenius Laboratory, Stockholm University, Sweden. The work has been conducted from august 2012 to august 2013, as a part of my MSc in chemistry.

I would like to thank Odd for offering me an interesting and challenging project. He is also thanked for valuable chemical guidance and for musical inspiration in the lab. Other members of Odd's group are thanked for creating a good environment in the lab and at the group meetings. Dr. Susana Villa Gonzales are highly appreciated for MS-results, and Roger Aarvik for supplying chemicals and solvents when needed.

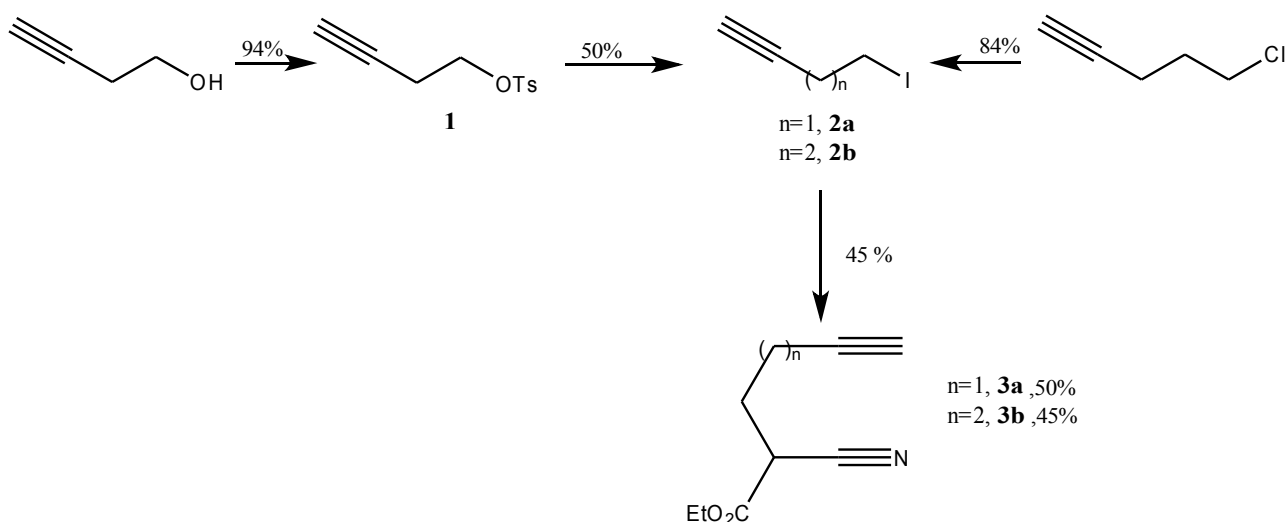
All friends and classmates in Trondheim who have made the last 6 years a fun and memorable time deserves a big thank you! The “12-kaffe” and my friends in Tindegruppera are highly appreciated for numerous lunch breaks and wonderful weekends in the mountains!

Last, but not least, my girlfriend Kristin and my family are thanked for their support and encouragement.

Sammendrag

Nye pyridin ringsystemer for anvendelse som ligander i iridium katalysert asymmetrisk hydrogenering har blitt syntetisert med syklotrimerisering som et nøkkelsteg. Dette var en effektiv metode for å variere det ønskede substitusjonsmønsteret.

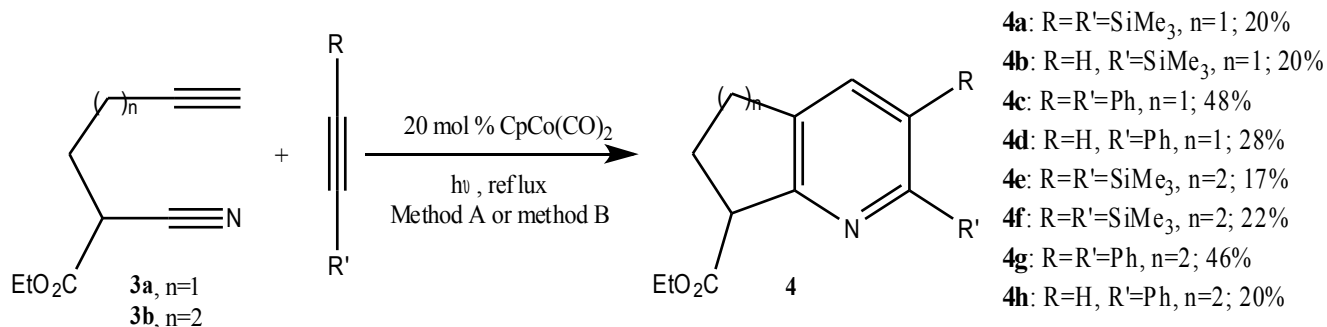
Først ble alkynnitriene **3a** og **3b** syntetisert fra kommersielt tilgjengelige utgangstoffer i henholdsvis 24 og 38% totale utbytter, som vist i figur 1. Utbyttene for de ulike trinnene er gitt i figuren.



Figur 1: Syntese av alkynnitriene **3a** og **3b**.

Butynalkoholen ble tosyleret til **1**, som videre ble omdannet til iodidet **2a** ved en Finkelstein reaksjon. Iodidet **2a** ble så reagert med etyl cyanoacetat i en alkyleringsreaksjon for å danne **3a**. Alkynenitrilet **3a** ble syntetisert på en lignende metode fra pentynklorid.

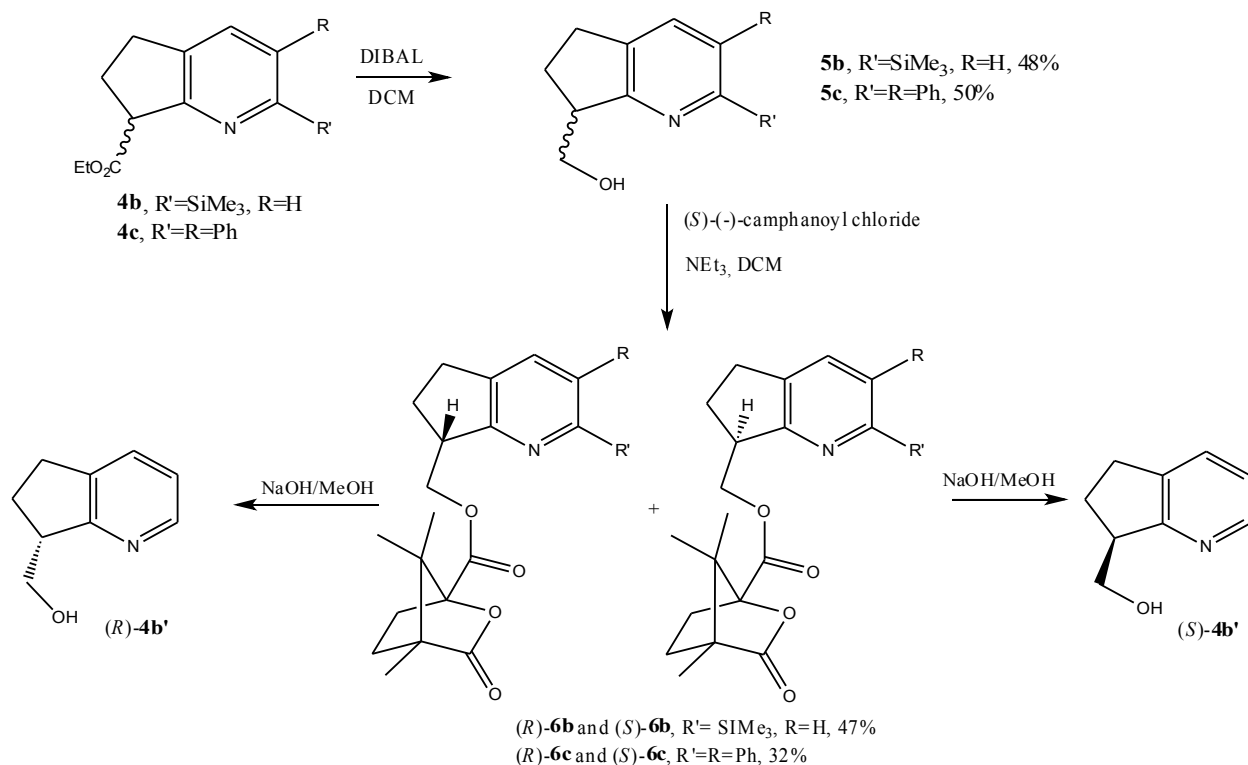
Ved å variere alkynene ble **3a** og **3b** omdannet til åtte nye forbindelser ved syklotrimerisering i 17-48% utbytte, som vist i figur 2.



Figur 2: Syklotrimerisering av **3** med ulike alkyner til **4a-h**.

Reaksjonene i figur 2 ble både utført i et trykkør og ved sakte-tilsettings metoder. CpCo(CO)₂ ble brukt som katalysator, og aktiveringen av pre-katalysatoren ble gjort med lys. Det ble vist at bruk av trykkør generelt poduserte **4** i bedre utbytter en ved sakte-tilsetting. Når mono-substituerte alkyner ble brukt, viste reaksjonene god regioselektivitet for den 2-substituerte regioisomeren, i samsvar med mekanistiske modeller beskrevet i litteraturen. Optimalisering av reaksjonene med andre katalysatorer (Fe(OAc)₂/ligand, Cp*RuCl(COD) og CpCo(COD)) og reaksjonsbetingelser var mislykket.

Foreløpig undersøkelse av **4d** som ligand i asymmetriske hydrogeneringsreaksjoner har gitt gode resultater, og testing av pyridin esterene **4a-4c** som ligander var derfor ønsket. Separasjon til rene enantiomerer via diastereomerene ble forsøkt som vist i figur 3.



Figur 3: Forsøkt separasjon av enantiomerene til **4b** og **4c**.

Reduksjon av pyridin esterene **4b** og **4c** ga alkoholene **5b** og **5c** i henholdsvis 48 og 50% utbytte. Alkoholene **5b** og **5c** ble videre reagert med (*S*)-camphanic klorid, og ga en 1:1 diastereomerisk blanding av **6b** og **6c** i henholdsvis 47 og 32% utbytte. Diastereomerene (*R*)-**6b** og (*S*)-**6b** ble i små mengder separert slik at optisk rotasjon kunne bli målt, og hydrolyse tilbake til **5b** kunne bli forsøkt. Total desilylering ble observert ved hydrolyse. Diastereomerene (*R*)-**6c** og (*S*)-**6c** ble ikke oppnådd i rene fraksjoner. Pyridinene **4a-4c** vil bli testet som ligander i asymmetrisk hydrogenering i Sverige av professor Pher Andersson.

Abstract

New fused pyridine ring systems for the application as ligands in iridium catalyzed asymmetric hydrogenation have been synthesized with cyclotrimerization as a key step. This proved to be an efficient method for varying the wanted substitution patterns in one step.

Firstly, alkyne nitriles **3a** and **3b** were synthesized from commercially available starting materials in 24 and 38% overall yields, respectively, as shown in figure 1. The yields for the individual steps are given in the figure.

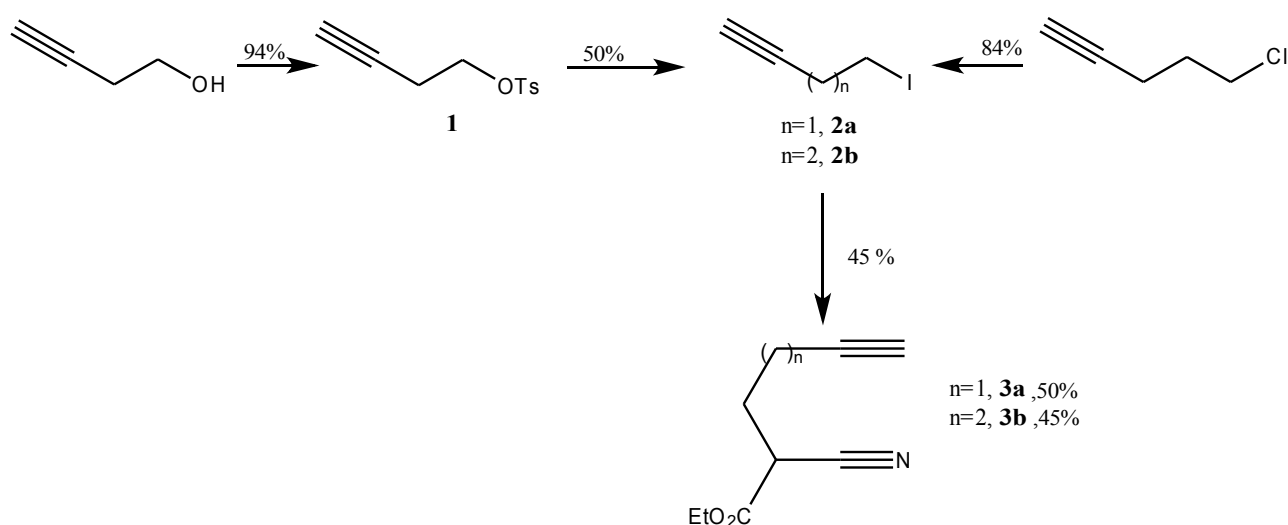


Figure 1: Synthesis of the alkyne nitriles **3a** and **3b**.

The starting butyn alcohol was tosylated to **1**, which was further converted to the iodide **2a** by a Finkelstein reaction. Iodide **2a** was then reacted with ethyl cyanoacetate in an alkylation reaction to form **3a**. Alkyne nitrile **3b** was synthesized in a similar manner from the pentyne chloride.

By varying the alkynes, were **3a** and **3b** converted into eight new structural entities by cyclotrimerization in 17-48% yields, as shown in figure 2.

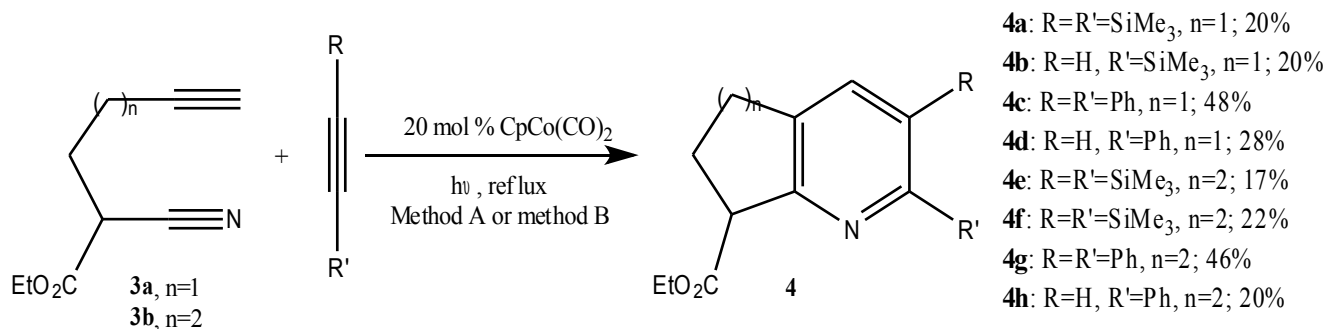


Figure 2: Cyclotrimerization of **3** with various alkynes towards **4a-h**.

The reactions shown in figure 2 were conducted both in a pressure vial, and by slow addition methods. $\text{CpCo}(\text{CO})_2$ was used as the catalyst, and activation of the pre-catalyst was done by irradiation. It was shown that usage of a pressure vial in general produced **4** in better yields than the slow addition method. When monosubstituted alkynes were employed, the reactions showed excellent regioselectivity towards the 2-substituted regioisomers, in accordance to mechanistic models described in the literature. Further improvements of the yields by using other catalysts ($\text{Fe}(\text{OAc})_2/\text{ligand}$, $\text{Cp}^*\text{RuCl}(\text{COD})$ and $\text{CpCo}(\text{COD})$) and reaction conditions did not succeed.

Due to good results from preliminary testing of **4d** as a ligand in asymmetric hydrogenations, evaluation of the pyridine esters **4a-4c** as ligands were therefore wanted. Separation into pure enantiomers via the diastereomers were attempted as described in figure 3.

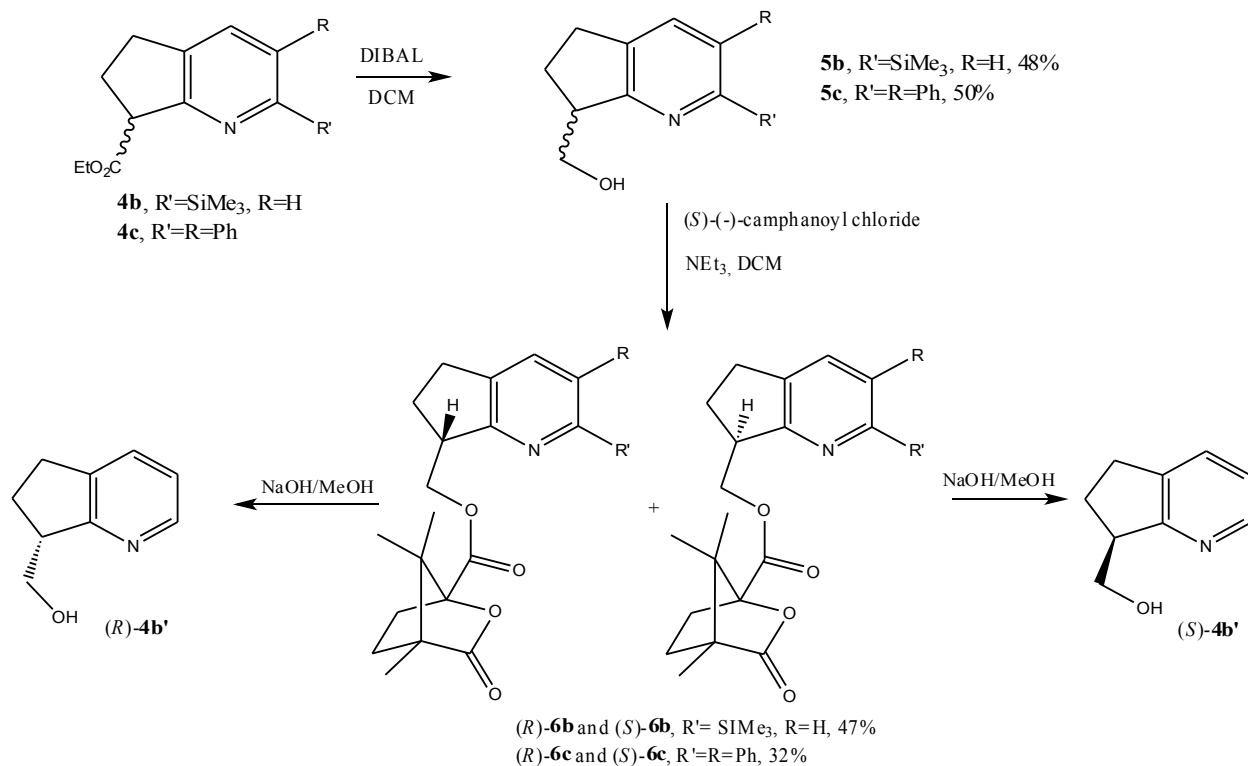


Figure 3: Attempted separation of the enantiomers of **4b** and **4c**.

Reduction of the pyridine esters **4b** and **4c** yielded the alcohols **5b** and **5c** in 48 and 50% yield, respectively. The alcohols **5b** and **5c** were further reacted with (*S*)-camphanic chloride to yield 1:1 diastereomeric mixtures of **6b** and **6c** in 47 and 32% yield, respectively. The diastereomers (*R*)-**6b** and (*S*)-**6b** was obtained pure in small amounts so that rotation could be measured, and hydrolysis back to (*R*)-**5b** and (*S*)-**5b** could be attempted. Here, total desilylation was observed. Separation of (*R*)-**6c** and (*S*)-**6c** were not successful with conventional chromatography. Based on these results is chiral preparative HPLC recommended as the method of choice for achieving pure enantiomers. The pyridines **4a-4c** will be tested as ligands in asymmetric hydrogenation in Sweden, by professor Pher Andersson.

Abbreviations and symbols

[α]_D²⁰	Optical rotation at 20 °C and sodium lamp
1D NMR	1-Dimensional NMR
2D NMR	2-Dimensional NMR
acac	Acetylacetonate
Ar	Aryl
ASAP	Atmospheric Solids Analysis Probe (MS)
atm.	Atmospheres (pressure)
BAr_F⁻	Tetrakis[3,5-bis(trifluoromethyl)phenyl]borate ion
b.p	Boiling point
BTMSA	Bis(trimethylsilyl)acetylene
c	g/100mL
COD	Cyclooctadiene
COSY	H,H Correlated Spectroscopy
Cp	Cyclopentadienyl
Cp*	1,2,3,4,5-pentamethylcyclopentadienyl
d	Doublet (NMR)
dd	Doublet of doublets
DMAP	4-dimethylaminopyridine
J	Coupling constant in ¹ H NMR spectroscopy
m/z	Mass over charge ratio
δ	Chemical shift in NMR spectroscopy
DCE	1,2-dichloroethane
DCM	Dichloromethane
DFT	Density Functional Theory
DIBAL	Diisobutylaluminium hydride
DMF	N,N-dimethyl formamide
dppp	1,3-bis(diphenylphosphino)propane
ee	Enantiomeric excess
ESI	Electron Spray Ionization

Et	Ethyl
Et₂O	Diethylether
EtOAc	Ethyl acetate
EtOH	Ethanol
eq.	Equivalents
HMBC	Heteronuclear multiple bond correlation
HPLC	High performance liquid chromatography
HRMS	High resolution mass spectroscopy
HSQC	Heteronuclear Single Quantum Coherence
Hz	Frequency
IR	Infrared radiation
NaH	Sodium hydride
N,P	Simplified nitrogen-phosphorus containing ligand
m	Multiplet (NMR)
Me	Methyl group
MeOH	Methanol
NMR	Nuclear magnetic resonance
Ph	Phenyl group
ppm	Parts per million
pyr-H	Pyridine proton
R_f	Retention factor in TLC
rt	Room temperature
S	Solvent
s	Singlet
S_N2	Bimolecular nucleophilic substitution
t	Triplet (NMR)
THF	Tetrahydrofuran
TLC	Thin-layer chromatography
TMS	Trimethylsilyl
TOF	Turn-over frequency
TON	Turn-over number

Table of contents

Acknowledgments.....	1
Sammendrag.....	2
Abstract.....	5
Abbreviations and symbols.....	8
1 Introduction.....	13
1.1 Background.....	13
1.2 Goal and synthetic strategy.....	14
2 Theory.....	17
2.1 Transition metals in organic synthesis.[9].....	17
2.2 Catalytic asymmetric hydrogenation.....	19
2.2.1 Introduction.....	19
2.2.2 Iridium-based catalysts.....	21
2.2.3 Mechanistic considerations.....	23
2.2.4 Stereoselection models.....	25
2.3 Cyclotrimerization.....	27
2.3.1 Mechanism.....	27
2.3.2 Reaction scope.....	30
2.3.3 Catalysts and conditions.....	36
3 Results and discussion.....	39
3.1 Preparation of alkynenitriles.....	39
3.2 Cyclotrimerization.....	42
3.2.1 CpCo(CO) ₂	42
3.2.2 Other catalytic systems tested.....	51
3.3 Resolution of enantiomers.....	55
3.4 Future work and other synthetic strategies.....	59
4 Conclusion.....	61
5 Spectroscopic data for new compounds.....	65
5.1 Ethyl 2,3-bis(Trimethylsilyl)-6,7-dihydro-5H-cyclopenta[b]pyridine-7-carboxylate (4a).....	65
5.2 Ethyl 2-(Trimethylsilyl)-6,7-dihydro-5H-cyclopenta[b]pyridine-7-carboxylate (4b).....	66
5.3 Ethyl 2,3-Diphenyl-6,7-dihydro-5H-cyclopenta[b]pyridine-7-carboxylate (4c).....	67
5.4 Ethyl 2-phenyl-6,7-dihydro-5H-cyclopenta[b]pyridine-7-carboxylate (4d).....	68
5.5 Ethyl 2,3-bis(Trimethylsilyl)-5,6,7,8-tetrahydroquinoline-8-carboxylate (4e).....	69
5.6 Ethyl 2-(Trimethylsilyl)-5,6,7,8-tetrahydroquinoline-8-carboxylate (4f).....	70
5.7 Ethyl 2,3-Diphenyl-5,6,7,8-tetrahydroquinoline-8-carboxylate (4g).....	71
5.8 Ethyl 2-phenyl-5,6,7,8-tetrahydroquinoline-8-carboxylate (4h).....	72
5.9 (2-(Trimethylsilyl)-6,7-dihydro-5H-cyclopenta[b]pyridin-7-yl)methanol (5b).....	73
5.10 (2,3-Diphenyl-6,7-dihydro-5H-cyclopenta[b]pyridin-7-yl)methanol (5c).....	74
5.11 (1S,4S)-((S)-2-(Trimethylsilyl)-6,7-dihydro-5H-cyclopenta[b]pyridin-7-yl)methyl 4,7,7-	

trimethyl-3-oxo-2-oxabicyclo[2.2.1]heptane-1-carboxylate ((S)-6b) and.....	75
(1S,4S)-((R)-2-(Trimethylsilyl)-6,7-dihydro-5H-cyclopenta[b]pyridin-7-yl)methyl 4,7,7-	
trimethyl-3-oxo-2-oxabicyclo[2.2.1]heptane-1-carboxylate ((R)-6b).....	75
5.12 (1S,4S)-((S)-2,3-diphenyl-6,7-dihydro-5H-cyclopenta[b]pyridin-7-yl)methyl 4,7,7-	
trimethyl-3-oxo-2-oxabicyclo[2.2.1]heptane-1-carboxylate ((S)-6c) and	76
(1S,4S)-((R)-2,3-diphenyl-6,7-dihydro-5H-cyclopenta[b]pyridin-7-yl)methyl 4,7,7-trimethyl-3-	
oxo-2-oxabicyclo[2.2.1]heptane-1-carboxylate ((R)-6c).....	76
6 Experimental data.....	77
6.1 General.....	77
6.2 Preparation of alkynenitriles	78
6.3 Cyclotrimerization.....	81
6.3.1 CpCo(CO) ₂	81
6.3.2 Other catalytic systems tested.....	89
6.3.3 Preparation of ligand for iron-catalysis.....	90
6.4 Resolution of enantiomers.....	93
References.....	100
Appendixes.....	100
A NMR spectra of 1	103
B NMR spectra of 2a	104
C NMR spectra of 2b	105
D NMR spectra of 3a	106
E NMR spectra of 3b	107
F NMR spectra of 4a	108
G NMR spectra of 4b	113
H NMR spectra of 4c	118
I NMR spectra of 4d	123
J NMR spectra of 4e	128
K NMR spectra of 4f	133
L NMR spectra of 4g	138
M NMR spectra of 4h	143
N NMR spectra of 5b	148
O NMR spectra of 5c	153
P NMR spectra of 6b , fraction 1	158
Q NMR spectra of 6b , fraction 2	163

R	NMR spectra of 6c , fraction 1	168
S	NMR spectra of 6c , fraction 2	173
T	Mass spectroscopy for 4a-h , 5b , 5c , 6b and 6c	178
U	IR spectra for 4a-h , 5b , 5c , 6b and 6c	190
V	Spectroscopy for 3a'	198
W	Spectroscopy for side-product in cyclotrimerization	202
X	Spectroscopy for side-product in cyclotrimerization	204
Y	NMR spectra for the synthesis of L	206
Z	NMR spectra of 5b'	209

1 Introduction

1.1 Background

Stereochemistry is very important in chemistry generally, and especially when it comes to molecular structures used in pharmaceutical chemistry.^[1] Reactions with high enantioselectivity are important in this context, and asymmetric hydrogenation is one reliable and popular procedure for this purpose.^[2] In this reaction, an prochiral alkene is converted into a saturated hydrocarbon containing a chiral center (figure 1.1). The popularity of this method is due to several factors;^[3] high conversions and enantioselectivity, small amounts of catalyst, perfect atom economy and mild conditions. Several transition metals have been explored for this purpose, and over the last couples of decades, iridium based catalysts have been developed and applied with success in asymmetric hydrogenations. They are especially valuable in the hydrogenation of unfunctionalized olefins, as they do not require a coordinating substituent nearby, as is the case for Ru- and Rh-catalysts.^[4] High conversions and enantiomeric excess (ee) have been achieved with several classes of ligands, and today the so called N-P ligands are important. One hydrogenation reaction with this kind of ligand is shown in figure 1.1, also showing typical reaction conditions.

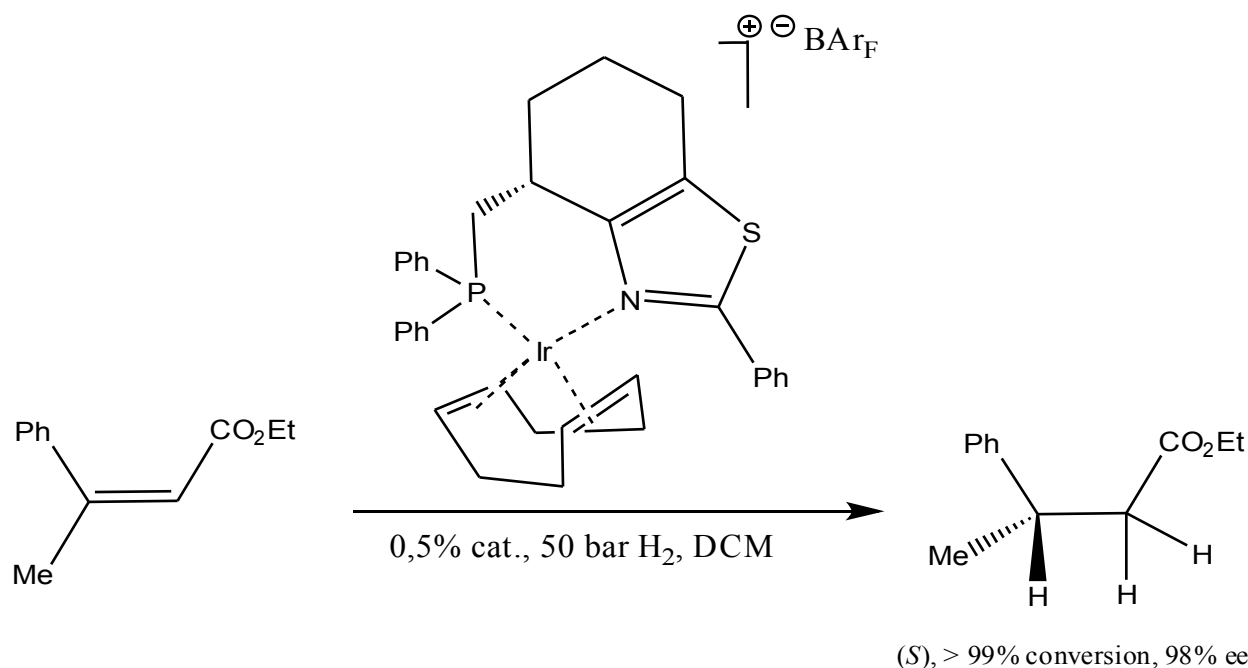


Figure 1.1: Example of an iridium catalyzed asymmetric hydrogenation with typical reaction conditions.

The first, and most famous, of the iridium-based catalysts were developed by Robert Crabtree in 1977.^[5] By altering the ligands, both in type and substitution pattern, better reactions have been achieved, and several catalytic systems today produce both conversion and ee of 99%.^[3] However, the field is far from completely explored, as the type of substrate to be hydrogenated determines very much the outcome of the reaction. New ligands are therefore very much needed to explore this reaction further, and extend the reaction scope.

1.2 Goal and synthetic strategy

As many challenges still are to be addressed in the field of asymmetric catalytic hydrogenation, new catalysts and ligands are highly wanted. The goal of this project is to develop such new ligands for iridium-based catalysts, for the hydrogenation of olefins. Figure 1.2 shows the general structure of the goal iridium complex, **I**. The catalyst is cationic, and the counterion are tetrakis[3,5-bis(trifluoromethyl)phenyl]borate, abbreviated BAr_F^- .

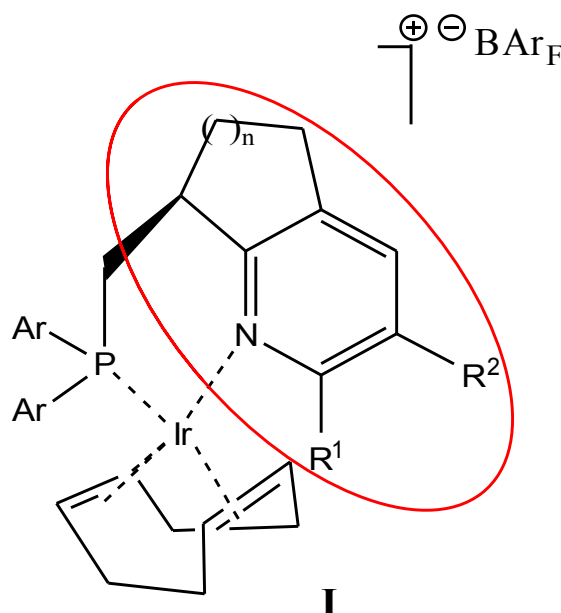


Figure 1.2: General structure of the goal molecule.

This new chiral pyridine fused ligand circled in figure 1.2, is suspected to be attractive in a catalytic system for several reasons. Large R groups that can induce steric interactions in the catalytic system is wanted, as this is earlier observed with other ligands to give good ee's. Two fused rings will make a rigid system, so that fewer conformations is allowed during the catalytic cycle. The type of Ar

groups at phosphor can also be varied, together with the ring size, for optimization purposes. A similar ligand as this has been developed earlier,^[6] although then with a oxygen linker from the fused ring to phosphor. It is expected that the type of linker can effect the conformations of the system, and hence outcome of the reaction. Other heterocycle ligands with a carbon linker have been developed earlier, so that comparison can be done to determine which features in the heterocycles that are important for achieving good ee and conversions.^[7]

The synthesis of the pyridine like ligand in the catalyst **I** will be the main challenge in this project. Substituents in 2-position of earlier developed ligands have been achieved in the past, but no studies have used methods that in one step can easily introduce diverse substituents in both 2- and 3-position. To be able to introduce, and vary, different R-groups in an relatively easy fashion, cyclotrimerization was intended as the key step. The retrosynthetic analysis towards **I** is shown in figure 1.3.

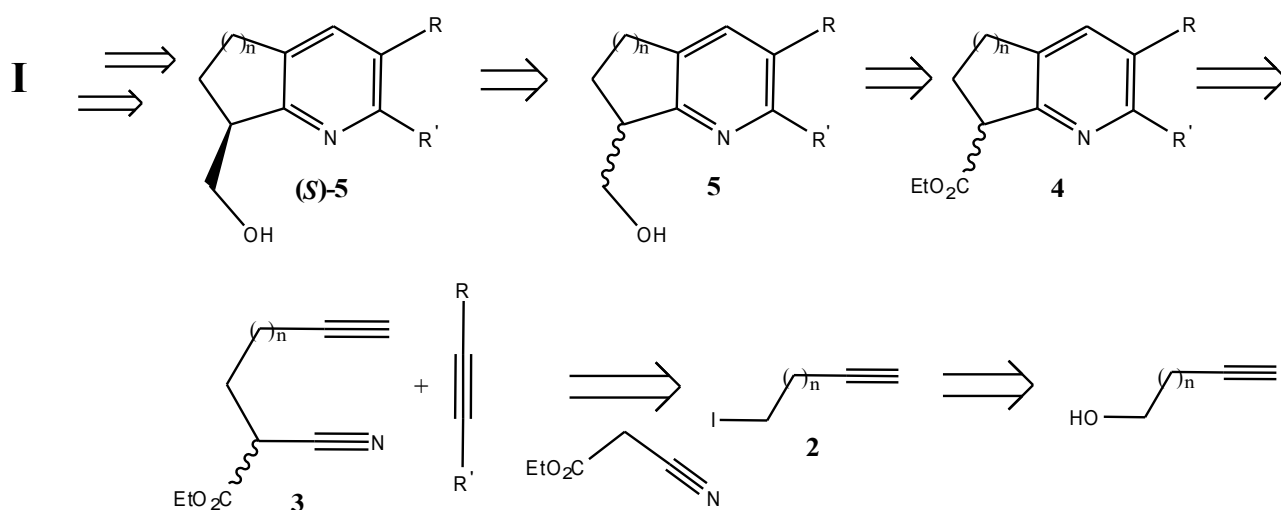


Figure 1.3: Retrosynthetic analysis towards the catalyst **I**, via the cyclotrimerization product **4**. $n=1,2$.

Cyclotrimerization is a transition metal catalyzed [2+2+2] cycloaddition that in one step forms three new bonds. It has successfully been applied to synthesize benzene- and pyridine derivatives.^[8] In this fashion, the R groups and ring sizes can be varied in only one step by applying different alkynes. To be able to affect the enantioselectivity in hydrogenations, the R groups must be relatively large, although examples with methyl groups have been seen.^[6] Phenyl and TMS will primarily be used as R groups. The alkyne nitriles **3**, which are used as the cyclotrimerization

substrate, can be synthesized from commercially available starting materials by substitution reactions and alkylations. When the main structure **4** is obtained, several steps toward **I** must be done, including separation of the racemic mixture into pure enantiomers. Several methods to achieve this exists, e.g. chiral preparative HPLC or derivatization to form diastereomers that can be separated by conventional chromatographic techniques. Chiral purity is crucial for **I** to function satisfactorily in hydrogenation reactions.

This project is in collaboration with Prof. Pher Andersson at the Department of Organic Chemistry, Arrhenius Laboratory, Stockholm University, Sweden. Due to the need for very high pressures of hydrogen gas (>50 atm), the catalyst will be tested at his group facilities.

2 Theory

2.1 Transition metals in organic synthesis.^[9]

Organometallic complexes have found its use in several applications in organic synthesis, among others the palladium catalyzed cross-couplings and hydrogenations. This area of chemistry grew out as an exchange between organic and inorganic chemistry by combining metal centers and organic fragments. It was observed that both elements experienced altered properties, and nowadays this is part of the toolbox of organic chemistry. Compared to more classic synthetic methods, the use of transition metals in organic chemistry have many advantages. Nearly all functional groups will coordinate to metals, and by doing this, reaction patterns are altered. Electrophilicity and nucleophilicity can be interchanged and reactions that are not achievable by other means can be accomplished. Further on, these complexes are often highly specific. That means that they carefully select between which functional groups they interact with, and in that way one can avoid using protective groups, and high chemoselectivity is often observed. Albeit this is of great advantage, it is also one of the disadvantages with organometallic chemistry. High specificity often means low generality in the reactions; small changes in the substrate and/or reaction conditions can alter the outcome of the synthesis completely. Due to the above mentioned consequences of the use of transition metal complexes in organic chemistry, it will be useful to mention some of their chemical characteristics.

By definition, transition metals have an incomplete d-shell. To achieve a stable state, electrons must be supplied into these shells, and this is done by ligands. For a metal to be relatively stable, it should posses around 18 valence electrons. This is often referred to as the “18-electron rule”, but can more conservatively be considered a strong trend. Deviations from this rule is far more common than deviations from the 8-electron rule in basic chemistry. Different ligands contribute with different number of electrons, and the mode of binding is also important. For instance, C_2H_4 binds by donating a pair of electrons from the π -orbital to the vacant d -orbital of the metal. In addition, there is another binding mode that is not taken into the electron count; the *backbonding* from the filled d -orbital to a vacant anti-bonding (π^*) orbital of C_2H_4 , as shown in figure 2.1.

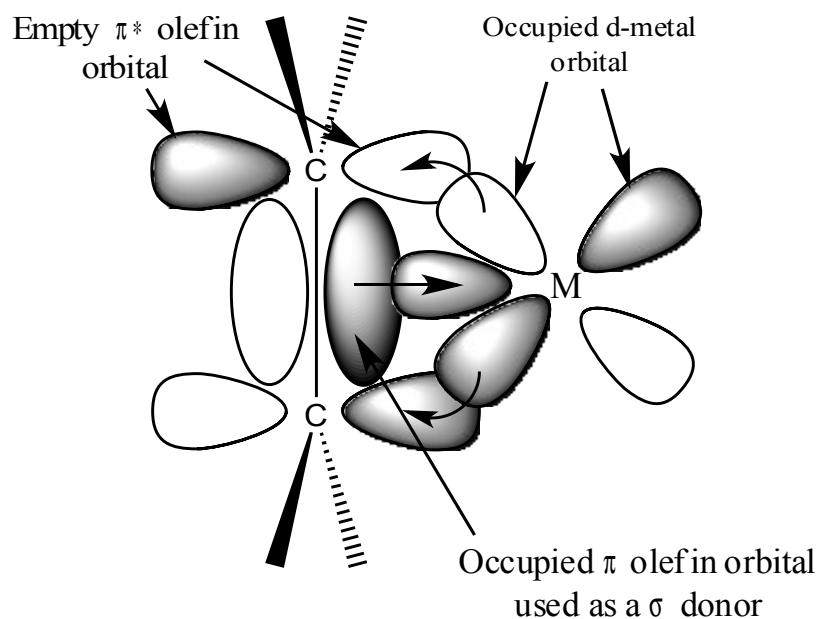


Figure 2.1: Binding modes in transition metal complexes, exemplified with ethene and a metal M. Adapted from Astruc.^[9a]

Here it is shown how the double bond donates electron density to the metal, and that the metal donates back to the available π^* orbital in the olefin. This stabilizes the complex by relieving the metal of electron density, and the same reasoning applies to all common ligands. The backbonding effect is also observed experimentally in X-ray analysis, where the C-C bond is longer in a complexed olefin than in a non-complexed one, due to electron filling of the antibonding orbitals. With inorganic ligands such as H_2O or NH_3 , this backbonding is impossible due to too high energy of the antibonding orbitals of O and N, and complexes such as $\text{M}(\text{H}_2\text{O})_6$ does not exist.

A property of transition metals is that they can exist in many oxidation states, and this is an important prerequisite for the participation in catalytic cycles. In these cycles, so-called dummy ligands are removed, resulting in free coordination sites at the metal. The substrates can then coordinate to the metal, combine with each other, and then subsequently be released as a product. In addition, other ancillary ligands have the role of securing the right electron density at the metal, apply steric effects and prevent the metal from precipitating out of solution. A measure of catalyst efficiency is the turn-over frequency (TOF); the number of turnovers per mol catalyst per unit of time, and the turn-over number (TON); the number of turnovers per mol of catalyst until it is no longer active. Examples of catalytic cycles are shown later for both hydrogenation and cyclootrimerization.

2.2 Catalytic asymmetric hydrogenation

2.2.1 Introduction

Various metals have been employed as catalysts for achieving higher conversion and/or higher ee in hydrogenation reactions. Efficient hydrogenation can be achieved with palladium on carbon (Pd/C) as a heterogeneous catalyst, although with no stereospecificity. The first homogenous catalyst was developed by Wilkinson in 1965 ($\text{RhCl}(\text{PPh})_3$), and chiral ligands were later developed by Kagan and Knowles.^[2a, 9a] This was the birth of catalytic asymmetric/enantioselective hydrogenation, and the metals employed in this developing period were rhodium (Rh) and ruthenium (Ru). These were developed in the late 60's, and the pioneers in this field have earned the Nobel prize for their work.^[2] With these catalysts, hydrogenation of functionalized olefins occurred with very good ee values. One famous example of application is the asymmetric synthesis of L-DOPA, shown in figure 2.2.

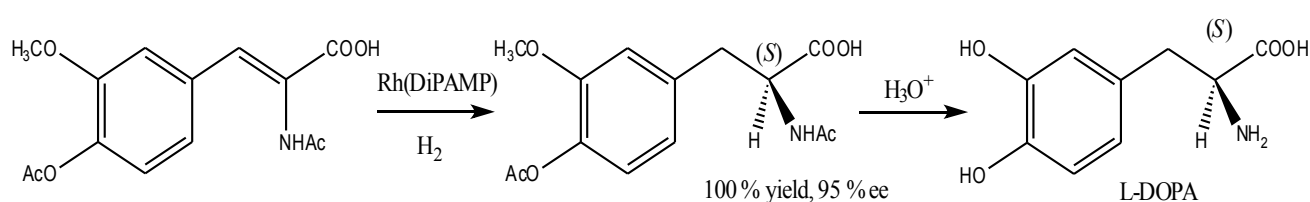


Figure 2.2: Asymmetric hydrogenation as a key step in the synthesis of L-DOPA.^[2a, 10]

Initially, this pharmaceutical for Parkinson's disease was marketed as a racemic mixture. However, it is only the (S) isomer that have biological effect and due to unwanted side effects because of high doses, an enantioselective synthetic route are highly important. The route in figure 2.2 is today a large scale industrial process.^[11]

The type of substrates to be hydrogenated effects the efficiency of the catalysts heavily. Mainly, they can be divided into two groups; functionalized or unfunctionalized olefins. The functionalized ones can further be divided on behalf of the nature of the nearby substituent; a carbonyl or an alcohol group will classify as a coordinating one, and e.g. heteroaromatics and halogens will classify as non-coordinating.^[12] This division is visualized in figure 2.3, but as Cui and Burgess points out, this division must be handled with care and that many substrates may fall into a gray area.^[13]

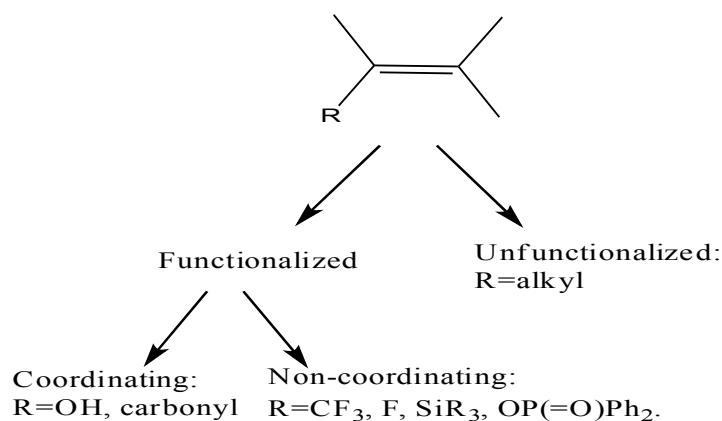


Figure 2.3: Scheme that shows the division of the various substrates that are subjected to hydrogenation. Substituents tested in reactions includes, but are not limited to, the one mentioned in the figure.

Ru- and Rh-catalysts have shown great efficiency and ee values for the substrates with coordinating substituents, but are less effective with non-coordinating and unfunctionalized olefines.^[4] This is due to the need for a coordinating moiety to form a chelate ring that directs the hydrogenation. Due to this dependency, the substrate scope is limited. However, a great breakthrough was achieved when iridium-based catalysts were introduced; hydrogenation of non-coordinating and even unfunctionalized olefins were made possible.

2.2.2 Iridium-based catalysts

In the late 70's, Robert Crabtree and coworkers developed as mentioned a new catalyst based on iridium, that showed great improvements on the hydrogenation of less functionalized olefins.^[5] This iridium complex is cationic with PF_6^- as the counterion, and the achiral catalyst, shown in figure 2.4 a), hydrogenated 1-hexene hundred times faster than Wilkinson's catalyst.^[12] It even hydrogenated tri- and tetra substituted alkenes in good yields. Wilkinson's catalyst is inactive towards the latter.

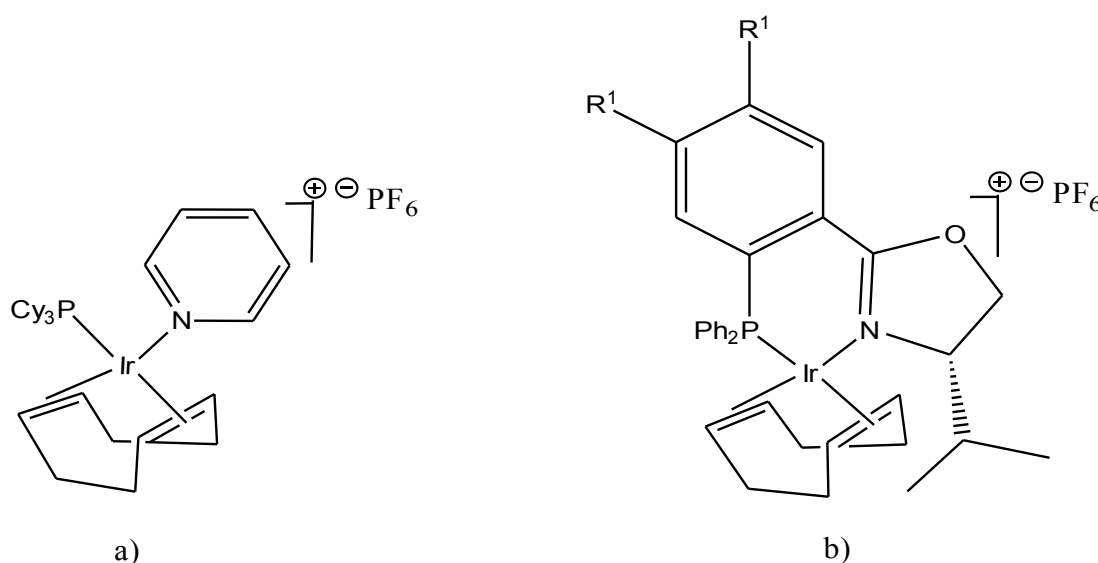


Figure 2.4: a) Crabtree's and b) Pfaltz' catalysts. COD is a common ligand in these catalysts.

It was early discovered that chiral ligands did improve the stereoselectivity in hydrogenations with rhodium- and ruthenium- based catalysts, so this was also tried implemented with iridium. The first iridium-based catalyst that employed a chiral ligand, reported by Pfaltz and coworkers,^[14] is shown to the right in figure 2.4. Different R groups gave various phosphinooxazoline ligands (PHOX) in the catalyst that hydrogenated imines with ee values up to 89% and olefins up to 98% ee.^[3] A drawback with this and the Crabtree catalyst, was that they were observed to form trimerized iridium complexes, which led to depletion of the catalyst. As a consequence, relatively high catalyst loadings (up to 4%) had to be applied. It was also observed that the turnover frequency (TOF) dropped from 2500 to 0 h^{-1} during one hour. Pfaltz' group tried to optimize the reaction conditions by, among other strategies, changing the counterion of the catalyst. It turned out that with tetrakis[3,5-bis(trifluoromethyl)phenyl]borate (BAr_F^-) as the anion, the reaction went to practically quantitative conversion with only 0.05% catalyst loading.^[15] This ion is today the anion of choice^[13] and is shown in figure 2.5.

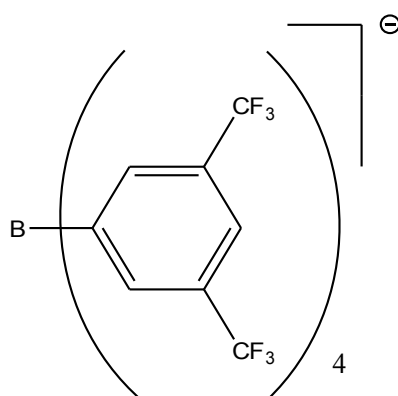


Figure 2.5: The tetrakis[3,5-bis(trifluoromethyl)phenyl]borate ion, BAr_F^- , now routinely used as counterion for cationic iridium catalysts.

This weakly coordinating anion made the catalyst stable to traces of moisture, which was suspected to be one of the causes for the trimerization observed with other anions. With BAr_F^- , the reaction solutions can therefore be prepared in air and without the need of dried solvents. TOF is also increased to 5000 h^{-1} . The reason for these observed effects were elucidated in a subsequent kinetic study by Pfaltz' group.^[16] It showed that with strong coordinating anions such as PF_6^- , the olefin is not involved in the turnover-limiting step, while the opposite is observed for BAr_F^- . By considering the formation of inactive trimerized complexes as the reason for catalyst depletion, the critical factor is the propensity to form trinuclear complexes over complexing with the olefin. With BAr_F^- the olefin insertion is fast, while for PF_6^- , which forms an tight anion pair, trimerization becomes more likely.^[3]

Considerations of the solvent is important in the hydrogenation reaction. Iridium complexes will precipitate in e.g. hexane, while the catalytic activity is preserved in chlorinated solvents.^[17] This is probably due to the high polarity and low coordinating power of the latter. Today, dichloromethane is the common solvent for the reactions. Because chlorinated solvents have an oxidizing power, DCM was for a long time considered unsuitable together with these metal catalysts. The resistance towards oxidations is one important advantage with iridium-based catalysts. Therefore, together with the anion effect, they are considerable more stable to air and moisture than the Ru- and Rh-counterparts.

2.2.3 Mechanistic considerations

Mechanistic rationalization is important to get a thorough understanding of the reactions and to make reliable selectivity models (*vide infra*). Compared to the mechanism of the rhodium-based catalysts^[18] the mechanism of iridium-based catalysts are not completely understood.^[12-13]

Different models of the iridium mechanism deviates mostly in the details in the catalytic cycle, while the structure of a initial iridium (III) dihydride complex is generally more accepted. The formation of this complex starts with that the COD-ligand is hydrogenated to cyclooctane and lost by the catalyst precursor. This gives a coordinatively unsaturated iridium complex which subsequently reacts with H₂ and the substrate to form a cationic iridium (III) dihydride, shown in figure 2.6. The understanding of the stereoselectivity of the catalyst lies mainly in how this complex looks like, and it has therefore been the subject of intense research. DFT- and NMR analysis together with X-ray crystallography in a thorough study by Pfaltz and coworkers,^[19] resulted in the structure below.

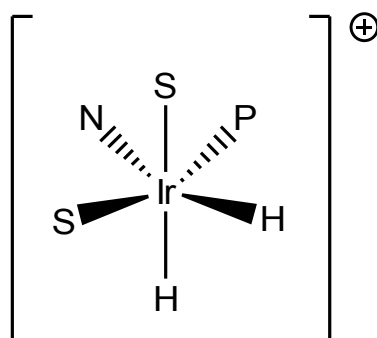


Figure 2.6: Optimized structure of the Ir (III) dihydride complex by DFT. S=solvent, N,P=simplified N,P-ligand.

Similar structures have been confirmed by other groups,^[20] and what they all conclude, is that electronic effects are more important than steric effects in deciding the structure. The hydrides, two strong σ -donors, can not be *trans* to one another, and preferably not *trans* to other strong σ -donors (e.g. the phosphine ligand). Therefore, they are placed *cis* to each other and the phosphine ligand, as shown in figure 2.6. In d₈-THF, the Pfaltz group was able to observe the calculated structure as the major isomer in NMR analysis, while in d₂-DCM, a more complex mixture was obtained. THF is

more strongly coordinating than DCM, which are commonly used in the hydrogenation reactions. This implies that the situation may be more complex than the study reveals.^[12]

Although several studies agrees on the same initial iridium (III) dihydride structure, the fate of this complex in the catalytic cycle, is subject to more debate. Among others, two possible cycles have been suggested; one with Ir^I and Ir^{III} intermediates by Chen^[21] and Pfaltz^[22] and one with Ir^{III} and Ir^V intermediates by Brandt^[20] and Burgess and Hall^[23], both shown in figure 2.7. The shared initial complex is shown in the center.

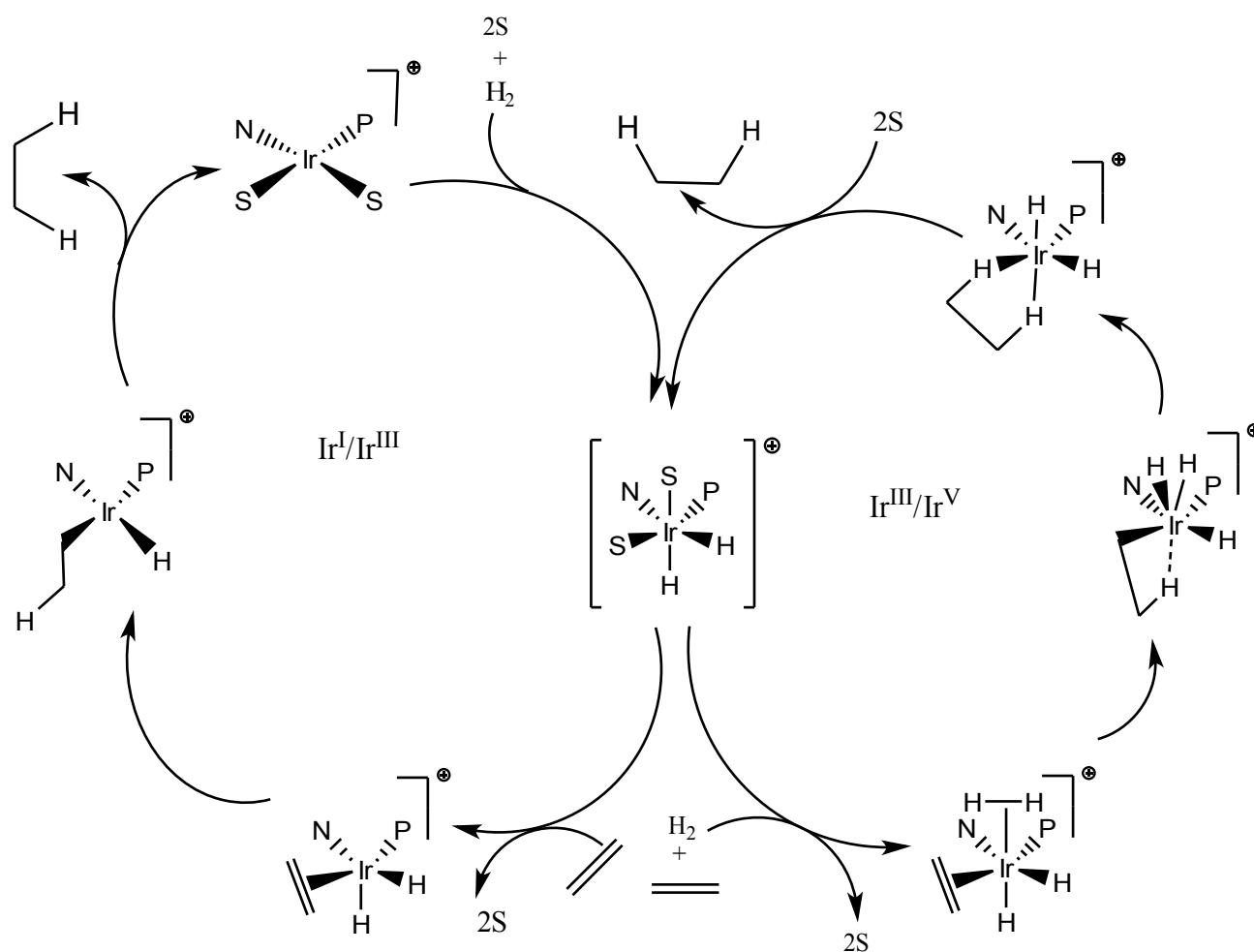


Figure 2.7: Two possible mechanisms for hydrogenation of olefins; Ir^I/Ir^{III} to the left and Ir^{III}/Ir^V to the right. Adapted from Church and Andersson.^[12]

The Ir^{III}/Ir^V cycle start by displacement of two solvent molecules by coordination of an olefin and H₂.^[12] Then, a migratory insertion of the olefin into a iridium-hydride bond occur. This is the rate-

determining step, and is made energetically favorable by the simultaneous oxidative addition of H_2 . Reductive elimination of the reduced hydrocarbon, and coordination of two solvent molecules completes the cycle. In the Ir^I / Ir^{III} cycle a migratory insertion followed by a reductive elimination finds place also here, however here via a Ir^I -complex. Clearly, many different reaction pathways are possible, but several highly enantioselective catalysts are reported, so it is likely that they have the ability to discriminate between competing reaction pathways.^[24]

2.2.4 Stereoselection models.

Although the complete mechanistic picture for iridium catalyzed hydrogenation remains uncertain, stereoselection models have been proposed on the basis of the above mentioned mechanistic studies. In a thorough study by Andersson et al. in 2010^[25] they evaluated four mechanistic pathways obtained to that date, including those in figure 2.7, with DFT calculations. As a result of this and earlier work, a stereoselection model was put forward. This has been established by performing calculations on the placement of the substrate in regards to the full catalyst. A similar model has also been established by the same group for other ligands,^[26] and the model is presented in figure 2.8.

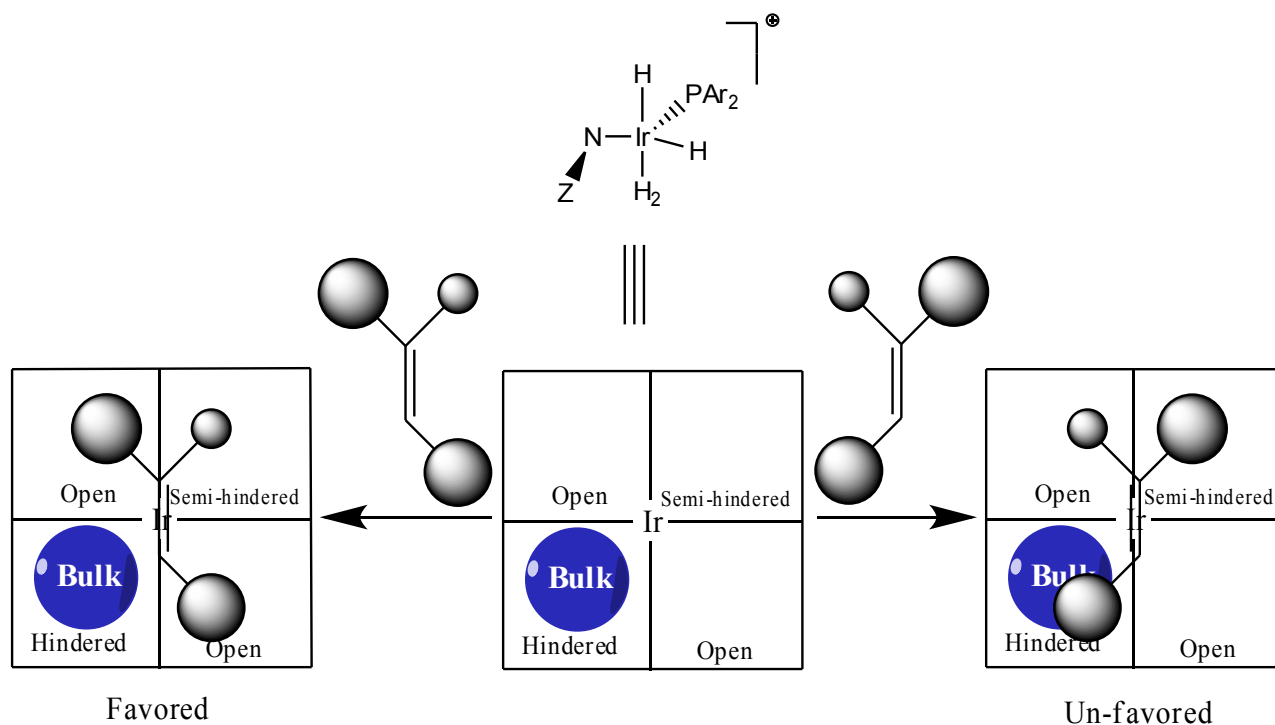


Figure 2.8: Stereoselection model exemplified with *trans*- α -methylstilbene.^[25-26]

By considering a N-Ir-H plane in the upper structure in figure 2.8, this intermediate can be interpreted as the schematic squares. Here, the most hindered part of the catalyst is the N-Z quadrant, where Z can be e.g. a phenyl substituent. The phosphine part of the ligand becomes the second most hindered position. On behalf of this, the least steric demanding substituent of the olefin, i.e. the proton, will be placed near the N-Z part. This models fits experimental findings, and in this example the preferred stereochemistry will be (*S*). While the model is highly applicable for substrates without electronic effects, the case is more complicated for substrates that have a polarizable double bond. Here it will be a mismatch between the electronic and steric preferences, and the reaction rates will be slower in addition to lower enantioselectivities.

2.3 Cyclotrimerization

Cyclotrimerizations can be considered as [2+2+2] cycloadditions, coupling three triple bonds in one step.^[8a] Although such reactions are thermally allowed, uncatalyzed reactions are rare. This is due to both entropic and enthalpic reasons; bringing three triple bonds together are not entropic favorable, and at the same time an high energy activation barrier must be overcome.^[8b]

This problem have been circumvented by applying transition metals as catalysts, and cyclotrimerization is now being considered an very efficient and versatile approach to several molecular structures. This is due to several reasons,^[27] the most important being that even under catalytic amount of catalyst and mild conditions, the methods provide a high degree of synthetic efficiency. Mild reaction condition also means that many functional groups are tolerated. In addition, the starting alkynes and nitriles are usually readily accessible. Most of the research on cyclotrimerizations have been done on the synthesis of pure carbocycles and pyridines. Fused pyridines have mostly been studied by the cycloaddition of a diyne and a nitrile, while cyclotrimerization of alkynenitriles are less studied (vide infra). This chapter will mostly focus on pyridine synthesis and structures resembling the ones sought fore in this thesis. Many different metals have shown catalytic effect in cyclotrimerizations (e.g. Fe, Co, Rh and Ru), and this is reviewed several places.^[8a, 28]

As an understanding of the mechanism is crucial for the subsequent discussion, it is presented first. Cobalt will be used for illustration, because it is most discussed in the literature, and it is also widely used in the experimental part of this thesis.

2.3.1 Mechanism

Several studies, both experimental and computational, have been conducted on the mechanism of cyclotrimerization.^[27-29] This have led to an common, general understanding of the catalytic cycle, which is outlined in figure 2.9. Although many studies focus on pure carbocycles, it is reasonable to assume the same pathways and intermediates for pyridine formation.^[29]

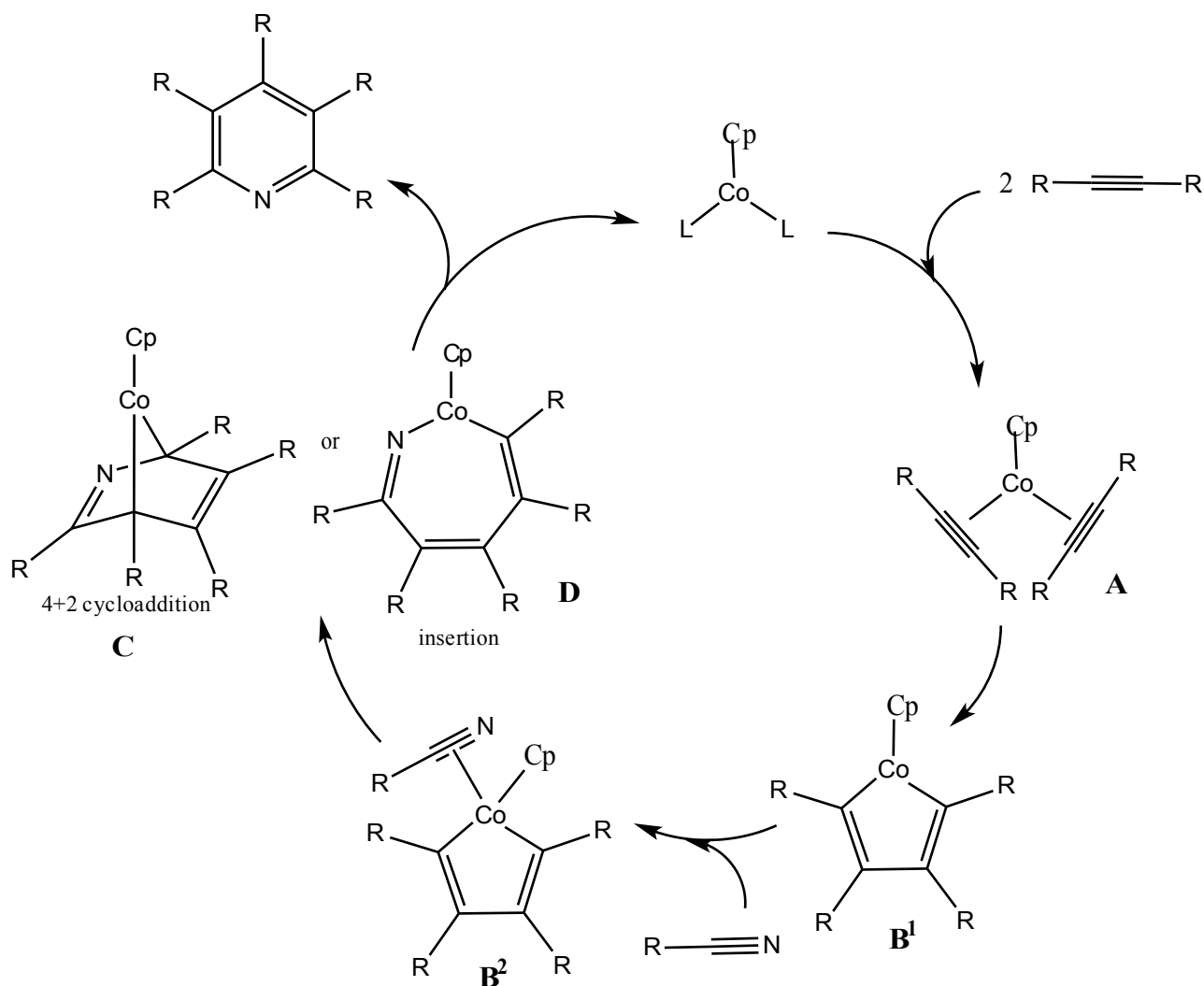


Figure 2.9: The catalytic cycle for the formation of pyridines from alkynes and nitriles.^[28-29]

The cycle starts with the displacement of the two ligands of the pre-catalyst by two alkynes, giving **A**. This is then followed by an oxidative coupling, leading to the formation of the cobaltacyclopentadiene **B¹**. Coordination of the nitrile leads to **B²**, and the subsequent incorporation of the nitrile into the metallacycle can either occur through addition (in a Diels-Alder fashion) or via insertion, giving **C** or **D**, respectively. Reductive elimination is the ultimate step which regenerates the catalyst and releases the product. Although the overall picture of the cycle is agreed upon, the step yielding **C** or **D** is a bit disputed.

In the formation of complex **B¹**, the oxidation number of Co is raised from I to III, and as a consequence, nitrile coordination in the next step is enhanced.^[29] This is a big advantage for

pyridine synthesis, since the addition of a nitrile will then be favored over an alkyne in the final step. The coordination occurs via the nitrogen lone pair, and relies on the electron donating ability of this group. This means that substituents close to the nitrile group with electron withdrawing effect will lower the coordinating ability of the nitrogen.^[28]

For cyclotrimerization to pure carbocycles, there is lacking experimental evidence of **A** and **D**, while the **B**-complexes are observed.^[28, 30] A more direct route to a η^4 -bound arene-Co complex from **B** is therefore considered, possibly via a [4+2] cycloaddition resembling **C**. This is supported by computational work by Hardesty et al.,^[31] and is thought to be due to the formation of an aromatic system and the extremely exothermic nature of this transformation.

From **B**¹ in figure 2.4, some side reactions have been observed, were the most common one being the formation of a η^4 -cyclobutadiene complex, **E**, as shown in figure 2.10.^[32]

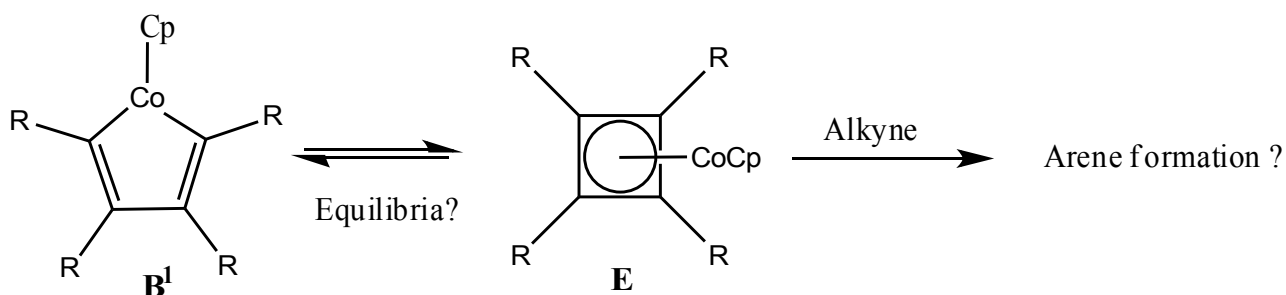


Figure 2.10: Formation of the cyclobutadiene **E** from cobaltacyclopentadiene **B**¹.

The main problem here is that a such side reaction may deplete the catalyst, and make it inactive towards the addition of a third triple bond. Vollhardt and Hillard^[32] tried to use isolated cyclobutadiene complexes as catalyst in further cyclotrimerization, but it turned out to be inert. They experienced bis-trimethylsilyl acetylene (BTMSA) to be prone to forming such complexes. In addition to catalyst depletion, starting materials as dienes or alkynenitriles can also be consumed, as they can also be incorporated in to structures like **E**^[32-33]. Although other groups^[34] have observed such complexes to be reintroduced into the catalytic cycle, it is generally understood that this side reaction is a reason for catalyst depletion.

Similar mechanisms as the one presented in figure 2.9 are assumed for other transition metals used as catalysts for cyclotrimerization, e.g. iron and ruthenium. Arene-iron and CpCo-complexes are isoelectronic, and therefore the same basic reaction patterns and mechanisms can be expected.^[28]

2.3.2 Reaction scope

As mentioned, the term cyclotrimerization applies to all kinds of cycloadditions of various triple bonds. The most thoroughly studied systems are the formation of benzene- and pyridine derivatives. Further on, cyclotrimerization has been employed to other substrates as well, including fused heterocycles from tethered diynes or alkyne nitriles.^[35] It also has several applications in total synthesis,^[27] and with chiral nitriles.^[36] For instance, the pharmaceutical Lysergene, was synthesized as shown in figure 2.11 by Vollhardt.^[37]

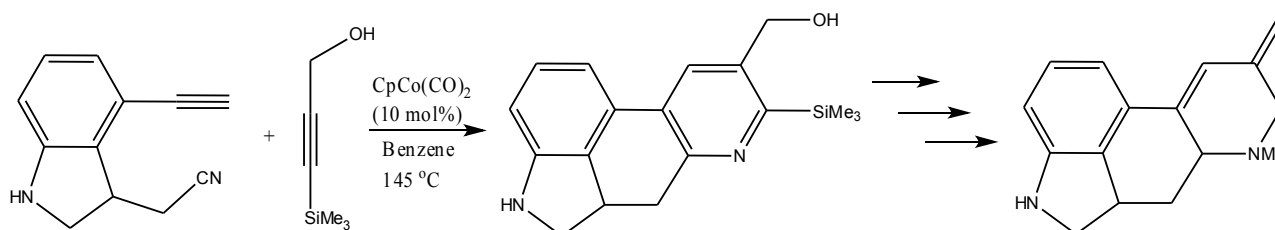


Figure 2.11: The total synthesis of Lysergene, with a cyclotrimerization as a key step.

Although cyclotrimerization have seen many applications, there are some limitations, the major one being regioselectivity.^[27] When the cyclization is totally intermolecular and unsymmetrical alkynes are being used, several regioisomers are possible, as shown in the top part in figure 2.12. Fortunately, the number of possibilities can in many cases be reduced by tethered multiple bonds, as the reaction becomes more intramolecular. In a cyclization with an α,ω -alkyne nitrile and an unsymmetrical alkyne as in the bottom part in figure 2.12, only two possible regioisomers are possible.

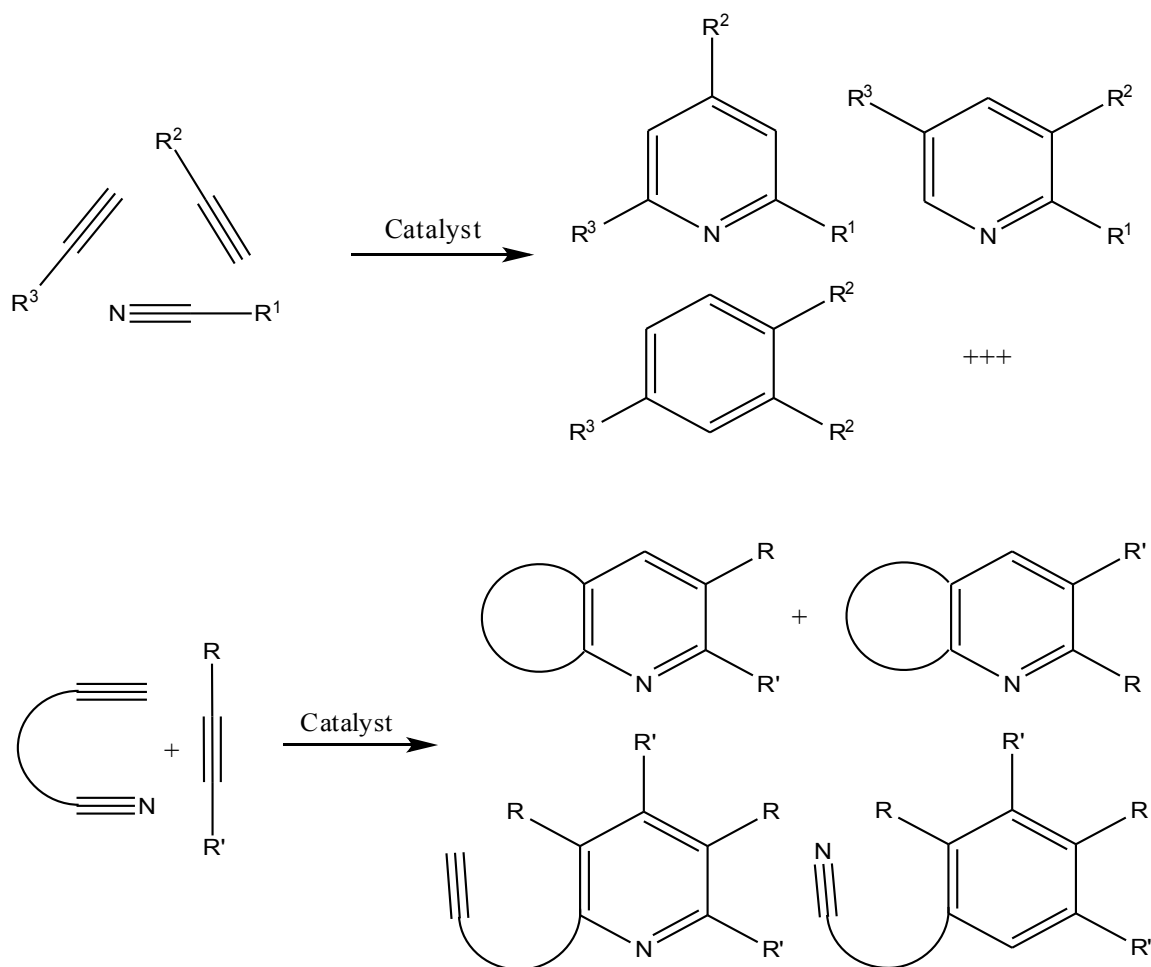
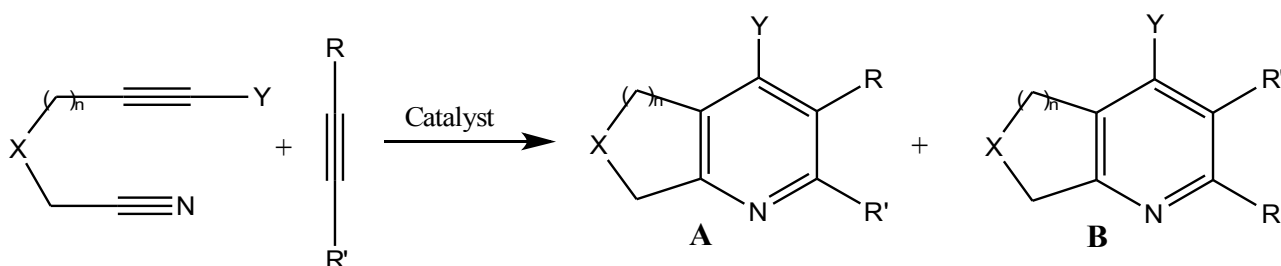


Figure 2.12: Regioselectivity and chemoselectivity in cyclotrimerization towards pyridines. The number of regioisomers is reduced by tethered triple bonds.^[27]

When synthesizing pyridines by cyclotrimerization, or using different alkynes for formation of carbocycles, the successful outcome relies on that the alkynes and nitrile combine in the wanted ratio and fashion; that is, the system must exercise the right chemoselectivity in addition to the right regioselectivity. For pyridine synthesis, it means that the alkynes and the nitriles must combine in a 2:1 fashion.^[28] Some of the possible sideproducts from this complication are also shown in figure 2.12. Even if a pyridine is the wanted product, a pure carbocycle can be achieved, this also with possibility of various regiochemistry. The same situation can happen for tethered alkynes and nitriles. How the triple bonds combine will largely depend on their reactivity toward the catalyst and each other. Fortunately, nitriles trimerize less readily than alkynes, so this is not a common side product.^[28]

Mainly two articles in the literature concerns the cyclizations of alkynes to alkynenitriles. Therefore, it is relatively little studied compared to the cyclizations of diynes to nitriles and cyclizations to pure carbocycles. Table 2.1 reviews selected reactions of alkynenitriles with varying alkynes to the formation of fused pyridines.

Table 2.1: Reactions of alkynenitriles with alkynes in the literature.



Entry	Catalyst	n	X	Y	R'	R	Ratio		Yield (%)
							A	B	
1 ^[38]	CpCo(CO) ₂	1	CH ₂	H	TMS	TMS	-	-	77
2 ^[38]	CpCo(CO) ₂	2	CH ₂	H	TMS	TMS	-	-	77
3 ^[38]	CpCo(CO) ₂	1	CH ₂	H	TMS	H	1:0	-	29
4 ^[38]	CpCo(CO) ₂	2	CH ₂	H	Ph	Ph	-	-	4
5 ^[38]	CpCo(CO) ₂	2	CH ₂	H	TMS	Me	1:0	-	70
6 ^[38]	CpCo(CO) ₂	2	CH ₂	H	Bu	Me	9:7	-	80
7 ^[39]	Fe(OAc) ₂ / ligand	1	C(CO ₂ Me) ₂	Me	Ph	Ph	-	-	54
8 ^[39]	Fe(OAc) ₂ / ligand	1	C(CO ₂ Me) ₂	Et	Bu	Bu	-	-	86
9 ^[39]	Fe(OAc) ₂ / ligand	1	C(CO ₂ Me) ₂	H	Bu	Bu	-	-	30
10 ^[39]	Fe(OAc) ₂ / ligand	1	C(CO ₂ Me) ₂	Me	^t Bu	Me	1:0	-	26

The yields in the reaction in table 2.1 varies from poor (4%) to good (86%). When terminal alkynes are used, which are capable of selftrimerizing, lower yields are in general observed (entry 3).^[38] Terminal alkynes are not tested in the iron catalyzed reactions. Low yield in entry 4, is explained by depletion of the catalyst due to formation of cyclobutadiene complex formation, as **E** in fig 2.10.

A common feature for many of the examples in table 2.1 are the quaternary center in the tether. This is a common choice for cyclization reactions, as these structures display easier and faster ring closing due to the Thorpe-Ingold effect.^[40] The substituents will repel each other, hence lower the angle inside the forming ring. The substituents taking part in the reaction, an alkyne and a nitrile in this case, will come closer to each other and therefore react faster. From table 2.1, for example comparing entry 8 and 9, it can also be seen that a substituent at the alkyne part of the alkynenitrile, increases the yield in the Fe-catalyzed reactions.

Table 2.1 shows some examples of regioselectivity in cyclotrimerizations of this kind. If an unsymmetrical alkyne is used in the reaction, complete regioselectivity can be achieved with the right substituents. Excellent regioselectivity are observed when the difference in size between the two R groups are sufficiently large (entry 3, 5 and 10). When two more similar R groups are used, the regioselectivity drops, as in entry 6. Due to their findings, Vollhardt et al. proposed a model for the formation of the cobaltacycle intermediates for alkynenitriles, shown in figure 2.13.^[37] Here, the larger R' group of the alkyne is placed proximal to the cobalt before addition of the nitrile group.

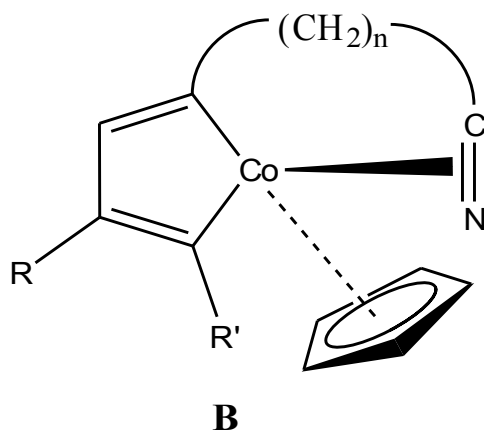


Figure 2.13: Proposed intermediate in the cyclotrimerization of an alkynenitrile with an alkyne where $R' > R$.^[38]

After the addition of nitrile, the bigger R' group will then be closest to the nitrogen in the resulting insertion- or cycloaddition stage in the Co-mechanism (figure 2.9). **B** is the equivalent to **B**² in the mechanistic cycle for tethered triple bonds. In an earlier article^[32] on the cyclization of alkynes and dienes, Vollhardt et al. discusses whether two alkynes or one diyne will preferably combine into the initial metallacycle **B**¹. They reach no conclusion, other than saying that several pathways may lead

to the same product, and that a mechanistic route via **B** in figure 2.13 explains the regioselectivity observed. However, in the synthesis of pyridines, the nitrile addition is as mentioned favored in the last step when cobalt has been oxidized, so here it is apparent that the cobaltocycle has the structure shown in figure 2.13. In the same article, the reason for the preferred regioselectivity in **B** from a substituted diyne and an substituted alkyne is discussed, and it is outlined in figure 2.14.

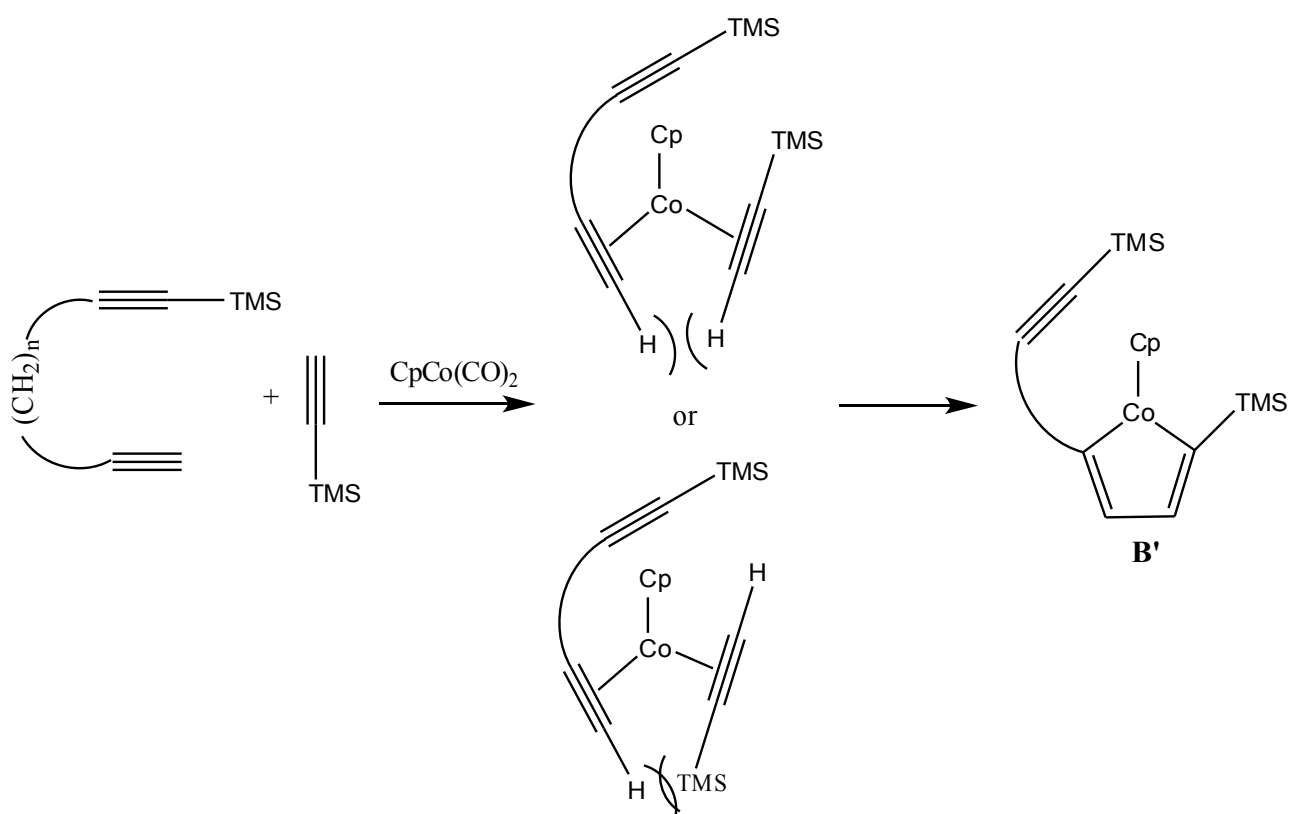


Figure 2.14: Formation of the more sterically hindered product from a diyne and an alkyne, via the upper less hindered precursor, here exemplified with TMS as substituents.^[32]

Here, two triple bonds are cyclized, yielding the intermediate **B'**. The reason for the selectivity is due to the lower steric interactions between the hydrogens in the upper structure, than between the alternative hydrogen-TMS interaction in the lower structure. This reasoning can be extrapolated to alkyne nitrile and alkynes, as the TMS substituted end of the diyne is interchanged with nitrogen. So in conclusion, by this model the reason for the 2-substituted pyridines or the more sterically hindered carbocycles are due to the lesser sterical interactions in the preceding intermediates. Also in the work of Louie et al.^[39] in table 2.1 with iron-catalysis, the same regioselectivity is found, albeit here it is not discussed to any extent. In addition, in this study opposite regioselectivity is

observed when applying substituents with electronic effects.

The importance of the electron donating ability of the nitrile group in the formation of pyridines was high-lighted in the discussion of the mechanistic aspect of cyclotrimerizations. An synthetic example that shows how this coordinating ability can be altered, is shown in figure 2.15, a work conducted by Varela et al.^[41]

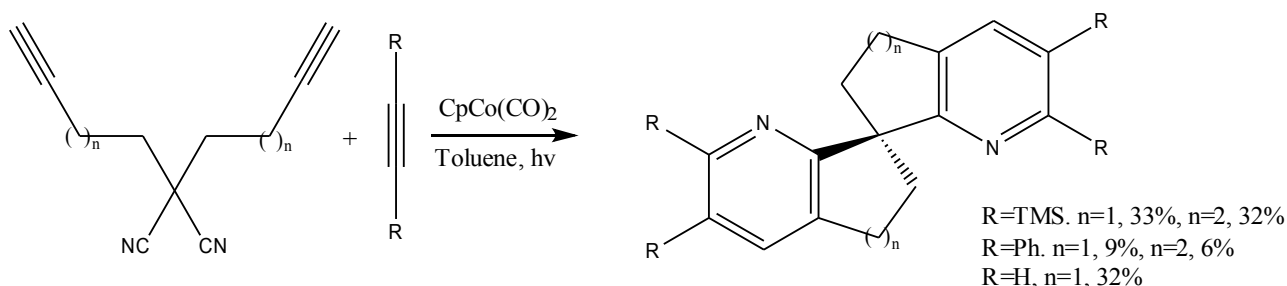


Figure 2.15: Cyclotrimerization where the nitrile group is deactivated by an electron withdrawing group.^[41]

Here a cyclization with an alkyne nitrile to an alkyne is performed, and an electron withdrawing group (another nitrile) is present close to the nitrile. This will lead to lower coordinating ability of the nitrile group, and the formation of **B**² in the catalytic cycle is not favored to the same extent. As a consequence of this, lower yields are observed. The same effect has been seen in cyclizations between diynes and nitriles by Vollhardt.^[42] It can also be noted from figure 2.15 that when acetylene is applied (R=H), the same yield is obtained as for R=TMS. This implies that steric hindrance is of little importance in this reaction. Again is the outcome of the cyclotrimerization poor when diphenylacetylene is used, as was the case for entry 4 in table 2.1.

2.3.3 Catalysts and conditions

Metals throughout the whole transition metals series have been found to mediate or catalyze cyclotrimerizations, but the group 9 metals stands out in popularity.^[43] The structure of two common cobalt catalyst are shown in figure 2.16,

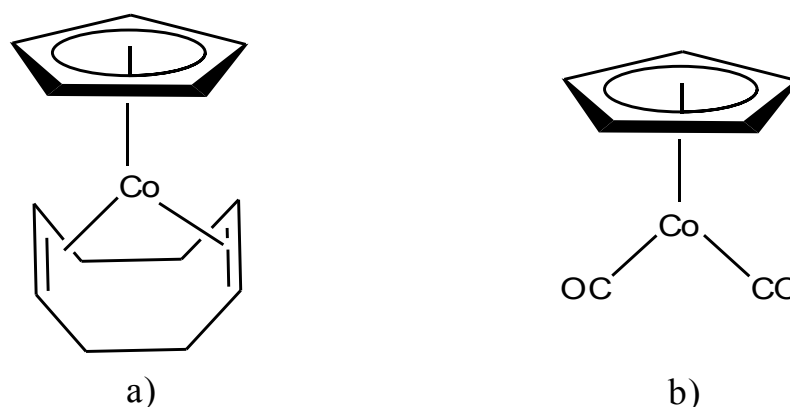


Figure 2.16: Examples and structures of two common catalysts for cyclotrimerization. a) CpCo(COD), b) CpCo(CO)₂, Vollhardts catalyst.

These two catalysts are among the most frequently used, especially in pyridine synthesis. CpCo(COD) must be prepared in the lab, while CpCo(CO)₂ is commercially available. In addition to these two, a range of quite different catalysts have been employed, but they share some common features:^[43] i) a spectator ligand, often the cyclopentadienyl moiety, that is attached to the metal throughout the reaction, and ii) neutral ligands such as CO, C₂H₄ or COD that are displaced from the metal to secure a smooth release of the active catalyst. These features can also be seen in the catalytic cycle in figure 2.9. The spectator ligand can be modified with respect to reactivity, selectivity and stability.^[43] Which catalyst to choose, depends among other things of the reactivity of the system. Low reactivity of the substrates, demands a highly reactive pre-catalyst, while a too highly reactive pre-catalyst can give a highly complex mixture. The choice of pre-catalyst and ligands can also affect the chemoselectivity in the system, as exemplified in figure 2.17.^[44]

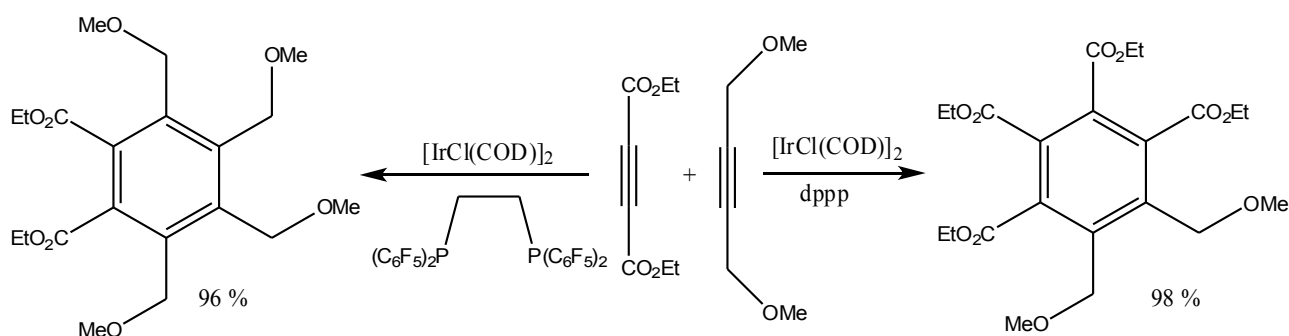


Figure 2.17: Example showing the different chemoselectivity when different ligands is used.^[44]

Both reactions uses the same pre-catalyst, and both give good yields, although of two different products. Different ligands are added to the reaction mixture, hence generating different active catalysts *in situ*. This approach is more common for iridium and rhodium systems than for cobalt systems.^[43] The coordination of different ligands in the catalytic cycle leads to a completely altered chemoselectivity.

As mentioned in chapter 2.1, organometallic chemistry is often quite specific, which often make the systems vulnerable to changes in the substrate. An example of that is from a work by Wang et al.,^[45] shown in figure 2.18.

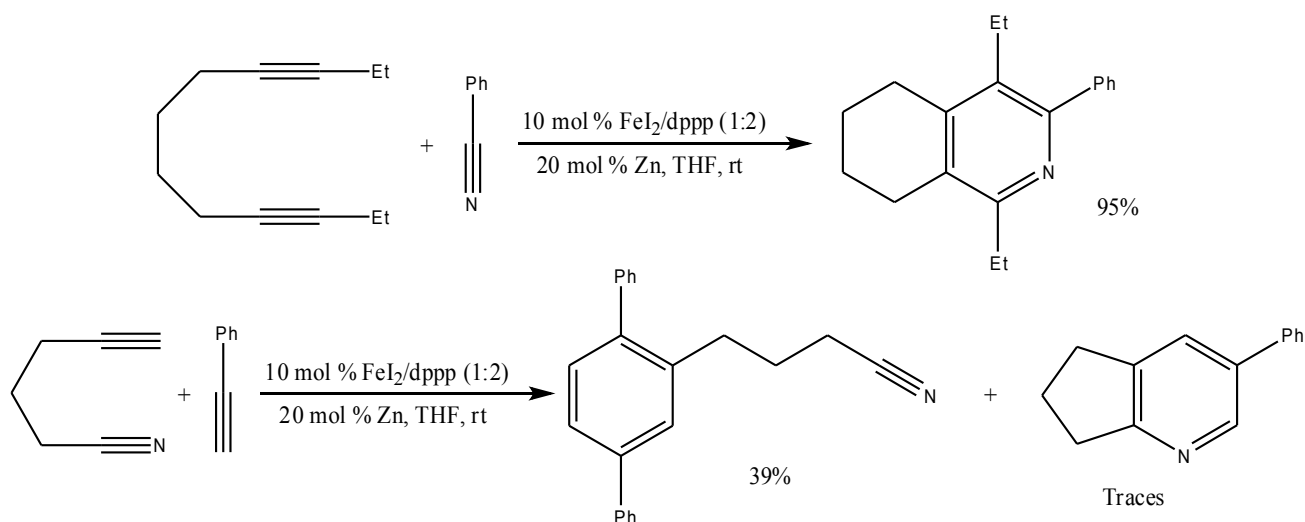


Figure 2.18: Example showing substrate specificity in a catalytic system for a cyclotrimerization.^[45]

This catalytic system is able to synthesize the wanted fused pyridine between a diene and a nitrile in excellent yield. When tested on an alkynenitrile and an alkyne, the wanted product is only observed in trace amounts. The main product is the structure achieved by cycloaddition of to alkynes and the

carbon triple bond in the alkynenitrile. Instead of an intramolecular nitrile insertion in an intermediate resembling **B** in figure 2.13, an extra alkyne seems to react more rapidly. Although the system showed good adaption to different dienes and nitriles in the top reaction of figure 2.18 by producing the wanted structures in good to excellent yields, a change in the connectivity between the triple bonds were not accepted.

The pre-catalyst must usually be transformed into the active catalytic species. The alternatives for catalyst activation are normally either heat or light, and the neutral ligands in the precatalyst determines the preferred method. C_2H_4 demands heating, while CO demands photochemical cleavage. The COD-ligand can be removed by either light or heat.^[28] A premise for a photo induced reaction is a light source with wavelengths above 360 nm, due to the decomposition of the catalyst at lower wavelengths.^[46]

Various reaction set ups have also been used in cyclotrimerizations. Continuous addition of catalyst and/or high dilution conditions have been applied to avoid self-trimerization of alkynes, dienes and alkynenitriles.^[32] This can be achieved by employing a slow addition method with a syringe-pump to a relatively large amount of solvent.

3 Results and discussion

The retrosynthetic route to the wanted ligands is shown in figure 1.3 in the introduction. In this chapter, the results from the various parts in the synthesis are presented and discussed. Detailed procedures are presented in the experimental data.

3.1 Preparation of alkynenitriles

The first main stage in the synthesis of **4** was to achieve the alkynenitriles **3** to be used in the cyclotrimerization step. This was done as shown in figure 3.1. All these steps are literature procedures, and the yields are given in the figure.

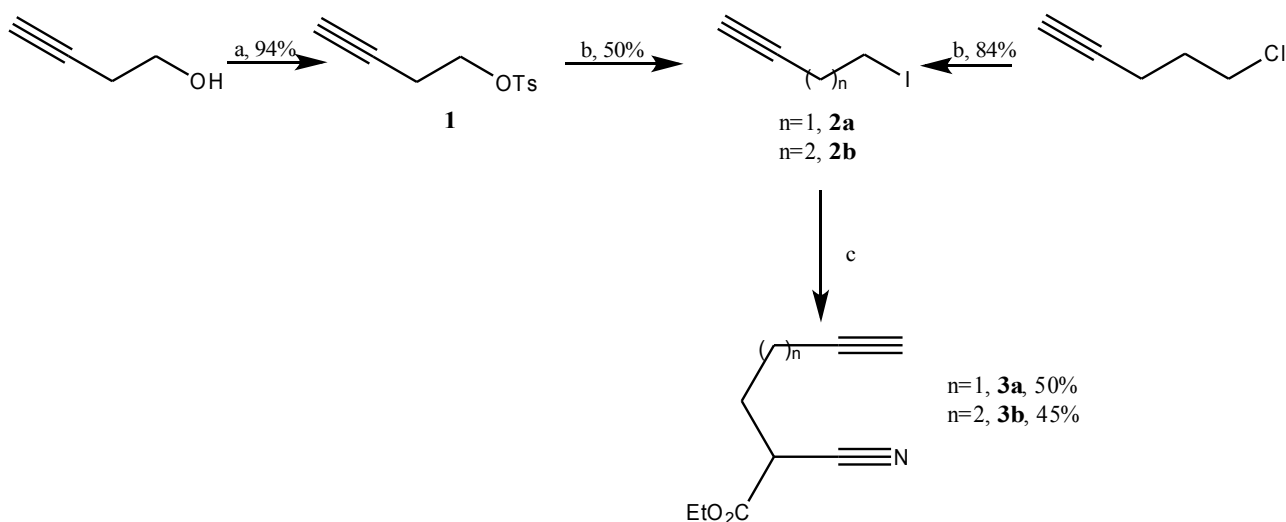


Fig 3.1: The synthetic route to the alkynenitriles **3**. (a) *p*-Toluenesulfonyl chloride, DMAP, NEt_3 ^[47] (b) NaI, acetone^[48] (c) NaH, ethyl cyanoacetate.^[49]

Firstly, the commercial starting materials but-3-yn-1-ol and 5-chloropent-1-yne were converted to better alkylation partners by substitution reactions on the alcohol or the chloride, respectively. 4-Iodo butyne, **2a**, was obtained via the tosylated alkyne **1**,^[47] and then a Finkelstein reaction.^[48a] 5-Iodo butyne, **2b**, was obtained by a Finkelstein reaction on 5-chloropent-1-yne.^[48b] Alkylation of ethyl cyanoacetate with **2a** and **2b** yielded **3a** and **3b**, respectively.^[49]

Tosylation was conducted in good yield and the product was used without any further purification. Initially, the direct alkylation of ethyl cyanoacetate with the tosylate was attempted. This did not give any of the desired alkynenitriles **3**, so focus was shifted towards the iodide. The transformation from tosylate to iodide was conducted in a relatively straight forward fashion with the Finkelstein reaction. This is a S_N2 reaction where one exploits the fact that sodium tosylate is insoluble in acetone, whereas sodium iodide dissolves readily.^[50] This will drive the reaction towards the iodated product, as shown in figure 3.2

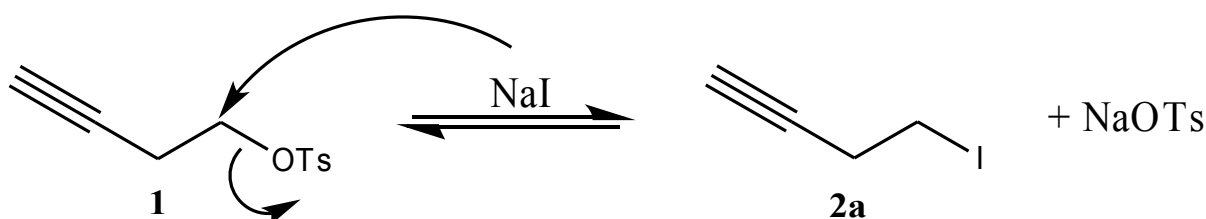


Figure 3.2: Mechanism for the Finkelstein reaction with the tosylate **1**.

Lower yields in the Finkelstein reaction towards **2a** than **2b** may be ascribed to the loss of product on the rotavapor, due to lower boiling point of the former. The direct iodation of but-3-yn-1-ol was also tried,^[51] but due to more tedious workup and purification, tosylation and Finkelstein reaction was the method of choice.

In the alkylation reactions, 2.1 equivalents of ethyl cyanoacetate and 2 equivalents of NaH was used. Here, fewer equivalents of NaH are to ensure that ethyl cyanoacetate will not be doubly deprotonated. Although both deprotonation and the addition of the electrophilic iodide was performed at 0 °C, amounts up to 40% of the dialkylated byproduct **3a'** were obtained (see appendix V for NMR and MS spectra). The reported literature value for these alkylations are 54 and 49%, for **3a** and **3b** respectively,^[49] so the reported values in figure 3.1 are in resemblance with earlier results. This is however somewhat lower than what can be expected in alkylation reactions in general, and can be due to the fact that ethyl cyanoacetate is doubly activated to deprotonation by two electron withdrawing groups that stabilizes the formed anion, as depicted in figure 3.3.

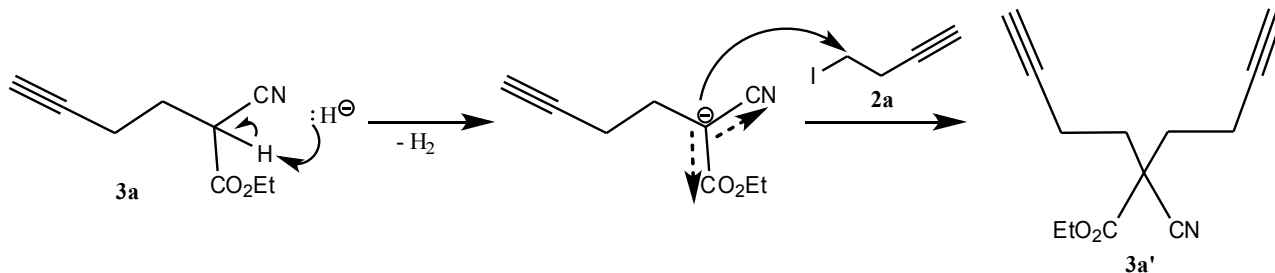


Figure 3.3: Ethyl cyanoacetate is activated to deprotonation by two activating groups, stabilizing a potential anion that can attack another molecule of **2a**.

This formed anion can then attack another molecule of **2a**, forming the dialkylated side-product **3a'**. Therefore is dialkylation more probable with this compound than for compounds with only one activating group.

Another challenge with this reaction was the purification. The product **3a** has similar chromatographic properties as the byproduct **3a'**, and similar boiling point as ethyl cyanoacetate. Therefore, distillation with subsequent column chromatography were performed to achieve a pure product. For **3b**, the difference in boiling points are large enough so that distillation was sufficient.

3.2 Cyclotrimerization

The next step in the synthesis of **I** was the cyclotrimerization of the alkyne nitriles **3** with alkynes to form **4** (figure 1.3). Several catalytic systems were tried to achieve the desired reactions. The general reaction is shown in figure 3.4. From the literature, the most similar reactions done earlier are the work of Vollhardt et al.^[38] and Louie et al.^[39] as discussed in chapter 2.3.2. Due to the similarities, these strategies were also tried for our system.

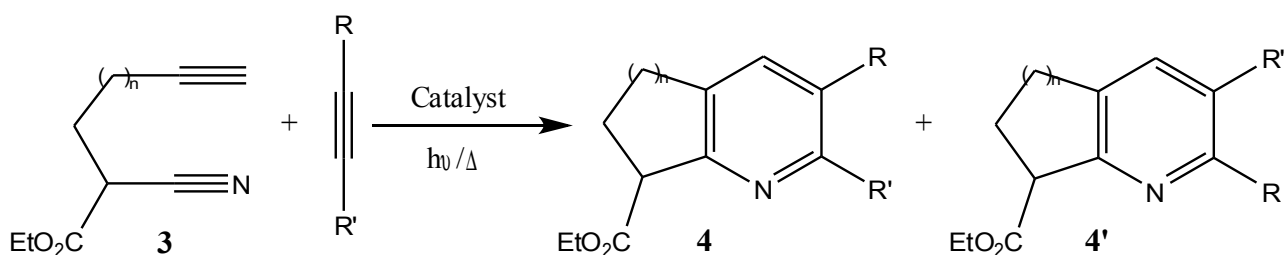


Figure 3.4: General scheme for the cyclotrimerizations.

The alkyne cyclization partners were chosen to be mono- or disubstituted phenyl or SiMe₃ alkynes. In addition to being of interest as ligands in a iridium catalyst, they also possess somewhat different electronic and steric properties, so that different outcomes in the cyclotrimerization reactions might be expected. In the following, the results are presented according to the catalyst employed.

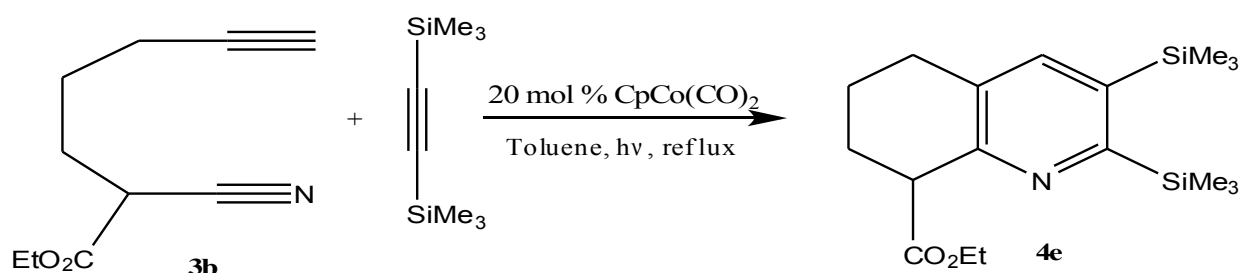
3.2.1 CpCo(CO)₂

The commercial dicarbonylcyclopentadienyl cobalt(I), CpCo(CO)₂, is a catalyst that is widely used in many cyclotrimerization reactions.^[28] Therefore, it was desirable to test it on the substrates in figure 3.4, and it turned out to produce the wanted cyclization products in poor to moderate yields under photoinduced conditions. Irradiation was performed with visible light from a conventional hardware store lamp (400 W, 118 mm, 50 Hz). In the following, the way through several reaction methods and conditions to the optimized system will be presented and discussed.

Bis(trimethylsilyl)acetylene (BTMSA) was selected as the initial cyclization partner as it is, as mentioned, reported by Vollhardt et al. to cyclize in good yield (77%, table 2.1) to their

alkynenitrile.^[38] It was also expected that any possible steric effects would be less than for the corresponding diphenyl substituted acetylene. We also wanted to initially test the system with out any regioselectivity problems, so mono-substituted alkynes were avoided in this initial phase. **3b** was chosen as the alkynenitrile. Firstly, a one-pot procedure was attempted. Table 3.1 summarizes the results from this initial process with $\text{CpCo}(\text{CO})_2$.

Table 3.1: Initial reactions with $\text{CpCo}(\text{CO})_2$, comparing one-pot, slow addition techniques, and amounts of toluene applied.



Entry	Procedure	Amount of toluene (mL)	Equivalents of BTMSA	Yield (%)
1	One-pot, 13.5 h.	5	1	traces
2	Slow addition of 3b , BTMSA and $\text{CpCo}(\text{CO})_2$ to toluene over 5 h. Flow 0.7 mL/h.	90	1	7
3	Slow addition of 3b and $\text{CpCo}(\text{CO})_2$ to BTMSA in toluene over 6h. Flow 0,5 mL/h	22	5.7	17
4	Slow addition of 3b and $\text{CpCo}(\text{CO})_2$ to BTMSA in toluene over 6h. Flow 0,5 mL/h	3.5	5.5	20

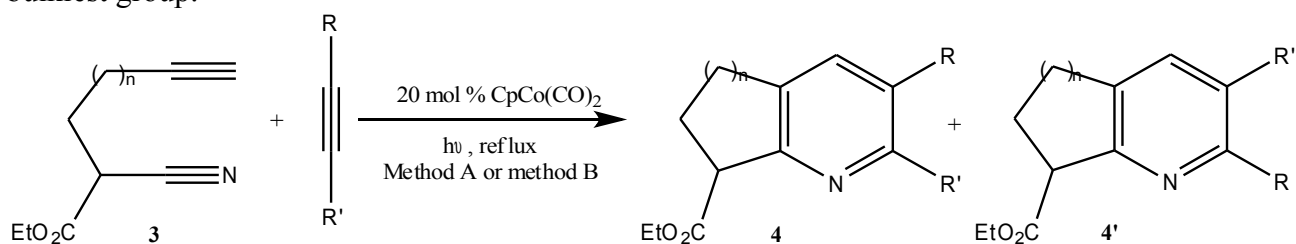
^a- Slow addition reactions were irradiated for 1.5 h after the addition was complete.

The one-pot procedure only produced trace amounts of **4e** (entry 1). Several articles on cyclotrimerization employs as mentioned high dilution and/or slow addition techniques, and this were therefore tested for this system as well. Firstly by addition of **3b**, BTMSA and $\text{CpCo}(\text{CO})_2$ to toluene (entry 2), then of **3b** and $\text{CpCo}(\text{CO})_2$ to BTMSA in toluene (entries 3 and 4). Total conversion of **3b** was observed by ^1H NMR as long as irradiation was continued for 1.5 h after the

addition was complete. Slow addition was according to table 3.1 better than the one-pot procedure, although only very poor yields were obtained initially. It was observed however, that more equivalents of BTMSA did increase the yields in the reactions (entry 3) and that reduction of the amount of toluene further improved the yield (entry 4), but only up to 20%. Further improvements were not achieved with this system, and other alkynes and ring sizes were therefore tested in this reaction setup to see how other cyclization partners would affect the outcome. The results are presented in table 3.2, entries 1-8, referred to as **method A**.

Still faced with poor yields, further optimization was wanted. Cyclotrimerization is an entropically unfavorable process, due to the coupling of three double bonds in one step, which leads to increased order in the system.^[8b] It is known that increased pressure can lead to better yields in such situations, as a consequence of Le Châteliers principle; an increase in the total pressure in a system will drive the equilibrium towards the side with fewer reactants/products.^[52] This will also apply here, and product formation will be favored. The cyclotrimerizations were therefore also conducted in a one-pot procedure in a pressure vial, and the yields with this method are also reported in table 3.2, entries 9-16, referred to as **method B**.

Table 3.2: Obtained yields for cobalt catalyzed cyclotrimerizations with varying size of alkyne nitrile and type of cyclization partner, conducted with method A and method B. R' is the bulkiest group.



Entry	n	R	R'	Yield (%)	Ratio 4:4' ^g
1, 4a ^a	1	SiMe ₃	SiMe ₃	20	-
2, 4b ^a	1	H	SiMe ₃	16	1:0
3, 4c ^a	1	Ph	Ph	37	-
4, 4d ^a	1	H	Ph	12 ^e	1:0
5, 4e ^a	2	SiMe ₃	SiMe ₃	17	-
6, 4f ^a	2	H	SiMe ₃	0	1:0
7, 4g ^a	2	Ph	Ph	32	-
8, 4h ^a	2	H	Ph	- ^d	1:0
9, 4a ^b	1	SiMe ₃	SiMe ₃	17	-
10, 4b ^b	1	H	SiMe ₃	20	1:0
11, 4c ^b	1	Ph	Ph	48	-
12, 4d ^b	1	H	Ph	28 ^e	1:0
13, 4e ^b	2	SiMe ₃	SiMe ₃	11 ^f	-
14, 4f ^b	2	H	SiMe ₃	22 ^e	1:0
15, 4g ^b	2	Ph	Ph	46	-
16, 4h ^b	2	H	Ph	20 ^e	1:0

^a- Method A: Slow addition of **3** and CpCo(CO)₂ in toluene (2 mL) to the alkyne in toluene (2 mL) over approximately 6h. Flow 0,5 mL/h.

^b- Method B: One-pot in a pressure vial, 5 h.

^c- Performed with 0.2 g of **3** and 3 eq. of the alkyne. (Entries 10 and 11 are 1 g scale).

^d- Not conducted.

^e- Not pure according to ¹H NMR analysis.

^f- With stoichiometric amount of CpCo(CO)₂.

^g- The other isomers were not observed in ¹H NMR; see further discussion below.

The wanted products were obtained in yields ranging from 17 to 46%, and quantitative conversion was observed by ^1H NMR analysis after chromatography. For disubstituted alkynes, better yields were observed when $\text{R}=\text{Ph}$ than $\text{R}=\text{SiMe}_3$ (entries 3, 7, 11 and 15 vs entries 1, 5, 9 and 13). When BTMSA was used, solids that were poorly soluble had to be filtered off before purification. Complete analysis of this side product was not conducted, but it may be ascribed to the cyclobutadiene complex **E** in figure 2.10, as BTMSA is as discussed known to form such complexes.^[32] Low yields in these reactions supports this theory as **E** is a cause to depletion of the catalyst. Diphenylacetylene however, was the most successful of the alkynes tested. When applying phenyl acetylene, lower yields were obtained, and this may be ascribed to competing self-trimerizations of the alkyne.^[38] Somewhat higher yields were obtained for the fused 5-rings than for the fused 6-rings (e.g entry 3 vs entry 7). Also structure elucidation were easier for the 5-rings.

Comparing the two methods in table 3.2, method B produced in general the wanted structures in the same or better yields than method A. Especially the reactions where alkynes with phenyl substituents were employed did benefit from this method (e.g entry 3 vs entry 11). Somewhat poorer yields were obtained with BTMSA in the pressure vial (entry 1 vs 9). Here it was observed that the reaction vial became very dark on the inside, and again the same poorly soluble side product was formed. As an extra benefit, method B did not yield any of another bothersome precipitation observed with the slow addition method. This precipitate, presumably cobalt itself, became visible on standing after purification on column. It tended to make NMR analysis difficult, and several filtrations were required to acquire good spectra after method A.

Some of the reactions in table 3.2 have similarities to the ones conducted by Vollhardt et al.^[38] where they studied the cyclization of alkyne nitriles without any ester group or any other functionality as shown in table 2.1. They used a slow addition and high dilution technique, and their yields are in general somewhat higher than those reported in table 3.2. This is especially true for cyclizations with BTMSA. Vollhardt et al. achieved a yield of 77% for both $n=1$ and $n=2$, whereas in this study a yield of only round 20% was obtained. Cyclizations with BTMSA were as mentioned also the only reaction that did not benefit of method B over method A, and for this case it seems like further optimization of method A could have been advantageous. High-dilution conditions and large excess of BTMSA could have been further tested. For SiMe_3 -ethylene (entry 14) relatively similar yields as reported by Vollhardt et al. was achieved (22 vs 29%). When diphenylacetylene was used (entry 15)

a much better yield than earlier reported was obtained; 46 vs 4%. Here, both method A and B did produce moderate yields of **4c** and **4g**. Catalyst depletion by cyclobutadiene formation as described by Vollhardt was apparently not occurring, at least not to such great extent. Vollhardt et al. also tested other alkynes than the ones used in table 3.2, and in general one can say that they obtained all over higher yields for the most cases. Lower yields in the reactions in this study may be due to the presence of the electron withdrawing ethyl ester group. Such effects were discussed in the theory in chapter 2.3, and these findings supports earlier work.^[35, 41] However, for some experiments the difference in yields are not big, and for diphenylacetylene much better yield was obtained in this study. Comparing literature on cyclizations as the one in this study with e.g. diene and nitriles it is clear that much higher chemoselectivity, and hence yields, are obtained in the latter. In general, cyclizations with alkyne nitriles are more difficult than with diynes,^[53] and this study confirms that trend in the literature.

Two possible regioisomers are possible in the reactions in table 3.2 with mono-substituted alkynes; **4** and **4'**. As discussed in chapter 2.3.2, the regioselectivity can be controlled by applying the right unsymmetrical alkynes, i.e. if the substituents differ greatly in size. This is the case for ethynyl-SiMe₃, and 1:0 regioselectivity was observed with this alkyne by Vollhardt et al.^[38] They did not test phenyl acetylene in their cyclizations, but as the phenyl group is sterically bigger than the SiMe₃ group, this alkyne should possess the same regioselectivity. In addition to give interesting substituents for the ligands in **I** (fig. 1.2), ethynyl-SiMe₃ turned out to be very useful in the determination of the regioselectivity of the reactions in table 3.2. In mono-SiMe₃ substituted **4**, the aromatic area of the ¹H NMR spectra will only contain the pyridine protons, which makes the interpretation more easy (see chapter 5.2 and 5.6, and appendix G and K for full spectra). Here, two clear doublets were observed, which corresponds to the 2-substituted isomer. In a 3-substituted isomer, two singlets would be expected, where the singlet corresponding to the proton in 2-position would possess a high ppm value, probably around 8.2 when comparing to 2,3,5-trimethyl pyridine in figure 3.5 a). For all the analyzed fractions from the reactions, no $\delta > 8.0$ were observed within the sensitivity of the NMR instrument, and it can be concluded that only the 2-substituted product was obtained. For **4f**, a impurity at δ 7.3 (s) is apparent, and several purifications did not remove it. But still no $\delta > 8.0$ was observed, so this do not correspond to **4f'**.

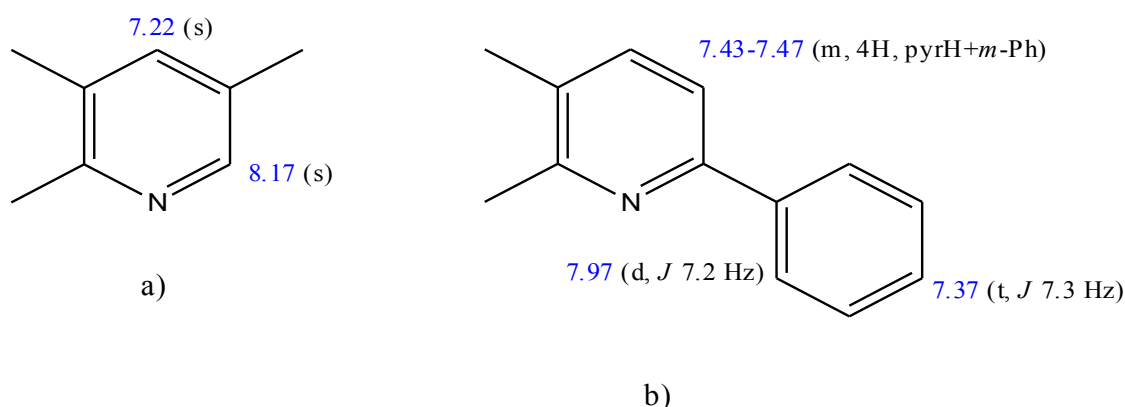


Figure 3.5: $^1\text{H-NMR}$ shifts of a) 2,3,5-trimethyl pyridine^[54] and b) 2,3-dimethylphenyl-6-phenyl pyridine.^[55]

The same reasoning applies to the phenyl substituted structures, and in figure 3.5 b) the proton shifts for 2,3-dimethylphenyl-6-phenyl pyridine can be seen. A doublet at δ 7.97 is observed for the *o*-Ph protons in this structure, which matches the observed values for **4d** and **4e** (see chapter 5.4 and 5.8 and appendix I and M). In addition, two doublets with $J = 8.05$ Hz and $J = 8.2$ Hz, were observed for **4d** and **4e**, respectively. These compounds were somewhat harder to purify than their SiMe_3 -substituted analogs **4b** and **4f**, but based on the above mentioned observations, and comparison with **4b** and **4f**, a conclusion of a 1:0 ratio of regioisomers seems justifiable also here. These observations are in agreement with earlier reported results, and with the mechanistic reasoning for the regioselectivity presented in chapter 2.3.2.^[38]

Both for method A and method B, the reactions produced quite “messy” columns, and in some cases it turned out difficult to achieve entirely pure compounds (entries 4, 12, 14 and 16). The complex crude products can probably be ascribed to low chemoselectivity in the system, as many different cyclization product can be produced besides **4**. However, when going from method A to method B, it was observed *empirically*, that higher chemoselectivity were obtained. A cleaner TLC of the crude and fewer fractions off the column underpins this observation. Apparently, when method B is employed, more of different cyclotrimerization products are produced, and lower degree of e.g. polymerization of alkyne nitriles is occurring, which is earlier reported as a way that start materials can be consumed in cyclotrimerization reactions.^[33] Some of the side-products from the reactions were further investigated. A thorough structure determination of all were not conducted, but two *m/z* values corresponding to expected side-products as described in figure 2.12 were observed in MS, and partly described by NMR. Figure 3.6 shows the assumed structures.

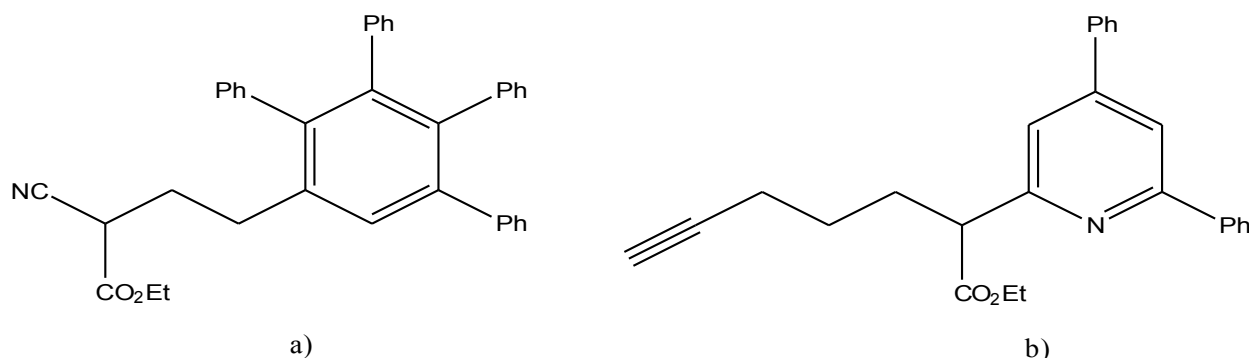


Figure 3.6: Assumed structures of two side-products observed in MS. a) From reaction of **3a** and diphenylacetylene and b) from reaction of **3b** and phenylacetylene. See appendix W and X, respectively, for HRMS and ¹H NMR spectra.

The connectivity in the structures have not been fully determined. From ¹H NMR of the structure to the left, it is seen that there are no signals above δ 7.5, and the methine proton of **3a** is lacking, so it is reasonable to assume a pure carbocycle. The structure to the right shows some signals around δ 8.0, which may correspond to a pyridine ring system. However, it should be noted that 2D-NMR were not conducted. Such side-products will consume alkyne nitrile in the reactions, and can partly explain the moderate yields in the cyclotrimerization reactions. It is also a good example of the chemoselectivity problems in such reactions. In this case the structures in figure 3.6 a) and b) consumed 10 and 14% of the alkyne nitrile, respectively.

Since relatively low and similar yields were obtained over several parallels for many of the entries in table 3.2, the reaction system was also tried with a stoichiometric amount of catalyst. The fact that the yield for many of the entries are around the amount of catalyst used, can imply that the reaction is Co-mediated and not Co-catalyzed, and this further motivates the testing of a higher amount of CpCo(CO)₂. Entry 13 in table 3.2 represents such an experiment, and shows that the obtained yield was not enhanced from higher catalyst loading. This, together with that other entries show higher yields than the applied amount of catalyst (entries 3, 11 and 15), suggest that the reactions are not directly catalyst mediated. However, a thorough investigation of this hypothesis with other alkynes and/or catalyst loadings were not conducted.

During this work, compounds **4d** and **4h** have been synthesized by other means by Anderssons

group, and their efficiency as ligands in iridium catalyzed asymmetric hydrogenation have been tested.^[7] Their initial results shows that the ligands having a fused 5-ring (**4d**) yields the greatest ee compared to the 6-rings (**4h**). Based on this, it became of great interest to analyze **4a-4c** as ligands in hydrogenations. Greater amounts of these structures were wanted and scale-up was performed with method B, and the results are reported in table 3.3.

Table 3.3: Results from the up scaling process of **4a-c**, with scale and yields from reactions according to method B.

Wanted product	Parallel	Scale (g)	Yield (%)
4a	I	0.98	3 ^a
	II	0.91	17
	III	1.75	2 ^a
4b	I	2.04	20
	II	2.06	28
4c	I	0.90	53

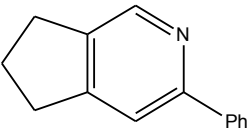
^a - Cobalt precipitate was observed.

Except from parallel I and III for **4a**, yields comparable to table 3.2 were observed. For both **4b** and **4c** the same or higher yields than reported in table 3.2 were observed, while **4a** did not facilitate from the up scaling conditions. It confirms the observations presented earlier that BTMSA was somewhat troublesome under the reaction conditions.

3.2.2 Other catalytic systems tested

In parallel with the initial screening of reaction conditions for the $\text{CpCo}(\text{CO})_2$ catalyst reported in table 3.1, other catalytic systems were tested as well. Because of the known ability of $\text{CpCo}(\text{COD})$ to be able to produce pyridines,^[56] it was tested in the process in figure 3.4. This was done both under heating with an oil bath and under irradiation (entries 1 and 2 in table 3.4). Under these conditions, no conversion of the alkynenitrile was observed. However, full conversion was observed when a pressure vial under irradiation was applied (entry 4).

Table 3.4: Tested catalytic systems under various reactions conditions.

Entry	Catalyst	Conditions	Wanted product	Conversion (%) ^b	Yield (%) ^b
1	$\text{CpCo}(\text{COD})$	Heat, 10% cat. 27 h	4c	0	-
2	$\text{CpCo}(\text{COD})$	Irradiation, 10% cat. 11 h	4c	0	-
3	$\text{CpCo}(\text{COD})$	Irradiation, 10% cat. 22 h.		100	0 ^c
4	$\text{CpCo}(\text{COD})$	Irradiation in pressure vial, 10% cat. 5 h	4g	100	0
5	$\text{Cp}^*\text{Ru}(\text{cod})\text{Cl}$	2% cat., DCM. 19 h	4g	0	-
6	$\text{Cp}^*\text{Ru}(\text{cod})\text{Cl}$	4% cat., DCE. 70 h	4c	0	-

^a - All reaction are one-pot.

^b - Analyzed by ^1H NMR analysis of the crude.

^c - No singlet at δ 8,51 in ^1H NMR was observed. ^[57]

This observation confirms that pressure is an advantage to achieve cyclotrimerizations, but still no product was observed, only unidentified side-products. Entry 3 shows a test reaction with benzonitrile and 1,6-heptadiyne that was conducted to see whether the $\text{CpCo}(\text{COD})$ was active as a catalyst, or had been destroyed on standing. This reaction proceeded with quantitative conversion under atmospheric pressure, however only unidentified side-products and no product were

observed. This indicates that the substrates employed here, reacts more easily than **3** under these reaction conditions. Although it did not give the wanted product, it is reasonable to conclude that it in some way coordinate with the catalyst, in contrast to **3**. CpCo(COD) had been prepared earlier from Co(acac)₂ in accordance with the literature procedure.^[58]

Cp*Ru(cod)Cl is a catalyst that are reported to give good yields in cyclotrimerizations of electron-poor nitriles.^[59] Due to the presence of the ethyl ester group in the alkynenitriles **3**, it was tested in the reactions towards **4**. Yamamoto et al.^[59] applied it with success to cyclotrimerizations of a wide range of diynes and nitriles, but it has not been used in reactions between alkynenitriles and alkynes. As can be seen in entries 5 and 6 in table 3.4, no conversion of the alkynenitrile were observed in the solvents DCM and DCE. As discussed in chapter 2.3.3 and exemplified in figure 2.18, a change in the connectivity of the triple bonds can heavily effect the outcome of the reactions. Pressurized conditions were not tested here.

Stimulated by the good results by Louie et al.^[39] for the reactions presented in table 2.1, iron was also tested as a catalyst. Figure 3.7 shows the general scheme with reaction conditions.

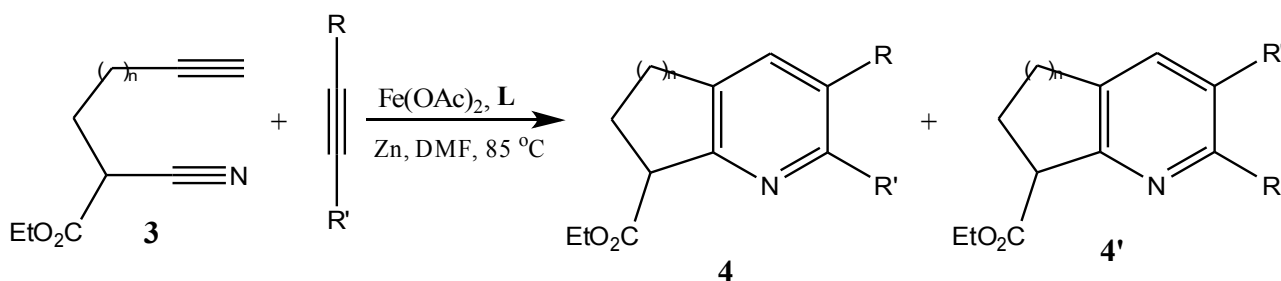


Figure 3.7 Reaction conditions in the iron-catalyzed reactions.

Here the pre-catalyst is Fe(OAc)₂ and this is reduced by zinc into the catalytic active species that can coordinate the ligand **L**. This ligand must be synthesized, and this was done as shown in figure 3.8. The procedure followed was adapted from Louie et al.^[39]

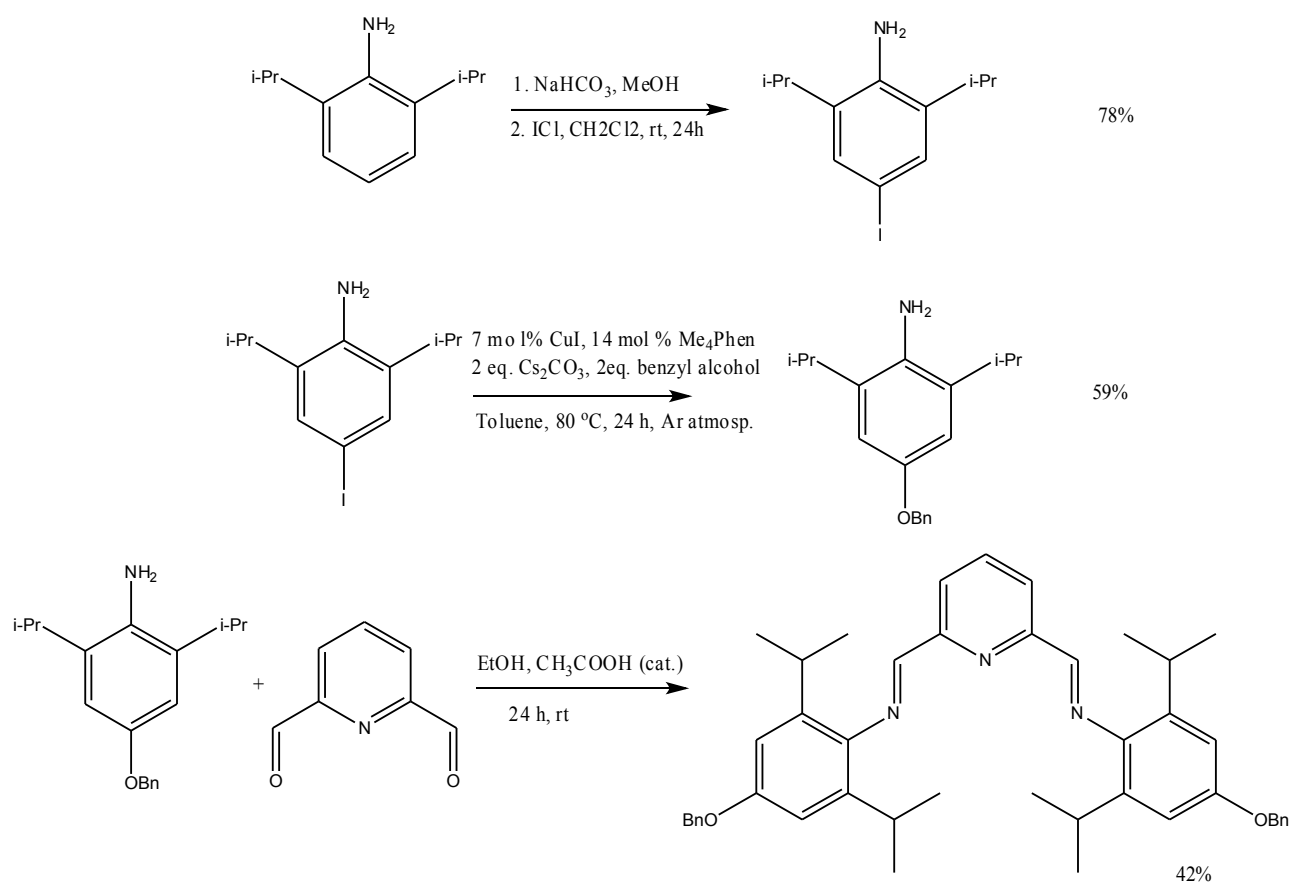
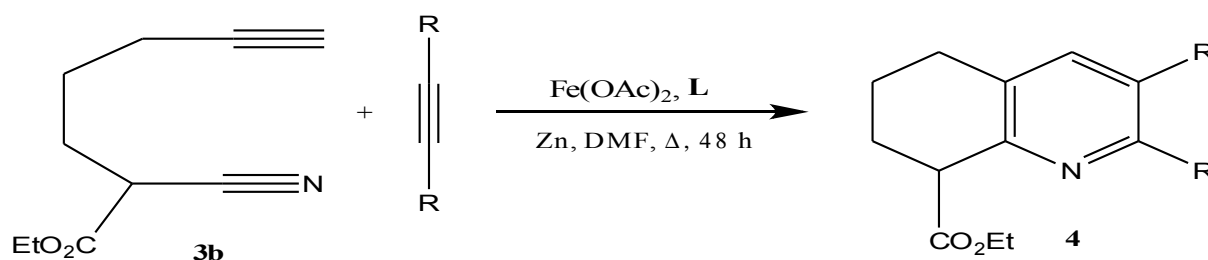


Figure 3.8: Synthesis of **L**, with reaction conditions and yields.^[39]

The synthesis of **L** starts by introducing iodine in *para* position, which can further be transformed in a Cu-catalyzed coupling reaction with benzyl alcohol. The last step in the formation of the bis-imine is a nucleophilic attack by the aniline nitrogen on the pyridine aldehyde.

With the wanted ligand in hand, the catalytic system was tested for the cyclotrimerization shown in figure 3.7. Table 3.5 gives an outline of the tested reactions.

Table 3.5: Tested iron catalytic systems.

Entry	Alkyne	Reaction conditions	Conversion (%)	Yield (%) ^a
1	BTMSA	18% Fe(OAc) ₂ , 45% Zn, 14% L. 1 eq. alkyne. 85 °C .	0	-
2	Diphenylacetylene	9% Fe(OAc) ₂ , 72% Zn, 11% L. 2 eq. alkyne. 85-100 °C.	0	-

^a – Only starting materials and **L** were observed in ¹H NMR during purification.

Both entries in table 3.5 shows that no conversion were observed. Comparing the alkyne nitriles **3** with the substrates employed in the earlier reported study (table 2.1), the biggest difference is that **3** does not have any benefit from the Thorpe-Ingold effect. In addition, no substituents on the alkyne end of **3** is present, as was seen to be advantageous in table 2.1. Pressurized conditions should had been tested here to fully test the catalytic system.

Although tethered systems reduce the number of possible regioisomers, problems with chemoselectivity in catalytic systems may still arise. To what degree the three catalysts in table 3.4 and 3.5 will produce the wanted product or some byproducts, depends on the ability of the various triple bonds to take part in the catalytic cycle in the right place. As mentioned earlier, the nitrile group is considered to be more reactive than the alkyne group,^[28] hence the synthesis of pyridines is a good reaction. Although, in this case the nitrile group is somewhat electron deficient, due to the ethyl ester group in the β-position. This is thought to give lower yield of pyridines and fused pyridines, and is reported in several articles.^[41-42] In addition, alkyne nitriles are not considered to be the best substrates for cyclotrimerization.^[53] Sensitivity in a catalytic system may also affect the outcome of the reactions, as described in figure 2.18. The lack of reactivity of **3** observed with CpCo(COD), Cp*Rh(cod)Cl and Fe(OAc)₂ may be explained due to these factors.

3.3 Resolution of enantiomers

Ligands in a chiral hydrogenation catalyst must be enantiomeric pure to exercise its role satisfactorily. Hence, this had to be achieved with **4a-4c** before they could be used as ligands. From a racemic mixture, pure enantiomers can be obtained by, among other techniques, chiral preparative HPLC or separation by conventional chromatography after forming the corresponding diastereomers. The separation of the enantiomers in a similar system to the structures **4a-4h** is described by Pham et al.^[60] (**5** with $n=2$ and $R=R'=H$) by the latter strategy. Here, diastereomers are constructed from a racemic mixture of an alcohol by reaction with (*S*)-camphoric chloride. This mixture may then be separated by column chromatography, since diastereomers exhibit different physical properties,^[10] in contrast to enantiomers. As an alternative to preparative chiral HPLC, this method was tested for **4b** and **4c**. The strategy is presented in figure 3.9, together with the yields of the reductions and reactions with (*S*)-camphoric chloride.

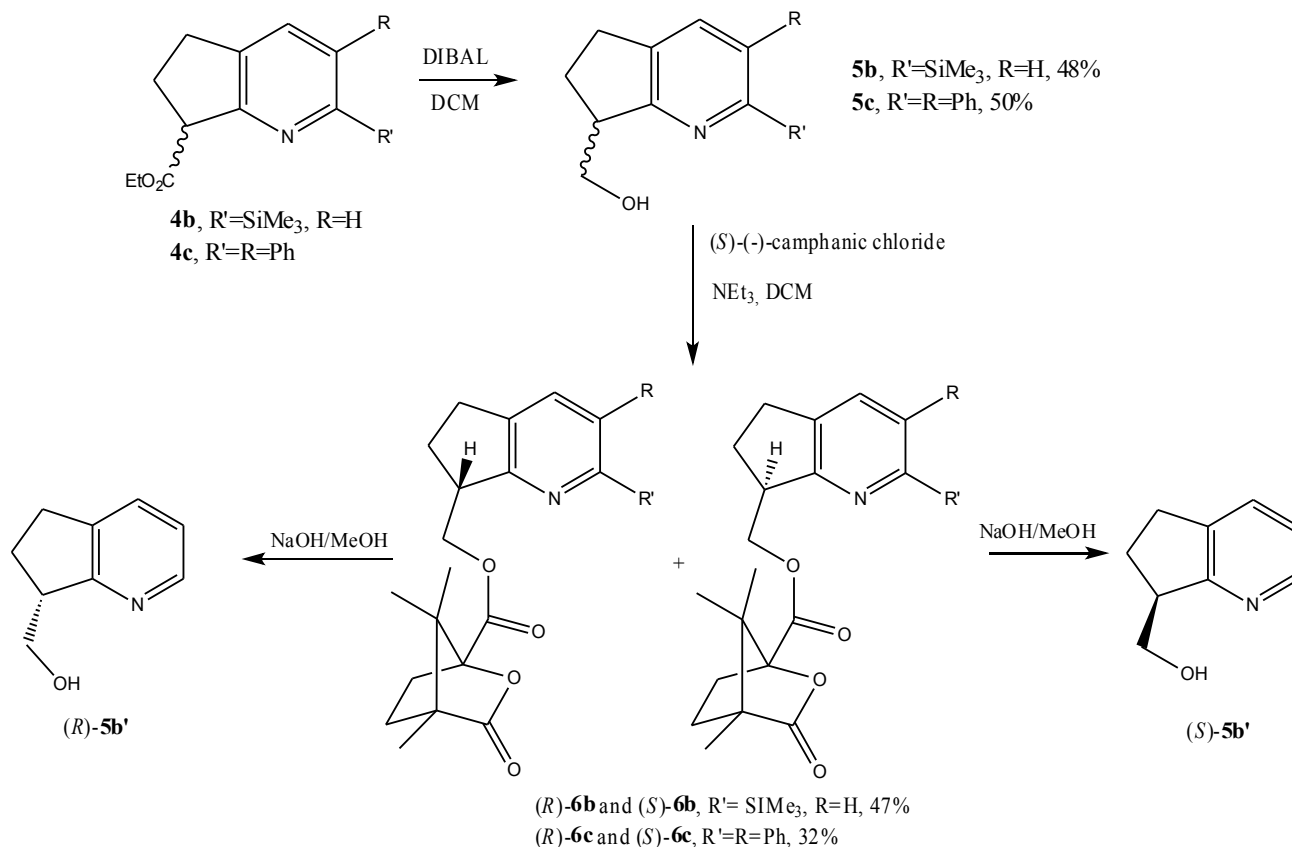


Figure 3.9: Separation of the enantiomers of **4b** and **4c**, via their camphoric esters, and then hydrolysis.

Firstly, the ester functionality is reduced by DIBAL to the alcohols **5b** and **5c**. DIBAL was chosen as reducing agent, as it is considered a more sensitive reagent,^[61] and to harsh conditions were not wanted due to the potential cleavage of the SiMe₃-groups. By this reduction, the electrophilic ester is converted into a nucleophilic alcohol, which can be reacted with (*S*)-camphonic chloride, creating the diastereomeric mixtures of **6b** and **6c**. This reaction mixture can then, hopefully, be separated by some conventional chromatographic technique.

As can be seen in figure 3.9, only around 50% yield in the reductions were obtained, and this is lower than what can be expected. During the course of this work, analysis by analytical TLC showed the appearance of several unwanted spots. This could indicate decomposition, and this was also apparent by NMR analysis. The relatively low yield in the reductions towards the alcohols **5b** and **5c** can therefore partly be explained by unpure starting esters **4b** and **4c**.

In the reaction of the alcohol **5c** with camphonic chloride, only 45% conversion was achieved, resulting in low yield (32%). Higher conversion was expected, and in the subsequent reaction of the alcohol **5b**, DMAP was added to ensure better turnover. This was effective, and full conversion of **5b** was observed, yielding **6b** in 47% yield. The diastereomers were achieved as an equimolar mixture (from ¹H NMR analysis), and the given yields are for the sum of both diastereomers. DMAP is commonly used in acylations of alcohols to ensure a high degree of conversion. The reason for this effect is due to the formation of an acyl pyridinium ion, as shown in figure 3.10.^[61]

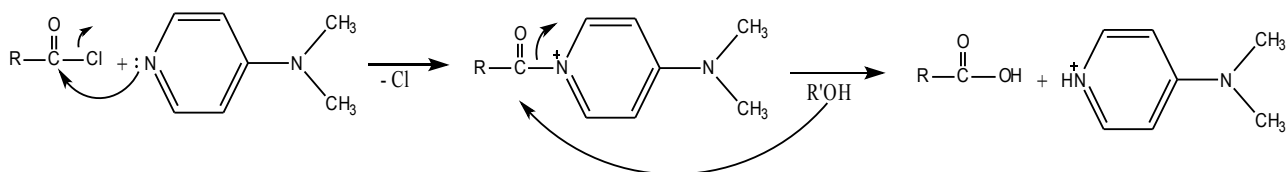


Figure 3.10: The catalytic action of DMAP in acylations of alcohols.

DMAP is a better nucleophile than neutral alcohols, so that the acid chloride will therefore initially be attacked by DMAP and not the alcohol. This will make a better leaving group than the chloride, so that the alcohol now will attack the carbonyl carbon more easily. The net effect will be higher reaction rates and successful acylation of most alcohols, even in catalytic amounts of DMAP.

The diastereomers (*R*)-**6c** and (*S*)-**6c** appeared as two closely located spots on analytical TLC, which were attempted separated on a flash column and VersaFlash. Several eluent systems were

tested, and the most promising one was hexane:Et₂O:EtOH (10:1:1), the one also used by Pham et al.^[60] Total separation was not achieved with column chromatography, only yielding both almost pure diastereomers and a intermediate mixture. However, it was observed that multiple elutions on analytical TLC gave increasing separation, which suggested that preparative TLC could be an appropriate method. This was tested, and yielded two closely placed bands, with an “less UV-active area” in between. Even carefully scraping off the silica, resulted in fractions contaminated by the other diastereomer. Since neither (*R*)-**6c** and (*S*)-**6c** were achieved in a pure form, optical rotation and further reaction by hydrolysis were not performed. However, the diastereomers were obtained sufficiently pure so that the structures could be elucidated by NMR. (See chapter 5.12, and appendix R and S for details).

To further test the strategy in figure 3.9, the separation was also attempted for (*R*)-**6b** and (*S*)-**6b**. It was anticipated that due to the change, and loss of one of the substituents, the chromatographic properties for this system would be different than for (*R*)-**6c** and (*S*)-**6c**. And encouragingly, this was observed on analytical TLC. Here the best eluent system, among many tested, was pentane:EtOAc (2:1) giving a *R_F*-difference of 0,06. Separation was tested on both flash column and preparative TLC, but also here total separation was not achieved. The best result was again observed with multiple elutions on preparative TLC, and the respective diastereomers were achieved pure in small amounts (by ¹H-NMR analysis), so that optical rotation could be measured, and hydrolysis performed. The separation ended with roughly the same amount of the (*S*), (*R*) and an intermediate racemic mixture (~8 mg). Figure 3.11 gives the rotational data for the diastereomers and the yields for the hydrolysis.

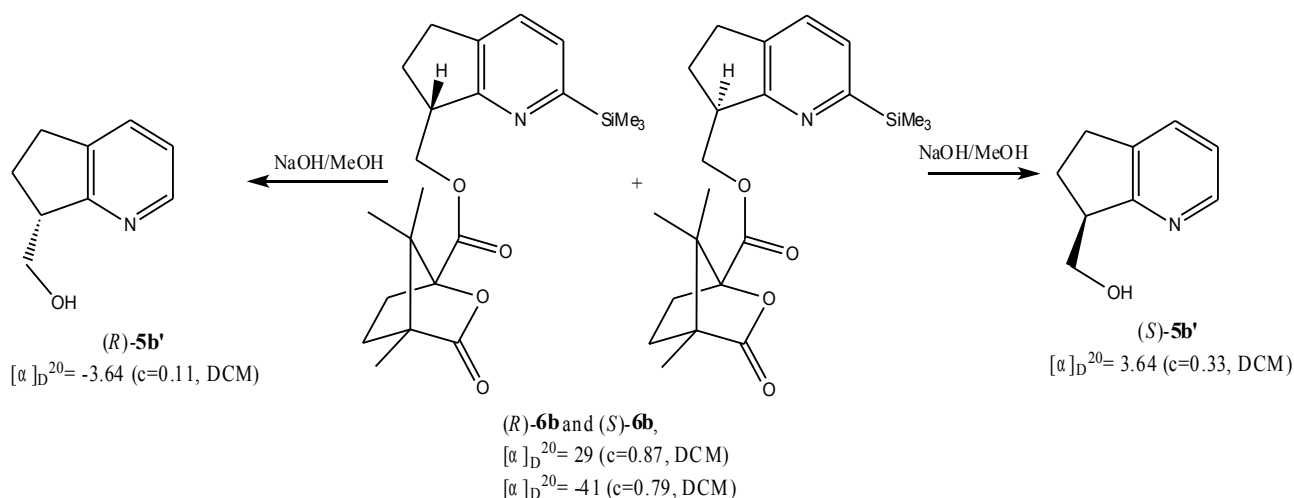


Figure 3.11: Attempted hydrolysis of **6b** to **5b**, yielding the disilylated **5b'**. Rotation of the diastereomers and **5b'** are given, but only arbitrary assigned to the structures.

As can be seen in the figure, complete desilylation was observed, giving **5b'**, with ¹H-NMR in agreement with literature data.^[57] Determination of the absolute stereochemistries were not conducted, so the rotation given are just arbitrary assigned to the structures. The observed rotation of the diastereomers showed resemblance with what was observed by Pham et al. for the similar system (+23 and -45). Hydrolysis of the camphanic ester occurred quantitatively for the one diastereomers and in only 37% for the other. This low yield in the latter case can only be explained by vulnerability to mechanical loss due to the low amounts of compound. In both cases, the SiMe₃-group was observed to be cleaved off. This indicates that such structures are susceptible to desilylation, which is also observed in similar systems even during purification on silica gel.^[62] An alternative method to remove the camphanic ester could have been the use of reducing agents, e.g. DIBAL which was used in the reduction of **4b**, and where the SiMe₃ group apparently survived. The similar absolute value for the rotation of the alcohols confirmed that pure enantiomers were obtained.

Since it appeared to be difficult to achieve the wanted enantiomers pure in a sufficiently high yield by this technique, separation was not tested for **4a** or in a larger scale for **4b** and **4c**. Reduction to the alcohols must be performed anyway in the synthesis of **I**, so the loss in this step must be included in the total strategy. In conclusion, due to the loss of compound in the formation of the diastereomers and hard separations in the strategy in figure 3.9, chiral preparative HPLC may be a better method to achieve the critical enantiomeric purity of the ligands.

3.4 Future work and other synthetic strategies.

Now as the pyridine framework of the ligands are in hand, also in gram scale for **4a-c**, their function in catalytic asymmetric hydrogenation must be evaluated. Firstly, the complete catalyst must be synthesized. This can be done by substitution from the alcohol to the iodide, and then reaction with the wanted phosphor group and iridium salt, described in the literature.^[6] As mentioned, **4d** has already been tested as a ligand, and the initial results shows both conversion and ee up to 99%.^[7] It is expected that **4a-c** can have a similar performance. Based on the results from the hydrogenations, the substitution pattern of **4** can be extended to see whether this can improve the ee's.

The cyclotrimerizations itself can be further studied, both regarding optimization of yields and reaction scope. From this study and other work,^[38] it is expected that other substitution patterns on the pyridine ring can be induced by cyclotrimerization, e.g. *tert*-butyl or ester groups. High yields with acetylene dicarboxylic esters have been observed,^[38] and it could be interesting to see if this also applies with our system.

Other alternatives for introducing substituents/groups that will not cyclotrimerize with **3** exist. An alternative can be cyclotrimerization with halogen alkynes, which can be further modified. With SiMe₃-substituted pyridines (e.g **4a**), desilylation and bromination can be accomplished.^[38] Such bromo-substituted structures can then be further reacted with other substituents or larger groups. Hence, cyclotrimerization can act as a part of a larger total synthesis.^[63] A second alternative can be cyclotrimerization with acetylene to construct the pyridine framework, and then alkylation with alkyl lithium reagents. This will probably occur in 2-position.^[64]

The iron-catalyzed reaction attempted in this study, seemed very promising from the results by Louie et al.^[39] However, no product formation was observed in the attempted reactions, and it would therefore be interesting to test this strategy further. Pressurized conditions and other alkynes would be a logical place to start.

Further investigations of the resolution of enantiomers can be possible. By systematically change the R-groups, other results can be achieved. Formation of other types of diastereomers by reaction with other chiral groups, can also be a possibility.



4 Conclusion

The goal of this thesis has been to synthesize new ligands for iridium catalysts as **I** for asymmetric hydrogenation. Based on previous work, these ligands are expected to give good enantiomeric excess, due to a rigid ring system together with sterically demanding substituents. Retro synthetic analysis showed that cyclotrimerization could be used as the key step, as this method is ideal for variation of substituents. Starting alkynenitriles **3a** and **3b** were synthesized in total yields of 24 and 38%, respectively, by literature procedures. The yields for the individual steps are shown in figure 4.1.

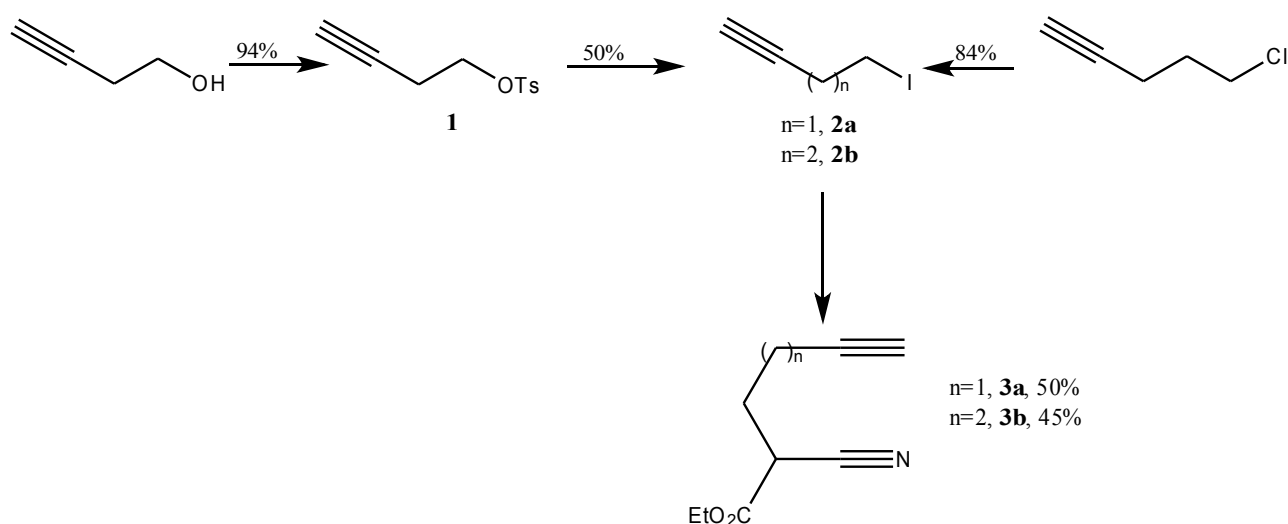


Figure 4.1: Synthesis of the alkynenitriles **3**.

Tosylation to **1** was conducted in excellent yield (94%), and the iodide **2a** was obtained by a Finkelstein reaction with **1** (50%). The iodide **2b** was also obtained by a Finkelstein reaction, now from the starting chloride (84%). Subsequently were the iodides **2** alkylated with ethyl cyanoacetate to **3a** and **3b** (50 and 45%, respectively). The yields in the alkylations is in correspondence to earlier reported results, and the relatively poor outcome can be explained by the formation of the dialkylated side-product, due to the very acidic α -protons of ethyl cyanoacetate.

Alkynenitriles **3a** and **3b** were used as starting materials for the cyclotrimerization reactions. The successful cyclotrimerization between **3** and phenyl or SiMe₃ substituted alkynes gave **4a-4h**, the main ligand framework, in poor to moderate yields (17 - 48 %), as shown in figure 4.2.

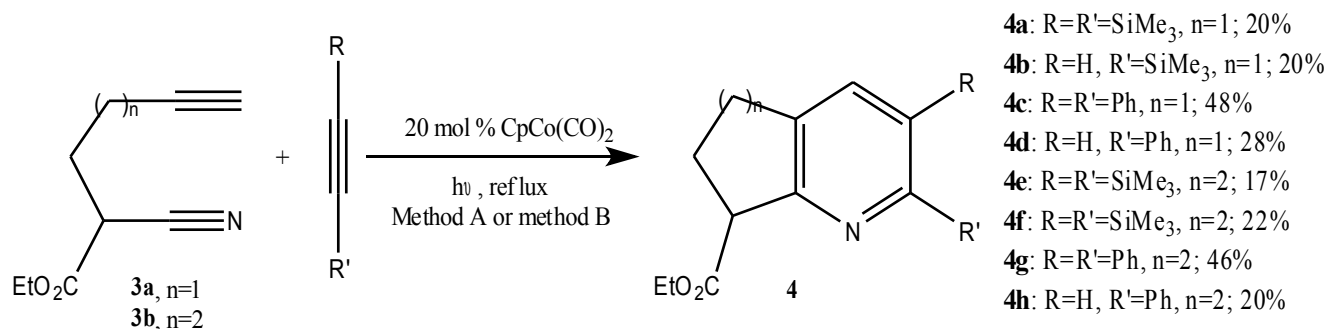


Figure 4.2: Synthesis of **4** by cyclotrimerization of **3** with various alkynes.

Two methods did give the wanted structure **4**; method A with a slow addition of alkyne nitrile and CpCo(CO)₂ to the alkyne, and method B applying a one-pot pressure vial. In most cases, method B proved to give the best yields. The pyridines **4a-4h** are all new compounds, and have been fully characterized. In comparison with similar reactions reported in the literature, the yields are acceptable, but somewhat lower, probably due to the electron withdrawing ester group nearby. Especially cyclizations of **3** with BTMSA did not give yields as expected, however this may be assigned to the formation of cobaltocycles leading to catalyst depletion, as indicated by previous research groups. Excellent regioselectivity in favor of the wanted 2-substituted pyridines were observed, and supports the existing mechanistic models for the reaction. The catalysts Fe(OAc)₂/ligand, CpCo(COD) and Cp*RuCl(COD) were also tested, but did not yield any product. Testing of **4d**, synthesized by other means, as ligand in hydrogenation reactions by prof. Andersson in Stockholm, suggested that the five-membered ring performed best in hydrogenation reactions. Therefore, upscaling of **4a-4c** were performed, without affecting the outcome of the reactions.

Chiral purity of the pyridine ligands are important, and separation of pure enantiomers from the racemic mixtures of **4b** and **4c** were attempted as shown in figure 4.3.

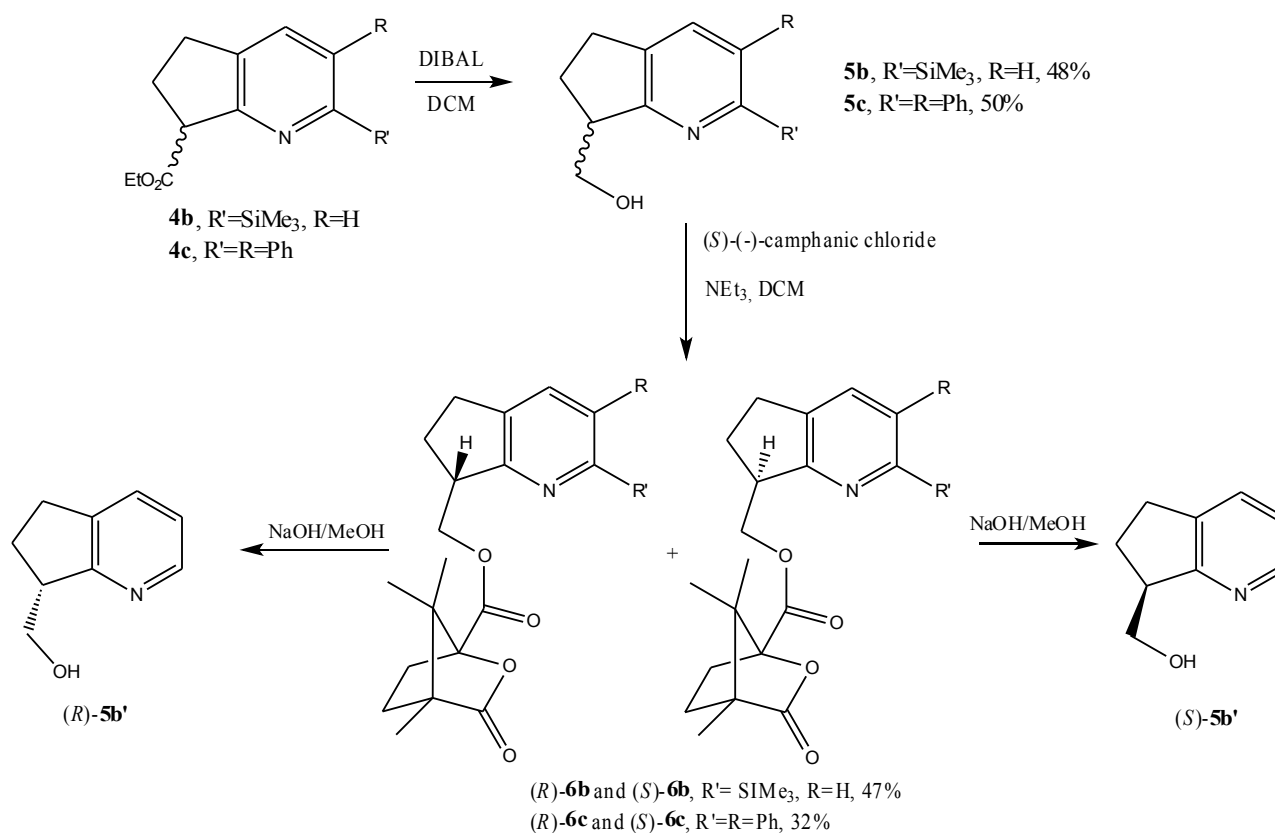


Figure 4.3: Attempted separation of enantiomers.

This was done by the reduction to the corresponding alcohols **5b** and **5c** (48 and 50 %) and subsequent reaction with (*S*)-camphoric chloride to construct the two diastereomeric pairs (*R*)-**6b** and (*S*)-**6b** and (*R*)-**6c** and (*S*)-**6c** (1:1 mixture, combined yields of 47 and 32 %, respectively). The diastereomers were attempted separated by conventional chromatographic methods, but total separation was not achieved, although to such extent that structures could be assigned by NMR. By preparative TLC, (*R*)-**6b** and (*S*)-**6b** were achieved pure in small amounts, so that rotation could be measured and hydrolysis performed. However, total desilylation occurred during hydrolysis, giving **5b'** in 99 and 37% yields. Due to the troublesome separation with this procedure, chiral preparative HPLC is proposed as a better method towards the pure enantiomers.

This study has shown that cyclotrimerization is a good method to introduce wanted substitution patterns, although not achieved in very good yields. Regioselectivity can also be controlled by applying suitable cyclization partners.



5 Spectroscopic data for new compounds

In this chapter, structural elucidation of new compounds will be presented. A figure with the respective NMR shifts will be shown; ^{13}C in red and ^1H in blue. Some features from 2D-NMR techniques for the compounds will be discussed to show how the structure was determined. Since most of the compounds share many common features, this it is not repeated for every structure. Multiples are given by their center value for the sake of clarity in the figures. The total range of the multiplets, together with additional coupling constants not mentioned here, are given in the experimental data. IR and MS analysis will be presented were it is appropriate. All structures are confirmed by HRMS.

5.1 Ethyl 2,3-bis(trimethylsilyl)-6,7-dihydro-5H-cyclopenta[b]pyridine-7-carboxylate (**4a**)

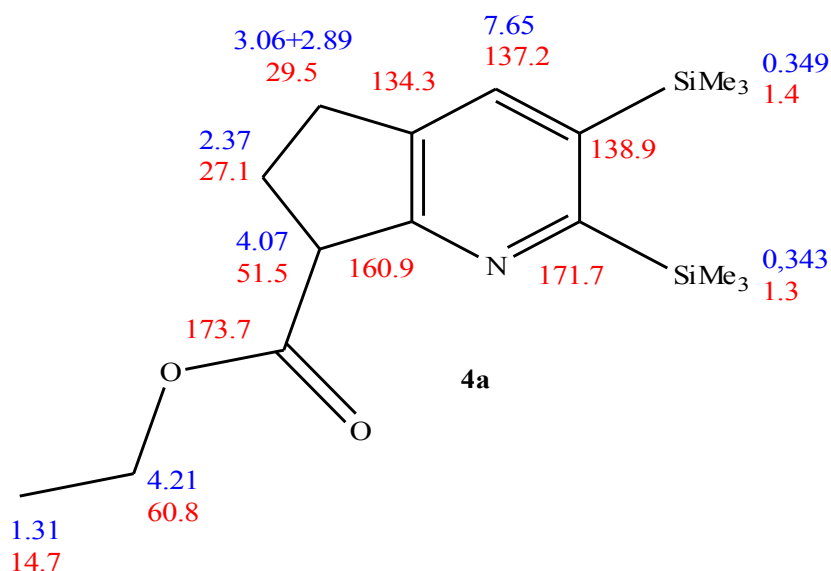


Figure 5.1: ^1H and ^{13}C NMR shifts for ethyl 2,3-bis(trimethylsilyl)-6,7-dihydro-5H-cyclopenta[b]pyridine-7-carboxylate (**4a**). See appendix F for full spectras.

The respective shifts observed in NMR are assigned in figure 5.1. From COSY, assignment of the aliphatic ring is relatively easy. HMBC from the carbonyl carbon is also valuable for this purpose. HMBC shows a coupling between the pyridine hydrogen and the carbons at 29.2, 138.9, 160.9 and 171.7, which is used for assignments in the pyridine ring. There are also coupling from the SiMe_3 -groups to the respective quaternary carbons in the aromatic ring.

5.2 Ethyl 2-(Trimethylsilyl)-6,7-dihydro-5H-cyclopenta[b]pyridine-7-carboxylate (4b)

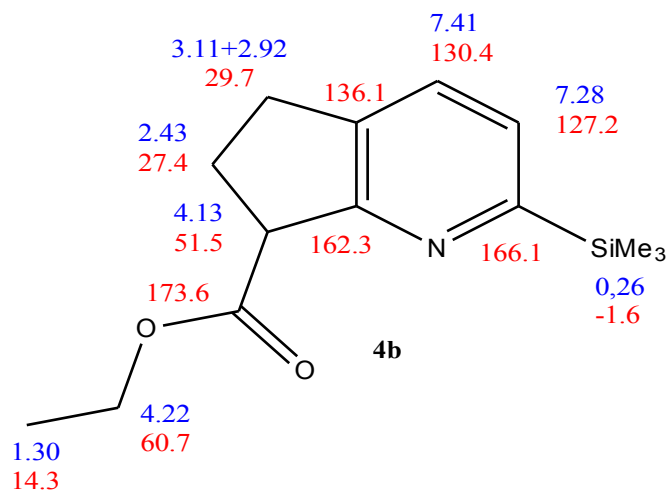


Figure 5.2: ¹H and ¹³C NMR shifts for ethyl 2-(trimethylsilyl)-6,7-dihydro-5H-cyclopenta[b]pyridine-7-carboxylate (**4b**). See appendix G for full spectras.

The respective shifts observed in NMR are assigned in figure 5.2. The same features as for **4a** are observed. In addition there is a clear doublet from the two pyridine protons, which couples with J 7.5 Hz. Only the 2-substituted regioisomer was observed in ¹H NMR. See chapter 3.2.1 for a discussion.

5.3 Ethyl 2,3-Diphenyl-6,7-dihydro-5H-cyclopenta[b]pyridine-7-carboxylate (4c)

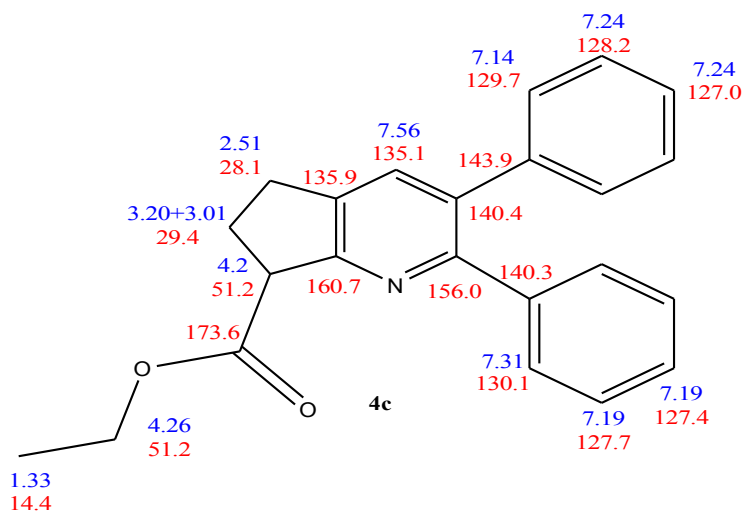


Figure 5.3: ¹H and ¹³C NMR shifts for ethyl 2,3-diphenyl-6,7-dihydro-5H-cyclopenta[b]pyridine-7-carboxylate (4c). See appendix H for full spectras.

The respective shifts observed in NMR are assigned in figure 5.3. The pyridine proton shows a clear singlet outside the phenyl region. Assignments of the phenyl rings are somewhat more complicated, but is made possible by observing coupling from carbon at 156.0 to the *o*-protons. In COSY, a clear coupling from the *o*-protons to the *m*- and *p*-protons are observed, and together with HMBC, two separate coupling systems from the two phenyl rings can be deduced.

5.4 Ethyl 2-phenyl-6,7-dihydro-5H-cyclopenta[b]pyridine-7-carboxylate (4d)

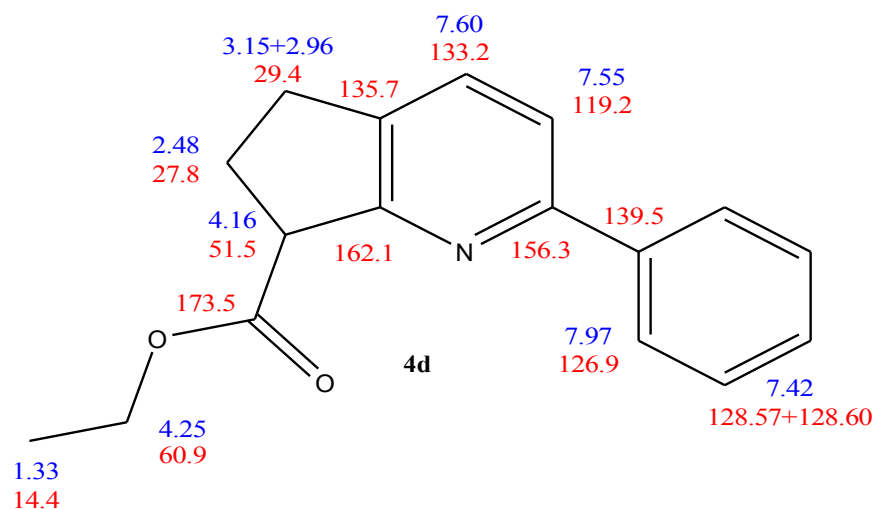


Figure 5.4: ¹H and ¹³C NMR shifts for ethyl 2-phenyl-6,7-dihydro-5H-cyclopenta[b]pyridine-7-carboxylate (**4d**). See appendix I for full spectras.

The respective shifts observed in NMR are assigned in figure 5.4. The two pyridine protons are observed with a coupling of J 8.05 Hz. It can be observed that the *o*-protons possess a relatively high shift compared to **4c**. This is in accordance with similar reported structures.^[6] Only the 2-substituted regioisomer was observed in ¹H NMR. See chapter 3.2.1 for a discussion.

5.5 Ethyl 2,3-bis(trimethylsilyl)-5,6,7,8-tetrahydroquinoline-8-carboxylate (4e)

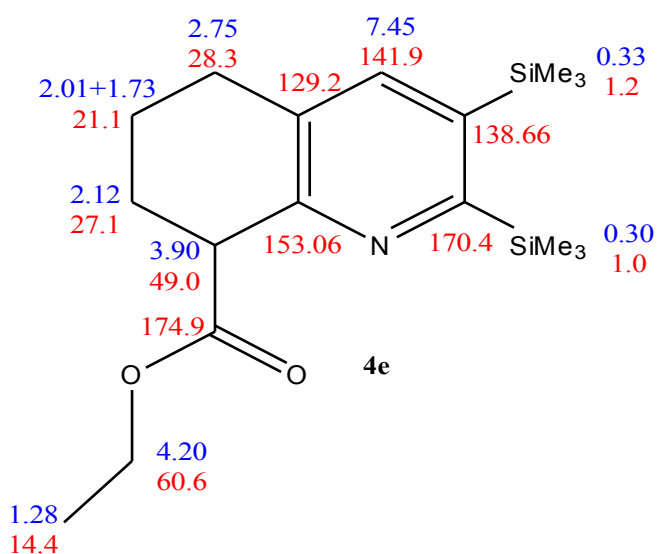


Figure 5.5: ¹H and ¹³C NMR shifts for ethyl 2,3-bis(trimethylsilyl)-5,6,7,8-tetrahydroquinoline-8-carboxylate (4e). See appendix J for full spectras.

The respective shifts observed in NMR are assigned in figure 5.3. From COSY, assignment of the aliphatic ring is relatively easy. HMBC from the carbonyl carbon is also valuable for this purpose. There are also coupling from the SiMe₃-groups to the respective quaternary carbons in the aromatic ring. In general, there are observed a lowering of the ¹³C-shifts of the fusion carbons when going from a fused 5-ring to a fused 6-ring.

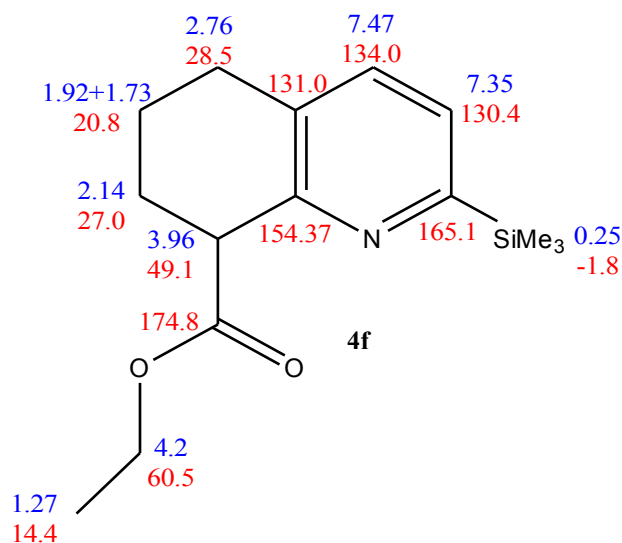
5.6 Ethyl 2-(Trimethylsilyl)-5,6,7,8-tetrahydroquinoline-8-carboxylate (4f)

Figure 5.6: ¹H and ¹³C NMR shifts for ethyl 2-(trimethylsilyl)-5,6,7,8-tetrahydroquinoline-8-carboxylate (**4f**). See appendix K for full spectras.

The respective shifts observed in NMR are assigned in figure 5.6. The same features as for **4e** are observed. In addition there is a clear doublet from the two pyridine protons, which couples with *J* 7.3 Hz. Only the 2-substituted regioisomer was observed in ¹H NMR. See chapter 3.2.1 for a discussion.

5.7 Ethyl 2,3-Diphenyl-5,6,7,8-tetrahydroquinoline-8-carboxylate (4g)

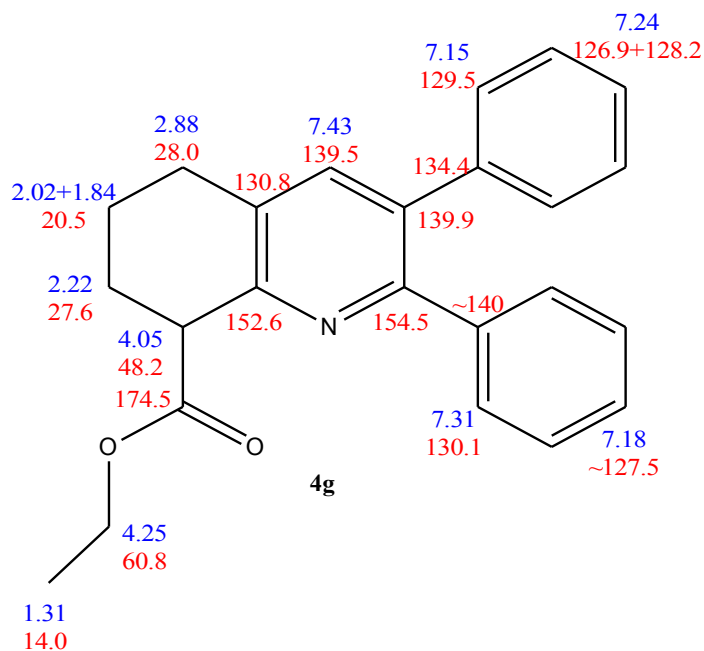


Figure 5.7: ¹H and ¹³C NMR shifts for ethyl 2,3-diphenyl-5,6,7,8-tetrahydroquinoline-8-carboxylate (**4g**). See appendix L for full spectras.

The respective shifts observed in NMR are assigned in figure 5.7, and the same method as for **4c** can be used. Some impurities made it hard do exactly assign the carbons in the *m*- and *p*-position in the phenyl rings.

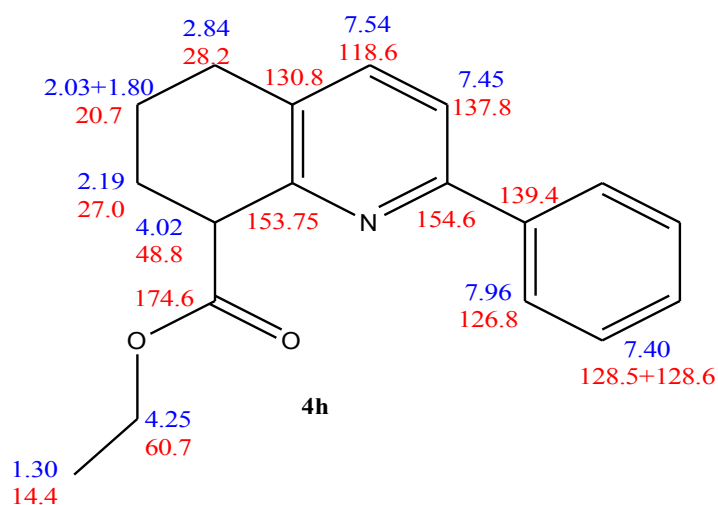
5.8 Ethyl 2-phenyl-5,6,7,8-tetrahydroquinoline-8-carboxylate (4h)

Figure 5.8: ¹H and ¹³C NMR shifts for ethyl 2-phenyl-5,6,7,8-tetrahydroquinoline-8-carboxylate (**4h**). See appendix M for full spectras.

The respective shifts observed in NMR are assigned in figure 5.8. The same observations as for **4d** are done. Only the 2-substituted regioisomer was observed in ¹H NMR. See chapter 3.2.1 for a discussion.

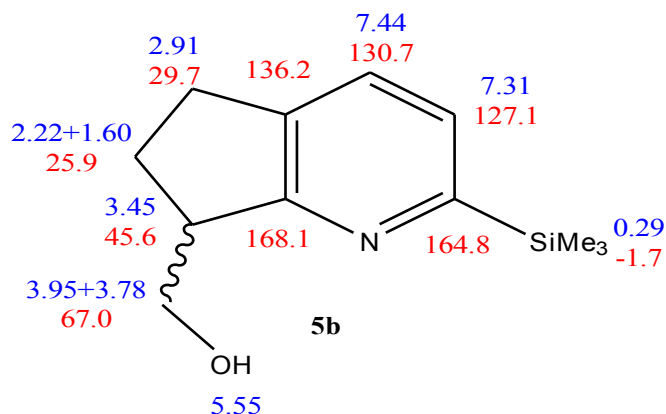
5.9 (2-(Trimethylsilyl)-6,7-dihydro-5H-cyclopenta[b]pyridin-7-yl)methanol (5b)

Figure 5.9: ¹H and ¹³C NMR shifts for (2-(trimethylsilyl)-6,7-dihydro-5H-cyclopenta[b]pyridin-7-yl)methanol (**5b**). See appendix N for full spectras.

The respective shifts observed in NMR are assigned in figure 5.9. Reduction to the alcohol naturally removes the ethyl signals. They are replaced by the -CH₂-OH signals that are split in two. C=O stretch absorption around 1730 cm⁻¹ disappears, and is replaced by a broad signal at 3400 cm⁻¹ resulting from OH stretching vibrations.

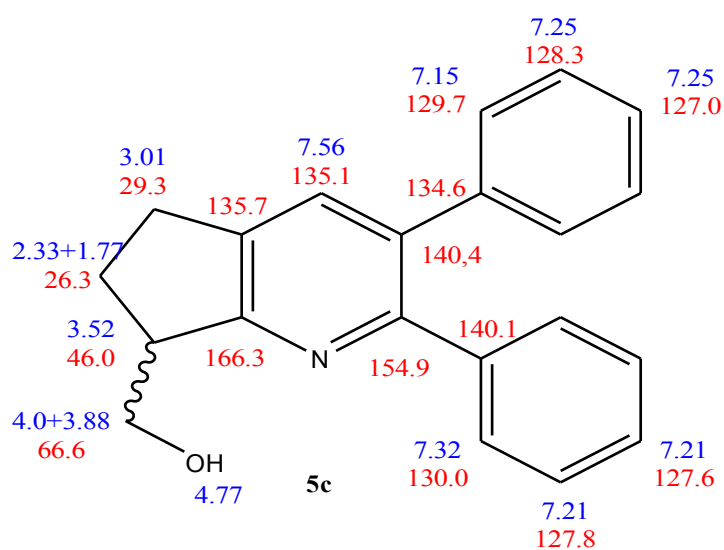
5.10 (2,3-Diphenyl-6,7-dihydro-5H-cyclopenta[b]pyridin-7-yl)methanol (5c)

Figure 5.10: ¹H and ¹³C NMR shifts for (2,3-diphenyl-6,7-dihydro-5H-cyclopenta[b]pyridin-7-yl)methanol (**5c**). See appendix O for full spectras.

The respective shifts observed in NMR are assigned in figure 5.10, and the same observations as for **5b** are done.

5.11 (1*S*,4*S*)-((*S*)-2-(Trimethylsilyl)-6,7-dihydro-5*H*-cyclopenta[*b*]pyridin-7-yl)methyl 4,7,7-trimethyl-3-oxo-2-oxabicyclo[2.2.1]heptane-1-carboxylate ((*S*)-6b) and

(1*S*,4*S*)-((*R*)-2-(Trimethylsilyl)-6,7-dihydro-5*H*-cyclopenta[*b*]pyridin-7-yl)methyl 4,7,7-trimethyl-3-oxo-2-oxabicyclo[2.2.1]heptane-1-carboxylate ((*R*)-6b)

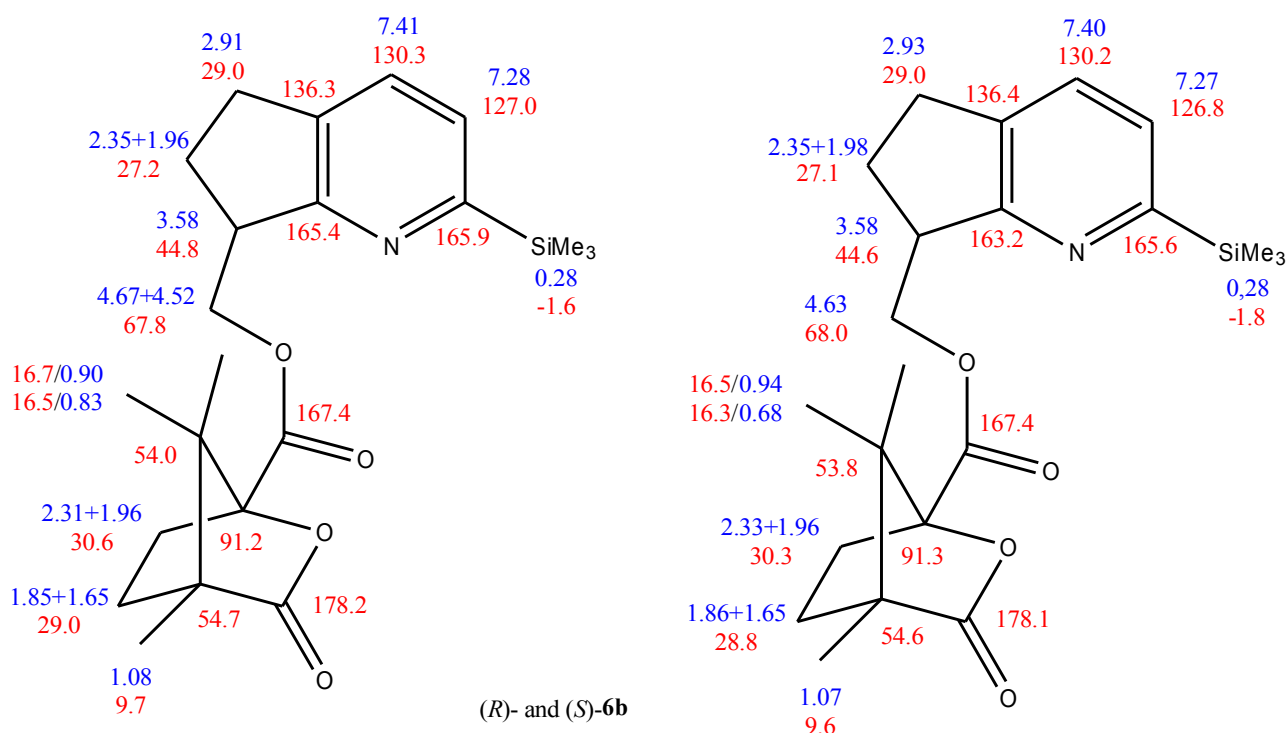


Figure 5.11 ¹H and ¹³C NMR shifts for (*R*)-6b and (*S*)-6b. See appendix P and Q for full spectra.

The respective shifts observed in NMR are assigned in figure 5.11. The absolute stereochemistry were not decided. Different ¹H NMR shift of the methyl signals make it easy to evaluate ratio of the two diastereomers. The -CH₂-O appears as either one doublet or two doublets of doublets. The camphor ring is assigned by HMBC from the two carbonyl carbons, and comparison with earlier reported similar structures.^[60] The two methyl groups in the bridge were hard to distinguish.

5.12 (1*S*,4*S*)-((*S*)-2,3-diphenyl-6,7-dihydro-5*H*-cyclopenta[*b*]pyridin-7-yl)methyl 4,7,7-trimethyl-3-oxo-2-oxabicyclo[2.2.1]heptane-1-carboxylate ((*S*)-**6c**) and

5.12 (1*S*,4*S*)-((*S*)-2,3-diphenyl-6,7-dihydro-5*H*-cyclopenta[*b*]pyridin-7-yl)methyl 4,7,7-trimethyl-3-oxo-2-oxabicyclo[2.2.1]heptane-1-carboxylate ((*S*)-6c**) and**

(1*S*,4*S*)-((*R*)-2,3-diphenyl-6,7-dihydro-5*H*-cyclopenta[*b*]pyridin-7-yl)methyl 4,7,7-trimethyl-3-oxo-2-oxabicyclo[2.2.1]heptane-1-carboxylate ((*R*)-6c**)**

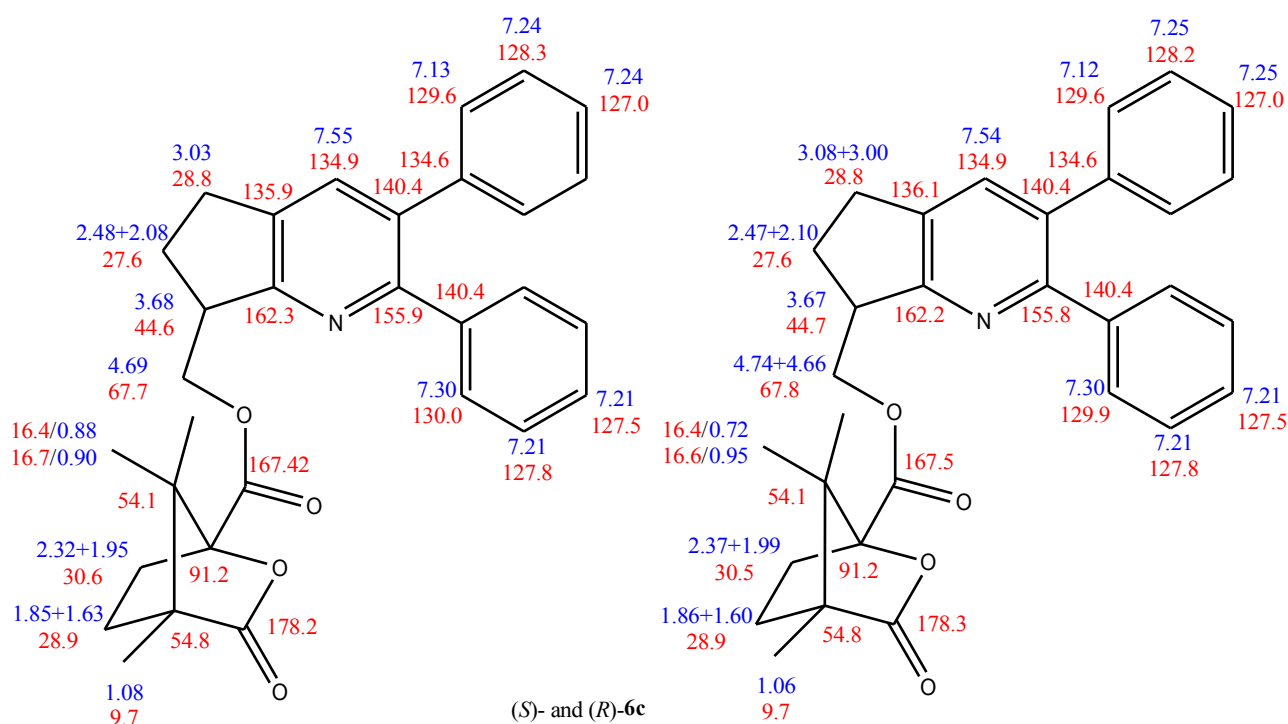


Figure 5.12 ¹H and ¹³C NMR shifts for (*R*)-**6c** and (*S*)-**6c**. See appendix R and S for full spectras.

The respective shifts observed in NMR are assigned in figure 5.12. The same features as for **6b** and **4b** are observed. The absolute stereochemistry were not decided.

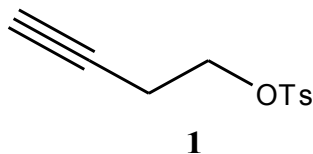
6 Experimental data

6.1 General

All chemicals were purchased from Sigma–Aldrich and used without further purification. Air and/or moisture sensitive reactions were performed under argon or nitrogen atmosphere with dried solvents and reagents. A Vacuum Atmosphere Company (VAC) HE-493 glove box was used for handling of very sensitive reagents. DCM, THF, and Et₂O were dried using MBRAUN solvent purification system (MB SPS-800). DCE and toluene were dried by distillation from CaH₂, then stored over activated 4 Å molecular sieves. Degassing of solvents with helium was performed for 20 min were indicated. TLC was performed on Merck silica gel 60 F₂₅₄ plates, and visualized using UV light at 312 nm or 365 nm, a phosphomolybdic acid solution (12 g phosphomolybdic acid in 250 mL EtOH) or a potassium permanganat (1,5 g KMnO₄, 10 g K₂CO₃, 2,5 mL 5M NaOH/H₂O, 200 mL H₂O) solution for detection. Column chromatography was performed with Silica gel (pore size 60 Å, 230–400 mesh particle size) purchased from Fluka. Preparative TLC was conducted with Kieselgel 60 PF₂₅₄₊₃₆₆ from Merck. ¹H and ¹³C NMR spectra were obtained on a Bruker Advance DPX instruments (300/75 MHz and 400/100 MHz). Chemical shifts (δ) are reported in parts per million. Where CDCl₃ has been used, shift values for proton are reported with reference to TMS (0.00) via the lock signal of the solvent. Signal patterns are indicated as s (singlet), d (doublet), t (triplet), q (quartet) or m (multiplet). ¹H and ¹³C NMR signals were assigned by 2D correlation techniques (COSY, HSQC, HMBC). IR spectra were recorded from a Thermo Nicolet FT-IR NEXUS instrument using a Smart Endurance reflection cell, and only the strongest/structurally most important peaks are listed (cm⁻¹). Accurate mass determination in positive or negative mode was performed on a “Synapt GS-2” Q-TOF instrument from Waters. Samples were ionized by electrospray (ESI) or by the use of ASAP probe (APCI). No chromatography was used previous to the mass analysis. Polarimetry was performed on a ParkinElmer Model 341 polarimeter. Irradiation in the cyclotrimerizations was performed with one or two halogen lamps (400 W, 118 mm, 50 Hz), bought from a standard hardware store.

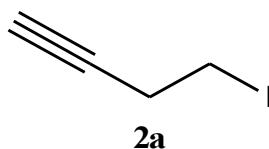
6.2 Preparation of alkynenitriles

But-3-yn-1-yl *p*-toluene sulphonate (**1**)^[47]



p-Toluenesulfonyl chloride (3.14 g, 16.5 mmol) and 4-(dimethylamino) pyridine (38 mg, 0.32 mmol) were dissolved in dry DCM (60 mL). The solution was cooled to 0 °C, and NEt₃ (2.70 mL, 19.0 mmol) and but-3-yn-1-ol (1.20 mL, 15.8 mmol) were added. The reaction vessel was then stirred for 24 hours. The reaction mixture was extracted with DCM (3x20 mL) and brine (20 mL), the organic phases dried over MgSO₄, and concentrated under reduced pressure. The product was obtained as a brown viscous oil (3.3 g, 94%), and used without any further purification. Spectroscopic data were in accordance with earlier reported results,^[47] and are presented in appendix A. R_f (Hexane:EtOAc, 1:1) 0.54. ¹H NMR (300 MHz, CDCl₃): δ 7.81 (d, 2H, *J* 8.3 Hz, Ar), 7.36 (d, 2H, *J* 8.3 Hz, Ar), 4.11 (t, 2H, *J* 7.0 Hz, O-CH₂), 2.56 (td, 2H, *J* 7.0, 2.6 Hz, CH₂), 2.47 (s, 3H), 1.98 (t, 1H, *J* 2.6 Hz, CH).

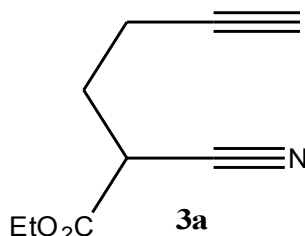
4-iodo-1-butyne (**2a**)



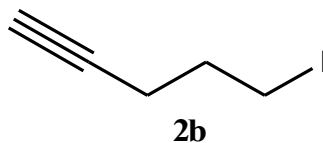
a) From but-3-yn-1-yl *p*-toluene sulphonate (Finkelstein reaction)^[48a]: NaI (76.15 g, 0.508 mol, 2.5 eq.) was dissolved in aceton (500 mL, reagent grade). **1** (44.35 g, 0.198 mol) was added, and the solution was stirred at reflux (68 °C) for 24 h. The solution was cooled, filtrated, and concentrated under reduced pressure. The crude product purified by column chromatography (pentane:Et₂O, 4:1), and the product was obtained as a clear, colorless liquid (24.86 g, 70%). Spectroscopic data were in accordance with earlier reported results,^[48a] and are presented in appendix B. R_f (pentane) 0.56. ¹H NMR (300 MHz, CDCl₃): δ 3.24 (t, 2H, *J* 7.3 Hz, I-CH₂), 2.79 (td, 2H, *J* 7.3, 2.1 Hz, CH₂), 2.16 (t, 1H, *J* 2.5 Hz, CH).

b) *Direct from but-3-yn-1-ol* ^[51]: I₂ (13.65 g, 53.11 mmol) were added over 1 h at 0 °C to PPh₃ (5.61 g, 21.41 mmol) and imidazole (2.43 g, 35.68 mmol) dissolved in dry DCM (120 mL). But-3-yn-1-ol (1.11 g, 15.86 mmol) was added slowly at 0 °C, and the mixture was stirred for 80 minutes at rt. The reaction mixture was quenched with Na₂S₂O₃ (50 mL saturated solution) and extracted with pentane (100 mL). The combined organic phases were washed with brine (30 mL) and water (30 mL), dried over MgSO₄ and concentrated under reduced pressure. The light yellow crude product was redissolved in pentane (30 mL), and the undissolved material was filtered off. The filtrate was purified by column chromatography (pentane) and 4-iodo-1-butyne was obtained as a clear, colorless liquid (0.24 g, 8%).

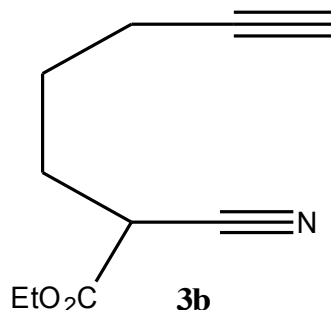
Ethyl 2-cyanohept-5-ynoate (**3a**) ^[49]



Ethyl cyanoacetate (29.4 g, 0.26 mol) was added to a stirred solution of NaH (6.03 g, 0.25 mol) in dry THF (400 mL), which then was stirred for 30 minutes. **2a** (22.34 g, 0.126 mol) was added, and the solution was refluxed at 68 °C for 48 h. A saturated aqueous solution of NaHCO₃ (15 mL) was added to the reaction mixture, which was extracted with Et₂O (3x80 mL), dried over MgSO₄ and concentrated under reduced pressure. The red-brown crude was purified by distillation and column chromatography (pentane:Et₂O, 4:1), and the product was obtained as a clear, colorless liquid (10.3 g, 50%). Spectroscopic data were in accordance with earlier reported results,^[49] and are presented in appendix D. R_f (pentane:Et₂O, 4:1) 0.37. B.p. 84 °C/0.84 mbar. ¹H NMR (300 MHz, CDCl₃): δ 4.28 (q, 2H, *J* 7.15 Hz, Et), 3.76 (dd, 1H, *J* 6.1 2.6 Hz, CH), 2.51-2.43 (m, 2H, CH₂), 2.28-2.08 (m, 2H, CH₂), 2.07 (t, 1H, *J* 2.6 Hz, C≡CH), 1.39 (t, 3H, *J* 7.15 Hz, Et).

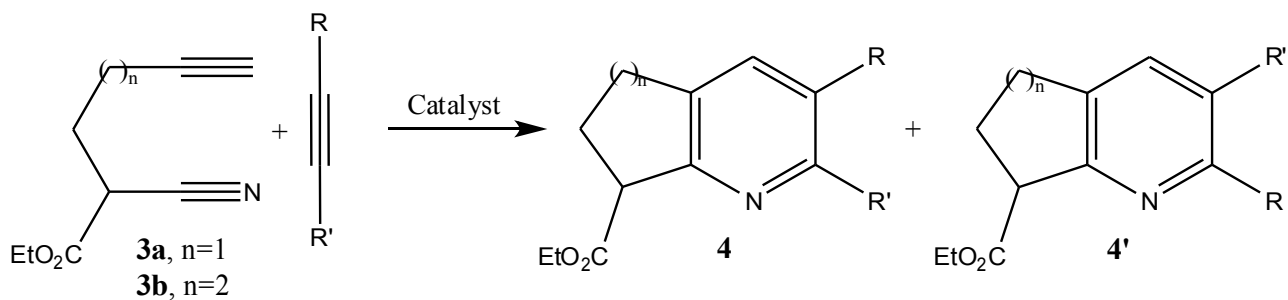
5-iodo-1-pentyne (2b) ^[48a]

NaI (73.11 g, 0.49 mmol) was dissolved in acetone (350 mL), and 5-chloropent-1-yne (10.10 g, 98.4 mmol) was added. The mixture was refluxed for 38 h, then cooled and filtered. The filtrate was extracted with ether (3x50 mL), washed with brine (50 mL), dried over MgSO₄ and concentrated under reduced pressure. The crude product was purified by column chromatography (pentane:Et₂O, 9:1), and the product was obtained as a clear colorless liquid (16 g, 84%). Spectroscopic data were in accordance with earlier reported results,^[48a] and are presented in appendix C. R_f (pentane:Et₂O, 9:1) 0.68. ¹H NMR (300 MHz, CDCl₃): δ 3.32 (t, 2H, *J* 6.7 Hz, I-CH₂) 2.34 (td, 2H, *J* 6.7 2.7, CH₂) 2.05-1.96 (m, 3H, CH₂+CH).

Ethyl 2-cyanohept-6-ynoate (3b) ^[49]

Ethyl cyanoacetate (24.91 g, 0.22 mol) was added to a stirred solution of NaH (4.96 g, 0.21 mol) in dry THF (250 mL), which then were stirred for 30 minutes. **2b** (20 g, 0.103 mol) was added, and the solution was refluxed at 68 °C for 64 h. A saturated solution of NaHCO₃ (90 mL) was added to the reaction mixture, which was extracted with Et₂O, dried over MgSO₄ and concentrated under reduced pressure. The crude product was purified by distillation, and the product was obtained as a clear, colorless liquid (8.3 g, 45%). Spectroscopic data were in accordance with earlier reported results,^[49] and are presented in appendix E. B.p. 70 °C/0.065 mbar. ¹H NMR (300 MHz, CDCl₃): δ 4.29 (q, 2H, *J* 7.15 Hz, Et), 3.5 (dd, 1H, *J* 7.8 1.5 Hz, CH) 2.29 (td, 2H, *J* 7.8 2.6 Hz, CH₂), 2.18-2.02 (m, 2H, CH₂), 2.0 (t, 1H, *J* 2.6 Hz, C≡CH), 1.82-1.67 (m, 2H, CH₂), 1.33 (t, 3H, *J* 7.15 Hz, Et).

6.3 Cyclotrimerization



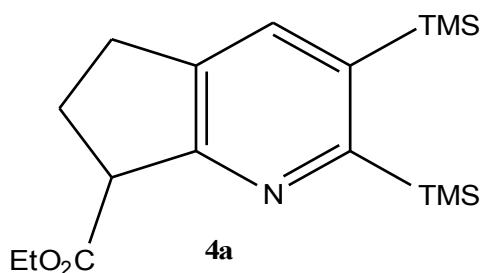
6.3.1 CpCo(CO)₂

The catalyst CpCo(CO)₂ was used with two different methods, referred to as Method A and B in table 3.2.

General procedure, method A:

CpCo(CO)₂ and alkyne nitrile **3** in dry, degassed toluene was added to the alkyne in toluene via a slow addition pump over the indicated period of time. The reaction was kept under Ar-atmosphere and irradiated with one halogen lamp (400 W, 118 mm, 50 Hz). Irradiation was continued for 1.5 h after the addition was complete. The reaction mixture was filtered, concentrated under reduced pressure and purified by column chromatography (EtOAc:pentane, 1:10)

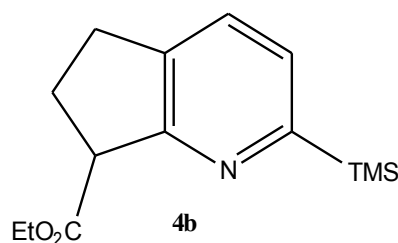
Ethyl 2,3-bis(trimethylsilyl)-6,7-dihydro-5H-cyclopenta[b]pyridine-7-carboxylate (**4a**)



CpCo(CO)₂ (30 μ L, 0.243 mmol) and **3a** (0.195 g, 1.18 mmol) in toluene (2 mL) was added to BTMSA (1.046 g, 6.14 mmol) in toluene (1 mL) via a slow addition pump over 6 h. The product was obtained as a dark red oil (80 mg, 20%). R_f (pentane:EtOAc, 4:1) 0.67. IR (neat): 2951 (w), 1729 (m), 1247 (m), 1174 (w), 1081 (w), 838 (s), 756 (m), 646 (w) cm^{-1} . ¹H NMR (400 MHz,

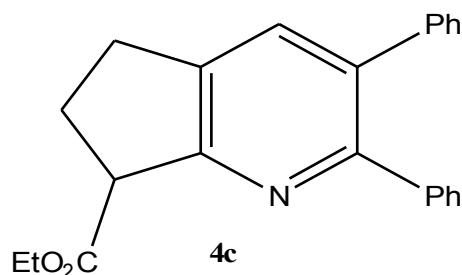
CDCl₃): δ 7.68 (s, 1H, pyr-H), 4.20 (q, 2H, *J* 7.2 Hz, Et), 4.07 (t, 1H, *J* 8.5 Hz, CH), 3.13-2.82 (m, 2H, CH₂), 2.49-2.28 (m, 2H, CH₂), 1.30 (t, 3H, *J* 7.2 Hz, Et), 0.349 (s, 9H, SiMe₃), 0.34 (s, 9H, NC-SiMe₃). ¹³C NMR (100 MHz, CDCl₃): δ 173.7 (C=O), 171.7 (NC-SiMe₃), 160.9 (NC), 138.9 (C-TMS), 137.3 (pyr-CH), 134.2 (NCC_q), 60.8 (Et), 51.5 (CH) 29.7 (CH₂), 27.1 (CH₂), 14.4, Et, 1.4 (SiMe₃), 1.3 (NC-SiMe₃). HRMS (TOF ASAP+) *m/z* calcd. for C₁₇H₃₀NO₂Si₂ [M+H]⁺: 336.1810 found 336.1815. Proton and carbon shift are assigned in chapter 5.1, and the spectras are given in appendix F.

Ethyl 2-(trimethylsilyl)-6,7-dihydro-5H-cyclopenta[b]pyridine-7-carboxylate (4b)



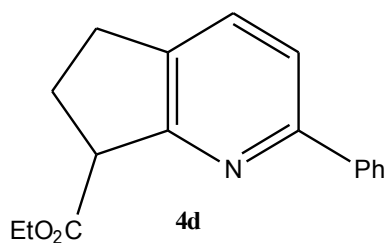
CpCo(CO)₂ (30 μL, 0.243 mmol) and **3a** (0.204 g, 1.23 mmol) in toluene (2 mL) was added to trimethylsilyl ethylene (0.376 g, 3.83 mmol) in toluene (2 mL) via a slow addition pump over 5 h. The product was obtained as a dark red oil (52 mg, 16%). R_f (pentane:EtOAc, 4:1) 0.44. IR (neat): 2951 (w), 2358 (w), 1731 (m), 1256 (m), 1199 (w), 1174 (w), 1045 (w), 838 (s), 756 (w) cm⁻¹. ¹H NMR (400 MHz, CDCl₃): δ 7.45 (d, 1H, *J* 7.5 Hz, pyr-H), 7.32 (d, 1H, *J* 7.5 Hz, NC(SiMe₃)CH), 4.23 (q, 2H, Et), 4.13 (dd, 1H, *J* 8.5 2.4 Hz, CH), 3.13-3.05 (m, 1H, CH₂), 2.94-2.86 (m, 1H, CH₂), 2.49-2.31 (m, 2H, CH₂), 1.30 (t, 3H, *J* 7.15 Hz, Et), 0.26 (s, 9H, SiMe₃). ¹³C NMR (100 MHz, CDCl₃): δ 173.6 (C=O), 166.2 (NC-SiMe₃) 162.2 (NC), 136.1 (NCC_q), 130.4 (pyr-CH), 127.2 (NC(SiMe₃)CH), 60.7 (Et), 51.5 (CH), 29.7 (CH₂), 27.4 (CH₂), 14.3 (Et), -1.6 (SiMe₃). HRMS (TOF ASAP+) *m/z* calcd. for C₁₄H₂₂NO₂Si [M+H]⁺: 264.1414, found 264.1423. Proton and carbon shift are assigned in chapter 5.2, and the spectras are given in appendix G.

Ethyl 2,3-diphenyl-6,7-dihydro-5H-cyclopenta[b]pyridine-7-carboxylate (**4c**)



CpCo(CO)₂ (30 μ L, 0.243 mmol) and **3a** (0.204 g, 1.23 mmol) in toluene (2 mL) was added to diphenylacetylene (0.655 g, 3.68 mmol) in toluene (2 mL) via a slow addition pump over 5 h. The product was obtained as a yellow oil (155 mg, 37%). *R_f* (pentane:EtOAc, 4:1) 0.5. IR (neat): 3044 (w), 2358 (w), 1742 (m), 1252 (w), 1199 (w), 1025 (w), 762 (m), 763 (m), 733 (m), 698 (s), 634 (w) cm^{-1} . ¹H NMR (400 MHz, CDCl₃): δ 7.56 (s, 1H, pyr-H), 7.32-7.13 (m, 10H, Ar), 4.26 (q, 2H, Et), 4.2 (dd, 1H, *J* 8.6 2.5 Hz, CH), 3.25-3.17 (m, 1H, CH₂), 3.05-2.97 (m, 1H, CH₂), 2.57-2.54 (m, 2H, CH₂), 1.33 (t, 3H, *J* 7.12 Hz, Et). ¹³C NMR (100 MHz, CDCl₃): δ 173.6 (C=O), 160.7 (NC-Ph), 156.0 (NC), 140.4 (C-Ph), 140.3 (Ar_q), 135.9 (NCC_q), 135.1 (pyr-CH), 134.9 (Ar_q), 130.1 (Ar), 129.7 (Ar), 128.2 (Ar), 127.7 (Ar), 127.4 (Ar), 127.0 (Ar), 61.0 (Et), 51.2 (CH), 29.4 (CH₂), 28.1 (CH₂), 14.4 (Et). HRMS (TOF ASAP+) *m/z* calcd. for C₂₃H₂₂NO₂ [M+H]⁺: 344.1651, found 344.1645. Proton and carbon shift are assigned in chapter 5.3, and the spectras are given in appendix H.

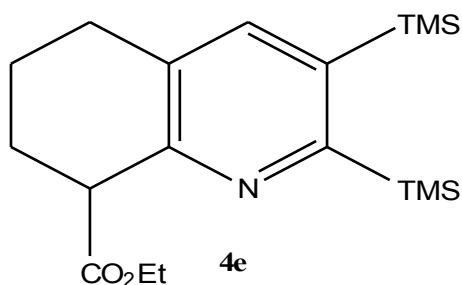
Ethyl 2-phenyl-6,7-dihydro-5H-cyclopenta[b]pyridine-7-carboxylate (**4d**)



CpCo(CO)₂ (30 μ L, 0.243 mmol) and **3a** (0.215 g, 1.30 mmol) in toluene (2 mL) was added to phenylacetylene (0.371 g, 3.63 mmol) in toluene (2 mL) via a slow addition pump over 6 h. The product was obtained as a yellow oil (43 mg, 12 %). *R_f* (pentane:EtOAc, 4:1) 0.33. IR (neat): 2977

(w), 2353 (w), 1778 (s), 1583 (m), 1444 (m), 1258 (m), 1177 (s), 763 (s), 697 (s) cm^{-1} . ^1H NMR (400 MHz, CDCl_3): δ 7.97 (d, 2H, J 7.3 Hz, Ar), 7.60 (d, 1H, J 8.05 Hz, pyr-H), 7.55 (d, 1H, J 8.05 Hz, NC(Ph)-CH), 7.5-7.35 (m, 3H, Ar), 4.25 (q, 2H, J 7.15 Hz, Et), 4.16 (dd, 1H, J 8.7 2.3 Hz, CH), 3.19-3.11 (m, 1H, CH_2), 3.0-2.94 (m, 1H, CH_2), 2.55-2.4 (m, 2H, CH_2), 1.33 (t, 3H, J 7.15 Hz, Et). ^{13}C NMR (100 MHz, CDCl_3): δ 173.5 (C=O), 162.1 (NC), 156.3 (NC-Ph), 139.5 (Ar_q), 135.7 (NCC $_q$), 133.2 (pyr-CH), 128.6 (Ar), 128.6 (Ar), 126.9 (Ar), 119.2 NC(Ph)-CH), 60.9 (Et), 51.5 (CH), 29.4 (CH_2), 27.8 (CH_2), 14.4 (Et). HRMS (TOF ASAP+) m/z calcd. for $\text{C}_{17}\text{H}_{18}\text{NO}_2$ $[\text{M}+\text{H}]^+$: 268.1332, found 268.1338. Proton and carbon shift are assigned in chapter 5.4, and the spectras are given in appendix I.

Ethyl 2,3-bis(trimethylsilyl)-5,6,7,8-tetrahydroquinoline-8-carboxylate (**4e**)

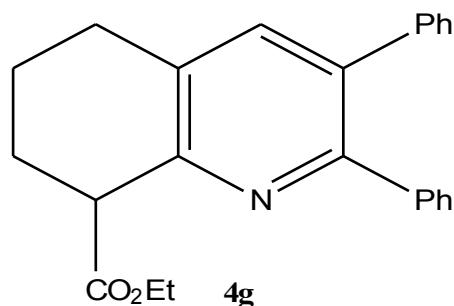


$\text{CpCo}(\text{CO})_2$ (30 μL , 0.243 mmol) and **3b** (0.205 g, 1.14 mmol) in toluene (3 mL) was added to bis(trimethylsilyl)acetylene (1.110 g, 6.51 mmol) in toluene (22 mL) via a slow addition pump over 6 h. The product was obtained as a light yellow oil (0.07 g, 17 %). R_f (pentane:EtOAc, 4:1) 0.82. IR (neat): 2940 (w), 2352 (w), 1736 (s), 1248 (s), 1155 (m), 755 (m) cm^{-1} . ^1H NMR (400 MHz, CDCl_3): δ 7.45 (s, 1H, pyr-H), 4.20 (q, 2H, J 7.12 Hz, Et), 3.90 (dd, 1H, J 9.12 2.95 Hz, CH), 2.86-2.65 (m, 2H, CH_2), 2.24-2.07 (m, 2H, CH_2), 2.06-1.96 (m, 1H, CH_2), 1.78-1.65 (m, 1H, CH_2), 1.29 (t, 3H, J 7.12 Hz Et), 0.33 (s, 9H, SiMe_3), 0.30 (s, 9H, NC- SiMe_3). ^{13}C NMR (100 MHz, CDCl_3): δ 174.9 (C=O), 170.4 (NC- SiMe_3), 153.1 (NC), 141.9 (pyr-CH), 138.7 (C- SiMe_3), 129.2 (NCC $_q$), 60.6 (Et), 49.0 (CH), 28.3 (CH_2), 27.1 (CH_2), 21.1 (CH_2), 14.4 (Et), 1.2 (SiMe_3), 1.0 (NC- SiMe_3). HRMS (TOF ASAP+) m/z calcd. for $\text{C}_{18}\text{H}_{32}\text{NO}_2\text{Si}_2$ $[\text{M}+\text{H}]^+$: 350.1966, found 350.1970. Proton and carbon shift are assigned in chapter 5.5, and the spectras are given in appendix J.

Ethyl 2-(trimethylsilyl)-5,6,7,8-tetrahydroquinoline-8-carboxylate (4f)

CpCo(CO)₂ (30 μ L, 0.243 mmol) and **3b** (0.2 g, 1.12 mmol) in toluene (2 mL) was added to trimethylsilyl ethylene (2.13 g, 21.69 mmol) in toluene (1.5 mL) via a slow addition pump over 5 h. ¹H NMR analysis of the crude showed only unidentified side-products.

Ethyl 2,3-diphenyl-5,6,7,8-tetrahydroquinoline-8-carboxylate (4g)



CpCo(CO)₂ (30 μ L, 0.243 mmol) and **3b** (0.195 g, 1.09 mmol) in toluene (2 mL) was added to diphenylacetylene (0.612 g, 3.43 mmol) in toluene (3 mL) via a slow addition pump over 6 h. The product was obtained as a yellow oil (0.124 g, 32%). IR (neat): 2930 (w), 2358 (w), 1731 (m), 1423 (m), 1177 (m), 1025 (m), 909 (m), 766 (m), 729 (s), 698 (s) cm⁻¹. R_f (pentane:EtOAc, 4:1) 0.56. ¹H NMR (400 MHz, CDCl₃): δ 7.43 (s, 1H, pyr-H), 7.32-7.29 (m, 2H, Ar), 7.26-7.23 (m, 3H, Ar), 7.21-7.17 (m, 2H, Ar), 7.17-7.12 (m, 2H, Ar), 4.25 (q, 2H, *J* 7.12 Hz, Et), 4.05 (t, 1H, *J* 6.65 Hz, CH), 2.98-2.79 (m, 2H, CH₂), 2.28-2.19 (m, 2H, CH₂), 2.09-1.97 (m, 1H, CH₂), 1.90-1.74 (m, 1H, CH₂), 14.02 (t, 3H, *J* 7.10 Hz, Et). ¹³C NMR (100 MHz, CDCl₃): δ 174.5 (C=O), 154.5 (NC(Ph)), 152.6 (NC), 140.0 (Ar_q), 139.9 (C-Ph), 139.5 (pyr-CH), 134.4 (Ar_q), 130.8 (NCC_q), 130.1 (Ar), 129.5 (Ar), 128.2 (Ar), 127.5 (Ar), 126.9 (Ar), 60.7 (Et), 48.2 (CH), 28.0 (CH₂), 27.2 (CH₂), 20.5 (CH₂), 14.0 (Et). HRMS (TOF ASAP+) *m/z* calcd. for C₂₄H₂₄NO₂ [M+H]⁺: 358.1802, found 358.1808. Proton and carbon shift are assigned in chapter 5.7, and the spectras are given in appendix L.

General procedure, method B:

The alkyne was added to a pressure vial and dissolved in dry, degassed toluene, which then was sealed with a rubber septum, and evacuated and back filled with argon gas three times. CpCo(CO)₂ and alkynenitrile **3** in toluene was added via a cannula, and the septum was replaced by a screw cork. The reaction mixture was irradiated for 5 h with two halogen lamps (400 W, 118 mm, 50 Hz) to ensure a high temperature, and hence pressure. The reaction mixture was filtered, concentrated under reduced pressure and purified by column chromatography (EtOAc:pentane, 1:10). The total amount of toluene is indicated for the respective reactions.

Ethyl 2,3-bis(trimethylsilyl)-6,7-dihydro-5H-cyclopenta[b]pyridine-7-carboxylate (4a)

CpCo(CO)₂ (135 μL, 1.09 mmol), **3a** (0.91 g, 5.51 mmol) and BTMSA (2.66 g, 15.6 mmol) in toluene (25 mL) was reacted according to the general procedure. The product was obtained as a dark red oil (0.31 g, 17%). For analytical data, see under method A.

Ethyl 2-(trimethylsilyl)-6,7-dihydro-5H-cyclopenta[b]pyridine-7-carboxylate (4b)

CpCo(CO)₂ (150 μL, 1.215 mmol), **3a** (1.036 g, 6.27 mmol) and trimethylsilyl ethylene (2.02 g, 20.6 mmol) in toluene (20 mL) was reacted according to the general procedure. The product was obtained as a dark red oil (0.335 g, 20%). For analytical data, see under method A.

Ethyl 2,3-diphenyl-6,7-dihydro-5H-cyclopenta[b]pyridine-7-carboxylate (4c)

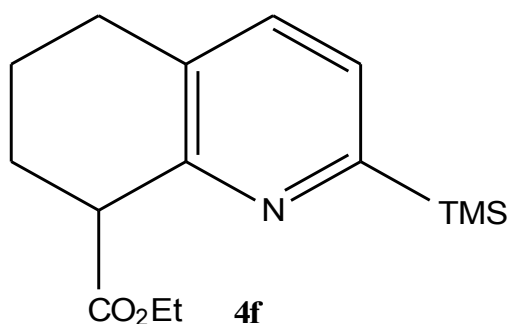
CpCo(CO)₂ (150 μL, 1.215 mmol), **3a** (1.003 g, 6.07 mmol) and diphenylacetylene (3.55 g, 19.9 mmol) in toluene (25 mL) was reacted according to the general procedure. The product was obtained as a yellow oil (0.993 g, 48%). For analytical data, see under method A.

Ethyl 2-phenyl-6,7-dihydro-5H-cyclopenta[b]pyridine-7-carboxylate (4d)

CpCo(CO)₂ (30 μL, 0.243 mmol), **3a** (0.197 g, 1.19 mmol) and phenylacetylene (0.335 g, 3.48 mmol) in toluene (8 mL) was reacted according to the general procedure. The product was obtained as a yellow oil (0.09 g, 28%). For analytical data, see under method A.

Ethyl 2,3-bis(trimethylsilyl)-5,6,7,8-tetrahydroquinoline-8-carboxylate (4e)

CpCo(CO)₂ (75 μL, 0.608 mmol, 1 eq.), **3b** (0.095 g, 0.53 mmol) and bis(trimethylsilyl)acetylene (0.57 g, 3.35 mmol) in toluene (8 mL) was reacted according to the general procedure. The product was obtained as a light yellow oil (21 mg, 11%). For analytical data, see under method A.

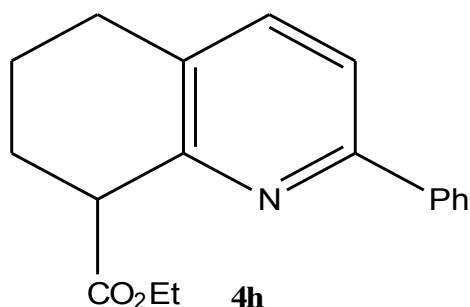
Ethyl 2-(trimethylsilyl)-5,6,7,8-tetrahydroquinoline-8-carboxylate (4f)

CpCo(CO)₂ (30 μL, 0.243 mmol), **3b** (0.201 g, 1.12 mmol) and trimethylsilyl ethylene (0.335 g, 3.41 mmol) in toluene (8 mL) was reacted according to the general procedure. The product was obtained as a yellow oil (68 mg, 22%). R_f (pentane:EtOAc, 4:1) 0.64. IR (neat): 2953 (w), 1754 (m), 1451 (w), 1247 (m), 1174 (w), 876 (w), 837 (s), 754 (w) cm⁻¹. ¹H NMR (400 MHz, CDCl₃): δ 7.47 (d, 1H, *J* 7.3 Hz, pyr-H), 7.35 (d, 1H, *J* 7.5 Hz, NC(Ph)-CH), 4.3-4.15 (m, 2H, Et), 3.96 (t, 1H, *J* 7.12 Hz, CH), 2.88-2.69 (m, 2H, CH₂), 2.23-2.1 (m, 2H, CH₂), 2.03-1.93 (m, 1H, CH₂), 1.8-1.68 (m, 1H, CH₂), 1.27 (t, 3H, *J* 7.1 Hz, Et), 0.25 (s, 3H, SiMe₃). ¹³C NMR (100 MHz, CDCl₃): δ 174.76 (C=O), 165.1 (NC-SiMe₃), 154.4 (NC), 134.0 (pyr-CH), 131.0 (NCC_q), 130.4 (NC(SiMe₃)-CH), 60.5 (Et), 49.1 (CH), 28.5 (CH₂), 27.0 (CH₂), 20.8 (CH₂), 14.4 (CH₂), -1.8 (SiMe₃). HRMS (TOF ASAP+) *m/z* calcd. for C₁₅H₂₄NO₂Si [M+H]⁺: 278.1571, found 278.1576. Proton and carbon shift are assigned in chapter 5.6, and the spectras are given in appendix K.

Ethyl 2,3-diphenyl-5,6,7,8-tetrahydroquinoline-8-carboxylate (4g)

CpCo(CO)₂ (30 μL, 0.243 mmol), **3b** (0.210 g, 1.17 mmol) and diphenylacetylene (0.55 g, 3.11 mmol) in toluene (8 mL) was reacted according to the general procedure. The product was obtained as a yellow oil (0.194 g, 46%). For analytical data, see under method A.

Ethyl 2-phenyl-5,6,7,8-tetrahydroquinoline-8-carboxylate (4h)



CpCo(CO)₂ (30 μL, 0.243 mmol), **3b** (0.215 g, 1.2 mmol) and phenylacetylene (0.34 g, 3.33 mmol) in toluene (8 mL) was reacted according to the general procedure. The product was obtained as a yellow oil (63 mg, 20%). R_f (pentane:EtOAc, 4:1) 0.6. IR (neat): 2930 (w), 2364 (w), 1731 (m), 1462 (m), 1245 (m), 1166 (m), 1025 (m), 761 (s), 730 (m), 695 (s) cm⁻¹. ¹H NMR (400 MHz, CDCl₃): δ 7.96 (dd, 2H, *J* 8.12 Hz, Ar), 7.54 (d, 1H, *J* 8.13 Hz, pyr-H), 7.48 (d, 1H, *J* 8.13 Hz, NC(Ph)-CH), 7.46-7.32 (m, 3H, Ar), 4.25 (q, 2H, Et), 4.02 (t, 1H, *J* 6.98 Hz, CH), 2.96-2.66 (m, 2H, CH₂), 2.26-2.17 (m, 2H, CH₂), 2.09-1.99 (m, 1H, CH₂), 1.90-1.76 (m, 1H, CH₂), 1.30 (t, 3H, *J* 7.1 Hz, Et). ¹³C NMR (100 MHz, CDCl₃): δ 174.6 (C=O), 154.6 (NC-Ph), 153.8 (NC), 139.4 (Ar_q), 137.8 (NC(Ph)-CH), 130.8 (NCC_q), 128.6 (Ar), 128.5 (Ar), 126.8 (Ar), 118.6 (pyr-H), 60.7 (Et), 48.8 (CH), 28.2 (CH₂), 27.0 (CH₂), 20.7 (CH₂), 14.4 (Et). HRMS (TOF ASAP+) *m/z* calcd. for C₁₈H₂₀NO₂ [M+H]⁺: 282.1489, found 282.1495. Proton and carbon shift are assigned in chapter 5.8, and the spectras are given in appendix M.

6.3.2 Other catalytic systems tested

The reactions tested in table 3.4 and 3.5 were conducted as outlined below.

Typical procedure for CpCo(COD)^[36]

CpCoCOD (62 mg, 0.29 mmol) was weighed out on the bench in a pressure vial which was then sealed with a septum, evacuated and back filled with argon gas three times, and dissolved in dry, degassed toluene (4 mL). **3b** (0.205 g, 1.14 mmol) and diphenylacetylene (0.617 g, 3.43 mmol) were dissolved in toluene (4 mL) and added via a cannula to the pressure vial. The reaction mixture was irradiated for 5 h. The reaction mixture was filtered, concentrated under reduced pressure and purified by column chromatography (pentane:EtOAc, 9:1). Only unidentified side-products were observed by ¹H NMR analysis.

Typical procedure for Cp*Ru(cod)Cl^[59]

Cp*Ru(cod)Cl (21 mg, 0.055 mmol) was weighed out in a glovebox to a round flask, equipped with a condenser sealed with a septum, removed from the glovebox and put under argon. **3a** (0.21 g, 1.27 mmol) and BTMSA (0.301 g, 1.76 mmol) in dry, degassed DCE (10 mL) were then added via a cannula, and the reaction mixture was refluxed for 70 h. TLC indicated only starting materials, which was confirmed by ¹H NMR analysis.

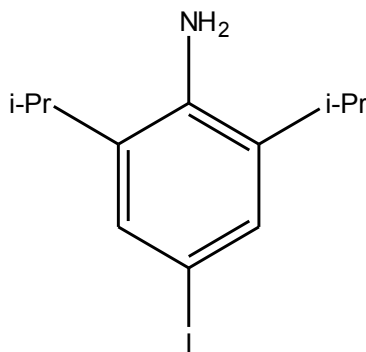
Typical procedure for Fe(OAc)₂^[39]

Fe(OAc)₂ (18.5 mg, 0.106 mmol,) and **L** (56.4 mg, 0.085 mmol) were weighed out in a glovebox to a round flask, sealed with a septum, removed from the glovebox and put under argon. Zn (17.3 mg, 0.265 mmol) was also weighed out in a glovebox and put in a GC-glass. **3b** in dry, degassed DMF (1.5 mL) was then added via a cannula, and the reaction mixture was stirred for 10 minutes. BTMSA (116 mg, 0.678 mmol) in DMF was added via a cannula before Zn was quickly added, and the flask was equipped with a condenser sealed with a septum. The reaction mixture refluxed for 48 h, then cooled and filtered. The crude product was concentrated under reduced pressure, and purified by column chromatography (pentane:EtOAc, 9:1). ¹H NMR analysis of the fractions showed only starting materials and ligand.

6.3.3 Preparation of ligand for iron-catalysis

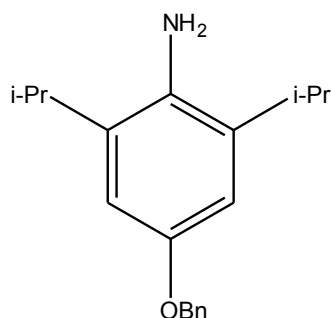
The ligand was synthesized according to the method described by Louie et al.^[39]

4-Iodo-2,6-diisopropylaniline



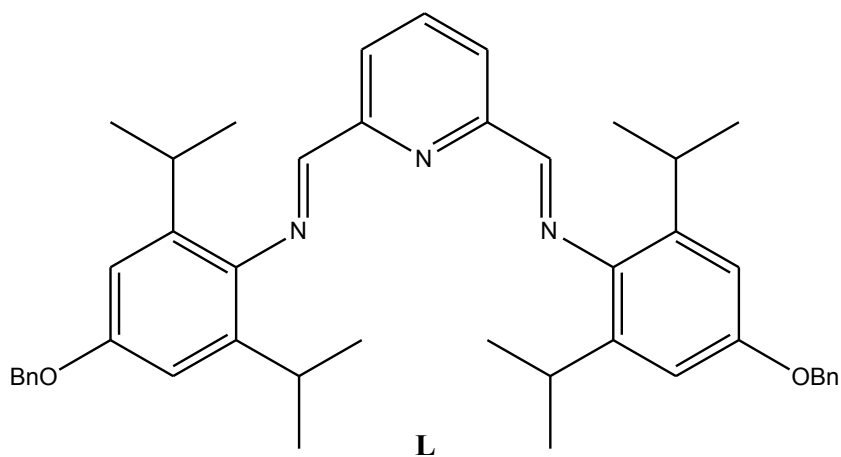
ICl (0.405 g, 2.49 mmol) in DCM (4 mL) was added dropwise to a stirring solution of 2,6-diisopropylaniline (0.435 g, 2.45 mmol) and NaHCO₃ (0.604 g, 7.18 mmol) in MeOH (5 mL). The reaction mixture was stirred for 19 h at room temperature. Solids were filtered off, rinsed with Et₂O (10 mL) and concentrated under reduced pressure. A aqueous saturated solution of Na₂S₂O₃ (10 mL) was added, and the solution was stirred for 10 minutes, then extracted with Et₂O (3x5 mL), washed with water (10 mL), dried over MgSO₄ and concentrated under reduced pressure. The crude product was obtained as a dark red, viscous liquid (0.58 g, 78%), and used without any further purification. Spectroscopic data were in accordance with earlier reported results,^[39] and are presented in appendix Y.1. R_f (pentane:Et₂O, 3:1) 0.43. ¹H NMR (300 MHz, CDCl₃): δ 7.27 (s, 2H, Ar), 3.73 (bs, 2H, NH₂), 2.84 (sep, 2H, *J* 6.8 Hz, CH), 1.23 (d, 12H, *J* 6.8 Hz, CH₃).

4-Benzyloxy-2,6-diisopropylaniline



In a glove box, a 25 mL round flask were filled with CuI (0.231 g, 0.121 mmol), Cs₂CO₃ (1.263 g, 3.88 mmol) and 3,4,7,8-tetramethyl-1,10-phenanthroline (Me₄Phen) (0.065 g, 0.275 mmol), and equipped with a condenser sealed with a septum. The reaction flask was removed from the glove box, and 4-Iodo-2,6-diisopropylaniline (0.58 g, 1.91 mmol) in dry, degassed toluene (2 mL) was added via a cannula. The mixture was then stirred at 80 °C for 20 minutes, before benzyl alcohol (0.418 g, 3.87 mmol) was added by syringe, and stirring was continued at 80 °C for 24 h. The reaction mixture was then cooled and filtered through a silica gel plug, which was washed with 150 mL ethyl acetate. The solution was then concentrated under reduced pressure and purified by column chromatography (EtOAc:pentane, 1:9 → 1:4). The product was obtained as a dark red liquid (0.32 g, 59%). Spectroscopic data were in accordance with earlier reported results,^[39] and are presented in appendix Y.2. R_f (pentane:EtOAc, 4:1) 0.51. ¹H NMR (300 MHz, CDCl₃): δ 7.50-7.27 (m, 5H, Bn), 6.71 (s, 2H, Ar), 5.0 (s, 2H, O-CH₂), 3.46 (bs, 2H, NH₂), 3.01-2.87 (sep, 2H, *J* 6.8 Hz, CH), 1.24 (d, 12H, *J* 6.8 Hz, CH₃).

(N,N'E,N,N'E)-N,N'-(pyridine-2,6-diylbis(methanylylidene))bis(4-(benzyloxy)-2,6-diisopropylaniline) (L)

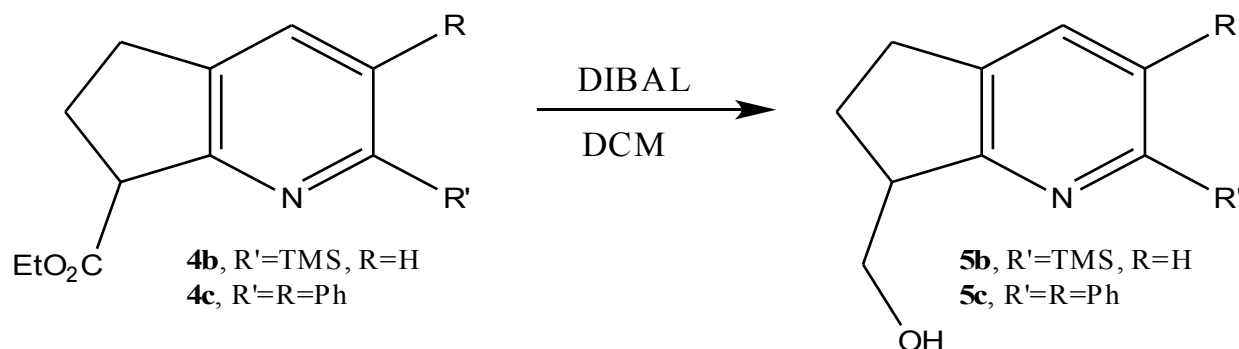


4-Benzyloxy-2,6-diisopropylaniline (0.32 g, 1.13 mmol), 2,6-pyridinedicarboxaldehyde (78.5 mg, 0.581 mmol) and 5 drops of concentrated acetic acid solution (>99 % purity) was dissolved in ethanol (5 mL), and stirred at room temperature for 20 h. The reaction mixture was cooled, then filtered and washed with cold ethanol (20 mL). The product was obtained as a yellow solid (0.31 g, 42%). Spectroscopic data were in accordance with earlier reported results,^[39] and are presented in appendix Y.3. R_f (pentane:EtOAc, 4:1) 0.59. $^1\text{H NMR}$ (300 MHz, CDCl_3): δ 8.38-8.34 (m, 4H, pyr-H), 7.98 (t, 1H, J 6.8 Hz, pyr-H), 7.49-7.32 (m, 10H, Bn), 6.81 (s, 4H, Ar), 5.07 (s, 4H), 3.06-2.97 (sep, 4H, J 6.8 Hz, CH), 1.17 (d, 24H, J 6.8 Hz, CH_3).

6.4 Resolution of enantiomers

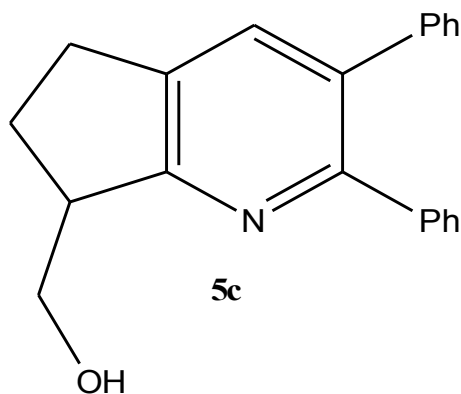
The overall strategy is presented in figure 3.6, and adapted from Pham et al.^[60]

General procedure for reduction of 4 to 5.



4 was dissolved in DCM (10 mL) under inert atmosphere and cooled to 0 °C. DIBAL was added slowly via syringe and the reaction mixture was stirred for 2 h at room temperature. A saturated solution of Rochell's salt (30 mL) was added and the solution was vigorously stirred for another 2 h. The organic layer was separated, and the aqueous phase was extracted with DCM. The combined organic phases was extracted with water and brine, dried over MgSO₄, and concentrated under reduced pressure. The crude was purified by column chromatography (EtOAc:pentane)

(2,3-Diphenyl-6,7-dihydro-5H-cyclopenta[b]pyridin-7-yl)methanol (**5c**)

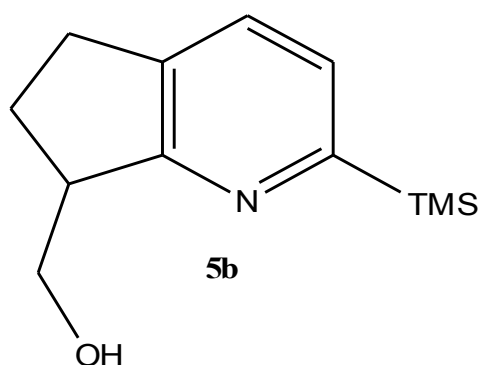


4c (0.14 g, 0.4 mmol) was reacted with DIBAL (1.8 mL, 1.8 mmol) according to the general procedure, and obtained as a white solid (60 mg, 50%). *R_f* (pentane:EtOAc, 1:1) 0.36. IR (neat):

3404 (b), 2939 (w), 1448 (w), 1423 (m), 1398 (w), 1074 (w), 1026 (w), 769 (m), 699 (s) cm^{-1} .

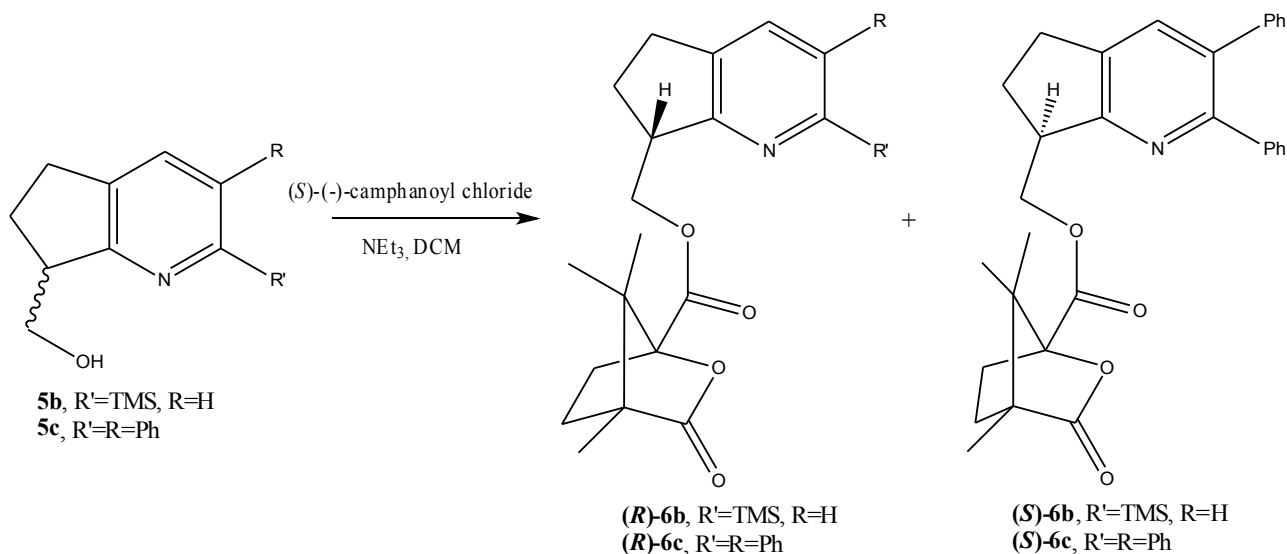
^1H NMR (400 MHz, CDCl_3): δ 7.56 (s, 1H, pyr-H), 7.33-7.29 (m, 2H, Ar), 7.27-7.23 (m, 3H, Ar), 7.23-7.18 (m, 3H, Ar), 7.17-7.12 (m, 2H, Ar), 4.77 (bs, 1H, OH), 4.02-3.98 (m, 1H, O- CH_2), 3.88 (t, 1H, J 9.9 Hz O- CH_2), 3.56-3.48 (m, 1H, CH), 3.03-2.99 (m, 2H, CH_2), 2.38-2.30 (m, 1H, CH_2), 1.82-1.72 (m, 1H, CH_2). ^{13}C NMR (100 MHz, CDCl_3): δ 166.3 (NC), 154.9 (NC-Ph), 140.4 (NC(Ph)C), 140.1 (Ar_q), 135.7 (NCC $_q$), 135.1 (pyr- CH), 134.6 (Ar_q), 130.0 (Ar), 129.7 (Ar), 128.3 (Ar), 127.8 (Ar), 127.6 (Ar), 127.0 (Ar), 66.6 (O- CH_2), 46.0 (CH), 29.3 (CH_2), 26.3 (CH_2). HRMS (TOF ASAP+) m/z calcd. for $\text{C}_{21}\text{H}_{20}\text{NO}$ [$\text{M}+\text{H}$] $^+$: 302.1539, found 302.1542. Proton and carbon shift are assigned in chapter 5.9, and the spectras are given in appendix O.

(2-(Trimethylsilyl)-6,7-dihydro-5H-cyclopenta[b]pyridin-7-yl)methanol (**5b**)



4b (0.116 g, 0.44 mmol) was reacted with DIBAL (2.64 mL, 2.64 mmol) according to the general procedure, and obtained as a light yellow oil (47 mg, 48%). R_f (pentane:EtOAc, 2:1) 0.38. IR (neat): 3392 (b), 2955 (w), 1424 (w), 1247 (m), 1096 (w), 1032 (w), 885 (w), 838 (s), 748 (m) cm^{-1} . ^1H NMR (400 MHz, CDCl_3): δ 7.44 (d, 1H, J 7.45 Hz, pyr-H), 7.31 (d, 1H, J 7.45 Hz, NC(SiMe_3)CH), 5.55 (bs, 1H, OH), 3.99-3.94 (m, 1H, O- CH_2), 3.77 (t, 1H, J 10.3 Hz, O- CH_2), 3.5-3.4 (m, 1H, CH), 2.94-2.88 (m, 2H, CH_2), 2.27-2.18 (m, 1H, CH_2), 1.65-1.54 (m, 1H, CH_2), 0.29 (s, 9H, SiMe_3). ^{13}C NMR (100 MHz, CDCl_3): δ 168.1 (NC), 164.8 (NC SiMe_3), 136.2 (NCC $_q$), 130.7 (pyr- CH), 127.1 (NC(SiMe_3)CH), 67.0 (O- CH_2), 45.6 (CH), 29.7 (CH_2), 25.9 (CH_2), -1.7 (SiMe_3). HRMS (TOF ASAP+) m/z calcd. for $\text{C}_{12}\text{H}_{20}\text{NOSi}$ [$\text{M}+\text{H}$] $^+$: 222.1309, found 222.1315. Proton and carbon shift are assigned in chapter 5.10, and the spectras are given in appendix N.

Preparation of diastereomers



(1*S*,4*S*)-((*S*)-2,3-diphenyl-6,7-dihydro-5*H*-cyclopenta[*b*]pyridin-7-yl)methyl 4,7,7-trimethyl-3-oxo-2-oxabicyclo[2.2.1]heptane-1-carboxylate ((*S*)-6c) and
(1*S*,4*S*)-((*R*)-2,3-diphenyl-6,7-dihydro-5*H*-cyclopenta[*b*]pyridin-7-yl)methyl 4,7,7-trimethyl-3-oxo-2-oxabicyclo[2.2.1]heptane-1-carboxylate ((*R*)-6c)

The alcohol **5c** (60 mg, 0.2 mmol) was dissolved in DCM (5 ml), and NEt₃ (0.2 mL) and (*S*)-camphanic chloride in DCM (5 mL) was cannulated to the alcohol at 0 °C. The reaction was stirred at room temperature for 48 h, then added ice water (10 mL), extracted with DCM (3x5 mL), washed with NaHCO₃ (10 mL 5% solution) and water (10 mL), dried over MgSO₄ and concentrated under reduced pressure. The crude product was purified by column chromatography (hexane:Et₂O:EtOH, 10:1:0.5) and the products were obtained as a 1:1 diastereomeric mixture (by ¹H NMR) of waxy white crystals (31 mg, 32%). It was then further purified by preparative TLC (hexane:Et₂O:EtOH, 10:1:0.5, nine elutions), and the diastereomers was obtained with enough purity so that structure elucidation by ¹H NMR could be conducted. Polarimetry was not performed since ¹H NMR showed a mixture of diastereomers. The absolute stereochemistry were not decided, so the following data can not be assigned to the names; instead they are named Fraction 1 (lowest R_f-value) and Fraction 2 (Highest R_f-value). MS was taken of the mixture of diastereomers and are given at the end. Proton and carbon shift are assigned in chapter 5.12, and the spectras are given in appendix R and S.

Fraction 1

R_f (hexane:Et₂O:EtOH, 10:1:1) 0.088. IR (neat): 2927 (w), 2360 (w), 1798 (s), 1752 (m), 1444 (w), 1271 (m), 1170 (m), 1107 (m), 1063 (m), 770 (w), 700 (m) cm⁻¹. ¹H NMR (400 MHz, CDCl₃): δ 7.56 (1H, s, pyr-H), 7.33-7.12 (10H, m, Ar), 4.69 (2H, d, *J* 6.3 Hz, O-CH₂), 3.73-3.63 (m, 1H, CH), 3.12-2.95 (m, 2H, CH₂), 2.54-2.42 (m, 1H, CH₂), 2.38-2.29 (m, 1H, camp CH₂), 2.15-2.03 (m, 1H, CH₂), 2.02-1.92 (m, 1H, camp CH₂), 1.89-1.80 (m, 1H, camp CH₂), 1.69-1.59 (m, 1H, camp CH₂), 1.08 (s, 3H, CH₃), 0.90 (s, 3H, bridge CH₃), 0.88 (s, 3H, bridge CH₃). ¹³C NMR (100 MHz, CDCl₃): δ 178.18 (C=O ring), 167.42 (C=O), 162.27 (NC), 155.90 (NC-Ph), 140.43 (C-Ph), 140.30 (Ar_q), 135.90 (NCC_q), 134.94(pyr-CH), 134.64 (Ar_q), 130.00 (Ar), 129.62 (Ar), 128.27 (Ar), 127.81 (Ar), 127.53 (Ar), 127.01 (Ar), 91.21 (OC=OC_q), 67.65 (O-CH₂), 54.75 (OC=OC_q ring), 54.07 (C_q bridge), 44.64 (CH), 30.61 (camp CH₂), 28.90 (camp CH₂), 28.80 (CH₂), 27.55 (CH₂), 16.67 (bridge CH₃), 16.55 (bridge CH₃), 9.71 (CH₃).

Fraction 2

R_f (hexane:Et₂O:EtOH, 10:1:1) 0.11. IR (neat): 2961 (w), 2360 (m), 1789 (s), 1392 (w), 1271 (w), 1168 (w), 1104 (m), 1062 (m), 1018 (w), 770 (w), 700 (s) cm⁻¹. ¹H NMR (400 MHz, CDCl₃): δ 7.54 (s, 1H, pyr-H), 7.31-7.11 (m, 10H, Ar), 4.74 (dd, 1H, *J* 10.9 6.8 Hz, O-CH₂), 4.66 (dd, 1H, *J* 10.9 3.9 Hz, O-CH₂), 3.72-3.63 (m, 1H, CH), 3.15-2.04 (m, 2H, CH₂), 2.53-2.43 (m, 1H, CH₂), 2.42-2.33 (m, 1H, camp CH₂), 2.17-2.06 (m, 1H, CH₂), 2.04-1.94 (m, 1H, camp CH₂), 1.91-1.81 (m, 1H, camp CH₂), 1.69-1.60 (m, 1H, camp CH₂), 1.06 (s, 3H, CH₃), 0.95 (s, 3H, bridge CH₃), 0.72 (s, 3H, bridge CH₃). ¹³C NMR (100 MHz, CDCl₃): 178.25 (C=O ring), 167.46 (C=O), 162.23 (NC), 155.75 (NC-Ph), 140.44 (C-Ph), 140.36 (Ar_q), 136.13 (NCC_q), 134.91 (pyr-CH), 134.61 (Ar_q), 129.98 (Ar), 129.62 (Ar), 128.24 (Ar), 127.81 (Ar), 127.51 (Ar), 126.98 (Ar), 91.24 (OC=OC_q), 65.75 (O-CH₂), 54.76 (OC=OC_q ring), 54.05 (C_q bridge), 44.67 (CH), 30.52 (camp CH₂), 28.92 (camp CH₂), 28.83 (CH₂), 27.55 (CH₂), 16.62 (bridge CH₃), 16.41 (bridge CH₃), 9.73 (CH₃).

HRMS (TOF ASAP+) *m/z* calcd. for C₃₁H₃₂NO₄ [M+H]⁺: 482.2326, found 482.2329.

(1*S*,4*S*)-((*S*)-2-(trimethylsilyl)-6,7-dihydro-5*H*-cyclopenta[*b*]pyridin-7-yl)methyl 4,7,7-trimethyl-3-oxo-2-oxabicyclo[2.2.1]heptane-1-carboxylate ((*S*)-6b) and
(1*S*,4*S*)-((*R*)-2-(trimethylsilyl)-6,7-dihydro-5*H*-cyclopenta[*b*]pyridin-7-yl)methyl 4,7,7-trimethyl-3-oxo-2-oxabicyclo[2.2.1]heptane-1-carboxylate ((*R*)-6b)

The alcohol **5b** (47 mg, 0.212 mmol) was dissolved in DCM (5 ml), and cannulated over to a dry round-flask containing DMAP (20 mg, 0.164 mmol). NEt₃ (0.1 mL) and (*S*)-camphonic chloride 0.75 g, 3.46 mmol) in DCM (5 mL) was added through a septum at 0 °C. The reaction was then stirred at room temperature for 22 h, then added ice water (10 mL), extracted with DCM (3x5 mL), washed with NaHCO₃ (10 mL 5% solution) and water (10 mL), dried over MgSO₄ and concentrated under reduced pressure. The crude product was first purified by column chromatography (EtOAc:pentane, 1:4) and the product obtained as a 1:1 diastereomeric mixture (40 mg, 47%). It was then further purified by preparative TLC (EtOAc:pentane, 1:4, three elutions) and the products was obtained as waxy solids (8.7 mg and 7.9 mg plus and intermediate mixture of 9 mg) so that rotation of the compounds could be conducted. The absolute stereochemistry were not decided, so the following data can not be assigned to the names; instead they are named Fraction 1 (lowest R_f-value) and Fraction 2 (Highest R_f-value). MS was taken of the mixture of diastereomers and are given at the end. Proton and carbon shift are assigned in chapter 5.11, and the spectras are given in appendix P and Q.

Fraction 1

R_f(pentane:EtOAc, 2:1) 0.47. [α]_D²⁰=29 (c=0.87, DCM). IR (neat): 2956 (w), 2358 (w), 1789 (s), 1753 (m), 1263 (w), 1170 (w), 1107 (m), 1062 (m), 839 (s), 733 (m) cm⁻¹. ¹H NMR (400 MHz, CDCl₃): δ 7.41 (d, 1H, *J* 7.55 Hz, pyr-H), 7.28 (d, 1H, *J* 7.55 Hz, NC(SiMe₃)CH), 4.67 (dd, 1H, *J* 10.9 3.9 Hz, O-CH₂), 4.52 (dd, 1H, *J* 10.9 7.15 Hz, O-CH₂), 3.62-3.54 (m, 1H, CH), 3.0-2.83 (m, 2H, CH₂), 2.42-2.34 (m, 1H, CH₂), 2.33-2.27 (m, 1H, camp CH₂), 2.03-2.02 (m, 1H, camp CH₂), 2.02-1.94 (m, 1H, CH₂), 1.91-1.82 (m, 1H, camp CH₂), 1.70-1.61 (m, 1H, camp CH₂), 1.08 (s, 3H, CH₃), 0.90 (s, 3H, bridge CH₃), 0.83 (s, 3H, bridge CH₃), 0.28 (s, 9H, SiMe₃). ¹³C NMR (100 MHz, CDCl₃): δ 178.2 (C=O ring), 167.4 (C=O), 165.9 (NC-SiMe₃), 163.4 (NC), 136.3 (NCC_q), 130.3 (pyr-CH), 127.0 (NC(SiMe₃)CH), 91.2 (OC=OC_q), 67.8 (O-CH₂), 54.7 (OC=OC_q ring), 54.0 (C_q bridge), 44.8 (CH), 30.6 (camp CH₂), 29.0 (CH₂), 29.0 (camp CH₂), 27.2 (CH₂), 16.7 (bridge CH₃), 16.5 (bridge CH₃), 9.7 (CH₃), -1.6 (SiMe₃).

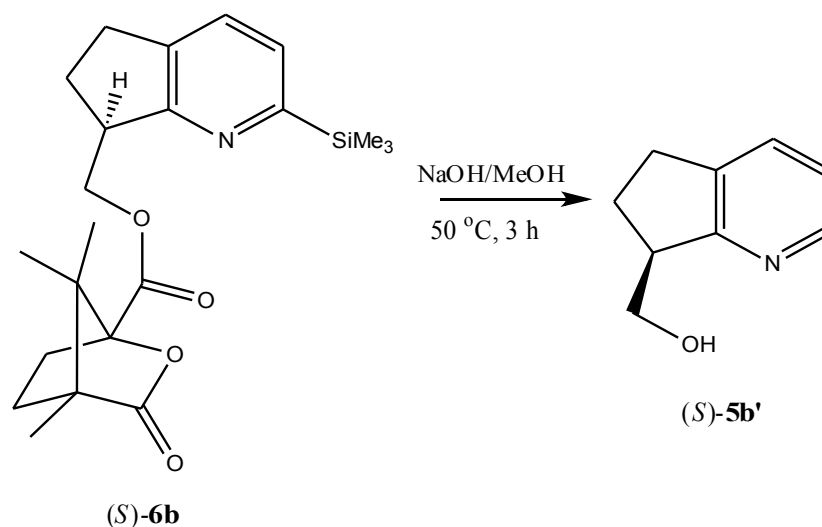
Fraction 2

R_f (pentane:EtOAc, 2:1) 0.53. $[\alpha]_D^{20} = -41$ ($c=0.79$, DCM). IR (neat): 2951 (w), 2353 (w), 1790(s), 1733 (w), 1264 (w), 1167 (w), 1105 (m), 1062 (m), 839 (s) cm^{-1} . ^1H NMR (400 MHz, CDCl_3): δ 7.40 (d, 1H, J 7.48 Hz, pyr-H), 7.27 (d, 1H, J 7.48 Hz, $\text{NC}(\text{SiMe}_3)\text{CH}$), 4.63 (d, 2H, J 5.12 Hz, O- CH_2), 3.62-3.54 (m, 1H, CH), 3.03-2.83 (m, 2H, CH_2), 2.42-2.35 (m, 1H, CH_2), 2.35-2.30 (m, 1H, camp CH_2), 2.04-1.99 (m, 1H, CH_2), 1.99-1.94 (m, 1H, camp CH_2), 1.91-1.82 (m, 1H, camp CH_2), 1.71-1.60 (m, 1H, camp CH_2), 1.07 (s, 3H, CH_3), 0.94 (s, 3H, bridge CH_3), 0.68 (s, 3H, bridge CH_3), 0.28 (s, 9H, SiMe_3). ^{13}C NMR (100 MHz, CDCl_3): δ 178.1 (C=O ring), 167.4 (C=O), 165.6 (NCSiMe_3), 163.2 (NC), 136.4 (NCC_q), 130.2 (pyr- CH), 126.8 ($\text{NC}(\text{SiMe}_3)\text{CH}$), 91.3 (OC=OC_q), 68.0 (O- CH_2), 54.6 (OC=OC_q ring), 53.8 (C_q bridge), 44.6 (CH), 30.3 (camp CH_2), 29.0 (CH_2), 28.8 (camp CH_2), 27.1 (CH_2), 16.5 (bridge CH_3), 16.3 (bridge CH_3), 9.6 (CH_3), -1.8 (SiMe_3).

HRMS (TOF ASAP+) m/z calcd. for $\text{C}_{22}\text{H}_{32}\text{NO}_4\text{Si}$ $[\text{M}+\text{H}]^+$: 402.2095, found 402.2099.

Hydrolysis of (*S*)-**6b** and (*R*)-**6b**

(*S*)-(2-(trimethylsilyl)-6,7-dihydro-5H-cyclopenta[*b*]pyridin-7-yl)methanol (*S*)-**5b**
and (*R*)-(2-(trimethylsilyl)-6,7-dihydro-5H-cyclopenta[*b*]pyridin-7-yl)methanol (*R*)-**5b**



The respective diastereomer was heated in NaOH (1 mL, 1M) and MeOH (5 mL) for 3 h. Methanol was removed on the rotavapor, and the water phase was extracted with DCM (3x5 mL). The combined organic phases was washed with NH₄Cl (10 mL saturated solution) and water (10 mL), then dried over MgSO₄. The solvent was removed and ¹H-NMR analysis was performed. In both cases, complete desilylation to **5b'** was observed. Obtained yields with respect to desilylation; 3.3 mg, 100 % and 1.1 mg, 37 %. [α]_D²⁰ = 3.64 (c=0.33, DCM), [α]_D²⁰ = - 3.64 (c=0.11, DCM). Absolute stereochemistry were not assigned. Spectroscopic data were in accordance with earlier reported results,^[57] and are presented in appendix Z. ¹H NMR (300 MHz, CDCl₃): δ 8.43-8.27 (m, 1H, N-CH), 7.55-7.49 (m, 1H, pyr-H), 7.13-7.06 (m, 1H, pyr-H), 4.41-4.34 (m, 1H, CH₂-O), 4.02-3.89 (m, 1H, CH₂-O), 3.85-3.75 (m, 1H, CH), 2.99-2.89 (m, 2H, CH₂), 2.33-2.21 (m, 1H, CH₂), 1.78-1.66 (m, 1H, CH₂).

References

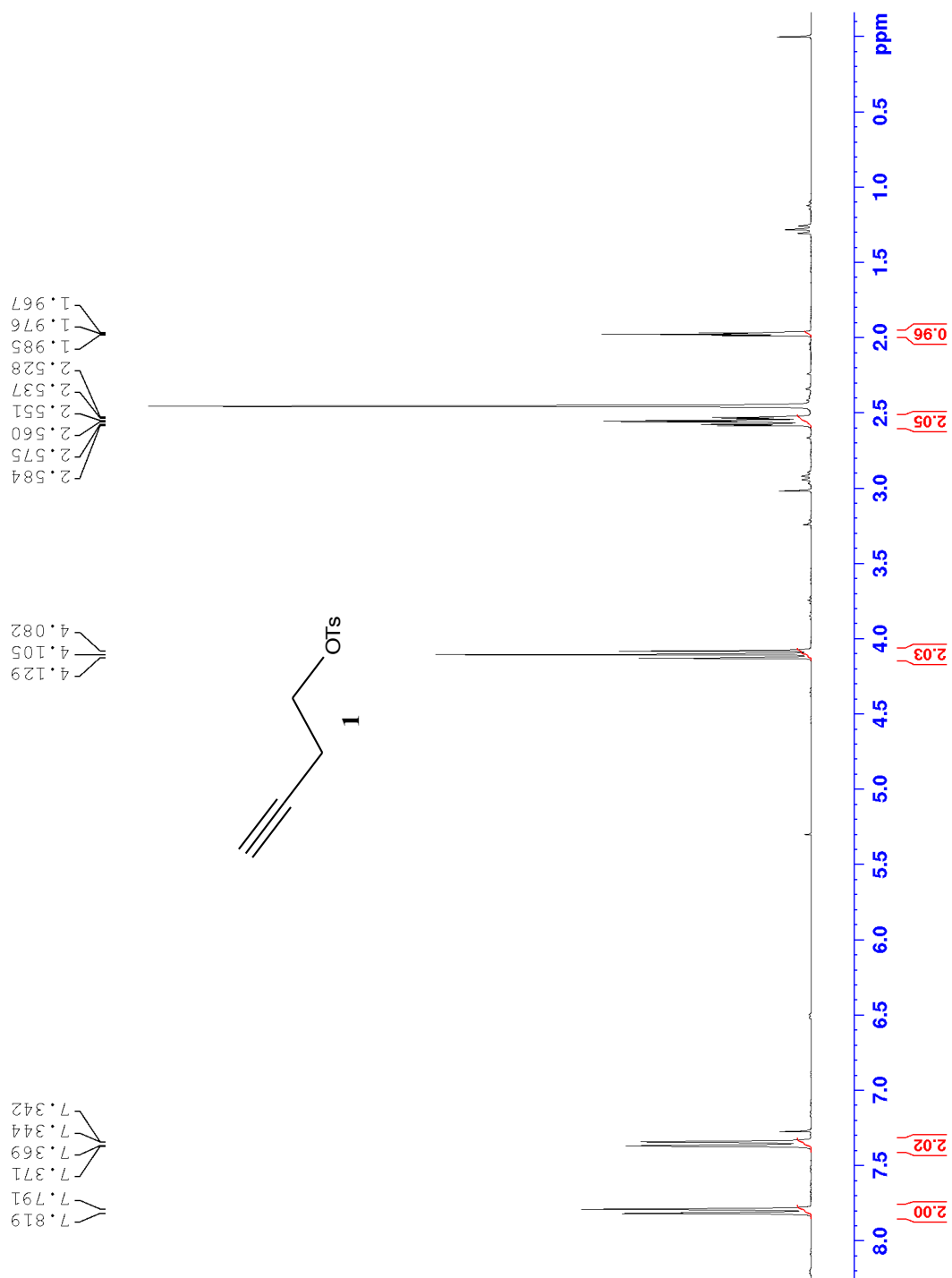
- [1] J. M. Brown, S. G. Davies, *Nature* **1989**, *342*, 631-636.
- [2] a) W. S. Knowles, *Angew. Chem., Int. Ed.* **2002**, *41*, 1998-2007; b) R. Noyori, *Angew. Chem., Int. Ed.* **2002**, *41*, 2008-2022.
- [3] D. H. Woodmansee, A. Pfaltz, *Top. Organomet. Chem.* **2011**, *34*, 31-76.
- [4] P. G. Andersson, Editor, *Iridium Catalysis. [In: Top. Organomet. Chem., 2011; 34]*, **2011**.
- [5] R. H. Crabtree, H. Felkin, G. E. Morris, *J. Organomet. Chem.* **1977**, *141*, 205-215.
- [6] S. Saiser, S. P. Smidt, A. Pfaltz, *Angew. Chem., Int. Ed.* **2006**, *45*, 5194-5197.
- [7] P. G. Andersson, *Unpublished results* **2013**.
- [8] a) P. R. Chopade, J. Louie, *Adv. Synth. Catal.* **2006**, *348*, 2307-2327; b) M. Lautens, W. Klute, W. Tam, *Chem. Rev.* **1996**, *96*, 49-92.
- [9] a) D. Astruc, *Organometallic chemistry and catalysis*, Springer, **2007**; b) R. H. Crabtree, *The organometallic chemistry of the transition metals*, 5. ed., Wiley, **2009**.
- [10] T. W. G. F. Solomons, Craig B. , *Organic chemistry*, 9 ed., Wiley, **2006**.
- [11] W. S. Knowles, *J. Chem. Educ.* **1986**, *63*, 222.
- [12] T. L. Church, P. G. Andersson, *Coord. Chem. Rev.* **2008**, *252*, 513-531.
- [13] X. Cui, K. Burgess, *Chem. Rev.* **2005**, *105*, 3272-3296.
- [14] P. Schnider, G. Koch, R. Pretot, G. Wang, F. M. Bohnen, C. Kruger, A. Pfaltz, *Chem.--Eur. J.* **1997**, *3*, 887-892.
- [15] A. Lightfoot, P. Schnider, A. Pfaltz, *Angew. Chem., Int. Ed.* **1998**, *37*, 2897-2899.
- [16] S. P. Smidt, N. Zimmermann, M. Studer, A. Pfaltz, *Chem.--Eur. J.* **2004**, *10*, 4685-4693.
- [17] R. Crabtree, *Acc. Chem. Res.* **1979**, *12*, 331-337.
- [18] J. A. Osborn, F. H. Jardine, J. F. Young, G. Wilkinson, *Journal of the Chemical Society A: Inorganic, Physical, Theoretical* **1966**, 1711-1732.
- [19] C. Mazet, S. P. Smidt, M. Meuwly, A. Pfaltz, *J. Am. Chem. Soc.* **2004**, *126*, 14176-14181.
- [20] P. Brandt, C. Hedberg, P. G. Andersson, *Chem.--Eur. J.* **2003**, *9*, 339-347.
- [21] R. Dietiker, P. Chen, *Angew. Chem., Int. Ed.* **2004**, *43*, 5513-5516.
- [22] S. J. Roseblade, A. Pfaltz, *C. R. Chim.* **2007**, *10*, 178-187.
- [23] Y. Fan, X. Cui, K. Burgess, M. B. Hall, *J. Am. Chem. Soc.* **2004**, *126*, 16688-16689.
- [24] K. Källström, I. Munslow, P. G. Andersson, *Chem.--Eur. J.* **2006**, *12*, 3194-3200.

- [25] T. L. Church, T. Rasmussen, P. G. Andersson, *Organometallics* **2010**, *29*, 6769-6781.
- [26] C. Hedberg, K. Källström, P. Brandt, L. K. Hansen, P. G. Andersson, *J. Am. Chem. Soc.* **2006**, *128*, 2995-3001.
- [27] P. Turek, M. Kotora, *Targets Heterocycl. Syst.* **2009**, *13*, 175-200.
- [28] J. A. Varela, C. Saa, *Chem. Rev.* **2003**, *103*, 3787-3801.
- [29] B. Heller, M. Hapke, *Chem. Soc. Rev.* **2007**, *36*, 1085-1094.
- [30] R. Diercks, B. E. Eaton, S. Gürtzgen, S. Jalisatgi, A. J. Matzger, R. H. Radde, K. P. C. Vollhardt, *J. Am. Chem. Soc.* **1998**, *120*, 8247-8248.
- [31] J. H. Hardesty, J. B. Koerner, T. A. Albright, G.-Y. Lee, *J. Am. Chem. Soc.* **1999**, *121*, 6055-6067.
- [32] R. L. Hillard, III, K. P. C. Vollhardt, *J. Am. Chem. Soc.* **1977**, *99*, 4058-4069.
- [33] B. E. Maryanoff, H.-C. Zhang, *ARKIVOC (Gainesville, FL, U. S.)* **2007**, 7-35.
- [34] L. P. McDonnell Bushnell, E. R. Evitt, R. G. Bergman, *J. Organomet. Chem.* **1978**, *157*, 445-456.
- [35] M. R. Shaaban, R. El-Sayed, A. H. M. Elwahy, *Tetrahedron* **2011**, *67*, 6095-6130.
- [36] B. Heller, B. Sundermann, C. Fischer, J. You, W. Chen, H.-J. Drexler, P. Knochel, W. Bonrath, A. Gutnov, *J. Org. Chem.* **2003**, *68*, 9221-9225.
- [37] C. Saa, D. D. Crotts, G. Hsu, K. P. C. Vollhardt, *Synlett* **1994**, 487-489.
- [38] D. J. Brien, A. Naiman, K. P. C. Vollhardt, *J. Chem. Soc., Chem. Commun.* **1982**, 133-134.
- [39] B. R. D'Souza, T. K. Lane, J. Louie, *Org. Lett.* **2011**, *13*, 2936-2939.
- [40] R. M. Beesley, C. K. Ingold, J. F. Thorpe, *J. Chem. Soc., Trans.* **1915**, *107*, 1080-1106.
- [41] J. A. Varela, L. Castedo, C. Saa, *Org. Lett.* **1999**, *1*, 2141-2143.
- [42] A. V. Naimann, K. P. C. , *Angew. Chem. Int. Edn Engl.* **1977**, *16*, 708-709.
- [43] N. Weding, M. Hapke, *Chem. Soc. Rev.* **2011**, *40*, 4525-4538.
- [44] R. Takeuchi, Y. Nakaya, *Org. Lett.* **2003**, *5*, 3659-3662.
- [45] C. Wang, X. Li, F. Wu, B. Wan, *Angew. Chem., Int. Ed.* **2011**, *50*, 7162-7166.
- [46] W. Schulz, H. Pracejus, G. Oehme, *Tetrahedron Lett.* **1989**, *30*, 1229-1232.
- [47] G. Belanger, M. Dupuis, R. Larouche-Gauthier, *J. Org. Chem.* **2012**, *77*, 3215-3221.
- [48] aG. Eglinton, M. C. Whiting, *J. Chem. Soc.* **1950**, 3650-3656; bB. M. Trost, A. Breder, B. Kai, *Org. Lett.* **2012**, *14*, 1708-1711.
- [49] E. C. Taylor, J. E. Macor, L. G. French, *J. Org. Chem.* **1991**, *56*, 1807-1812.
- [50] H. Finkelstein, *Ber. Dtsch. Chem. Ges.* **1910**, *43*, 1528-1532.
- [51] A. Mukherjee, R.-S. Liu, *Org. Lett.* **2011**, *13*, 660-663.

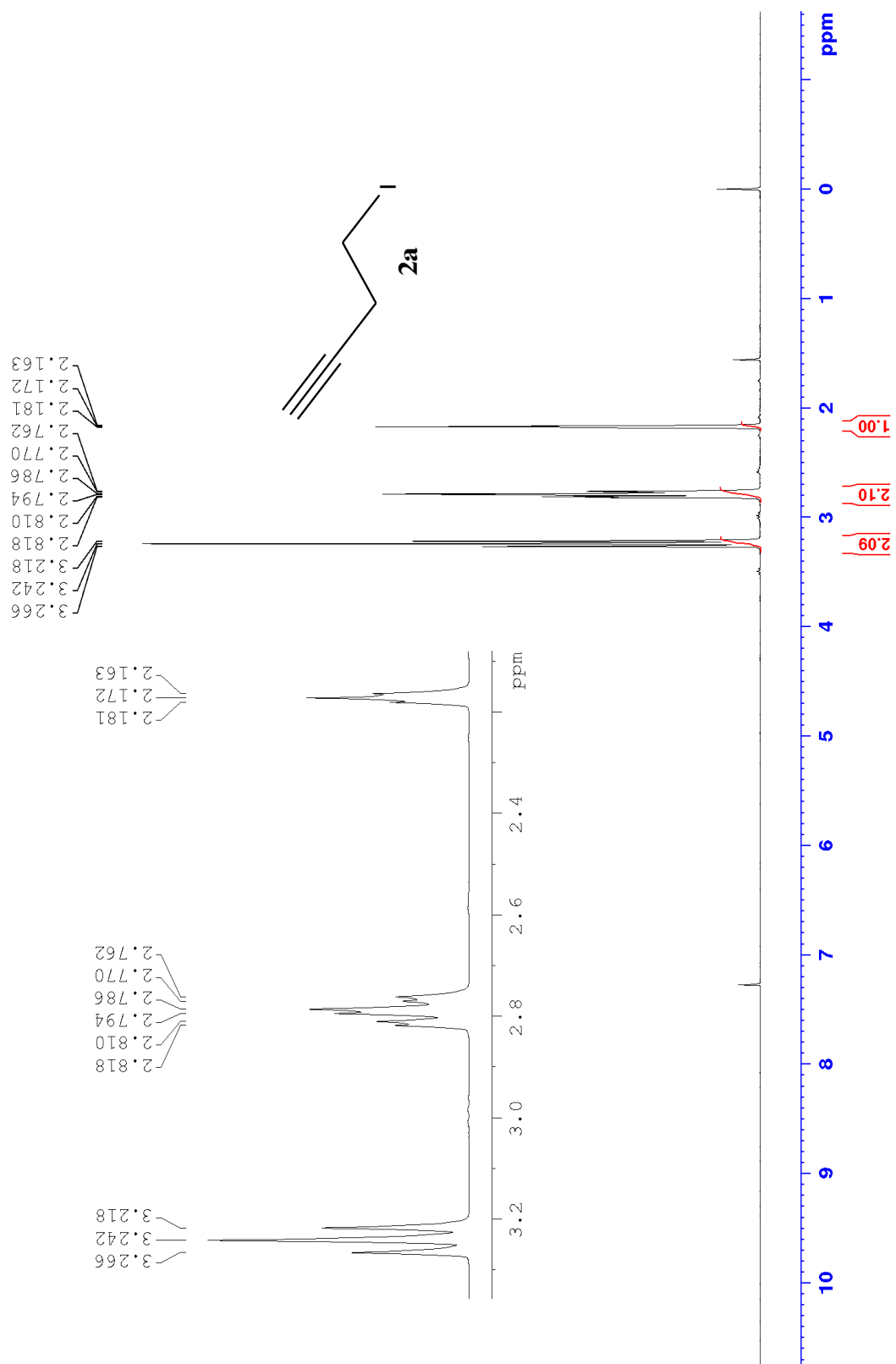
- [52] M. Helbæk, S. Kjelstrup, *Fysikalsk kjemi*, 2 ed., Fagbokforlaget, **2006**.
- [53] Y. Zou, Q.-Y. Liu, A. Deiters, *Org. Lett.* **2011**, *13*, 4352-4355.
- [54] M. Bröring, C. Kleeberg, *Synth. Commun.* **2008**, *38*, 3672-3682.
- [55] M. Ohashi, I. Takeda, M. Ikawa, S. Ogoshi, *J. Am. Chem. Soc.* **2011**, *133*, 18018-18021.
- [56] J. S. Viljoen, J. A. K. Du Plessis, *J. Mol. Catal.* **1993**, *79*, 75-84.
- [57] M. Hapke, N. Weding, A. Spannenberg, *Organometallics* **2010**, *29*, 4298-4304.
- [58] G. Chelucci, *Tetrahedron Asymmetry* **1995**, *6*, 811-826.
- [59] Y. Yamamoto, S. Okuda, K. Itoh, *Chem. Commun. (Cambridge, U. K.)* **2001**, 1102-1103.
- [60] V. C. Pham, A. Jossang, P. Grellier, T. Sevenet, V. H. Nguyen, B. Bodo, *J. Org. Chem.* **2008**, *73*, 7565-7573.
- [61] F. A. Carey, R. J. Sundberg, *Advanced organic chemistry Part B: Reaction and synthesis*, 5 ed., Springer, **2007**.
- [62] J. A. Varela, L. Castedo, C. Saa, *J. Org. Chem.* **1997**, *62*, 4189-4192.
- [63] S. Melnes, A. Bayer, O. R. Gautun, *Tetrahedron* **2012**, 8463-8471.
- [64] T. Gilchrist, *Heterocyclic chemistry*, 3 ed., Pearson Education, **1997**.

Appendixes

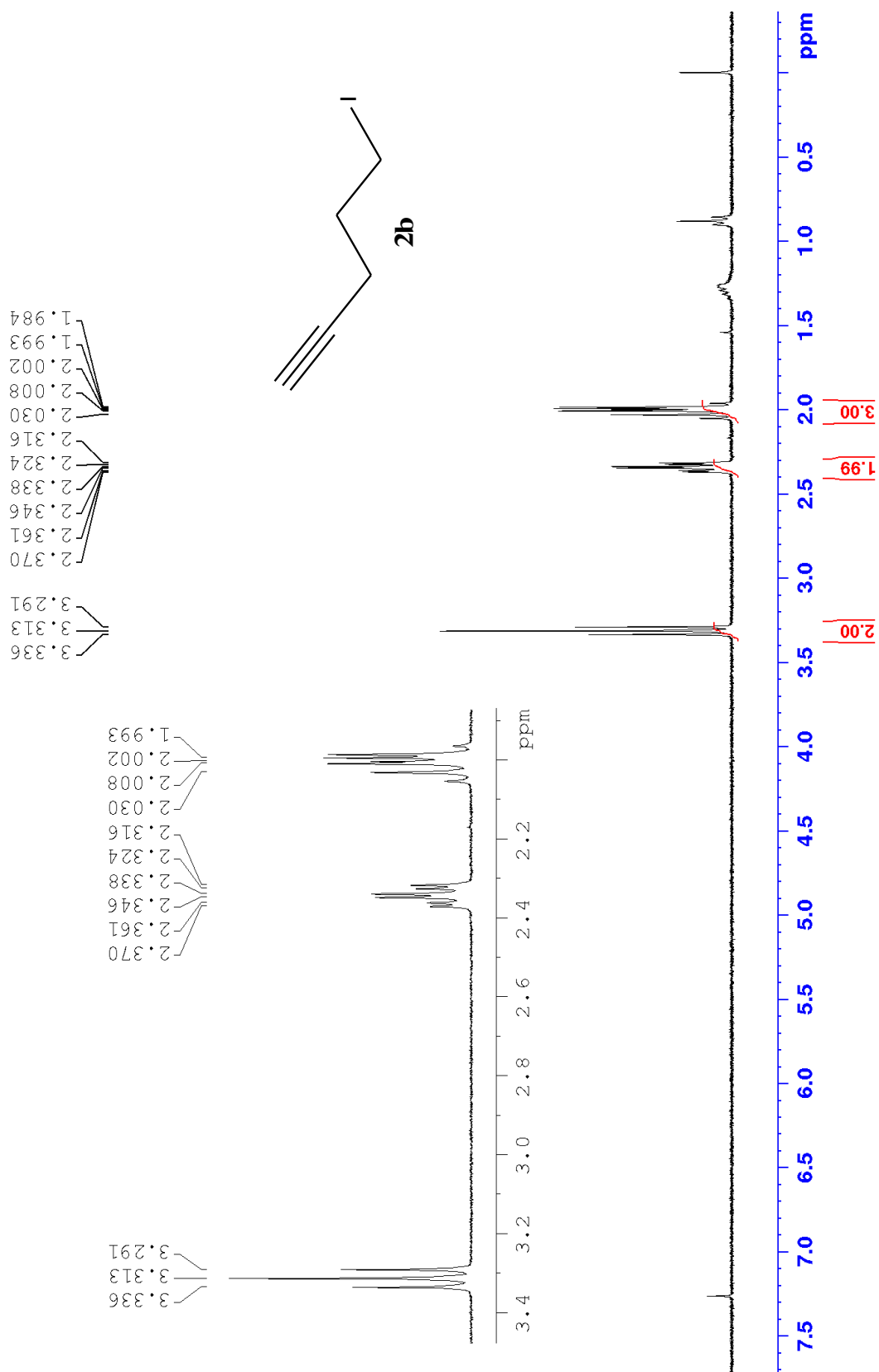
A.1 Proton of 1



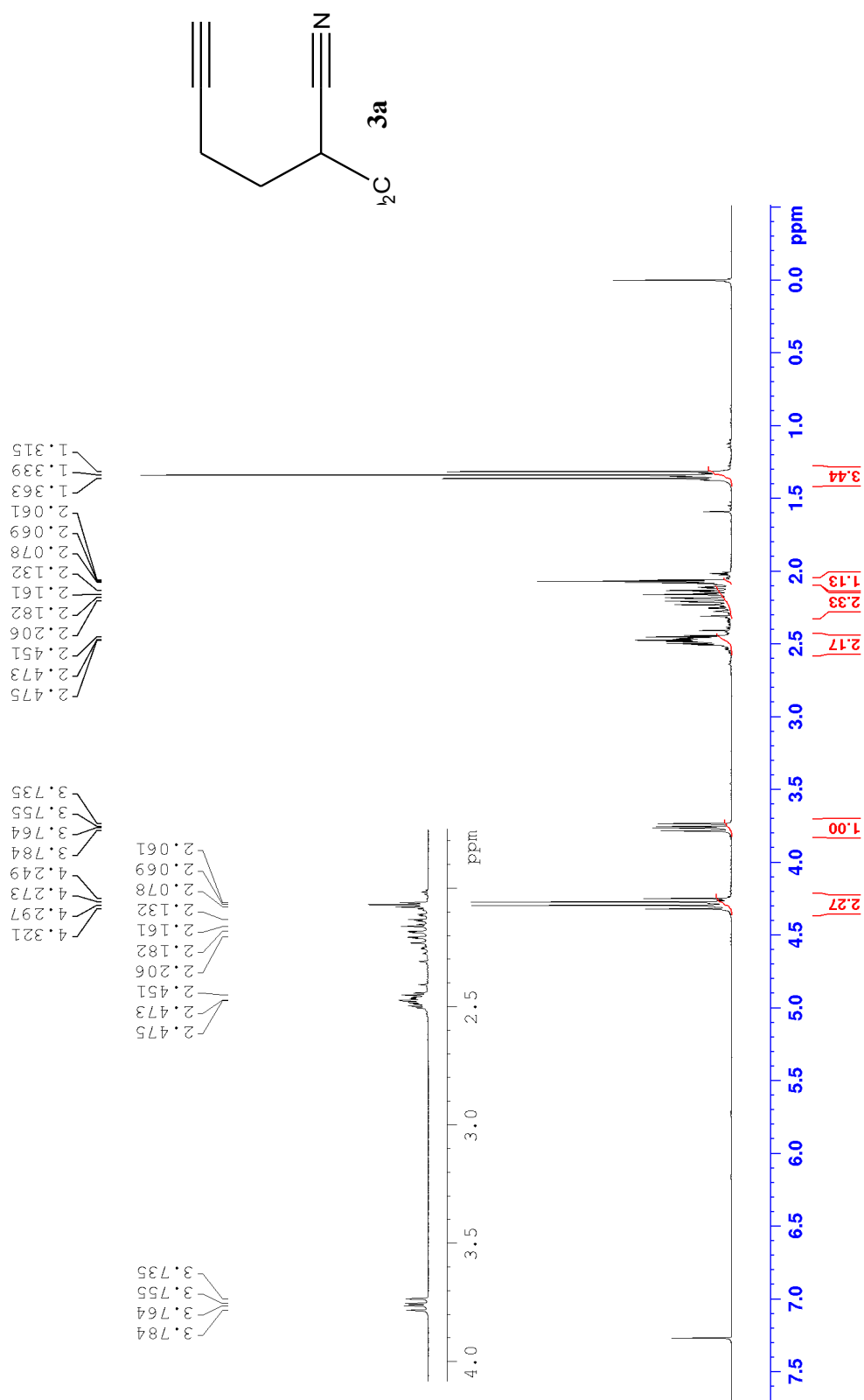
B.1 Proton of 2a



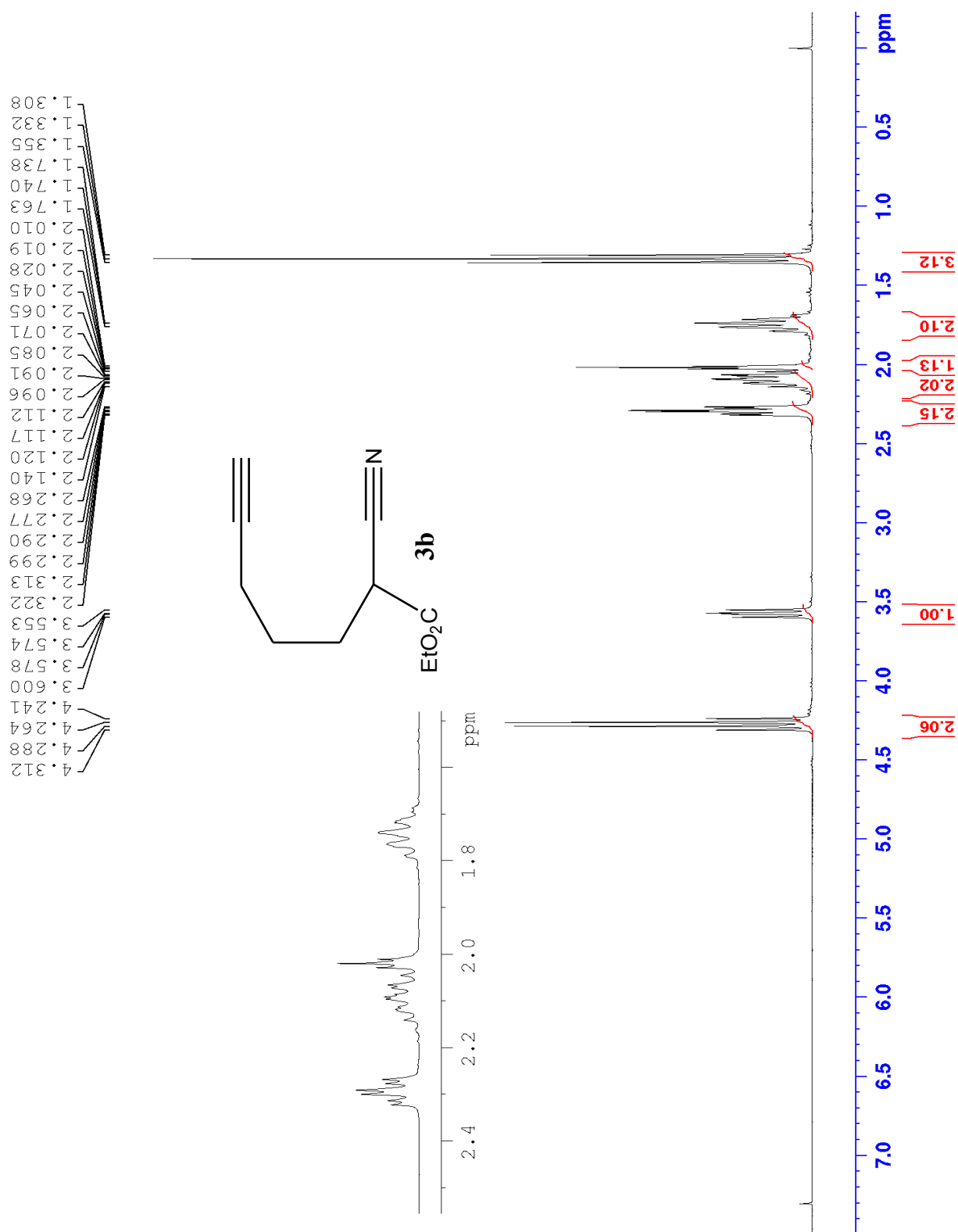
C.1 Proton NMR of 2b



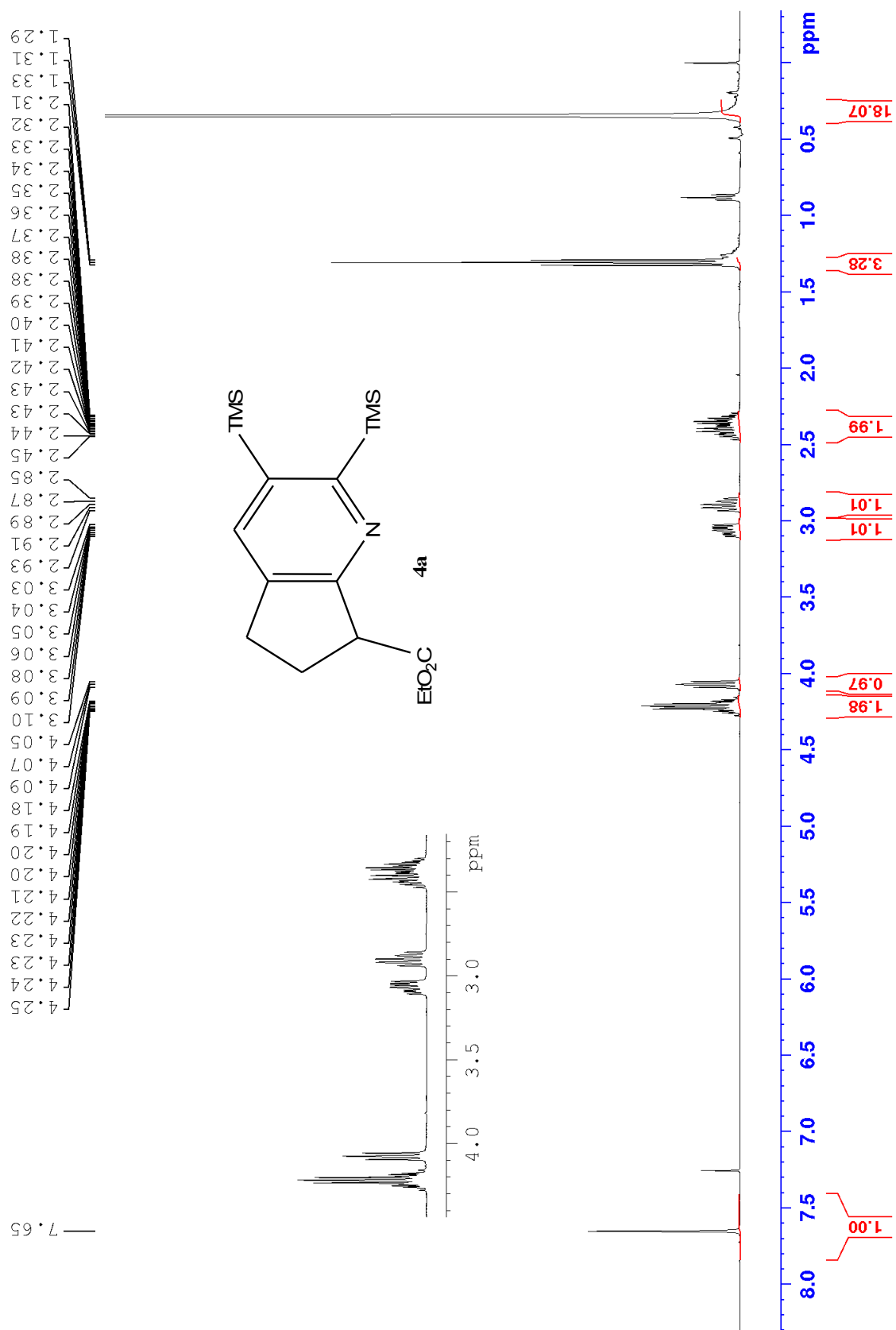
D.1 Proton NMR of 3a



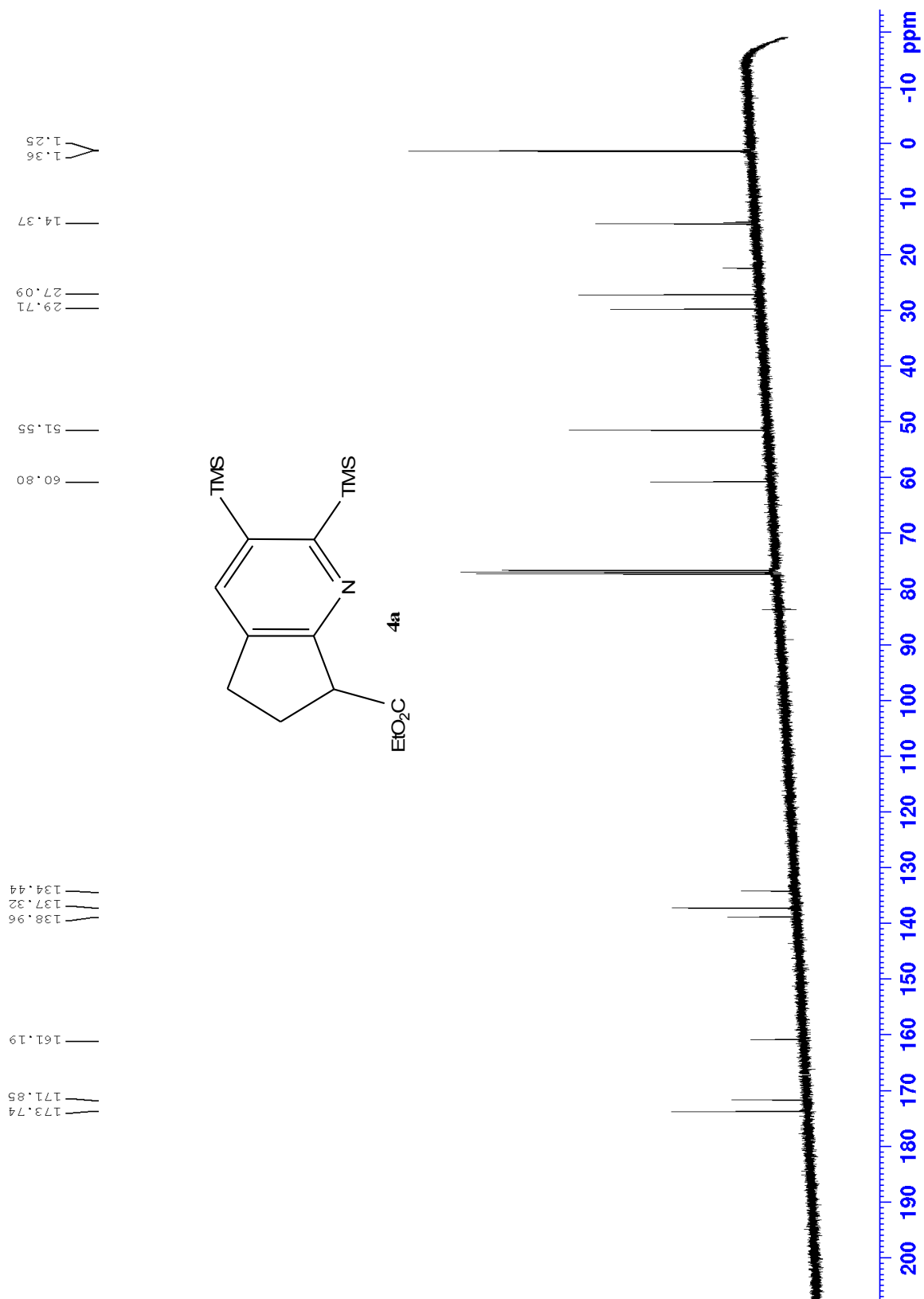
E.1 Proton NMR of 3b



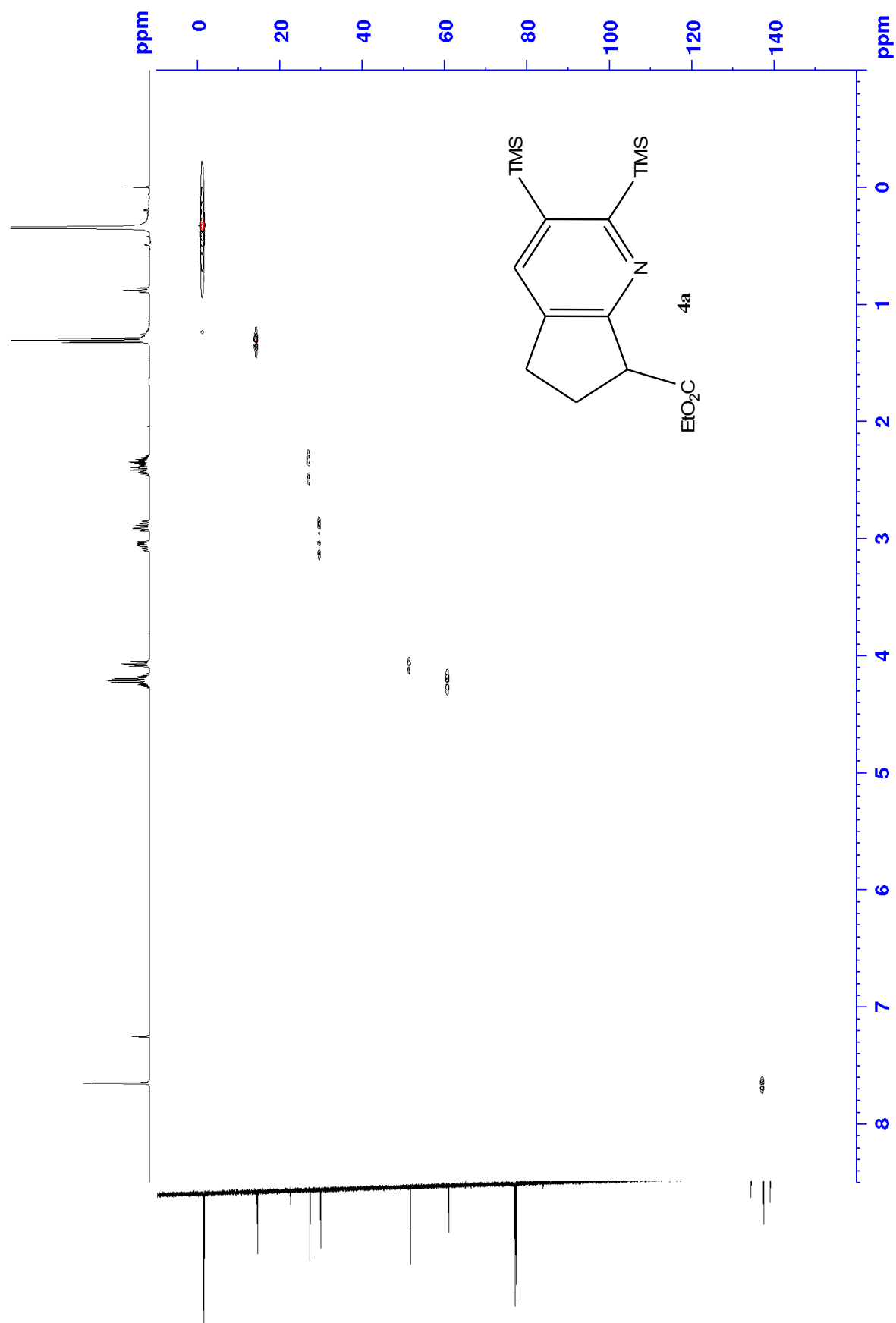
F.1 Proton NMR of 4a



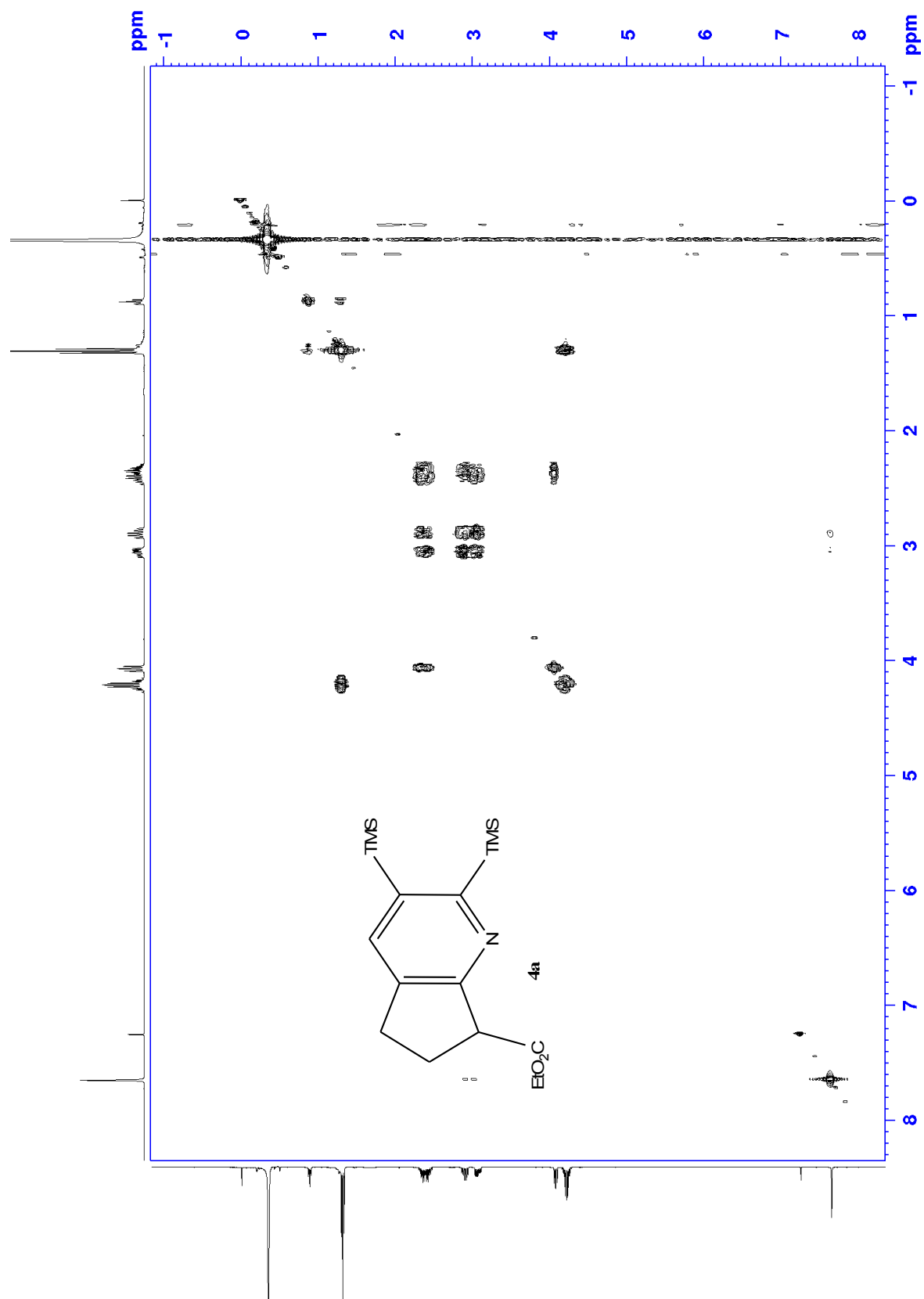
F.2 Carbon NMR of 4a



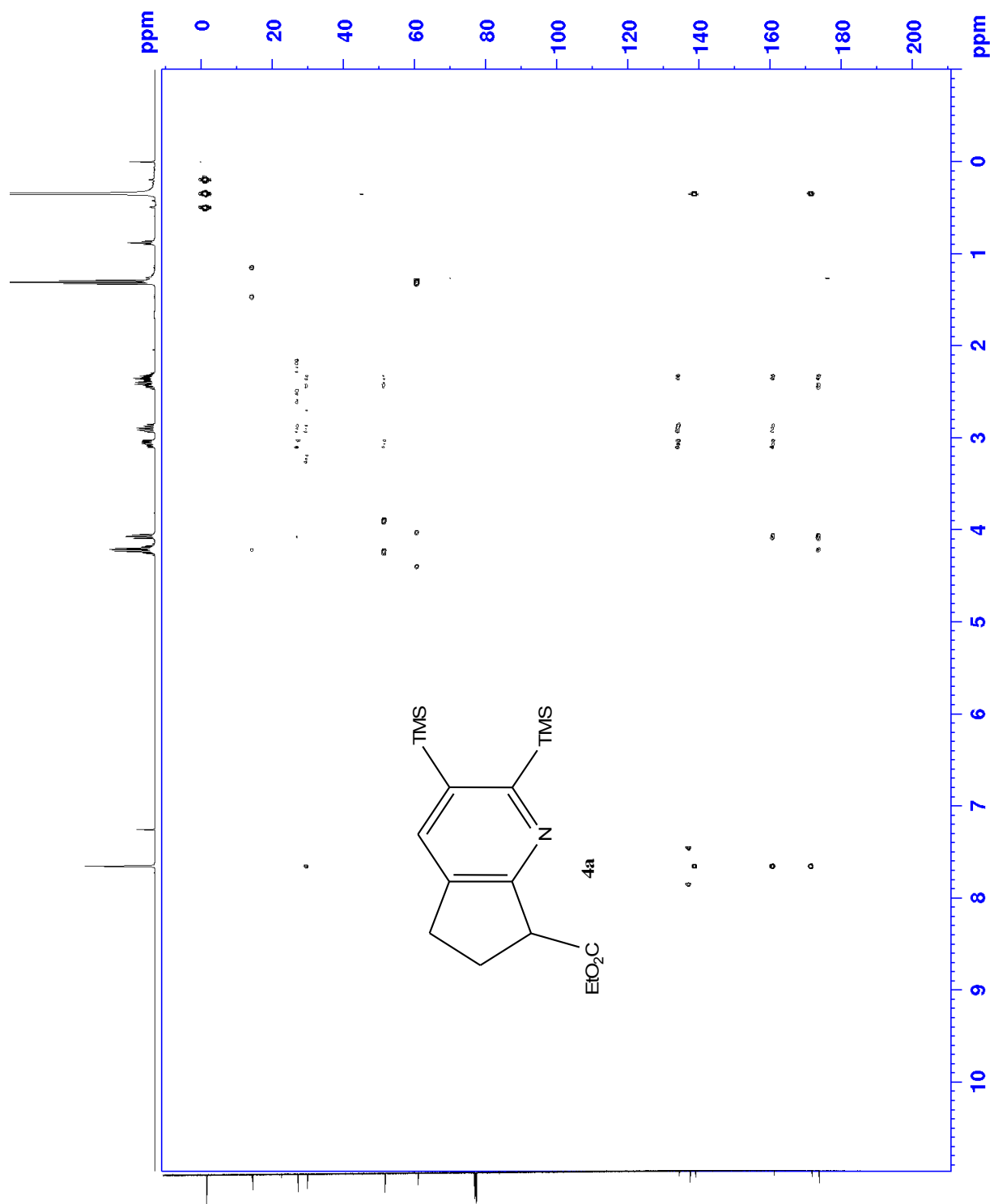
F.3 HSQC of 4a



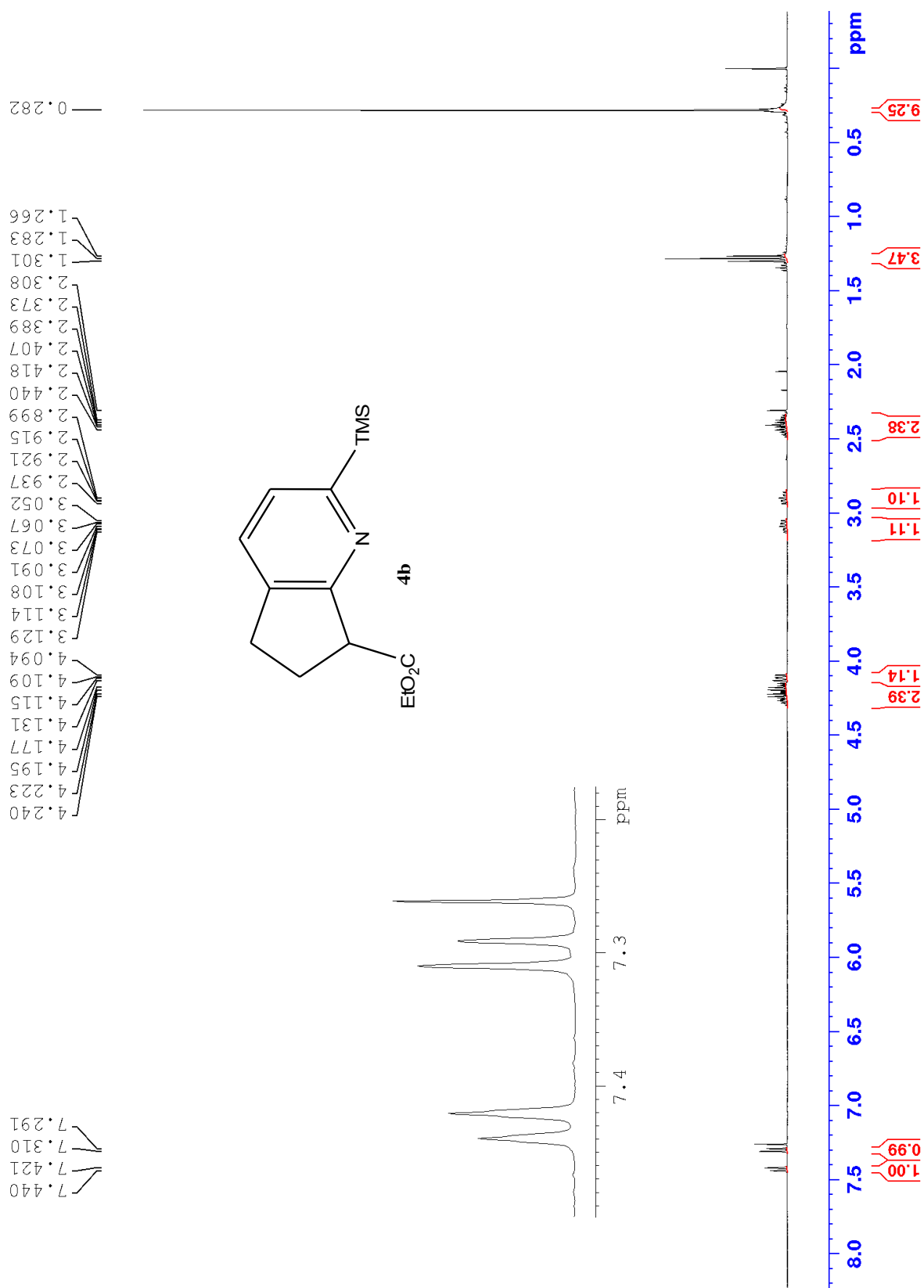
F.4 COSY of 4a



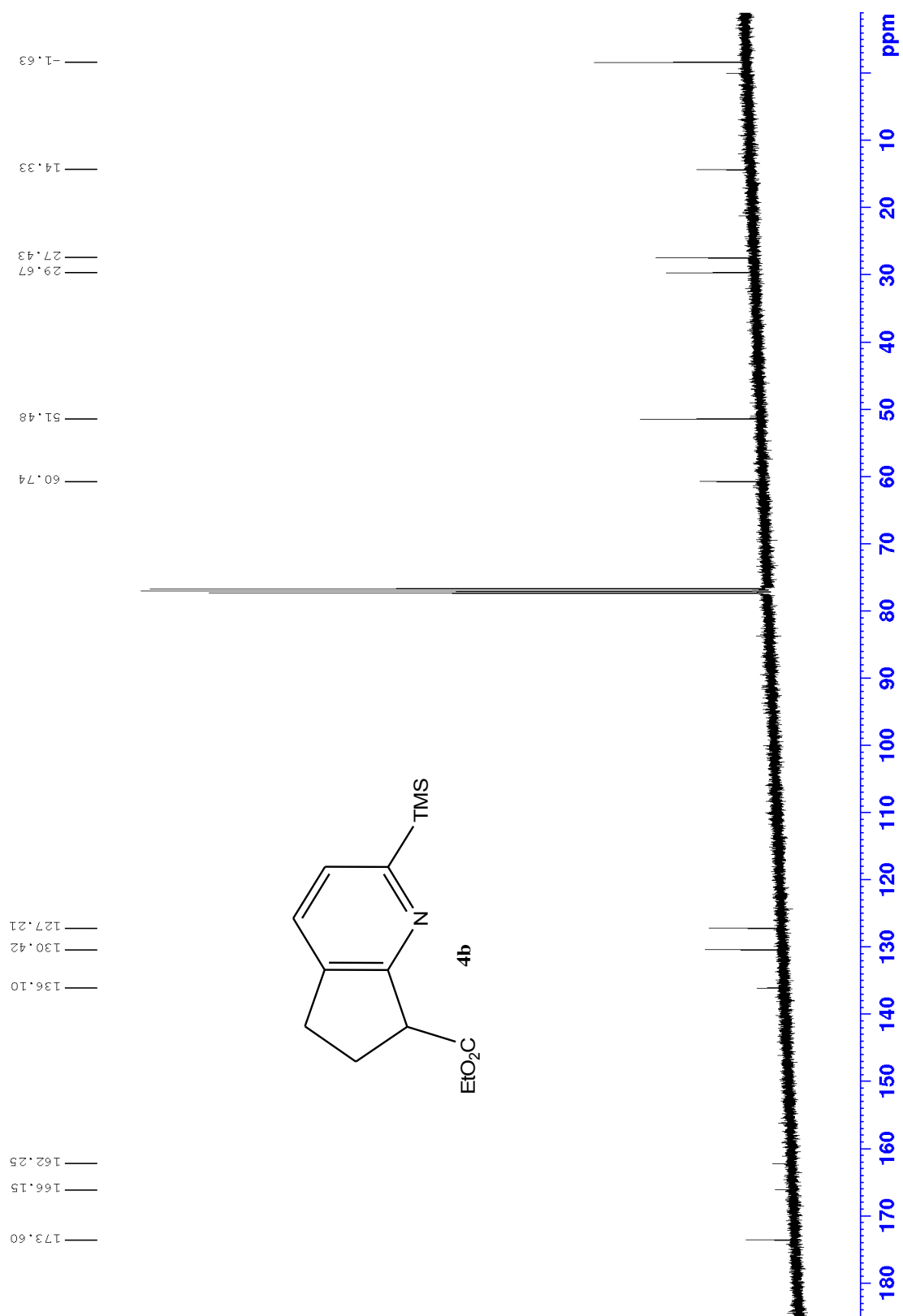
F.5 HMBC of 4a



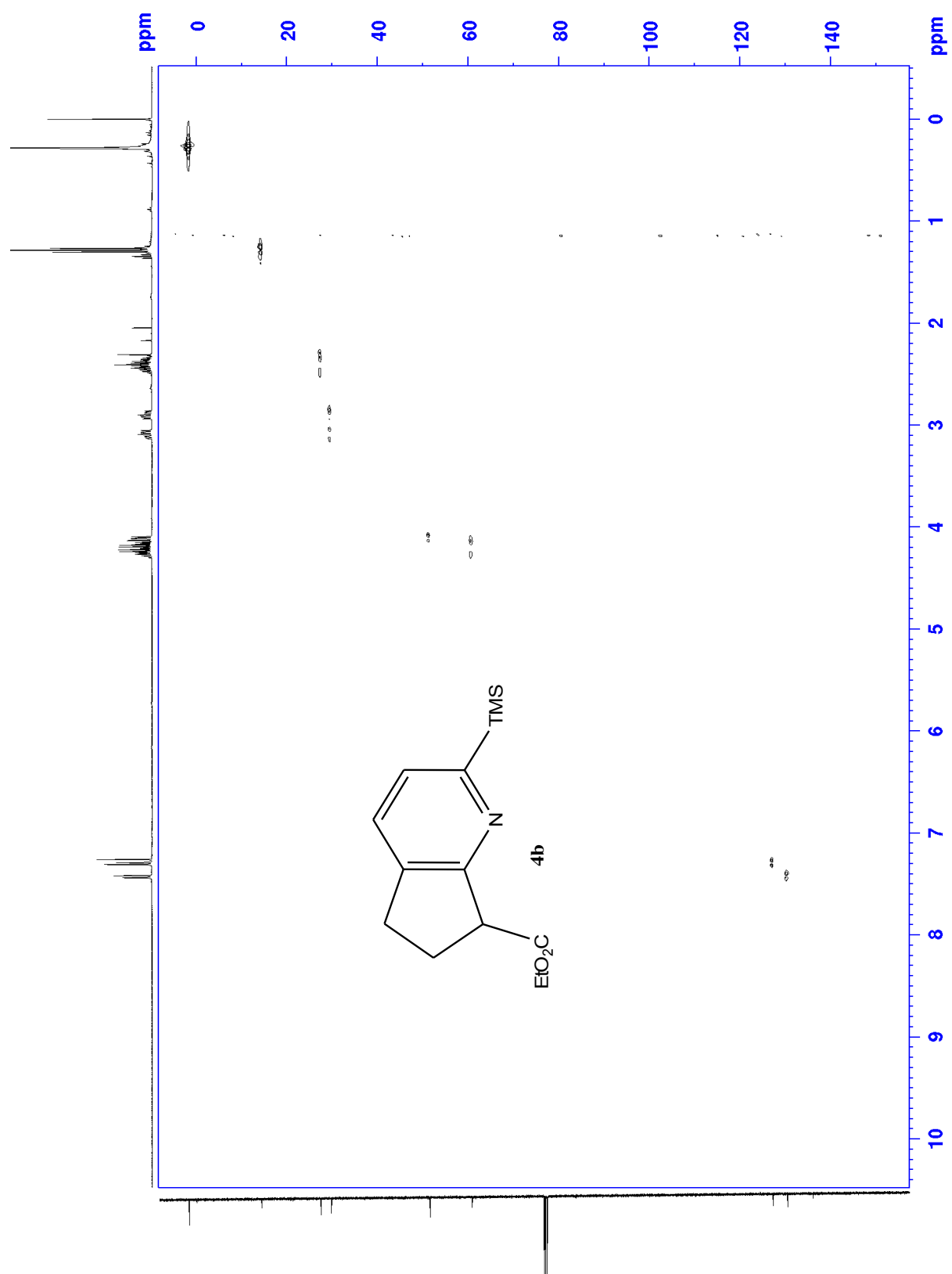
G.1 Proton of 4b



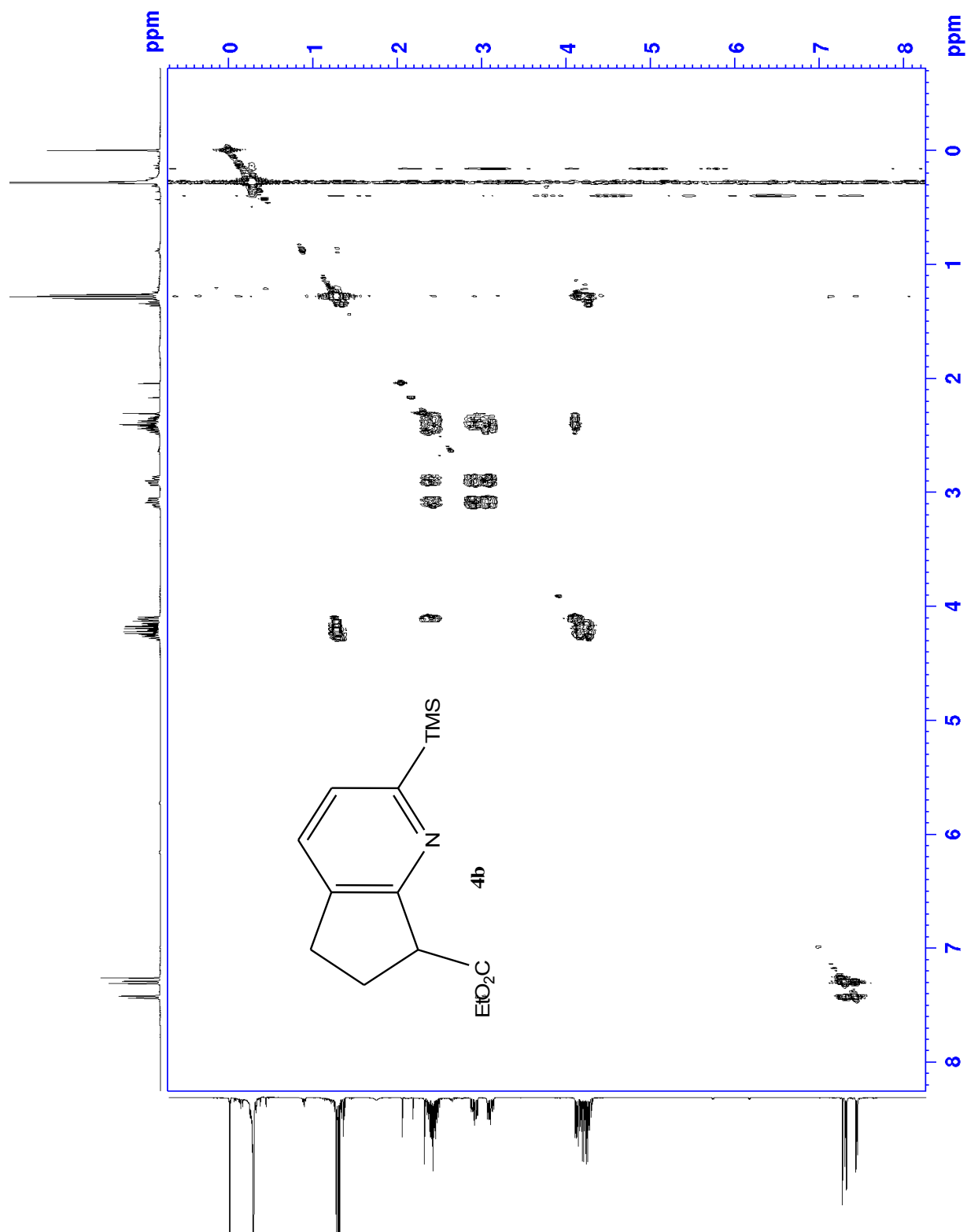
G.2 Carbon of 4b



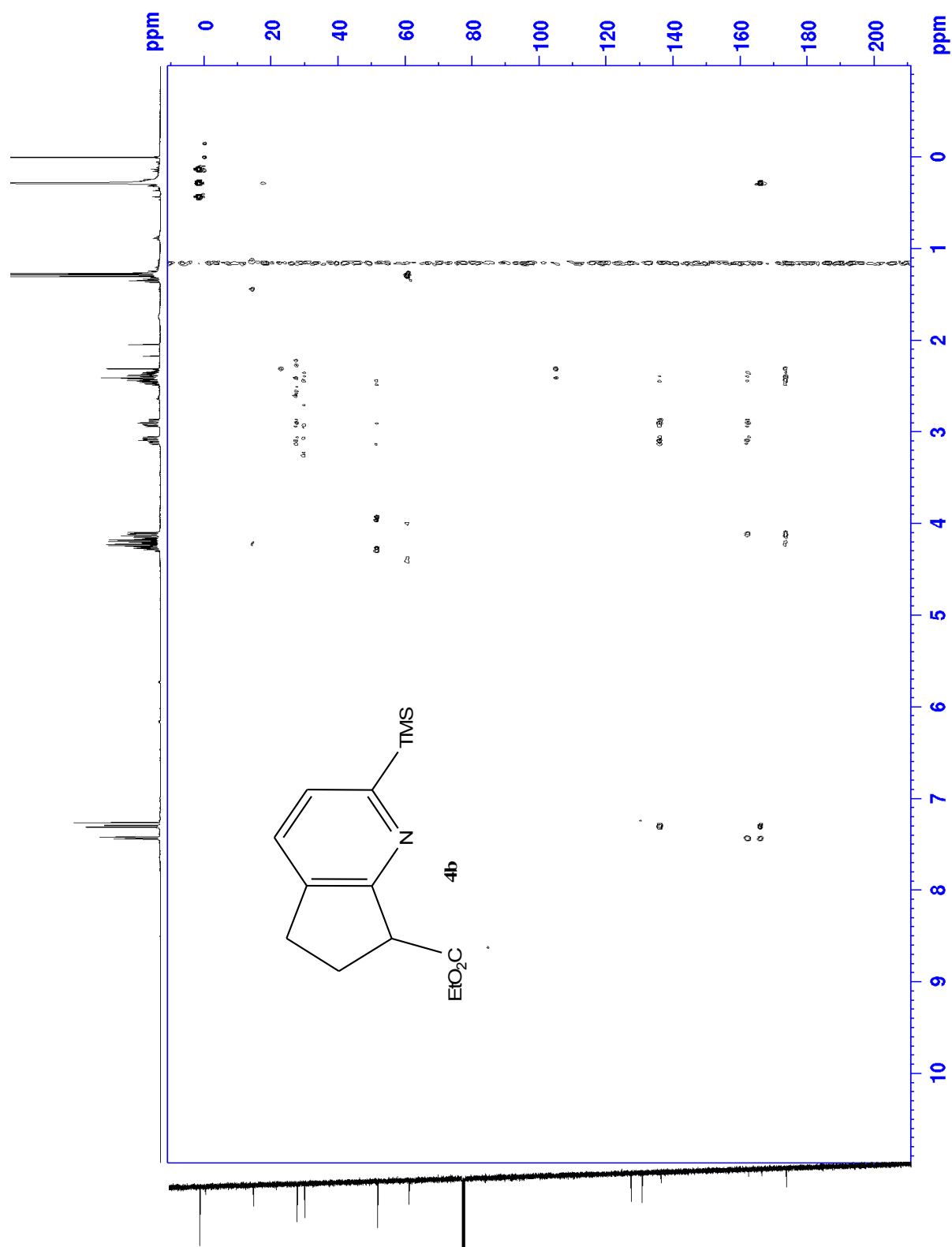
G.3 HSQC of 4b



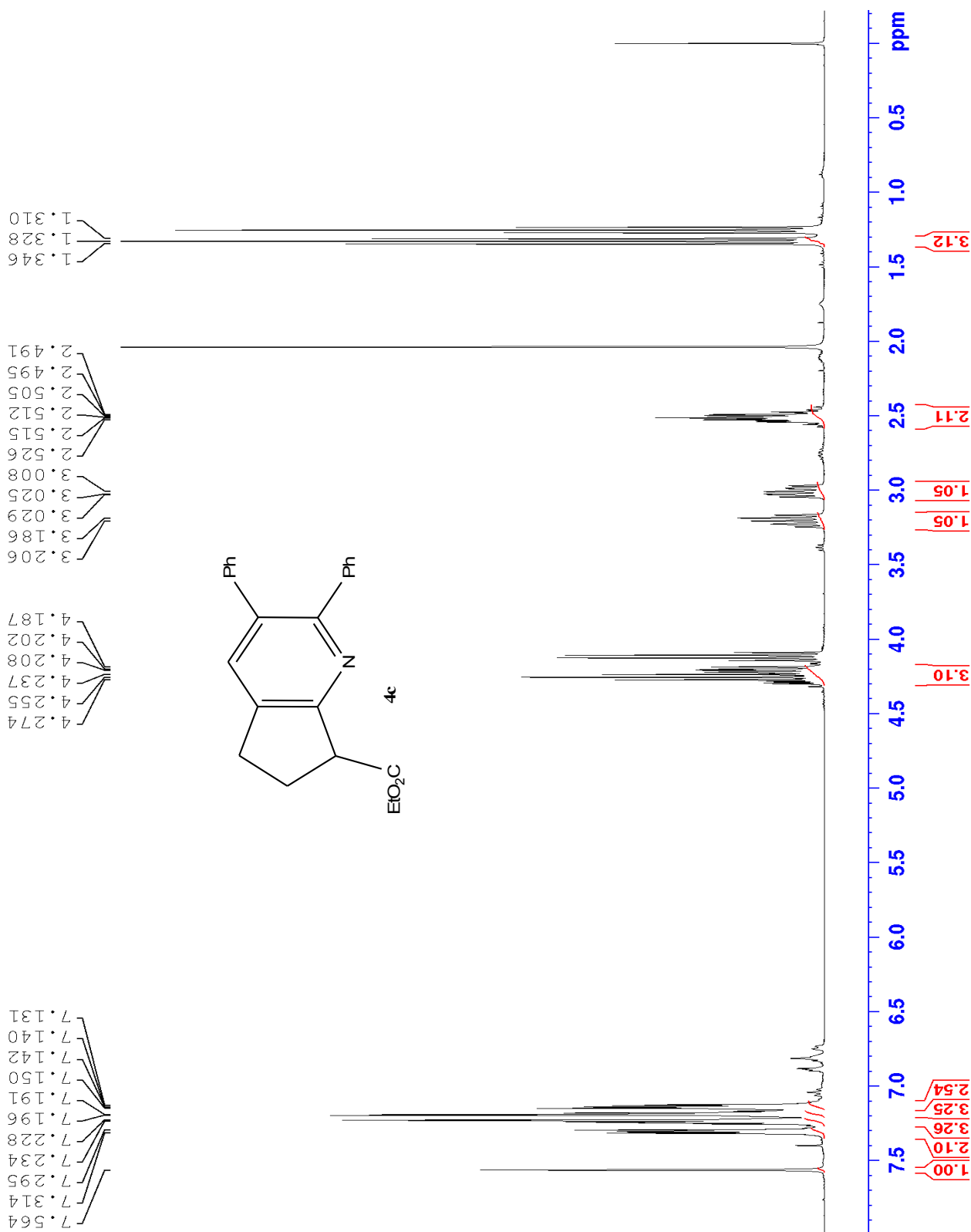
G.4 COSY of 4b



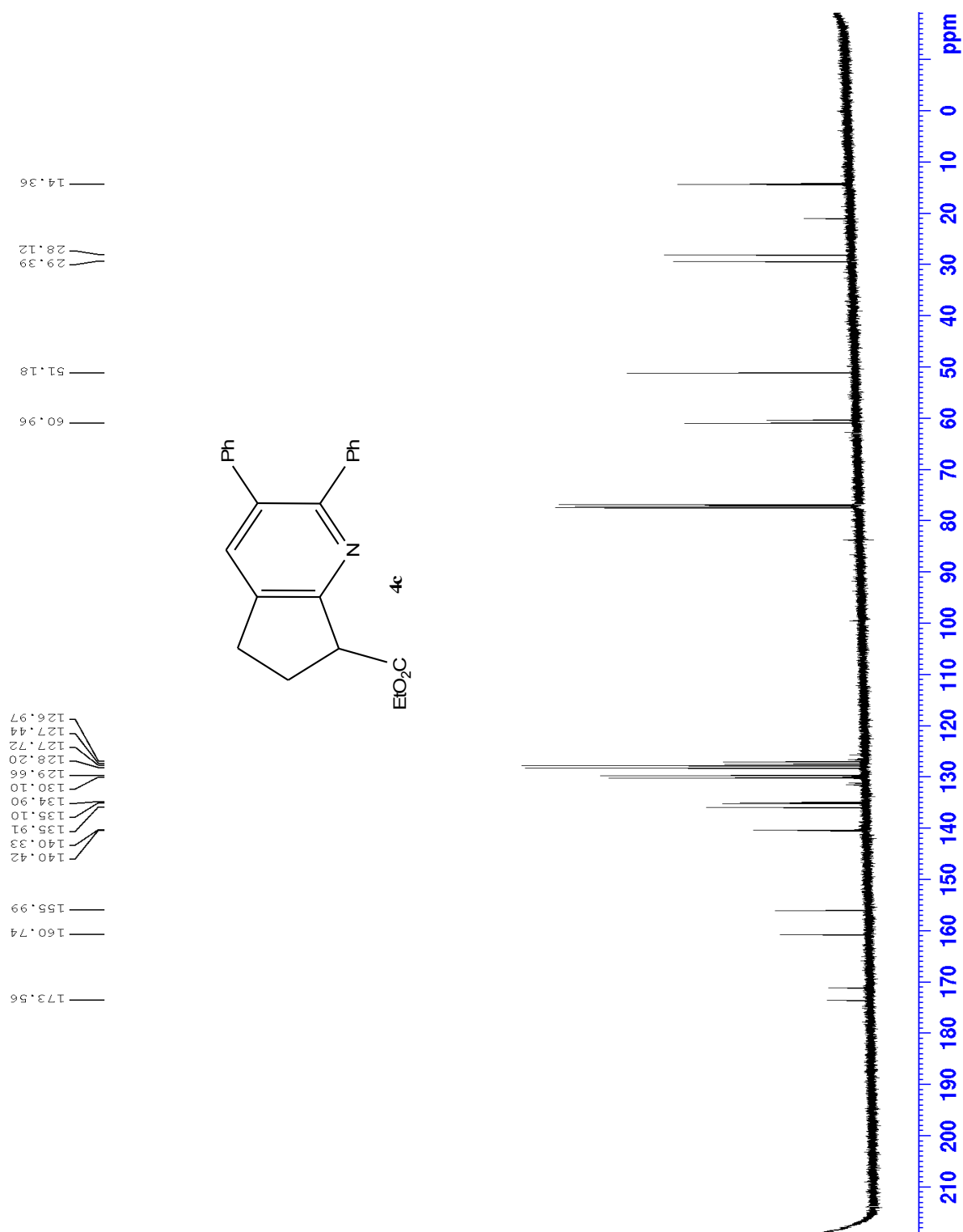
G.5 HMBC of 4b



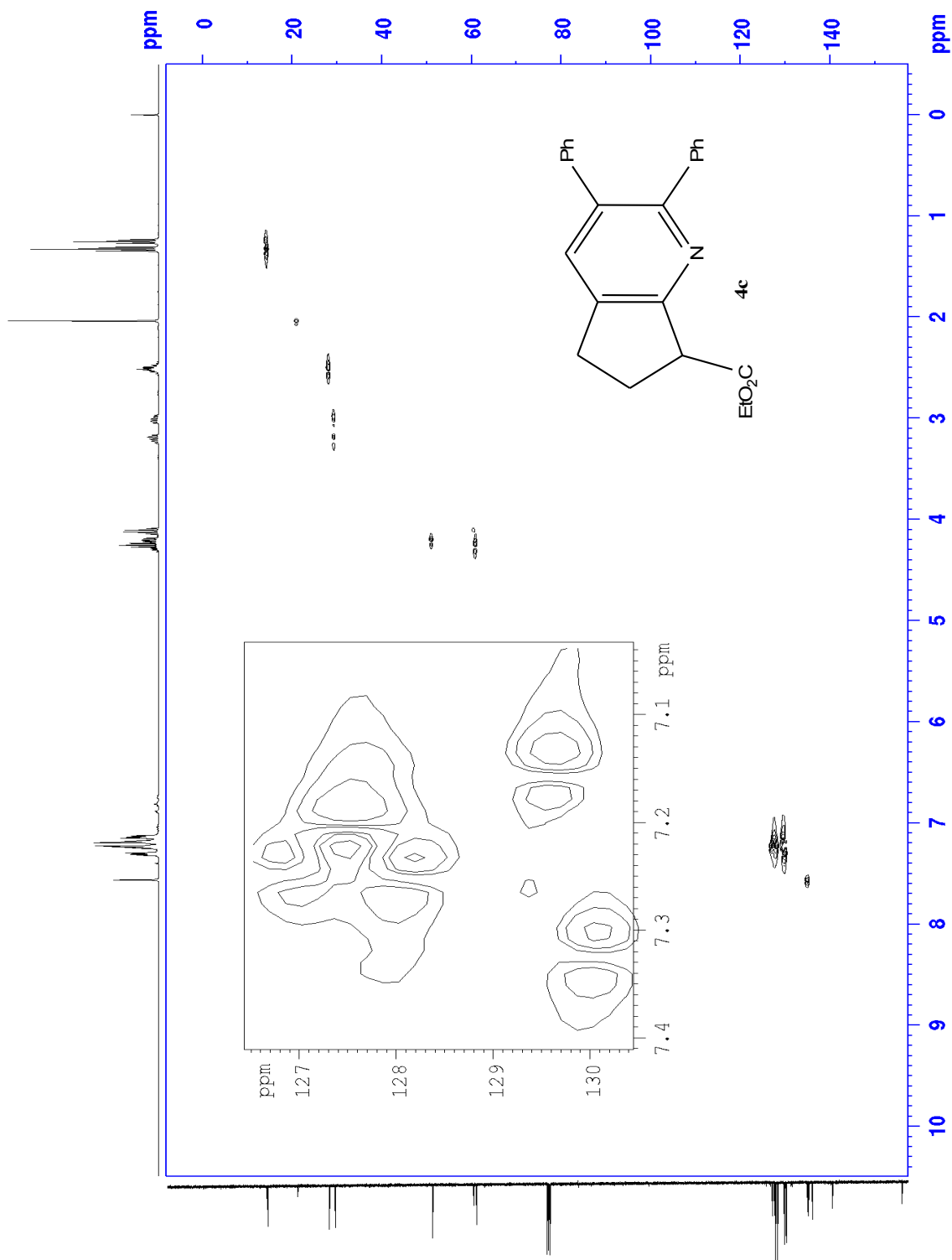
H.1 Proton of 4c



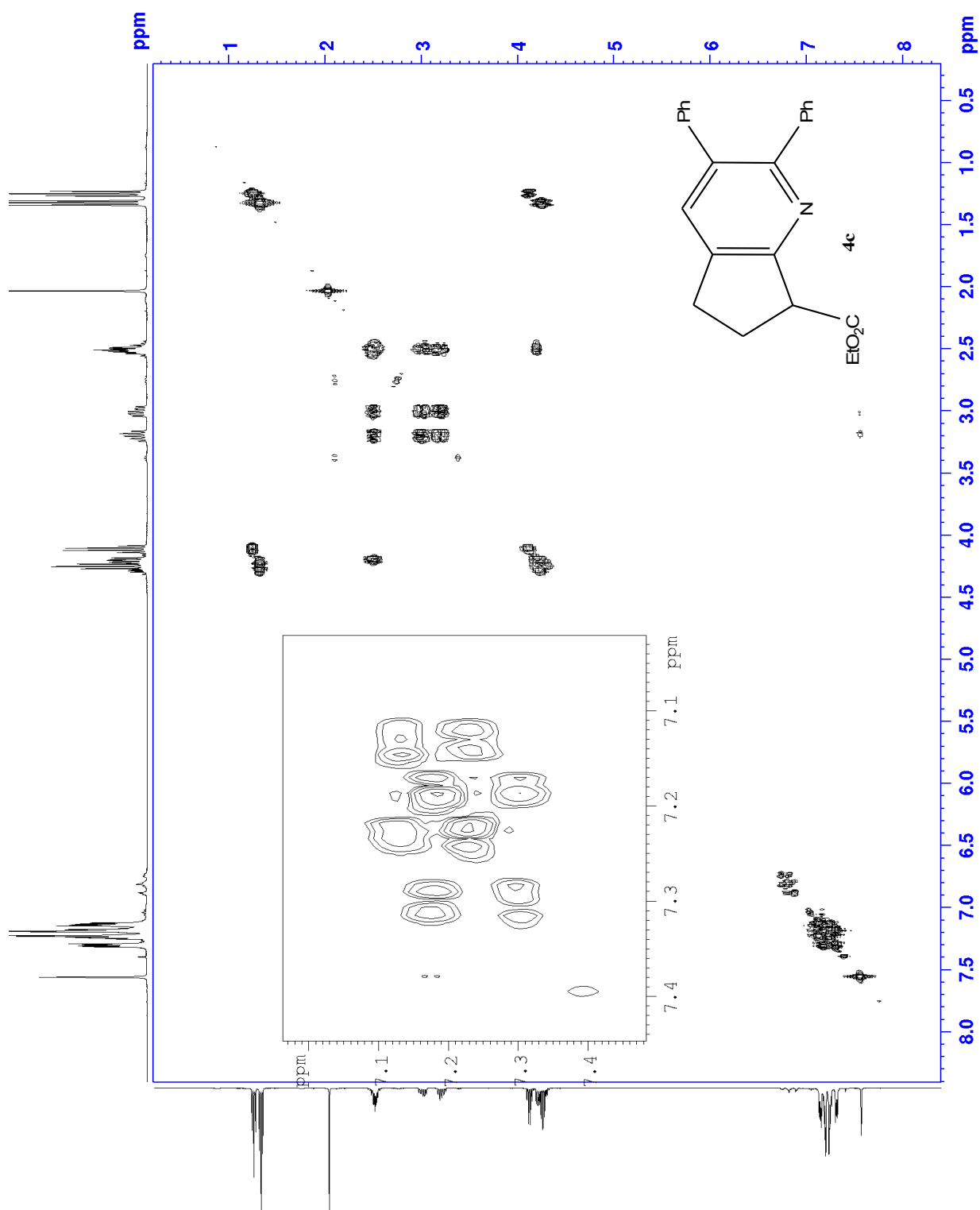
H.2 Carbon of 4c



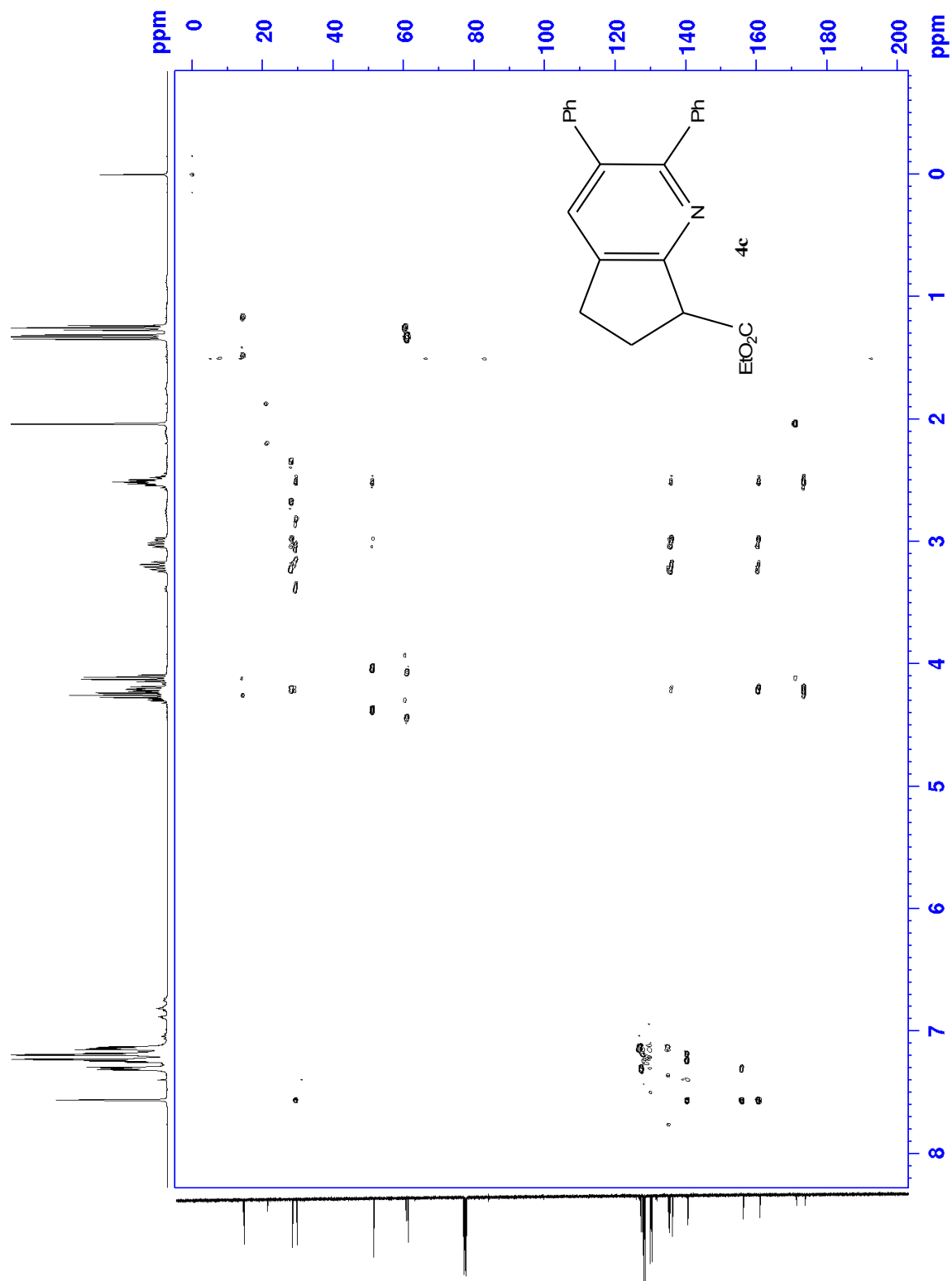
H.3 HSQC of 4c



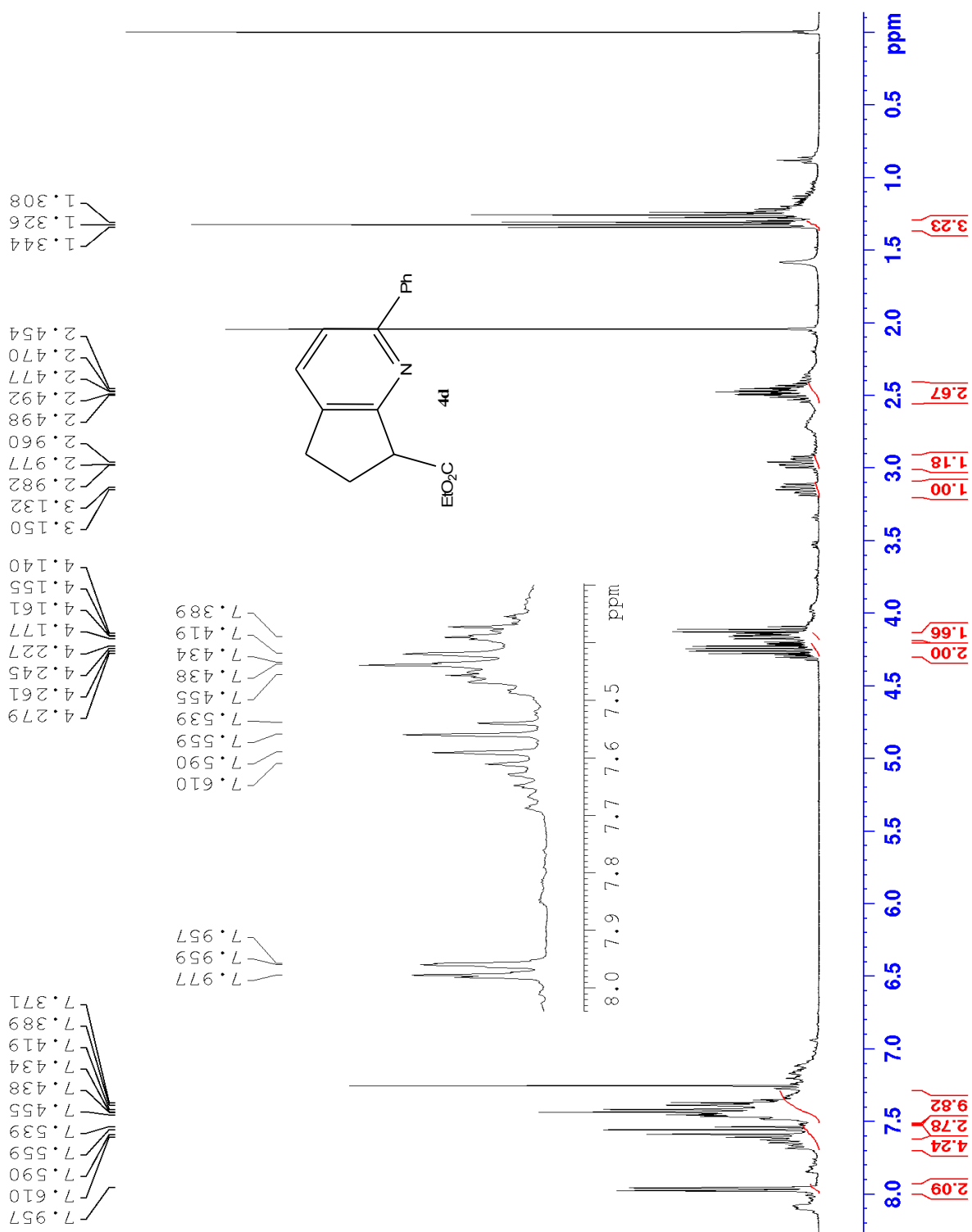
H.4 COSY of 4c



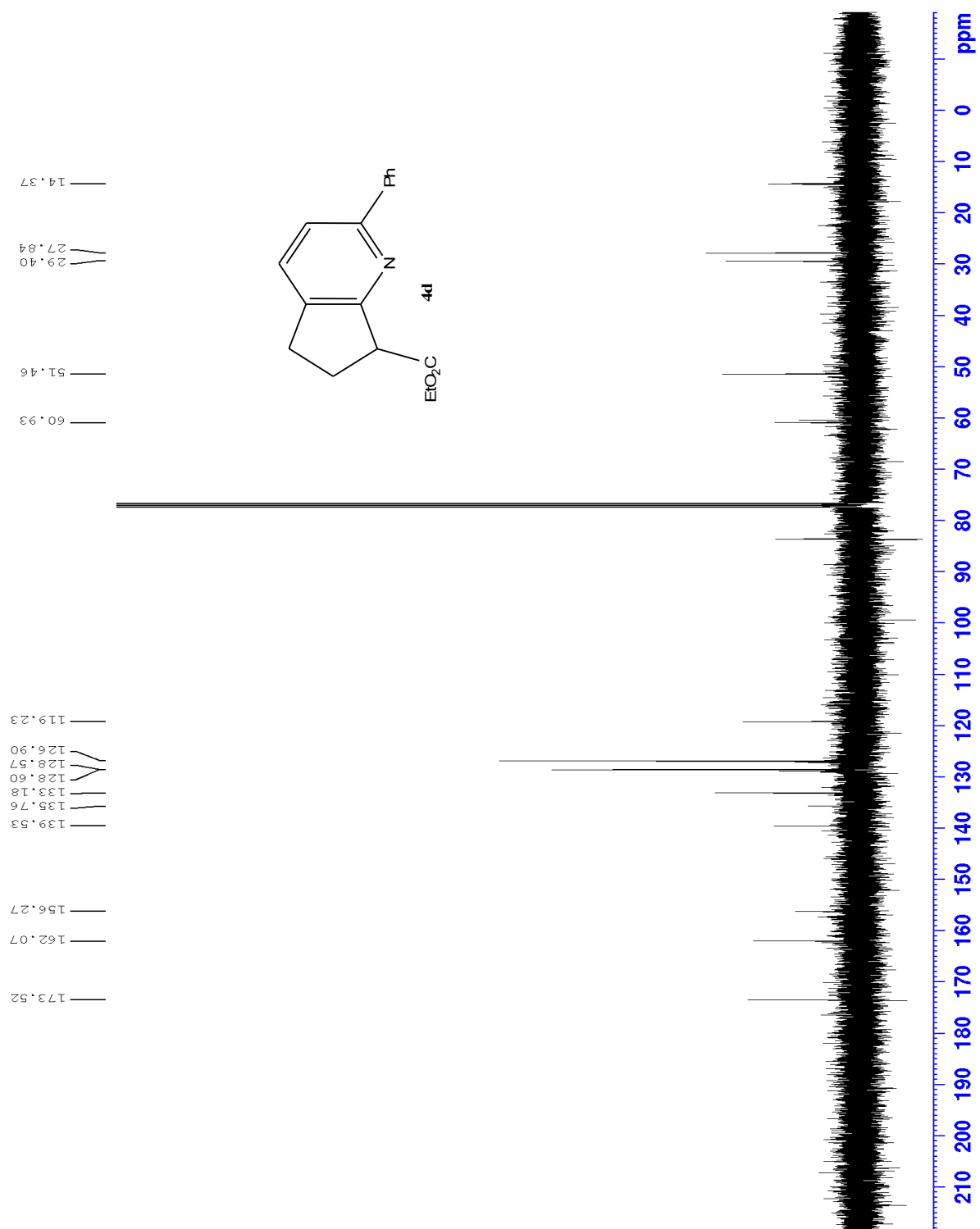
H.5 HMBC of 4c



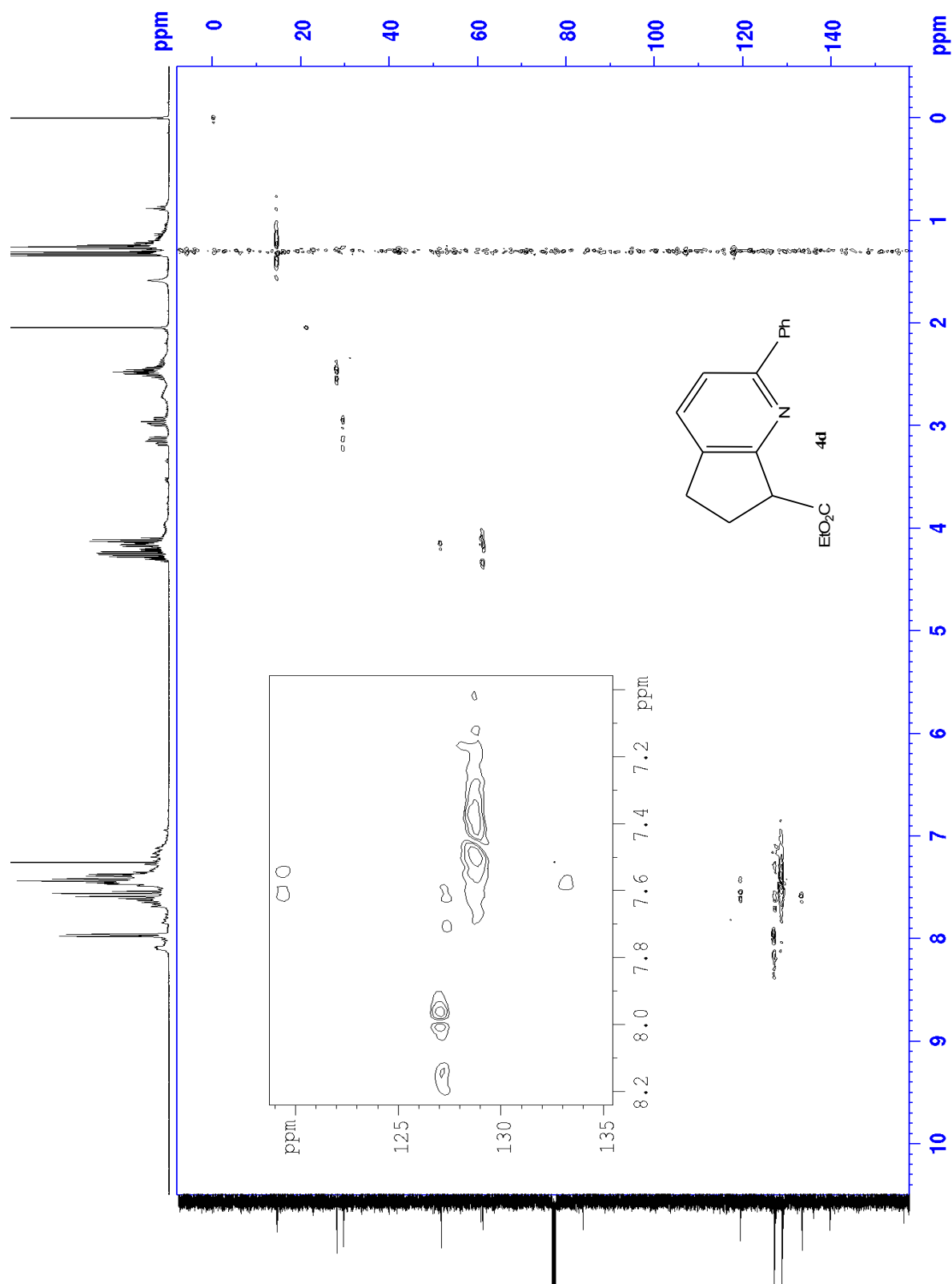
I.1 Proton of 4d



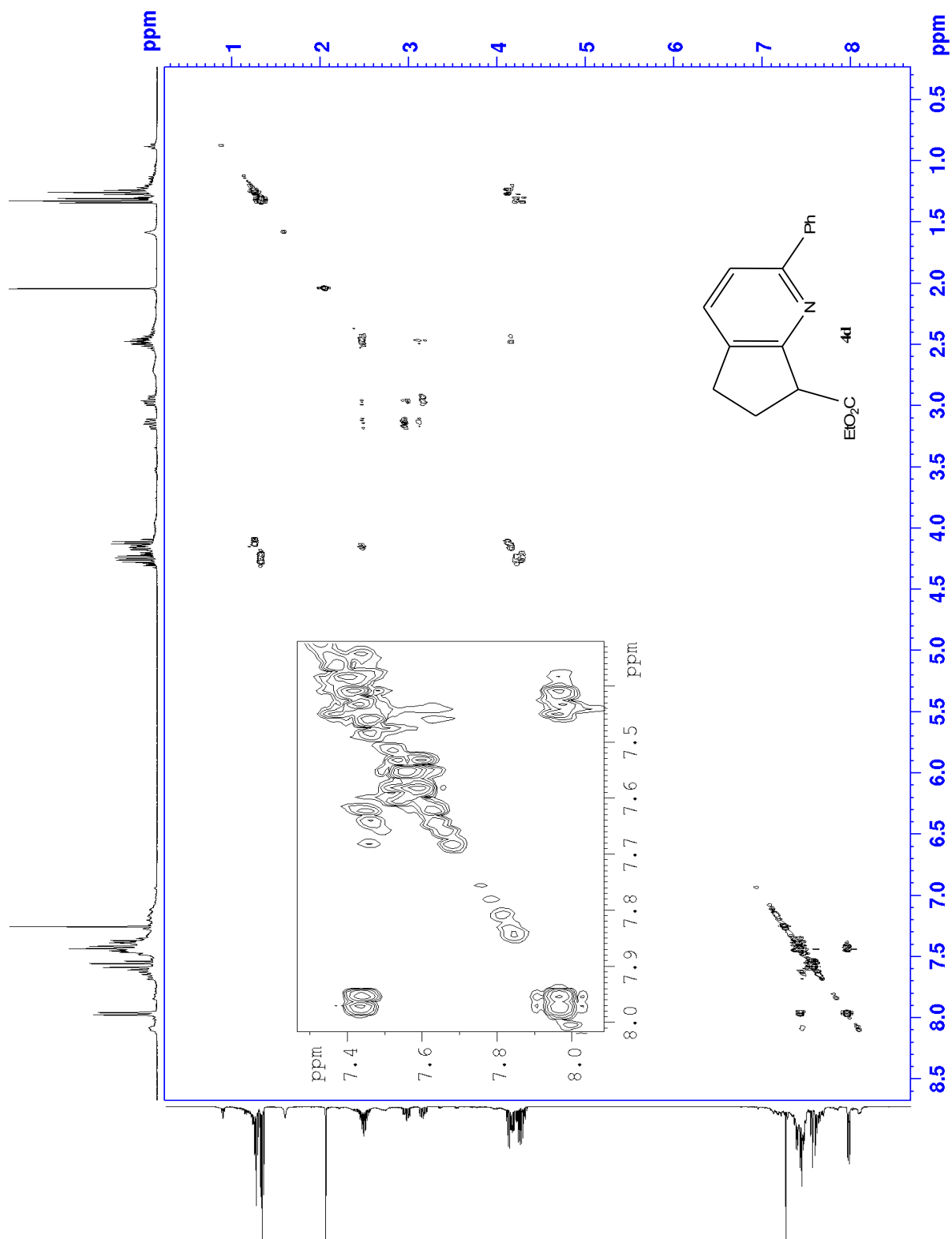
I.2 Carbon of 4d



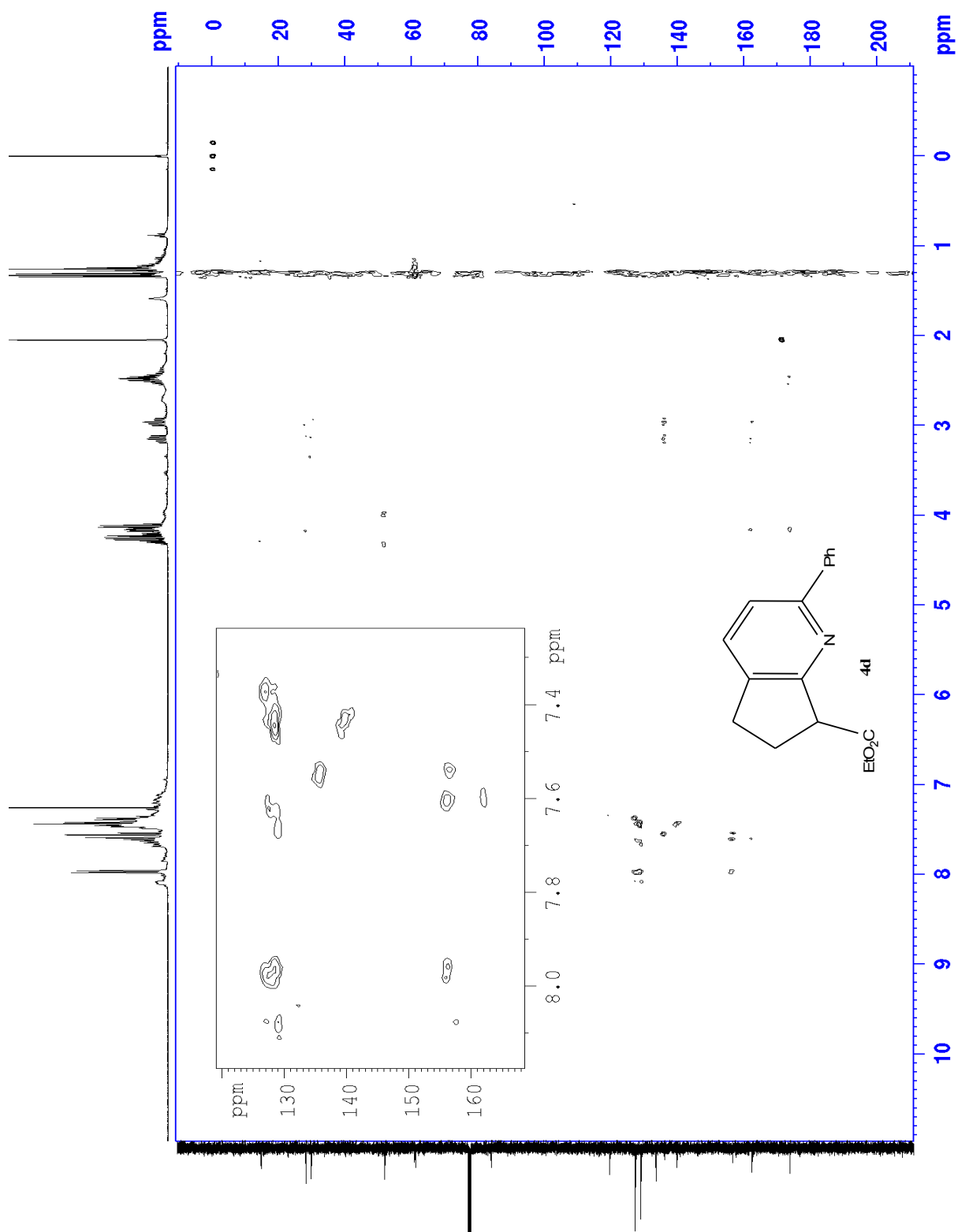
I.3 HSQC of 4d



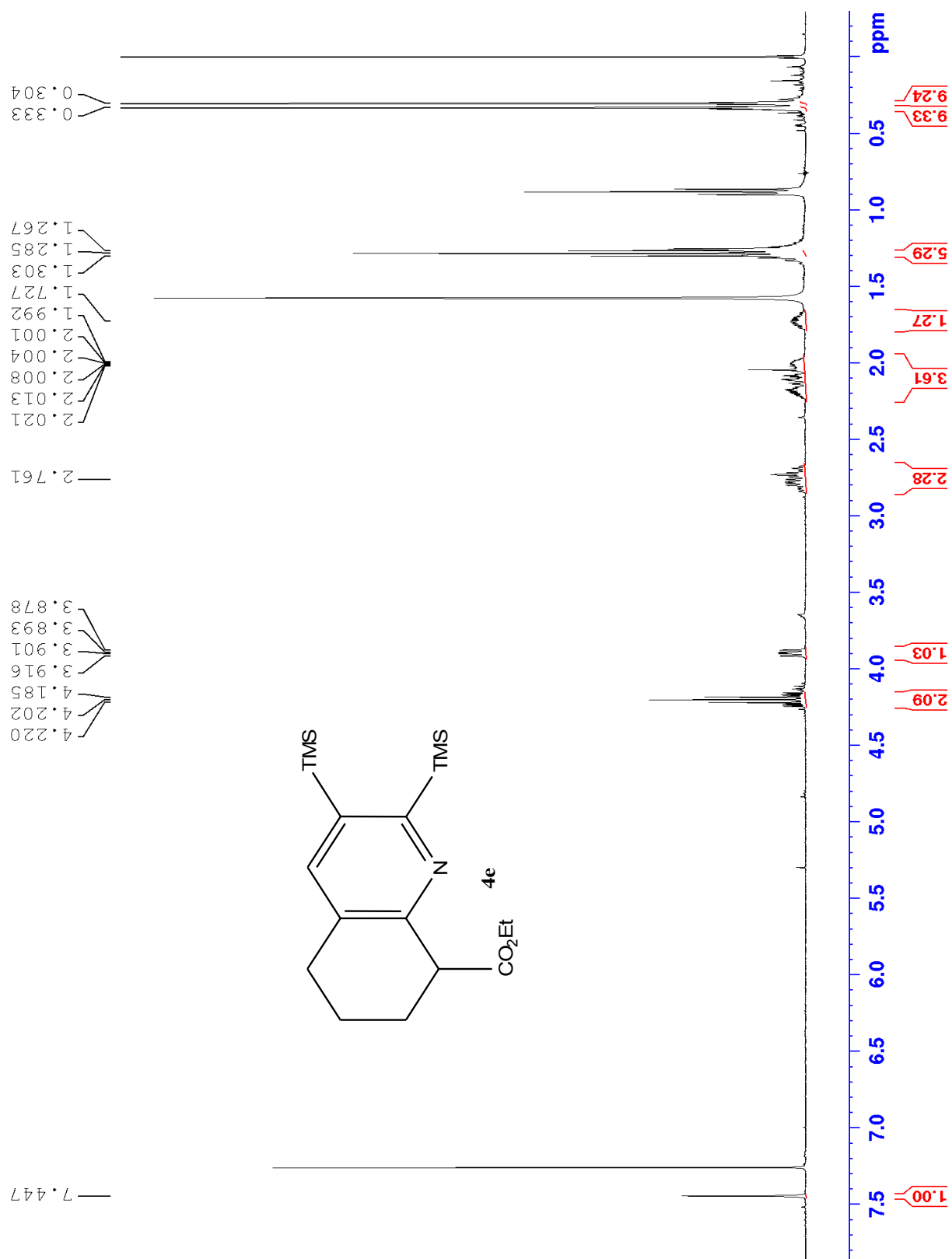
I.4 COSY of 4d



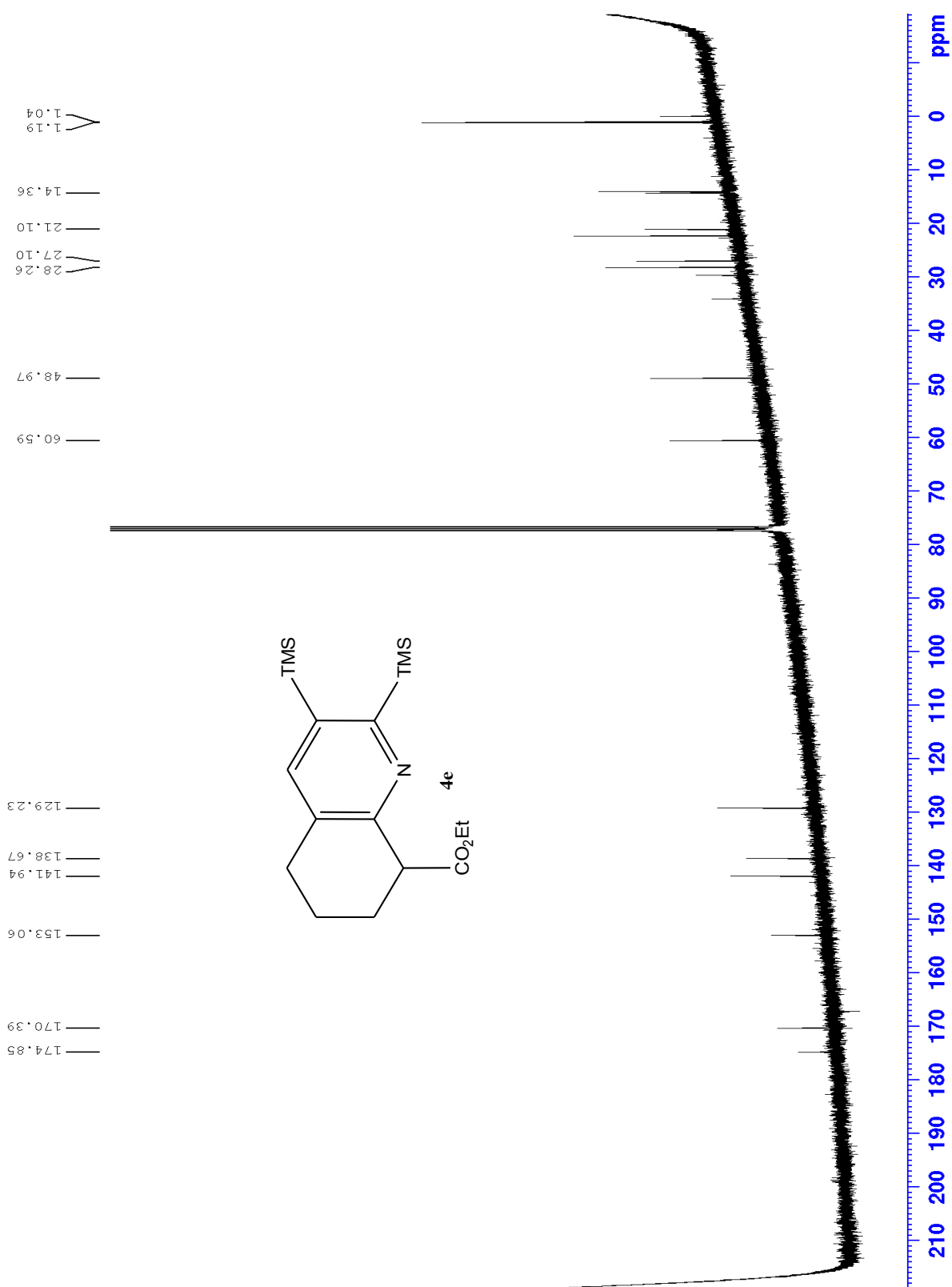
1.5 HMBC of 4d



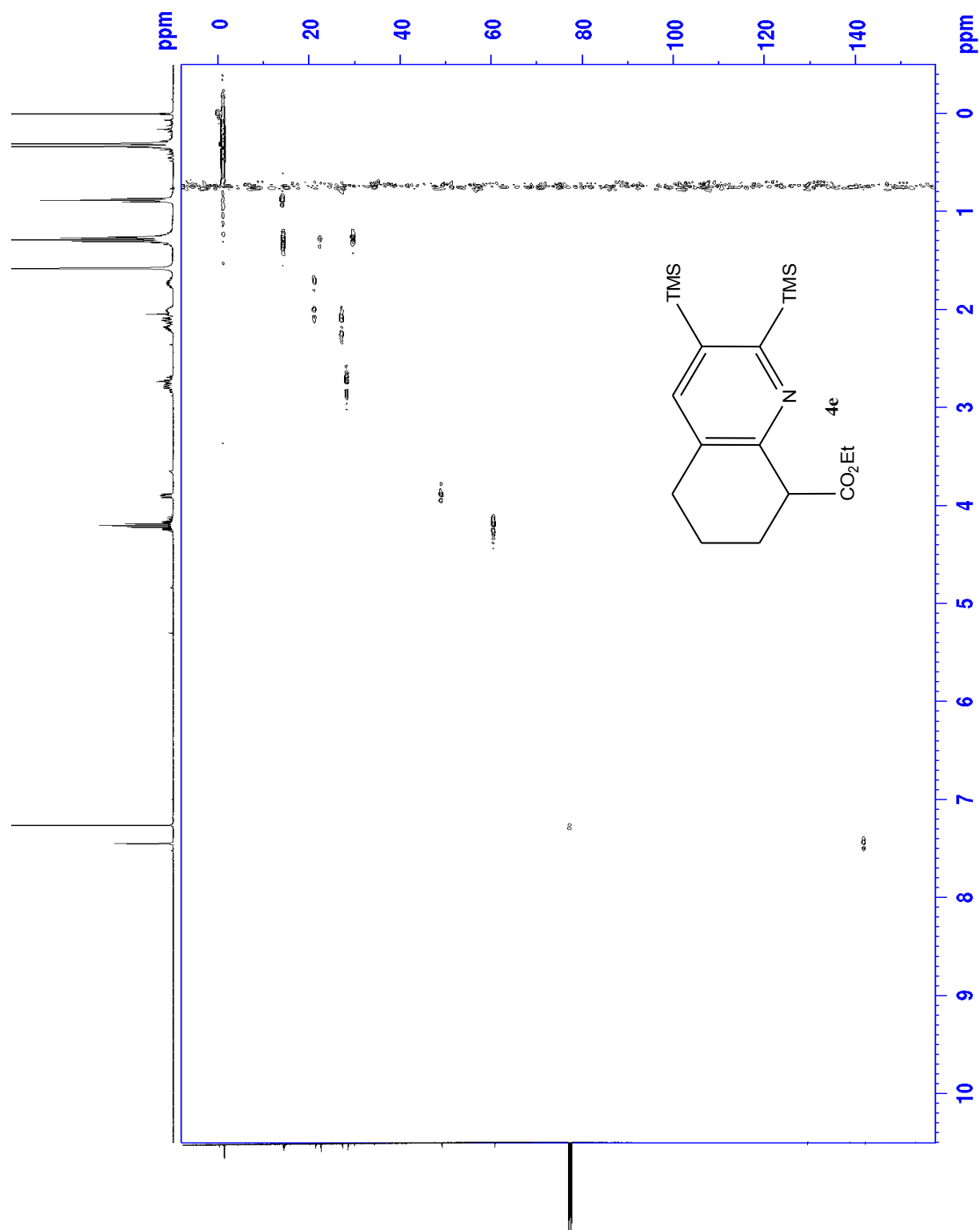
J.1 Proton of 4e



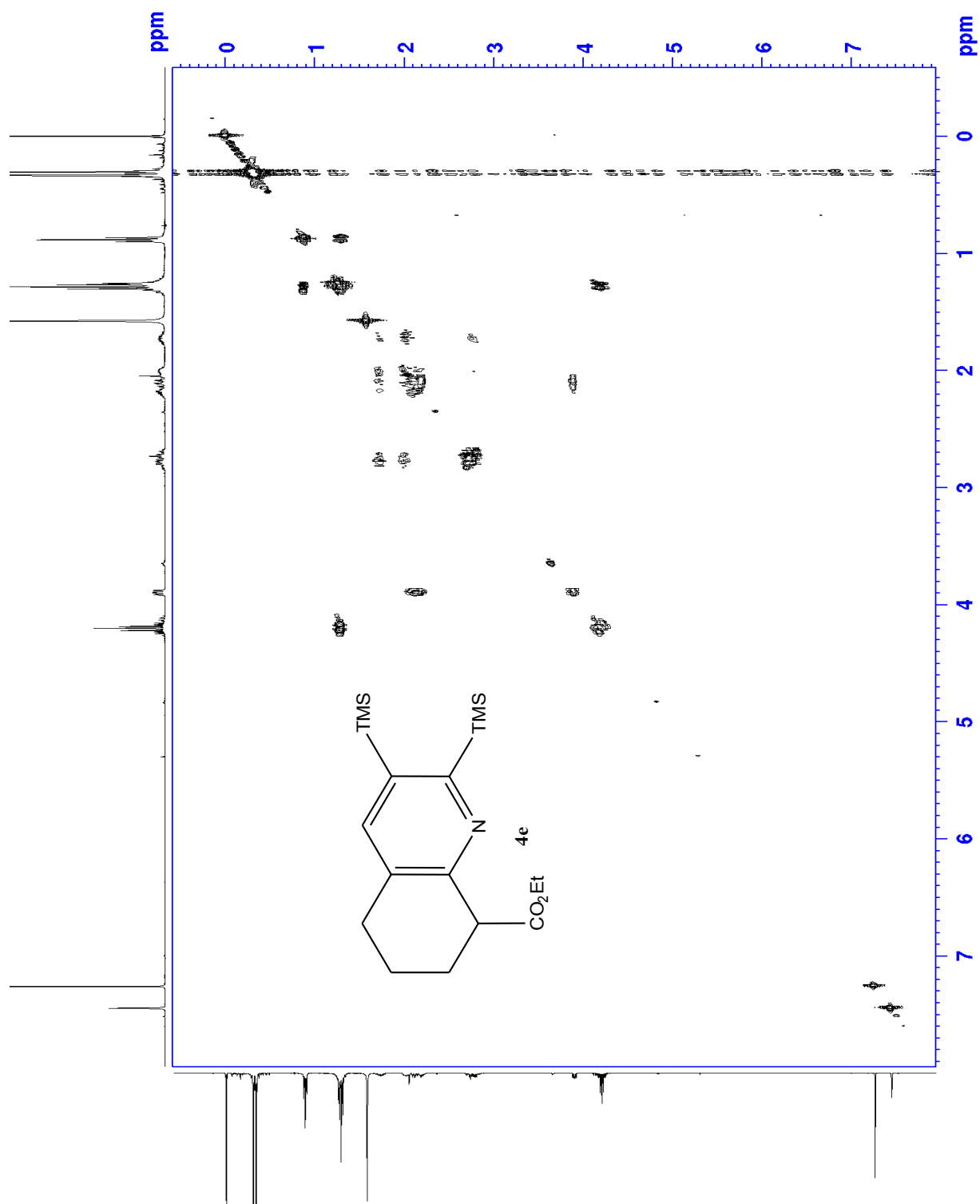
J.2 Carbon of 4e



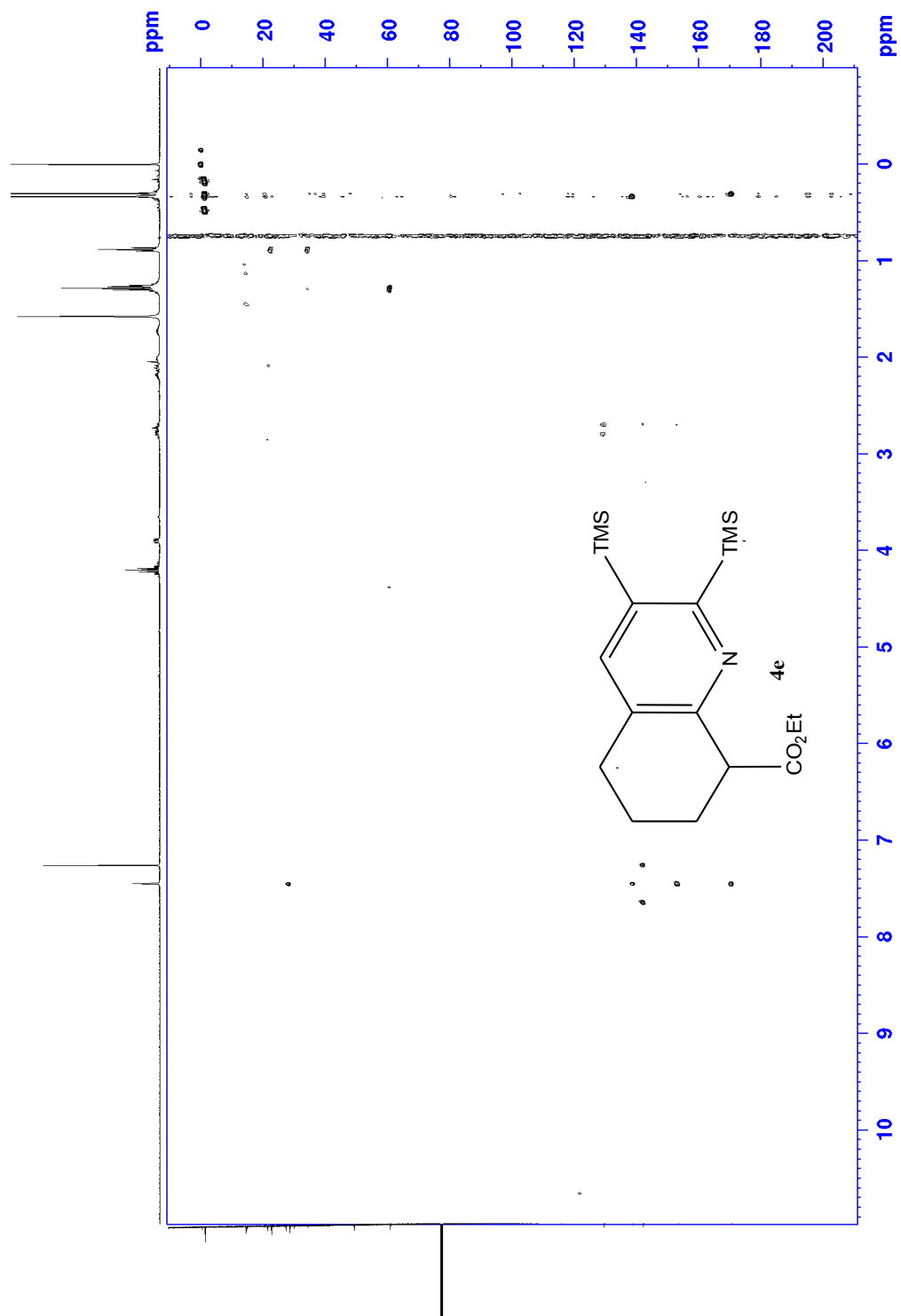
J.3 HSQC of 4e



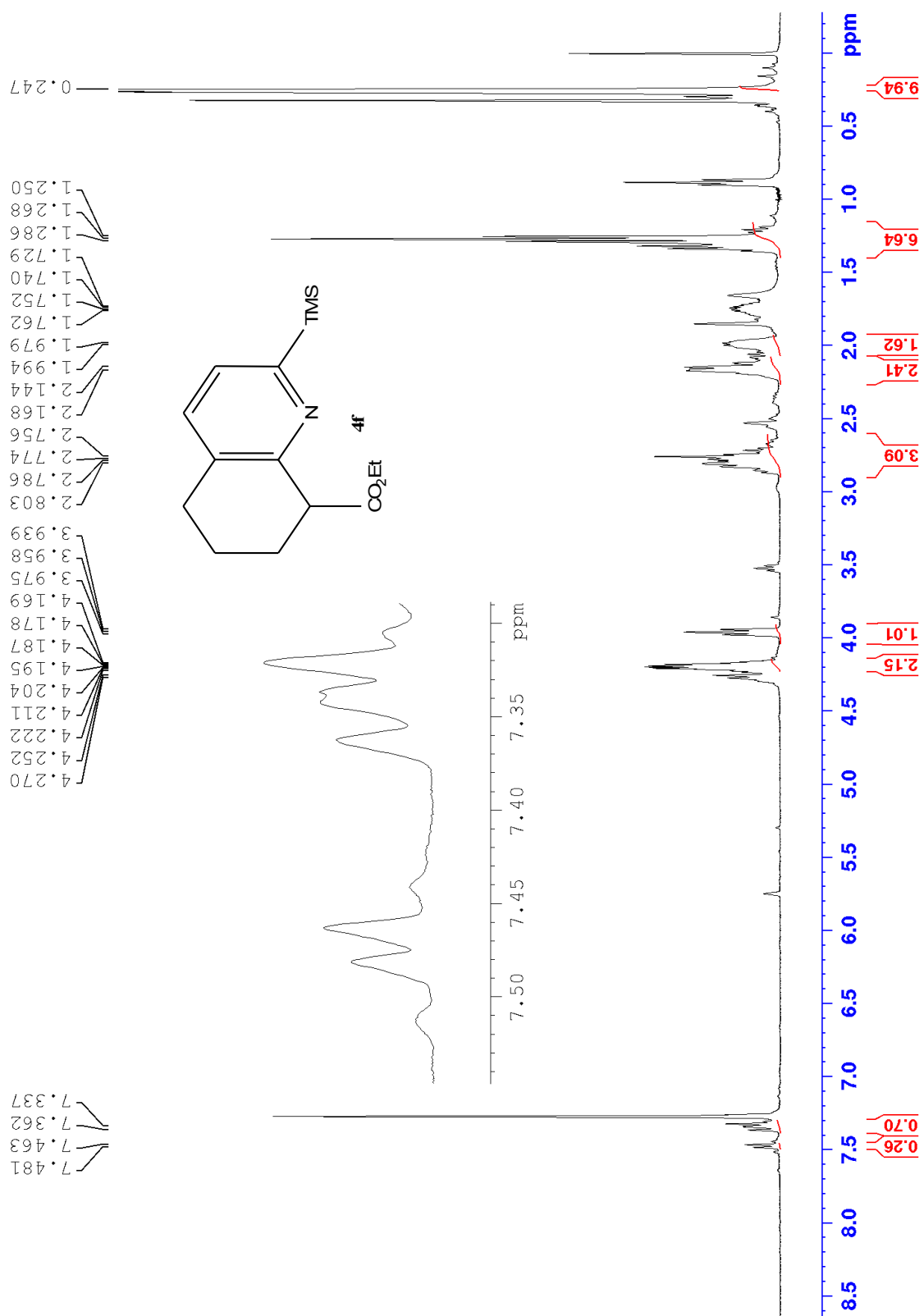
J.4 COSY of 4e



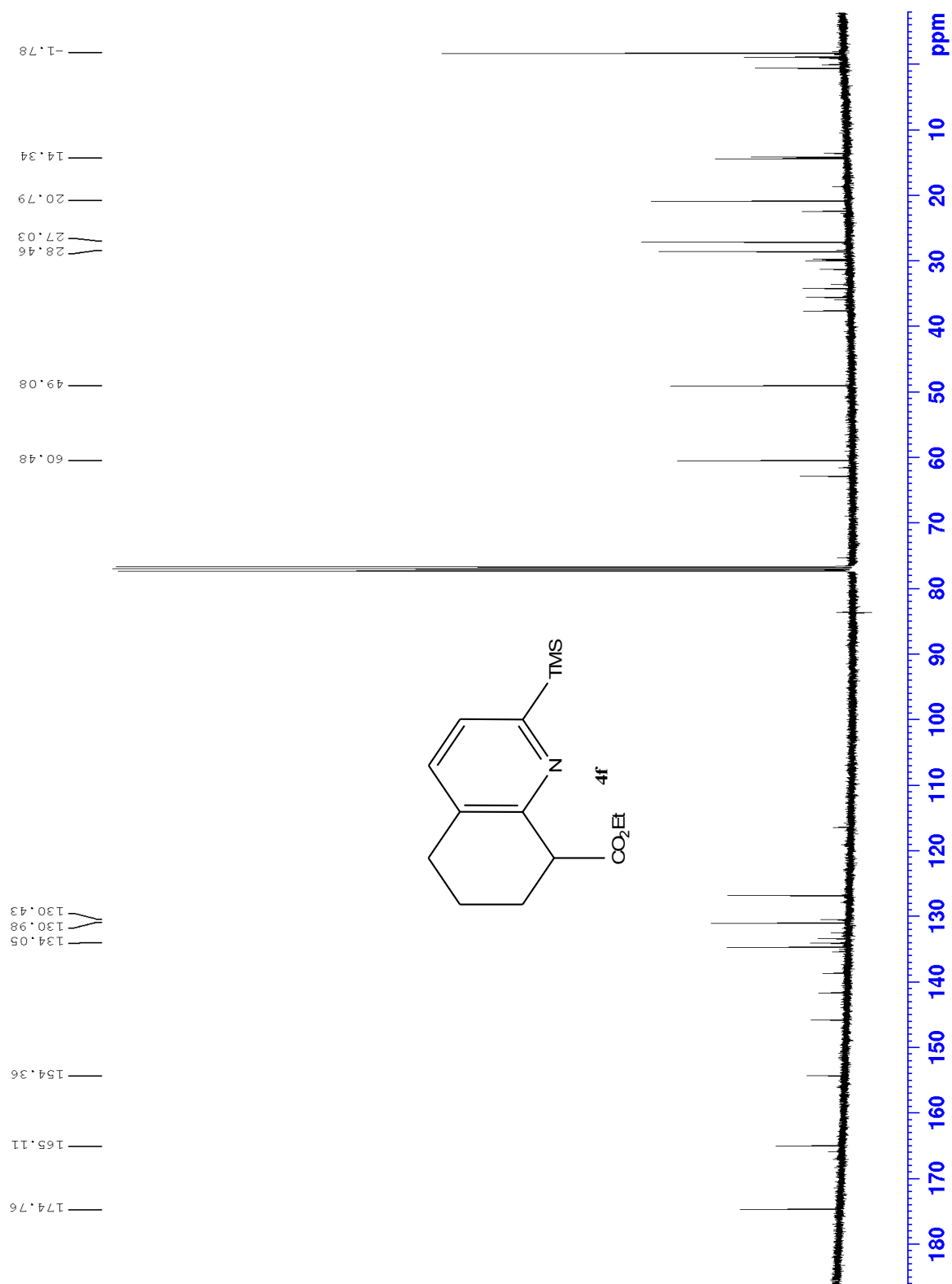
J.5 HMBC of 4e



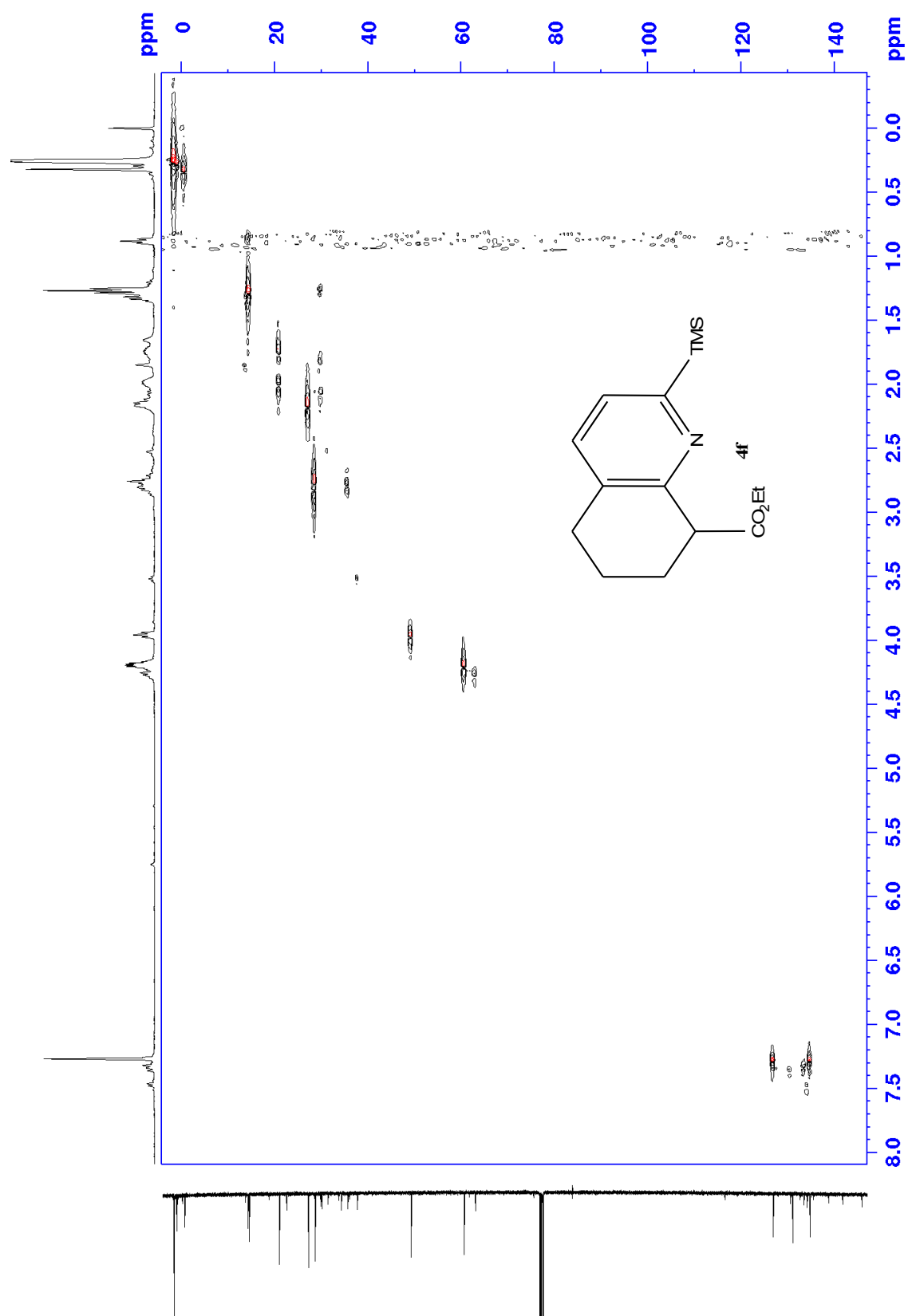
K.1 Proton of 4f



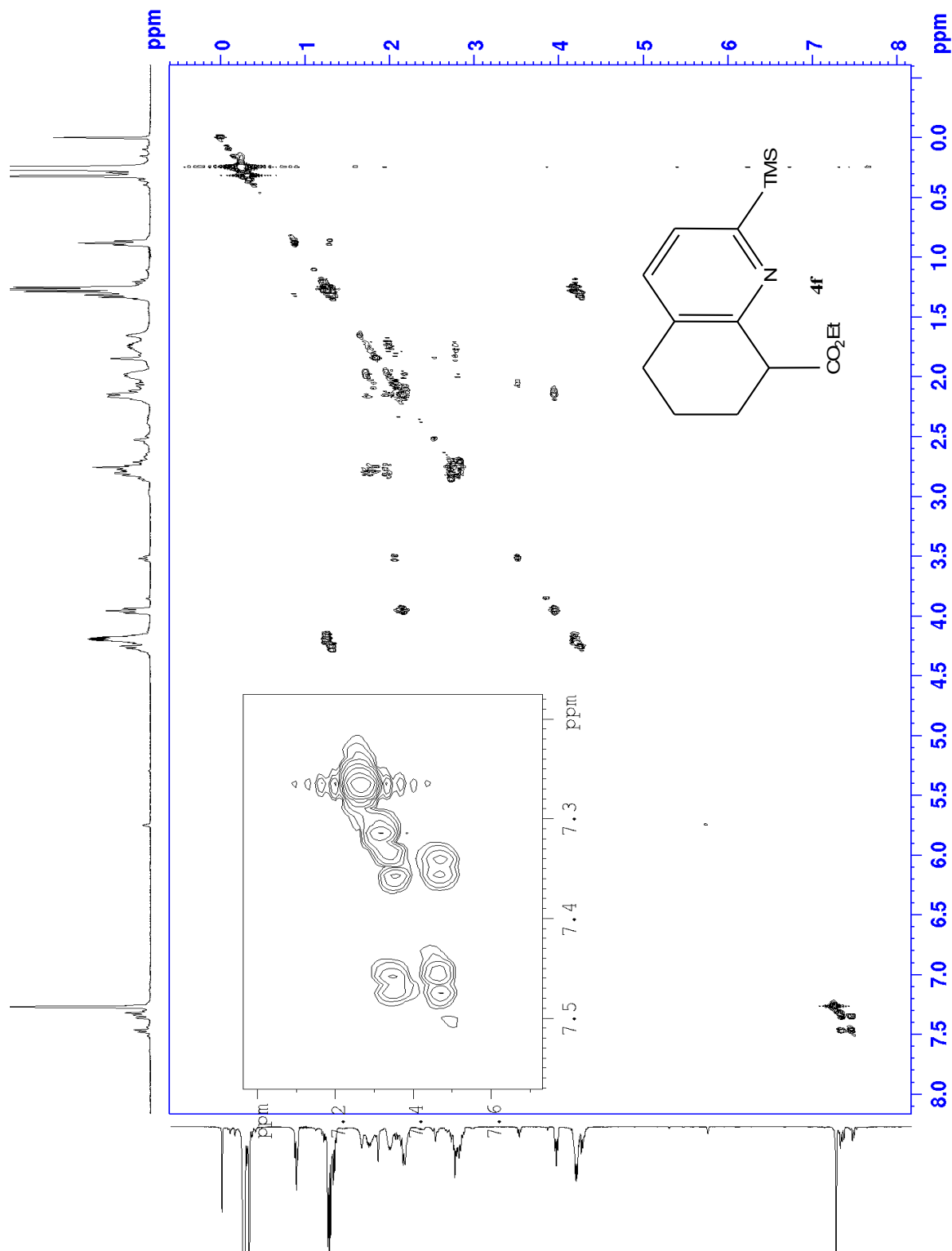
K.2 Carbon of 4f



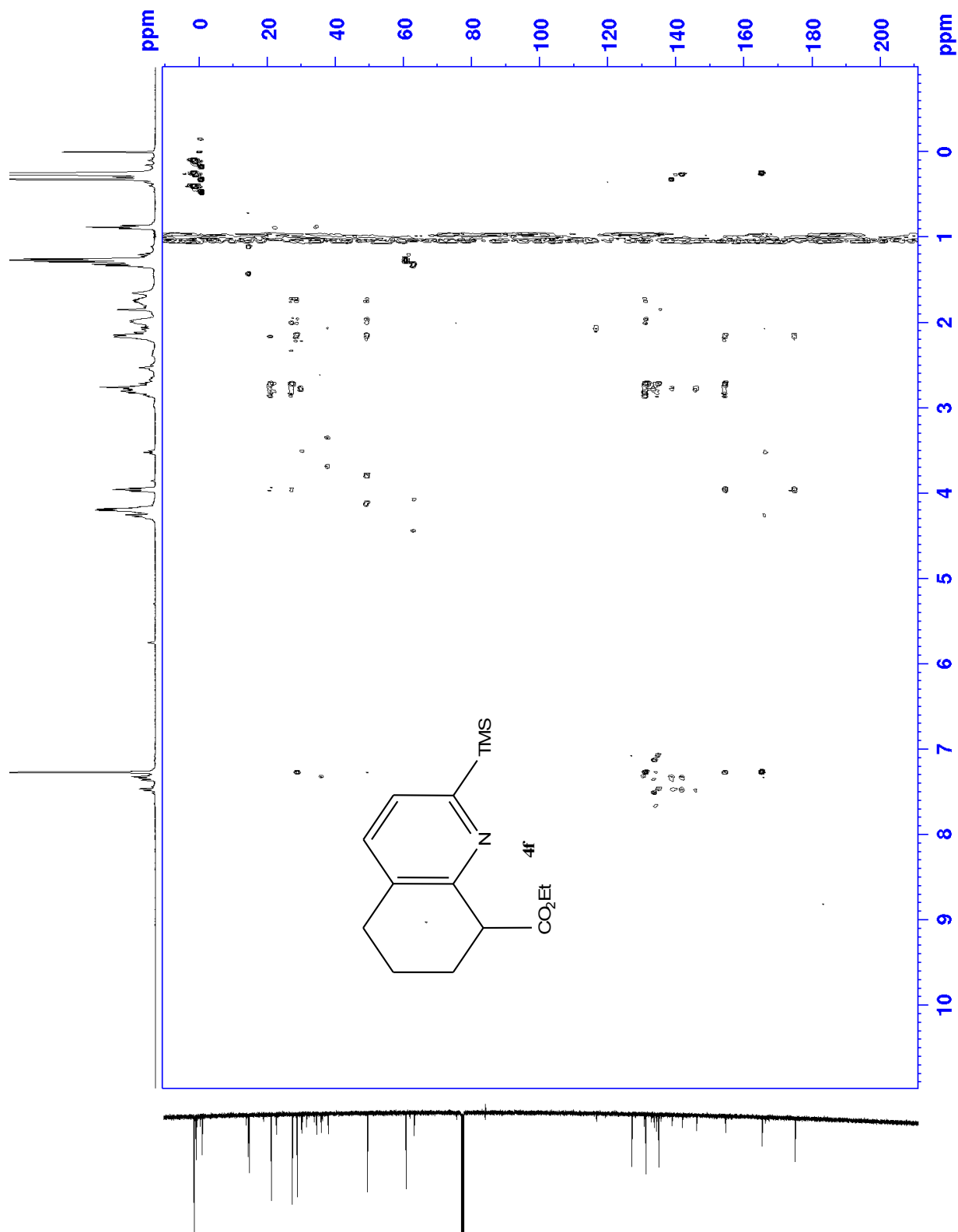
K.3 HSQC of 4f



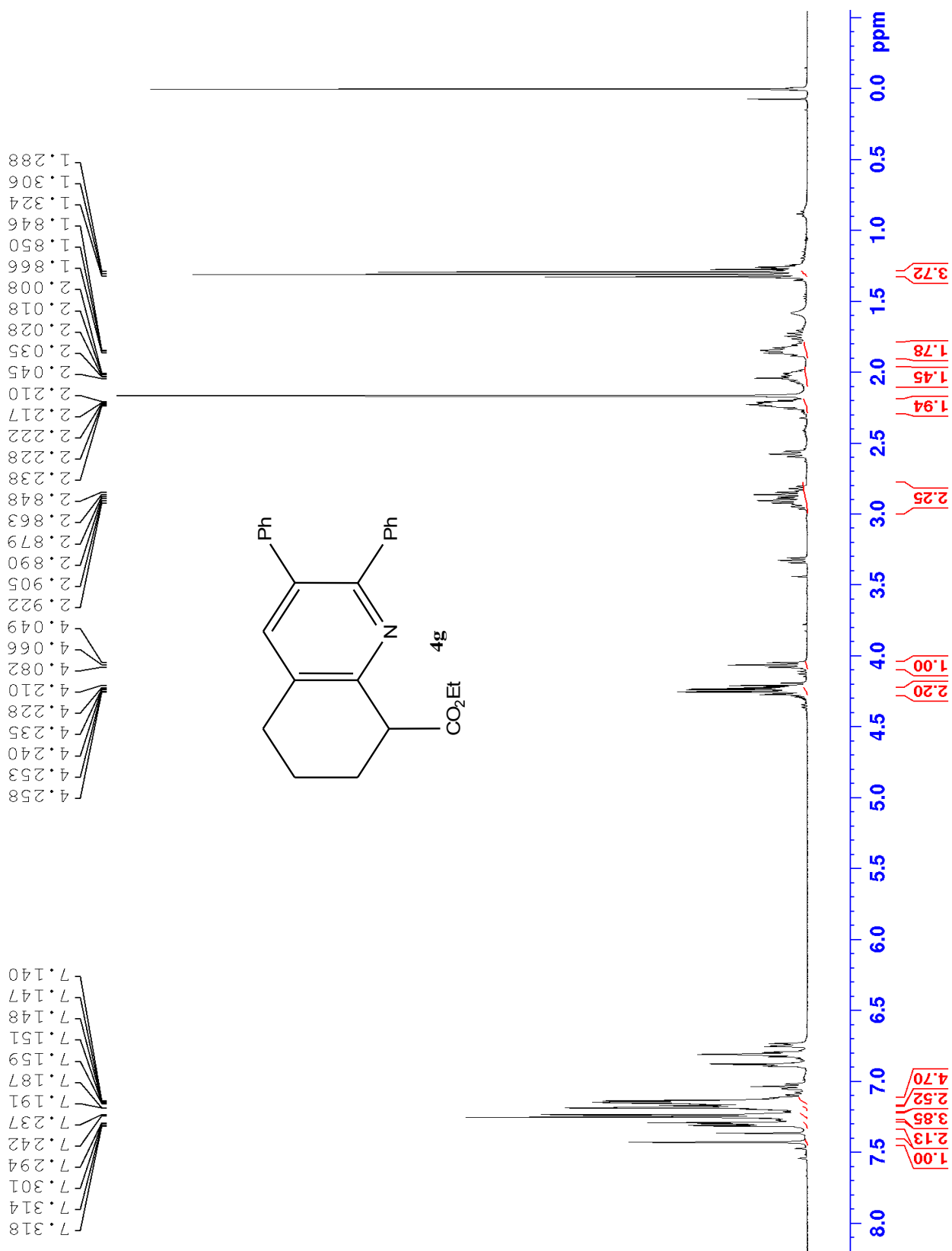
K.4 COSY of 4f



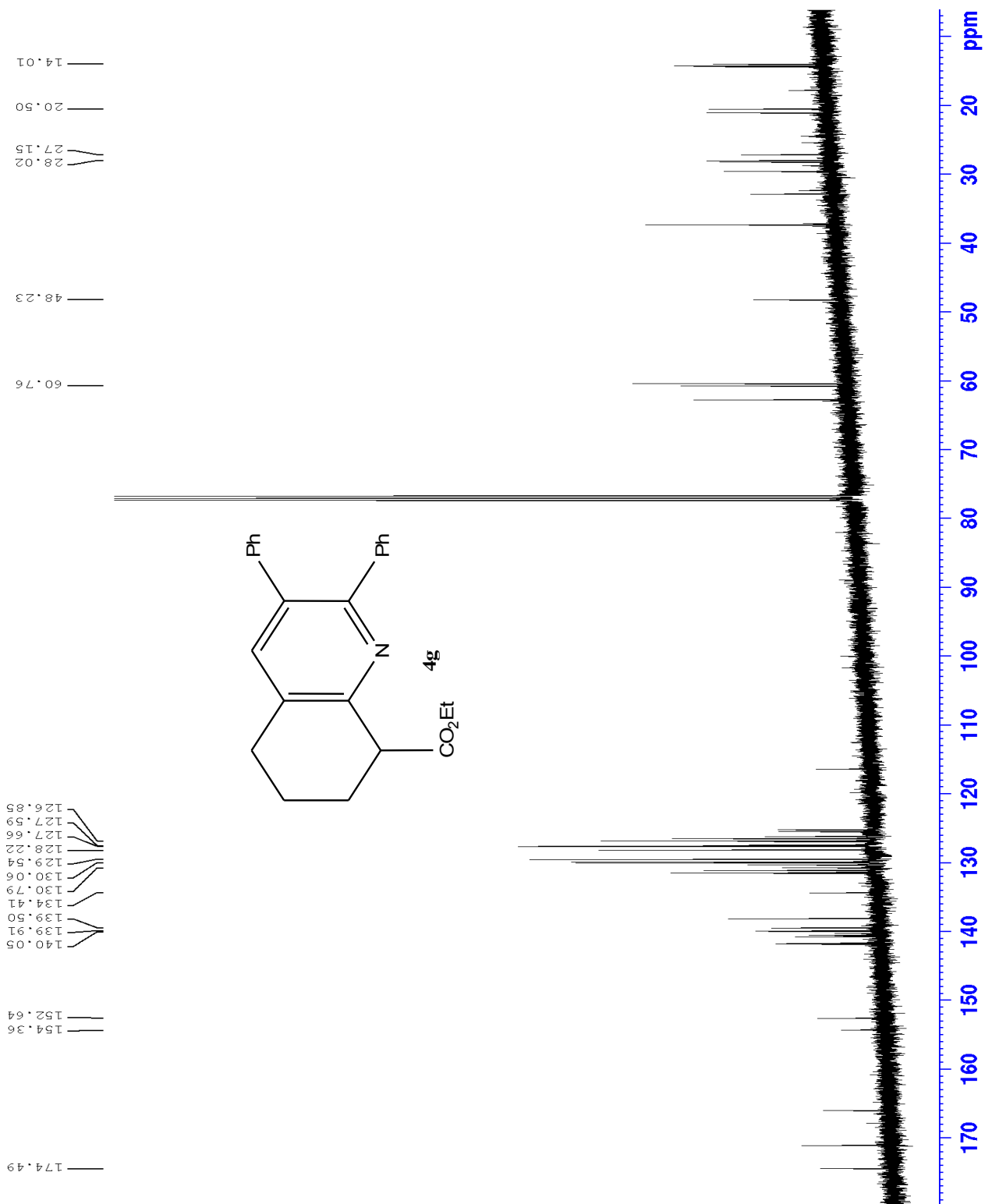
K.5 HMBC of 4f



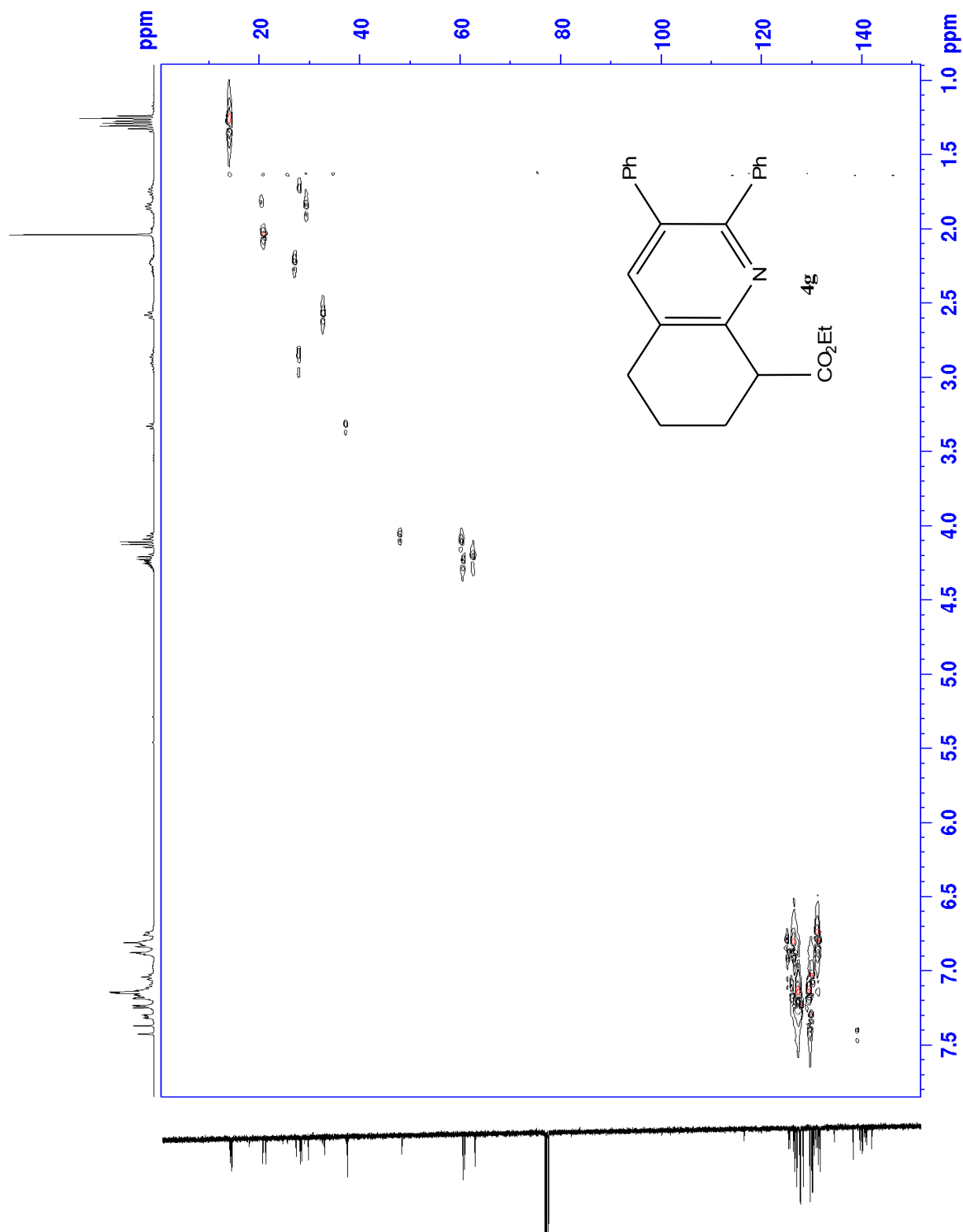
L.1 Proton of 4g



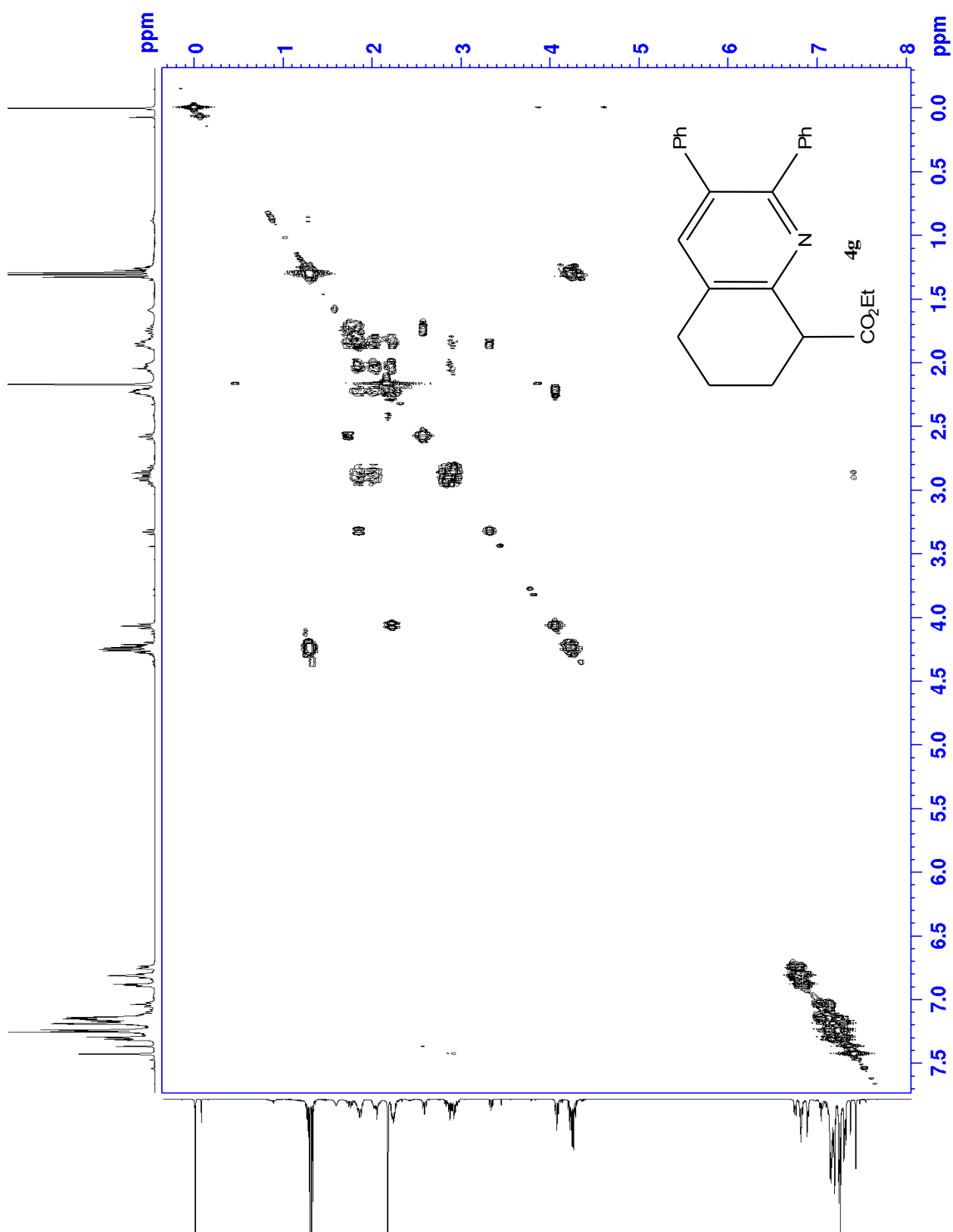
L.2 Carbon of 4g



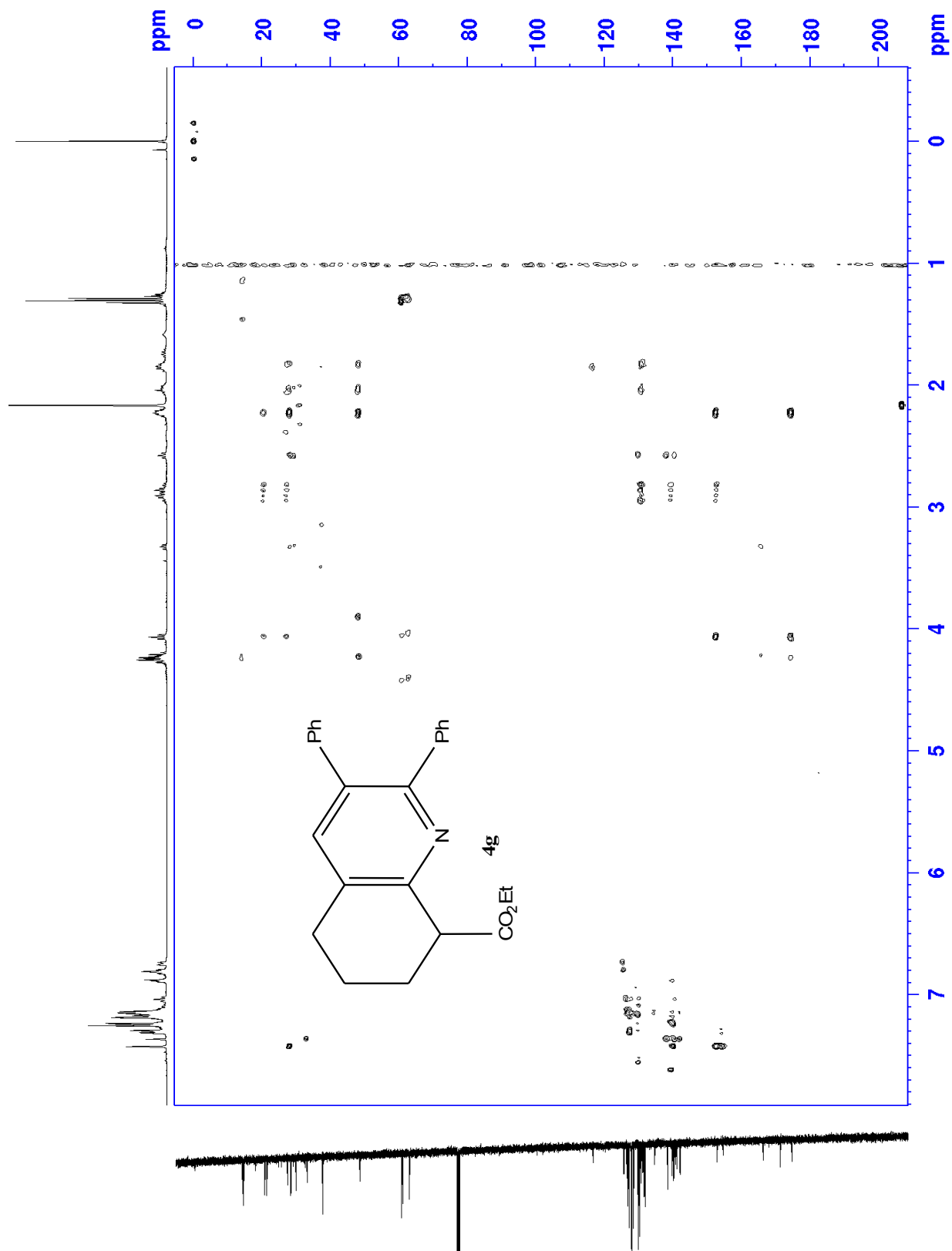
L.3 HSQC of 4g



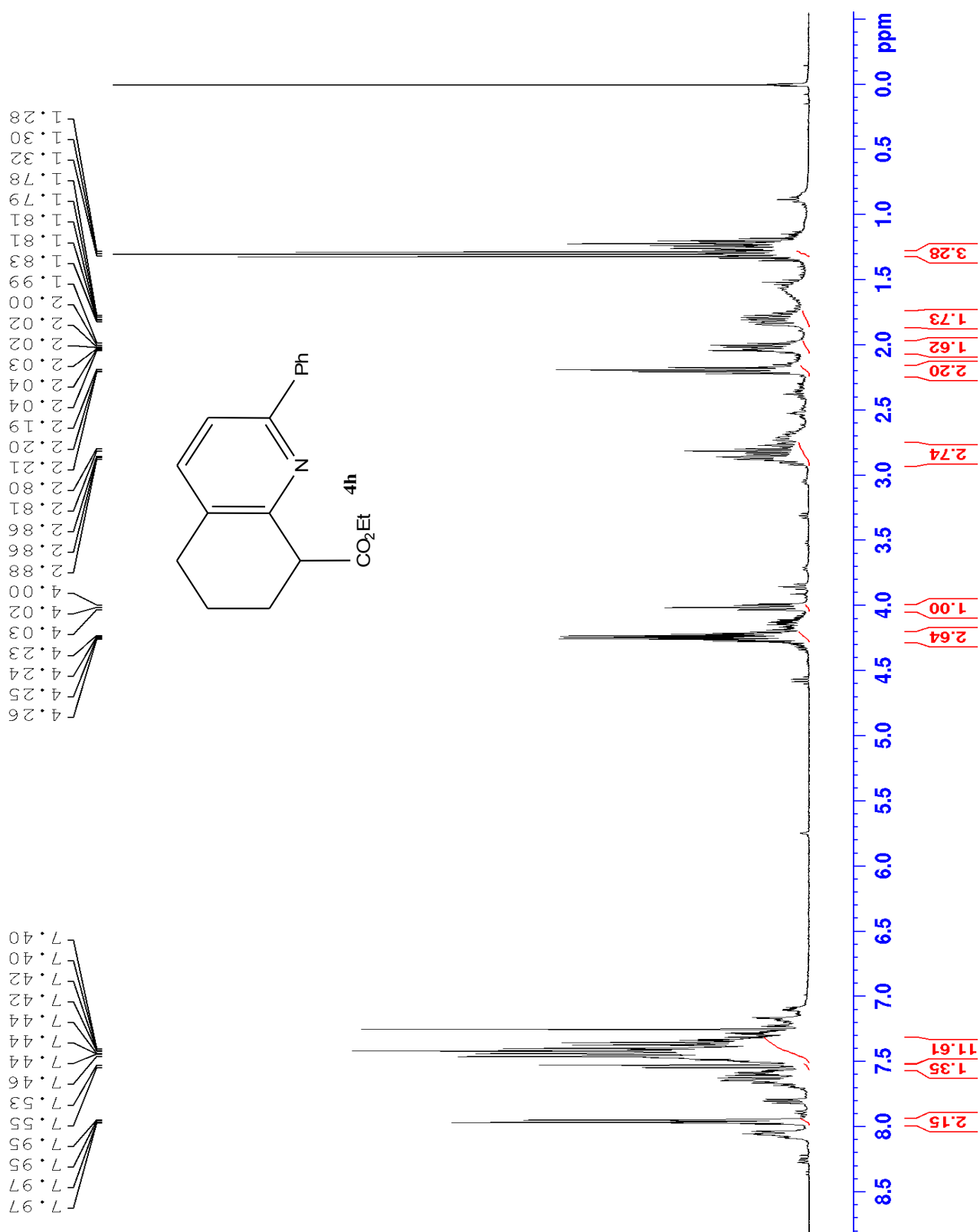
L.4 COSY of 4g



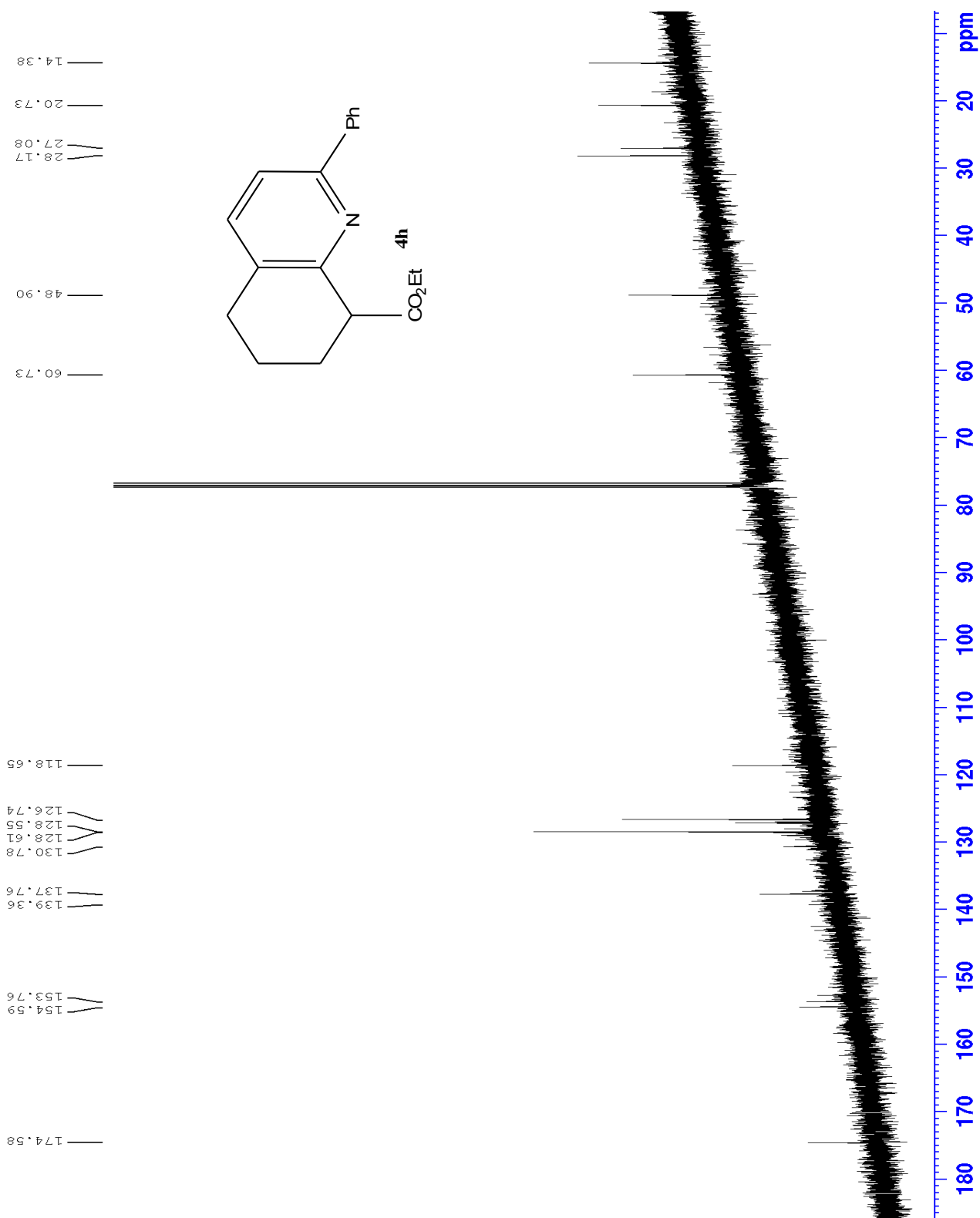
L.5 HMBC of 4g



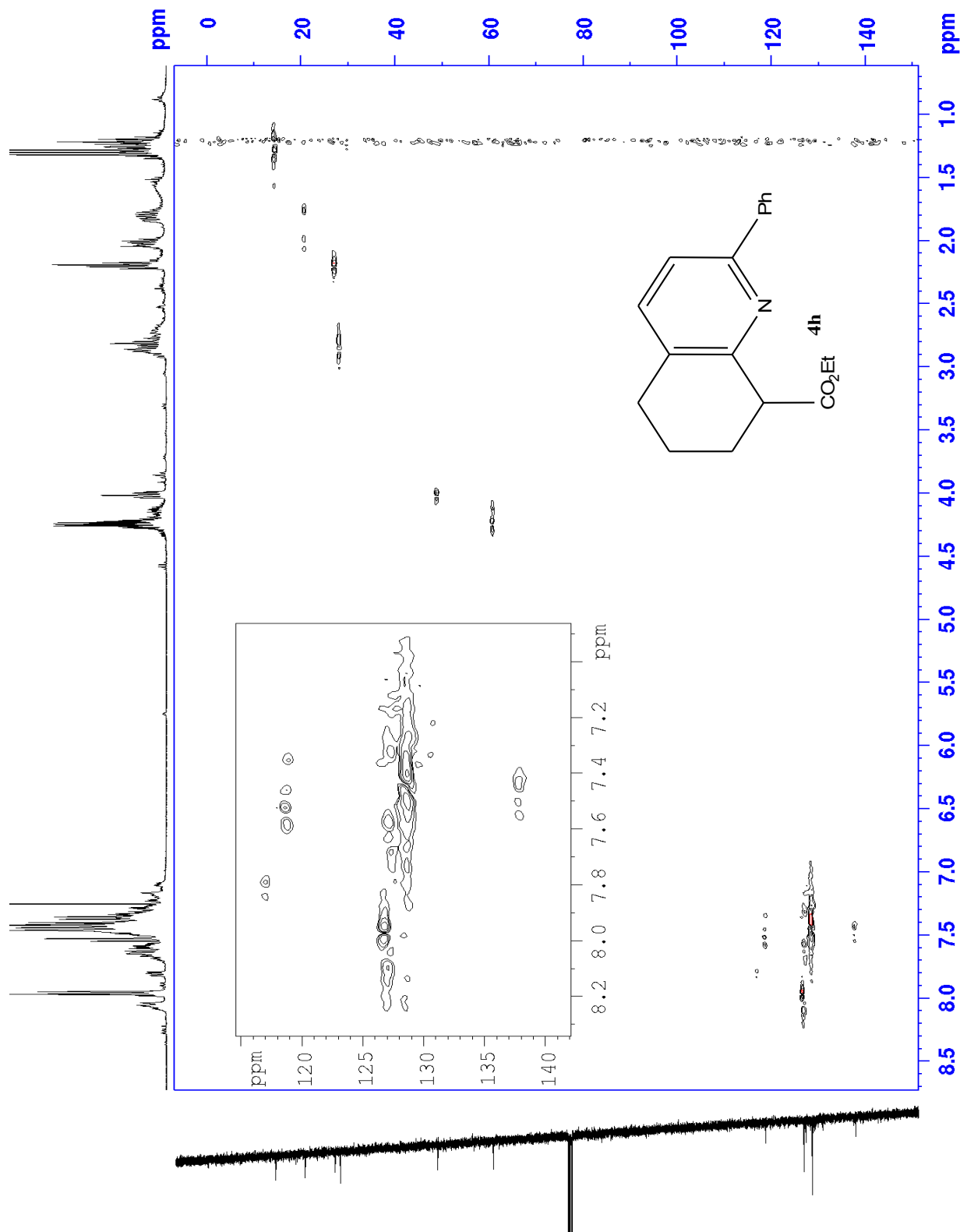
M.1 Proton of 4h



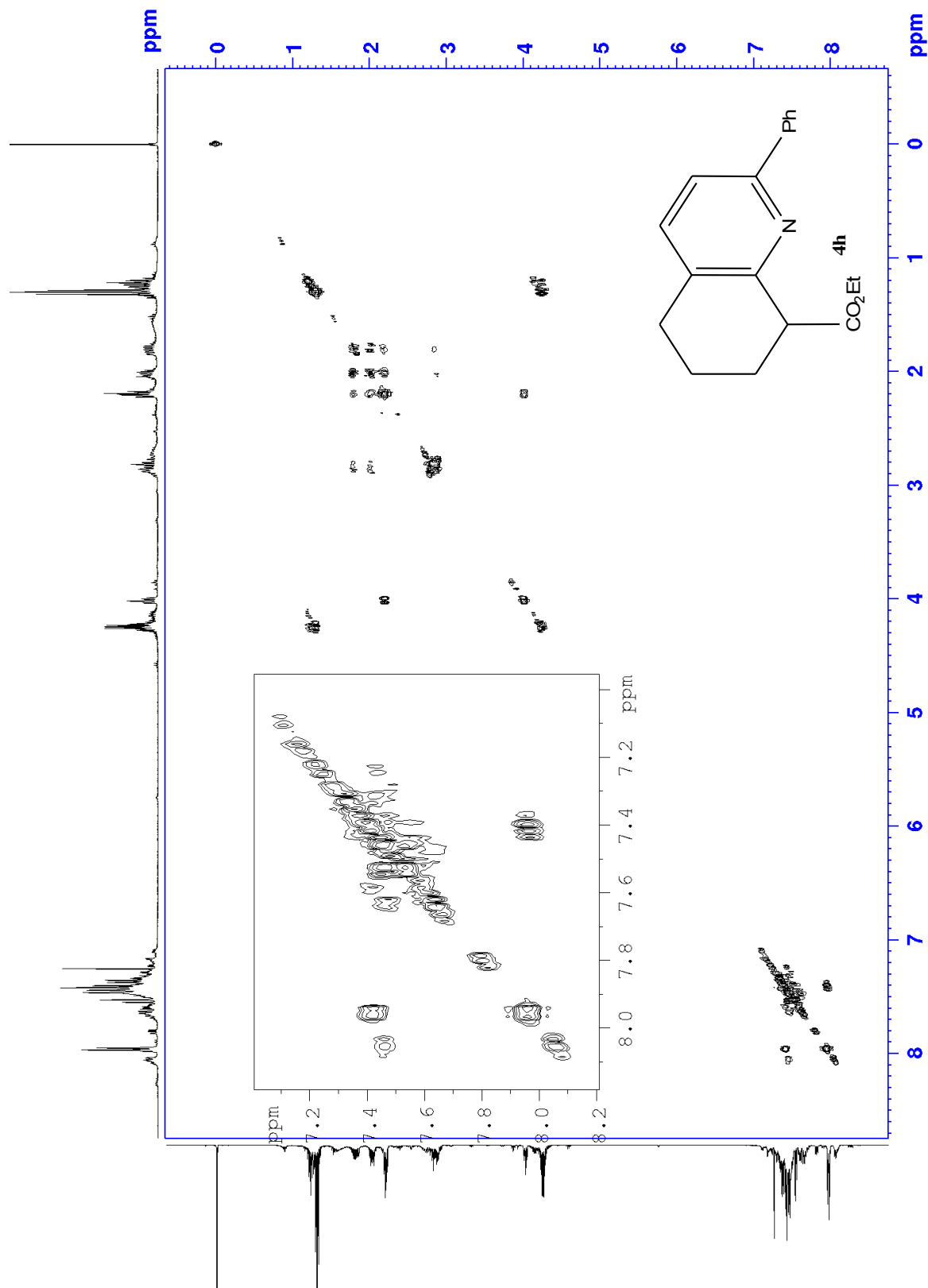
M.2 Carbon of 4h



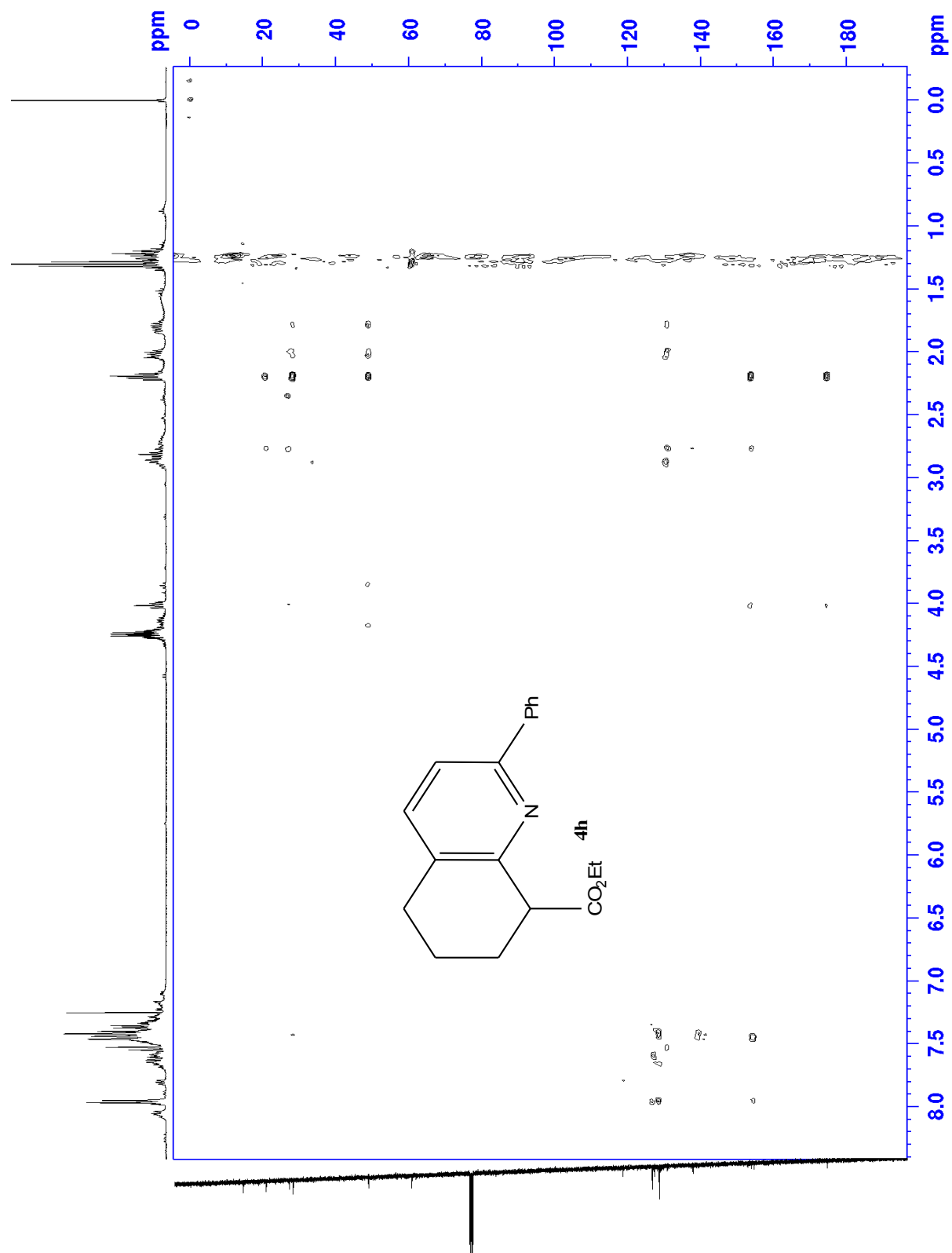
M.3 HSQC of 4h



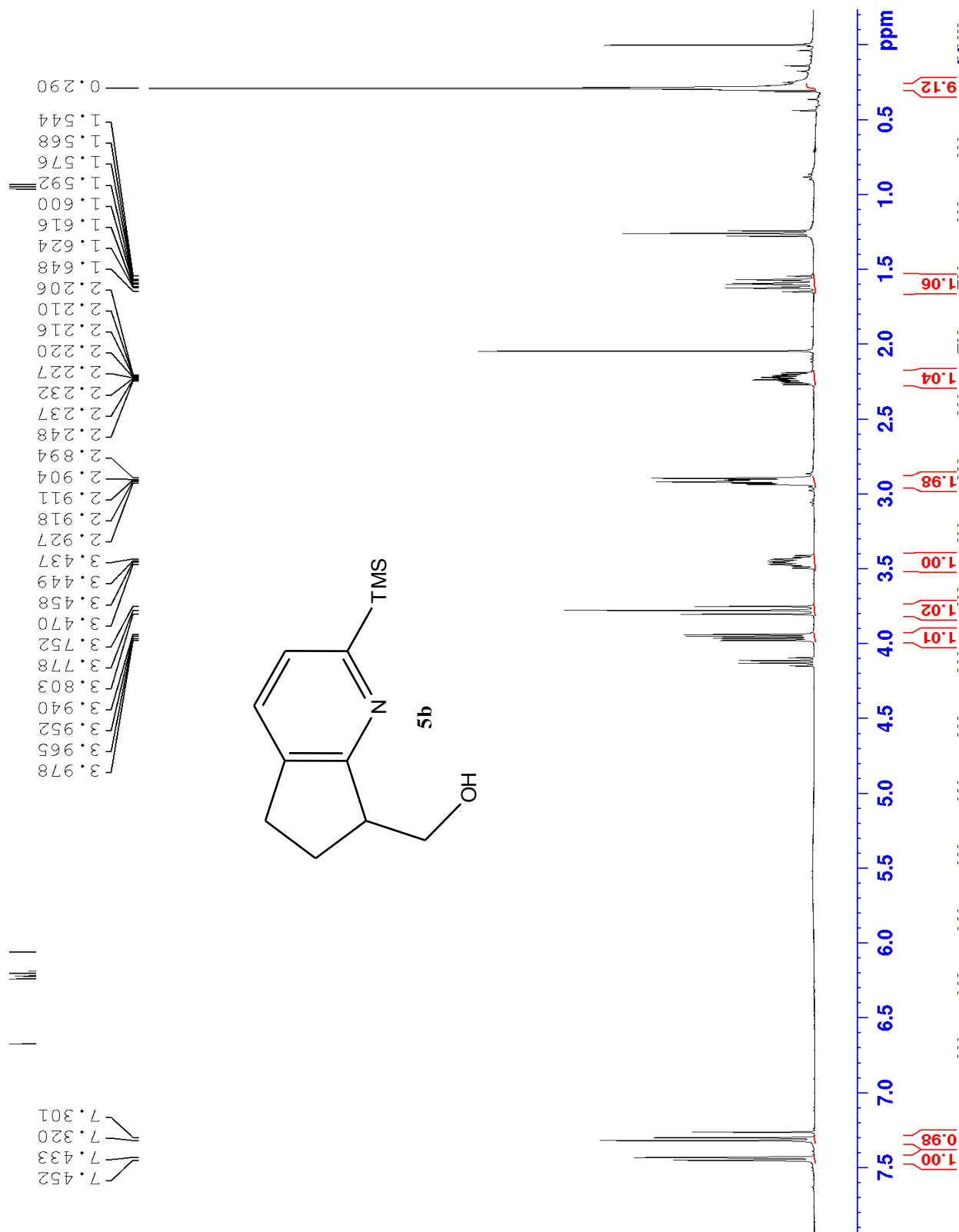
M.4 COSY of 4h



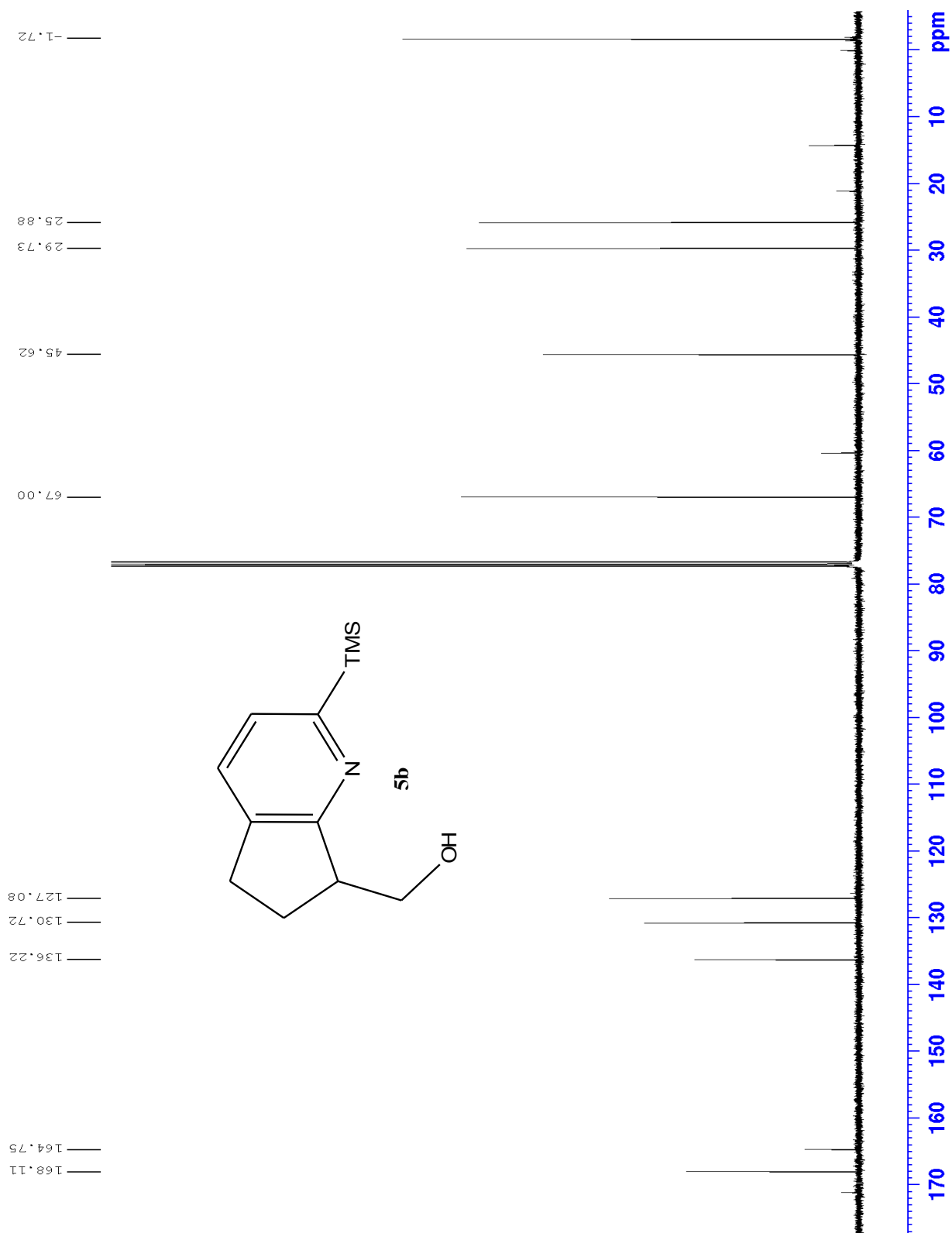
M.5 HMBC of 4h



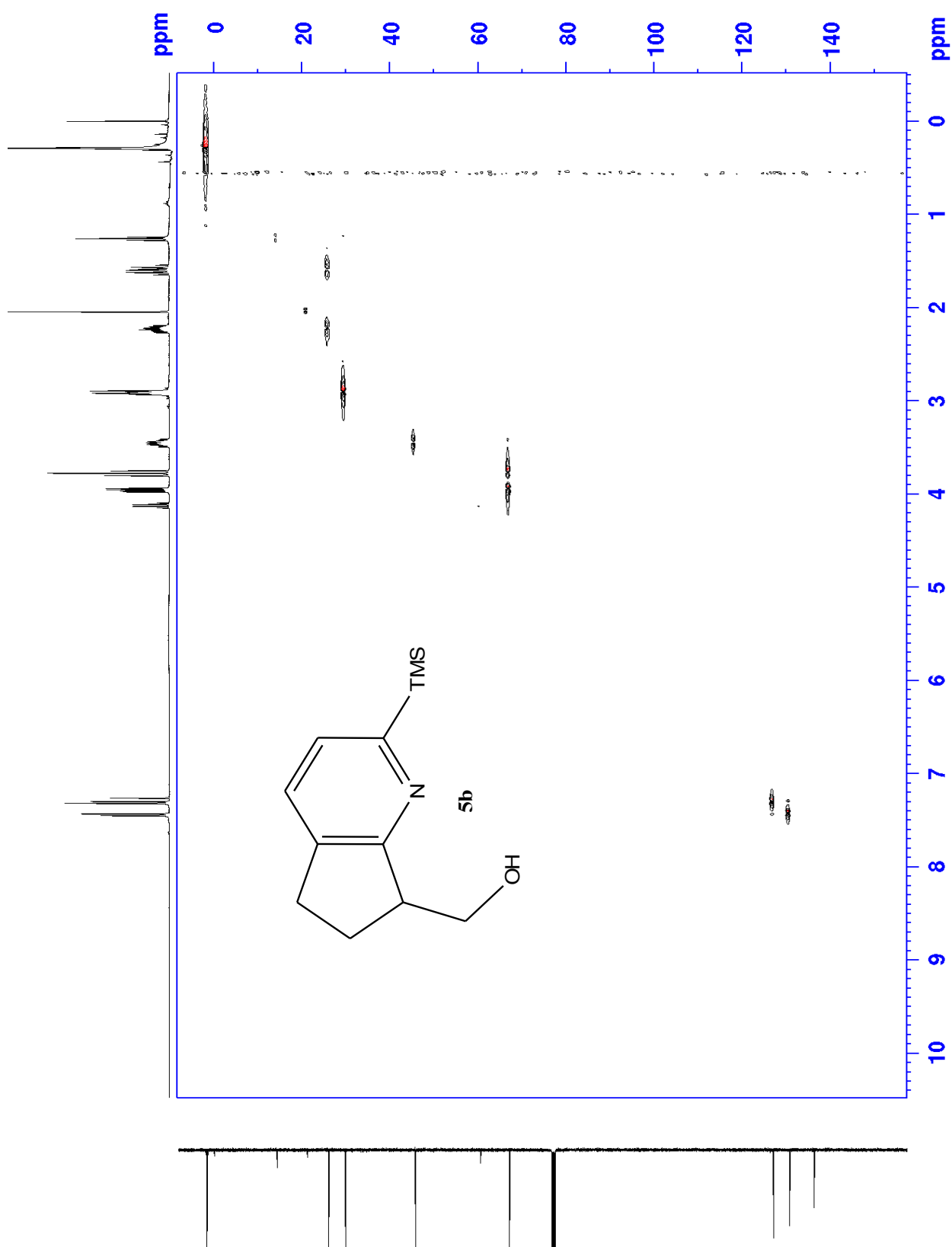
N.1 Proton of 5b



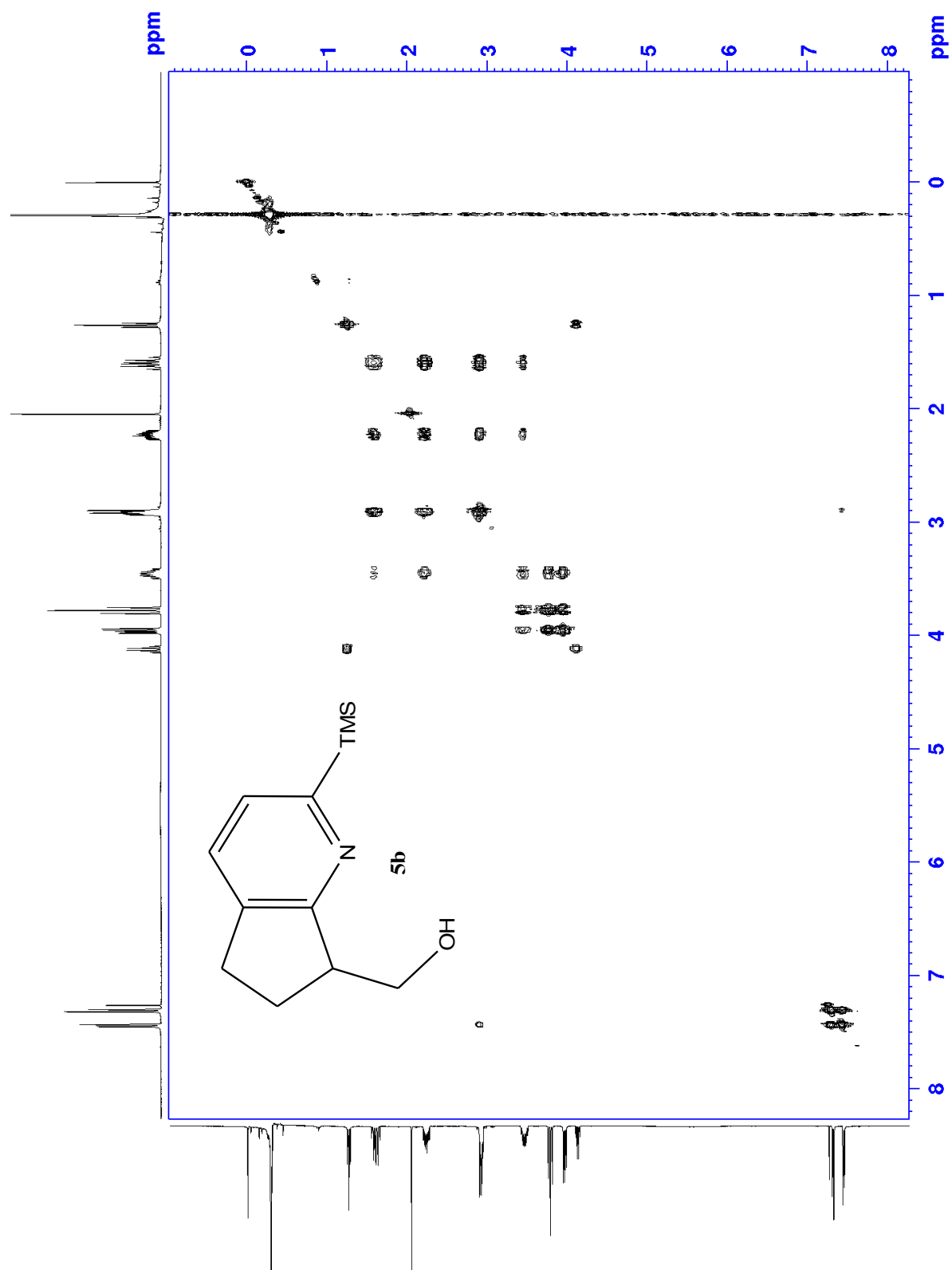
N.2 Carbon of 5b



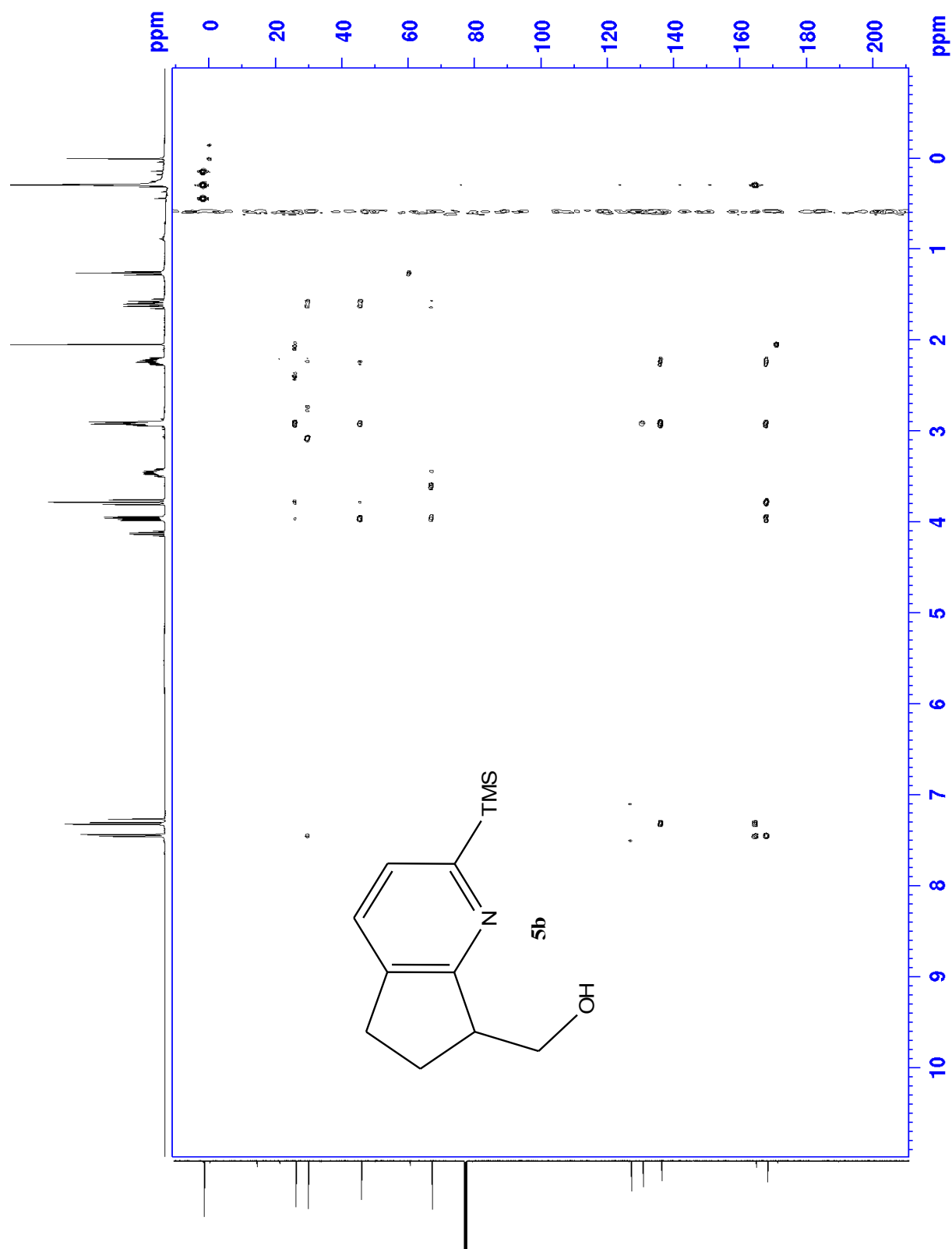
N.3 HSQC of 5b



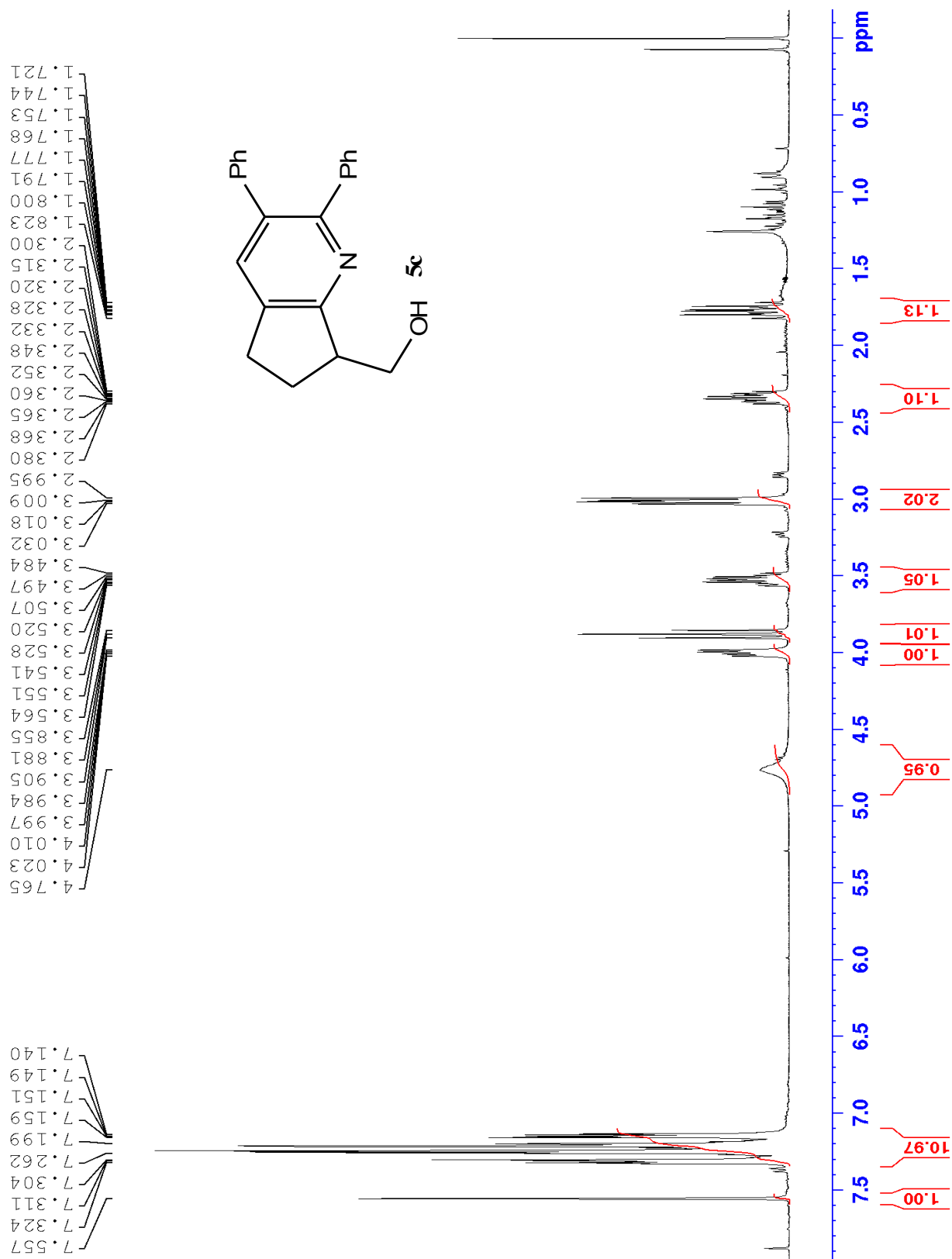
N.4 COSY of 5b



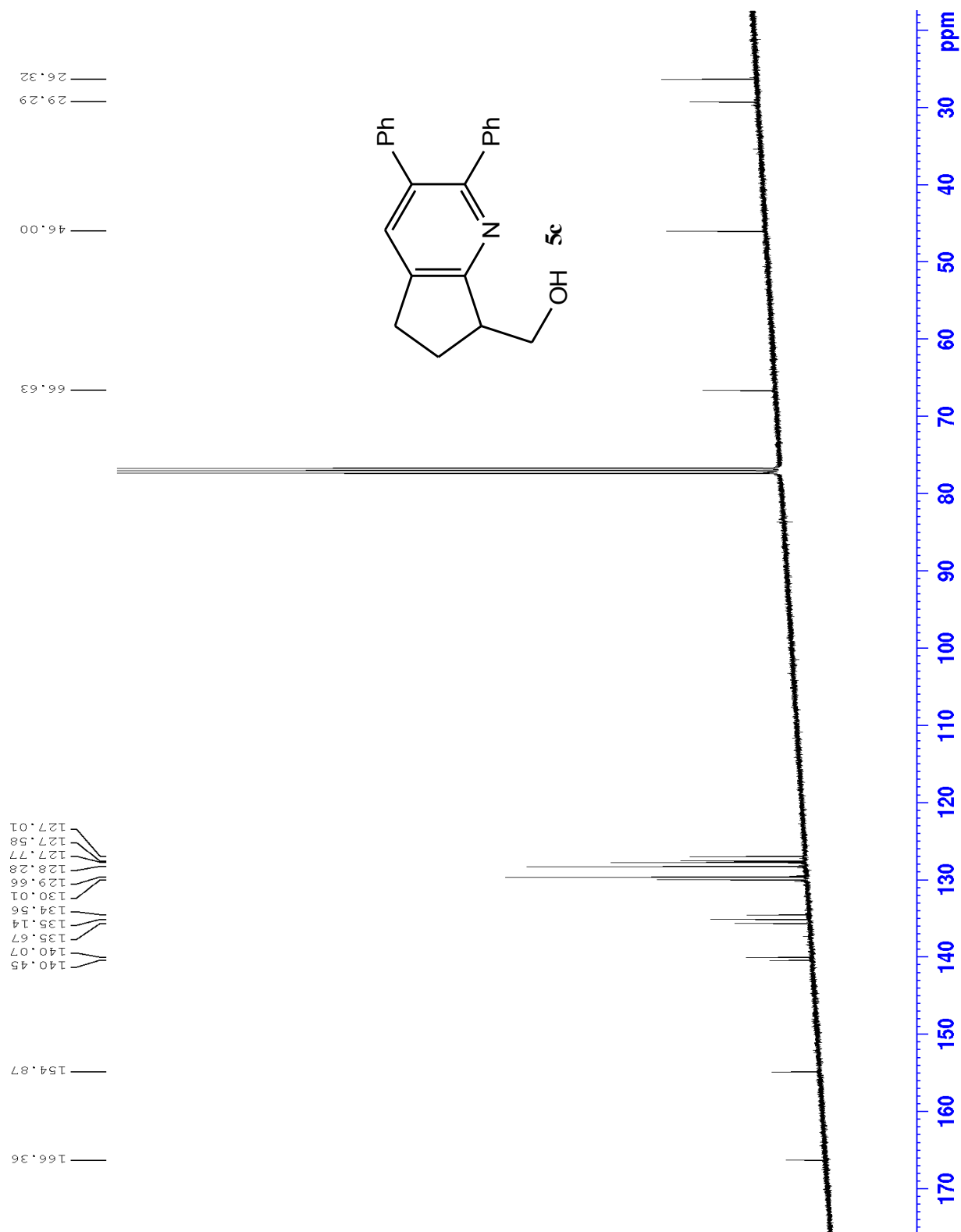
N.5 HMBC of 5b



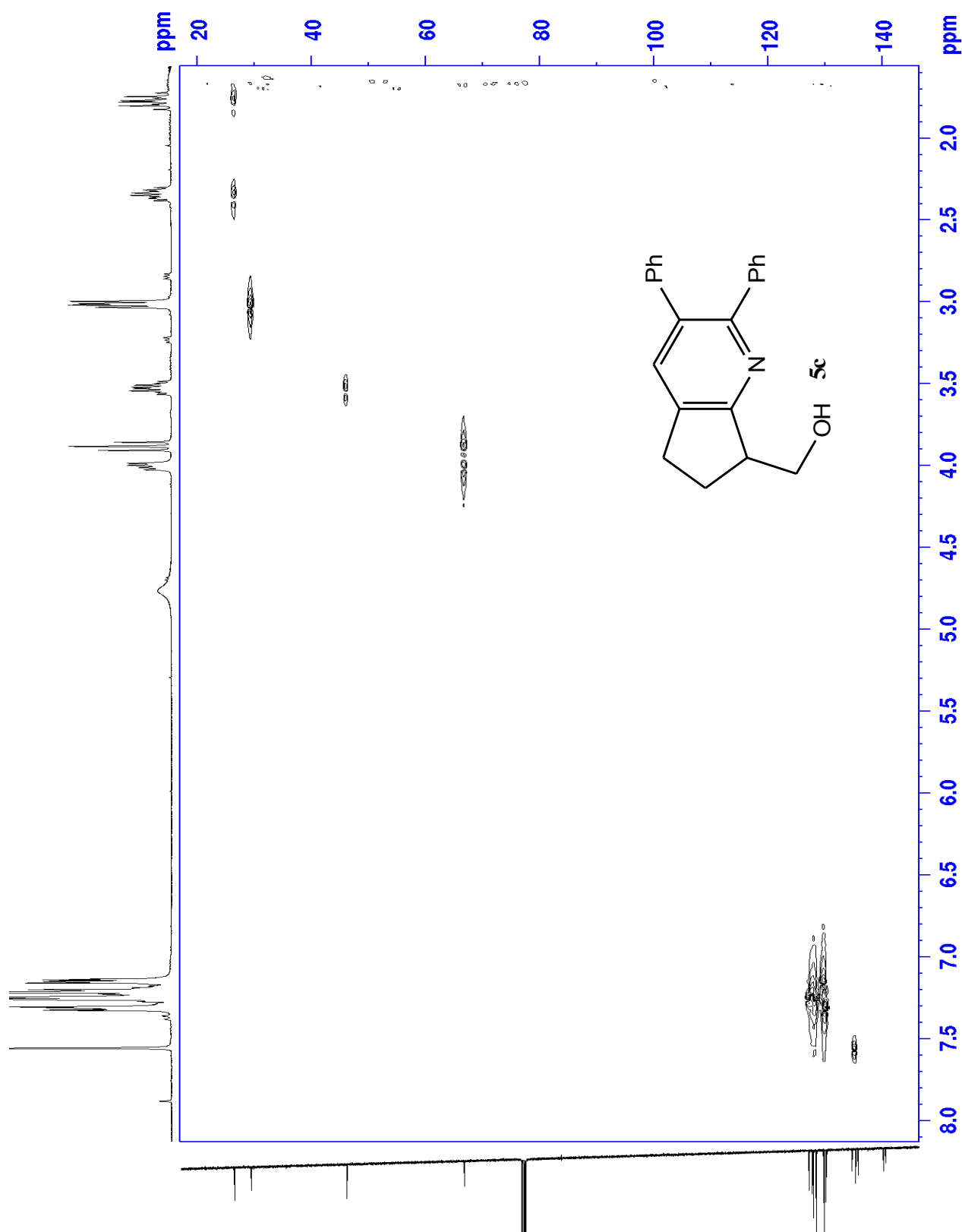
O.1 Proton of 5c



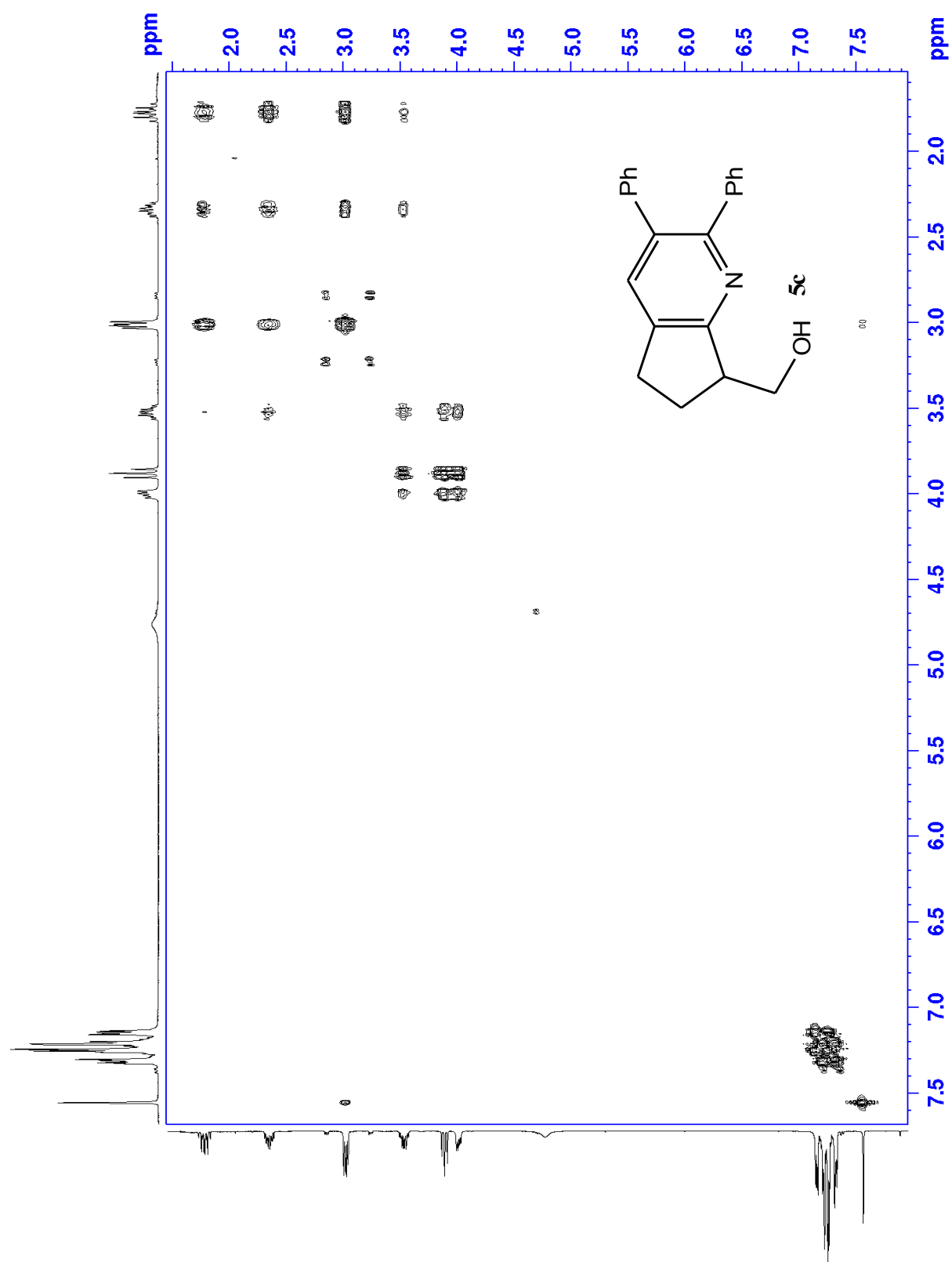
O.2 Carbon of 5c



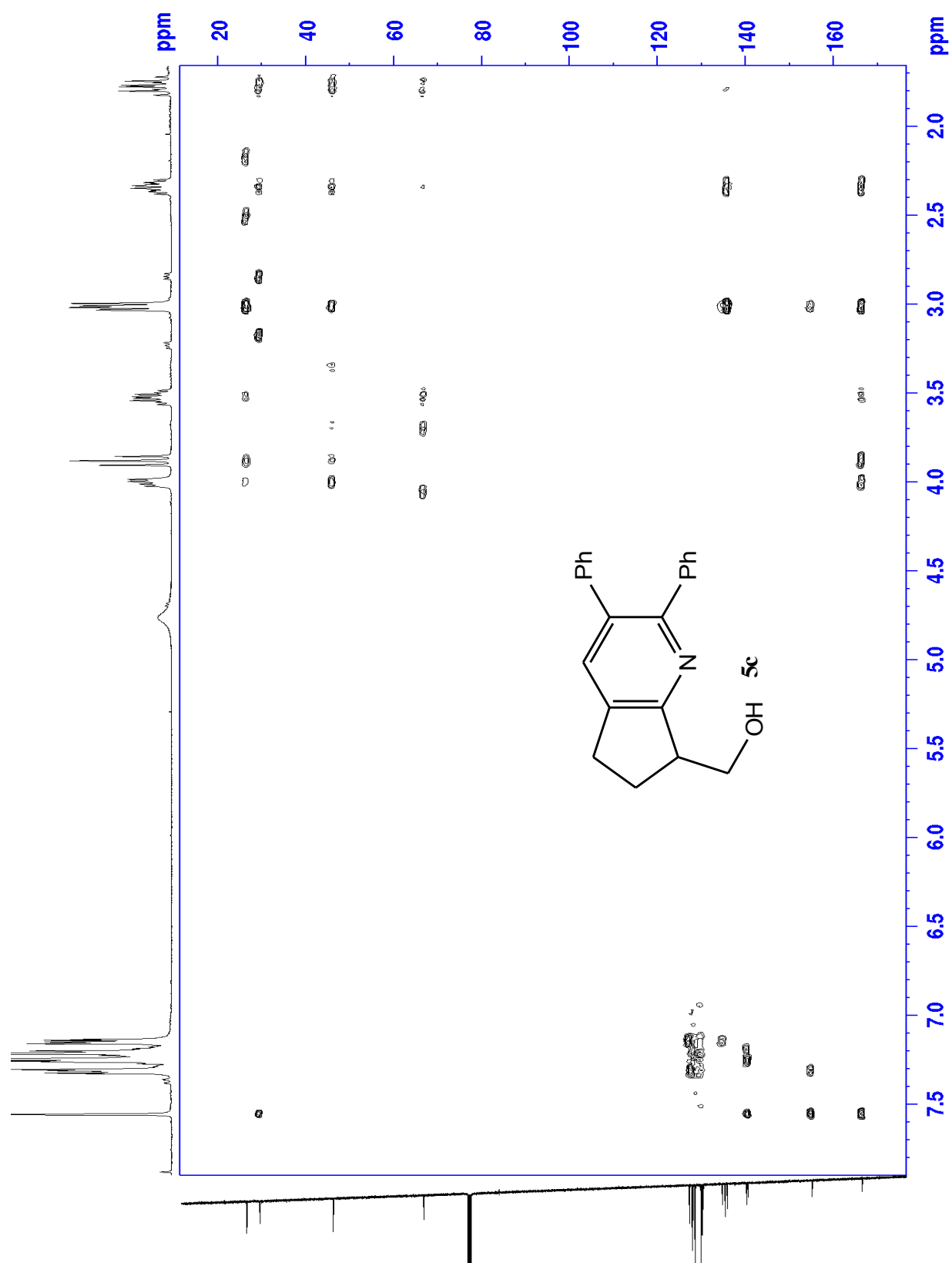
O.3 HSQC of 5c



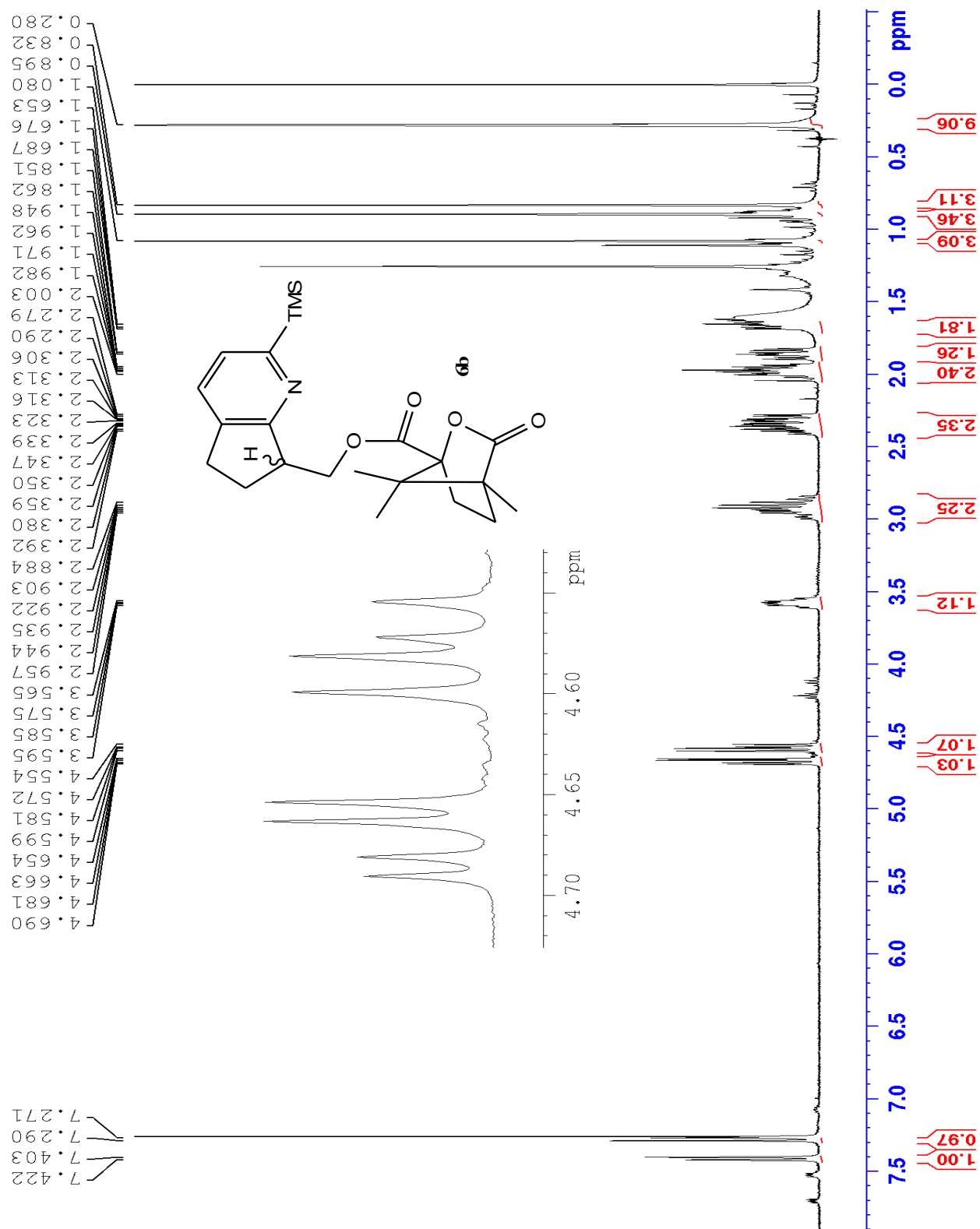
O.4 COSY of 5c



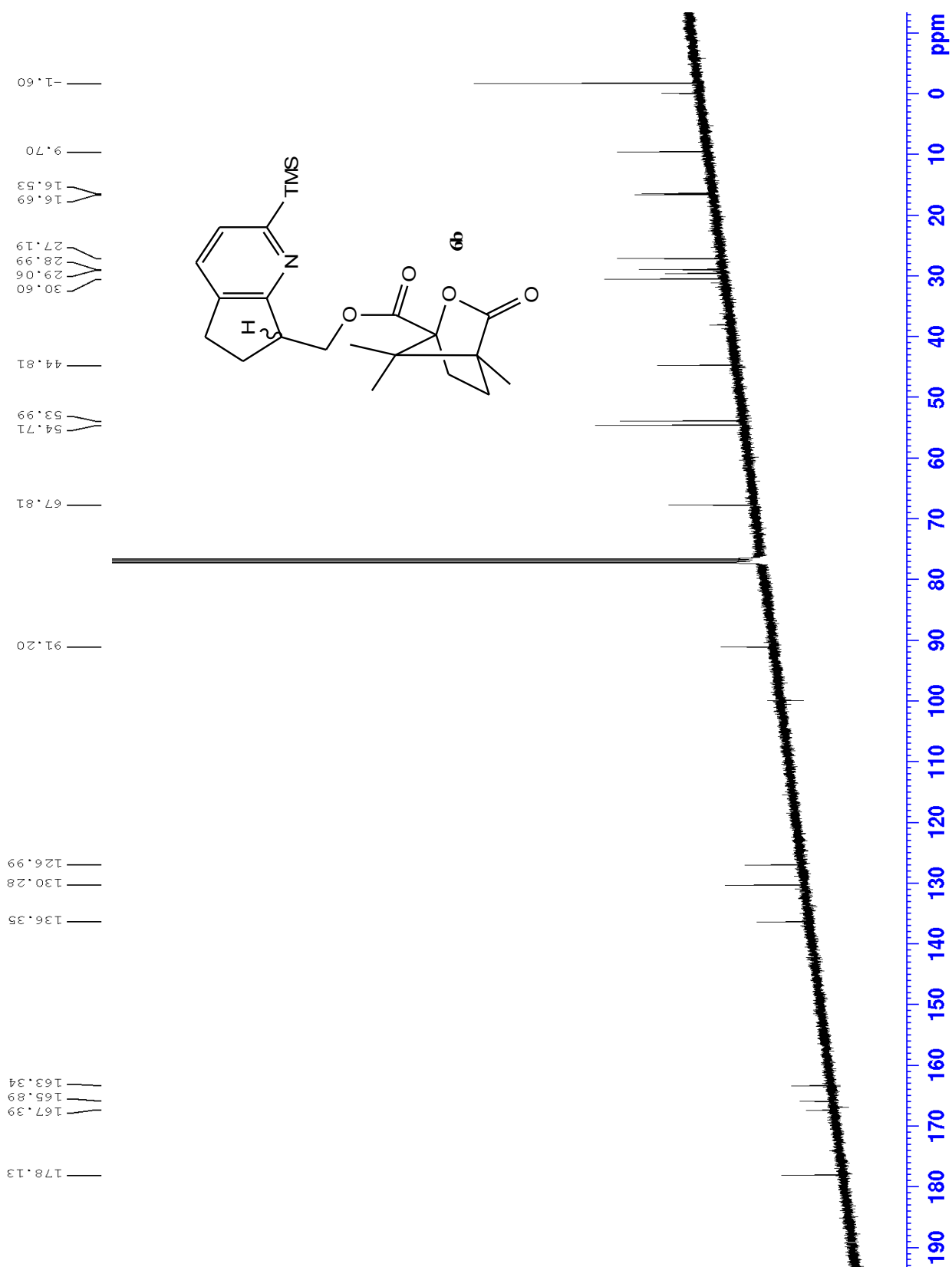
O.5 HMBC of 5c



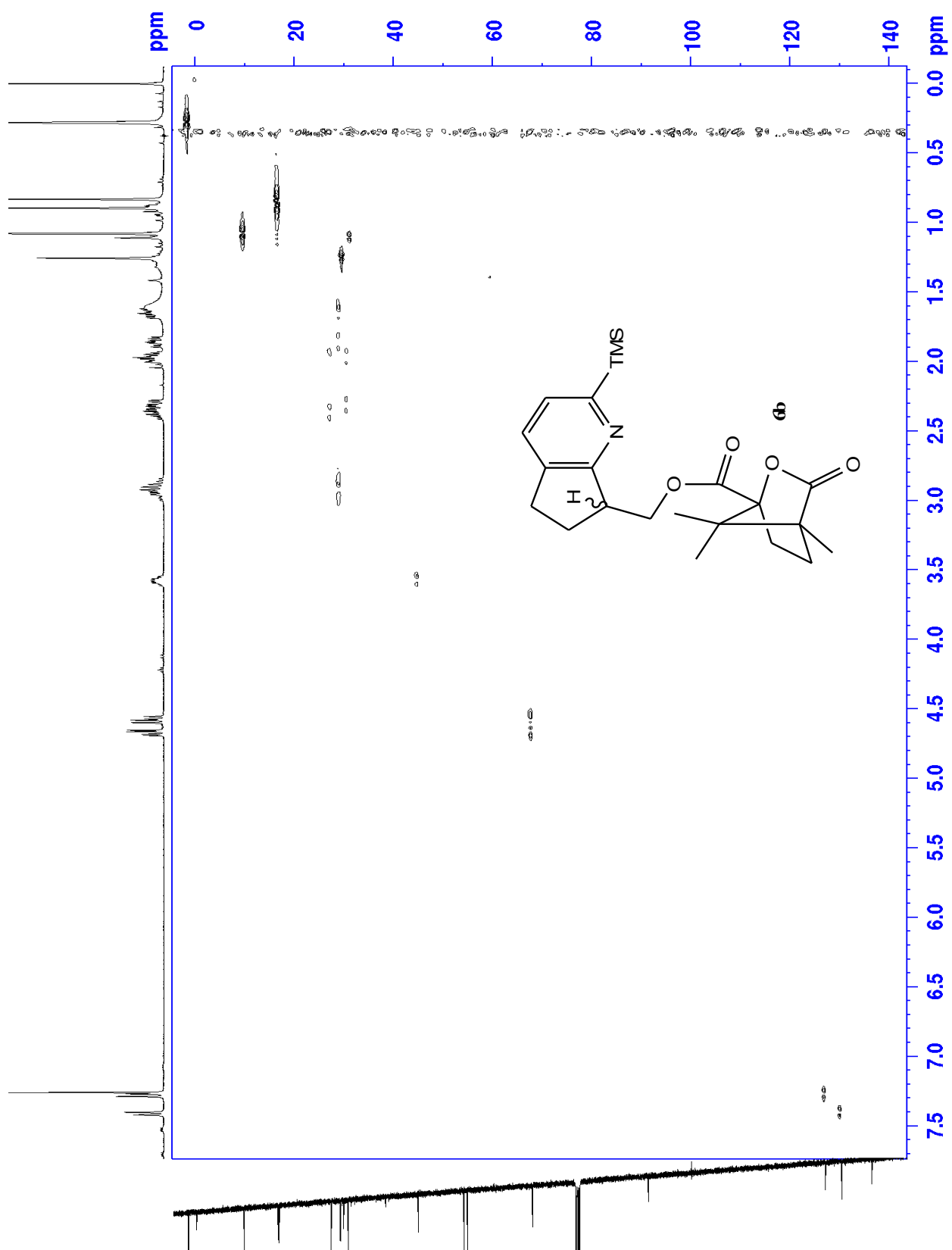
P.1 Proton of 6b (frac 1)



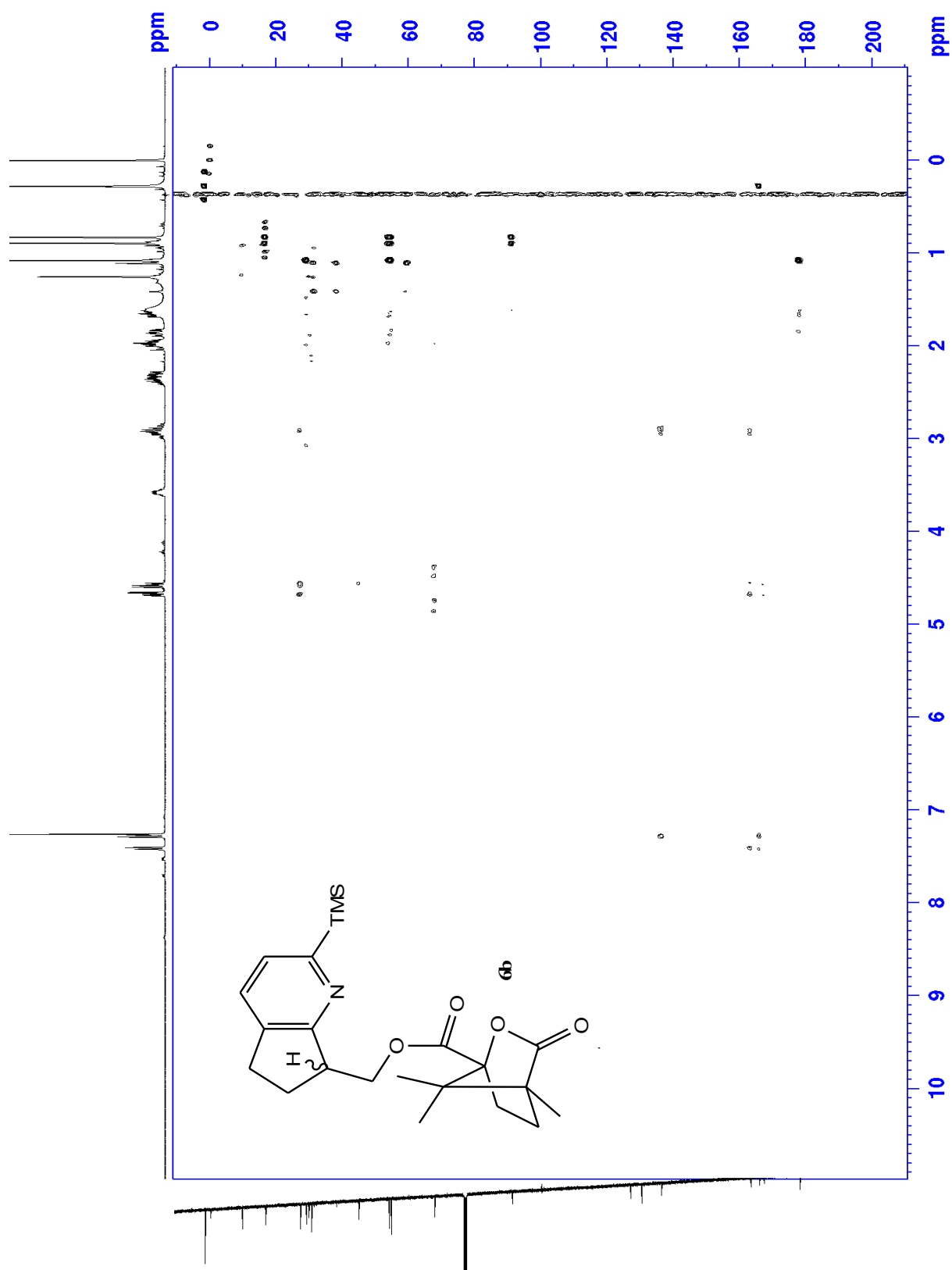
P.2 Carbon of 6b (frac 1)



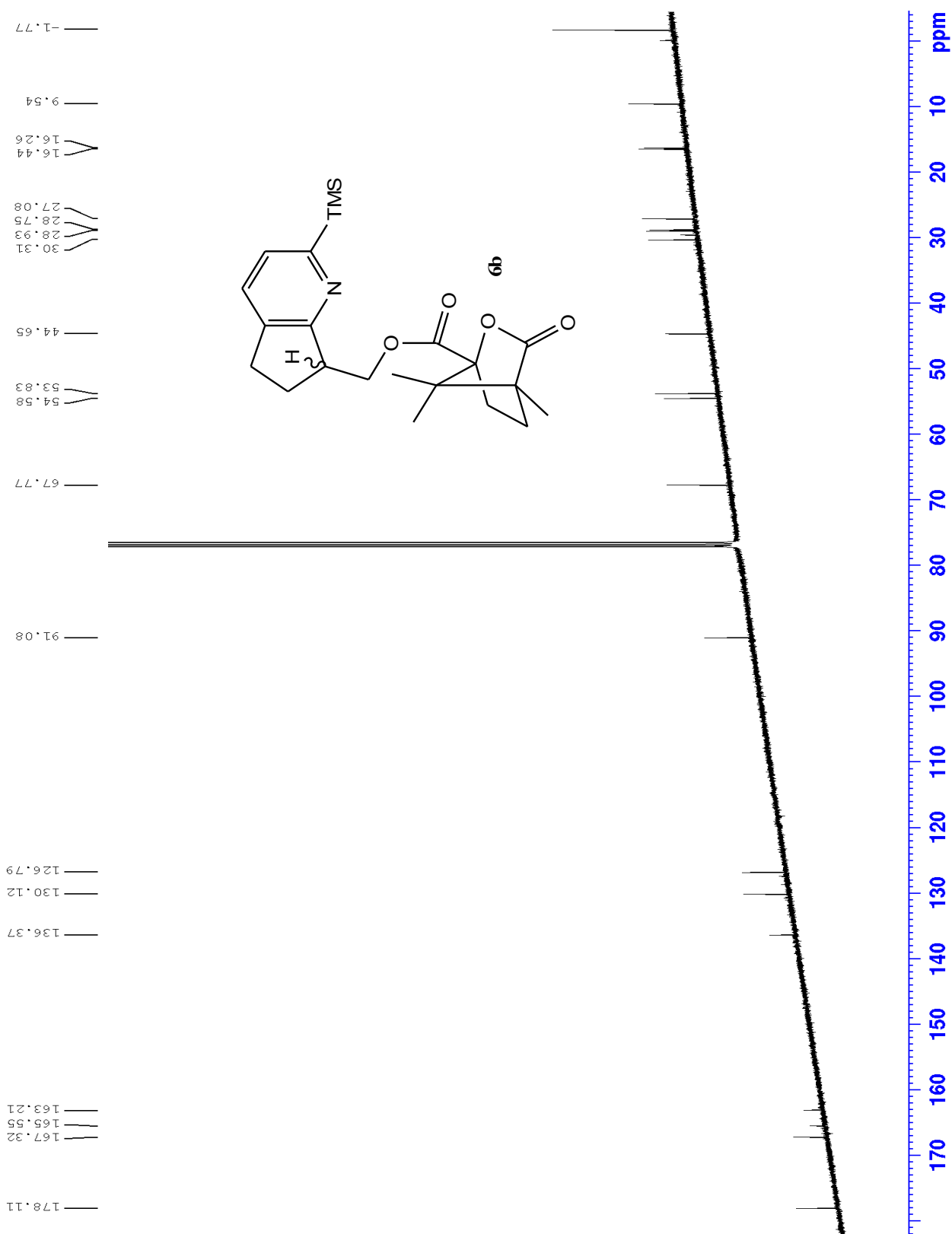
P.3 HSQC of 6b (frac 1)



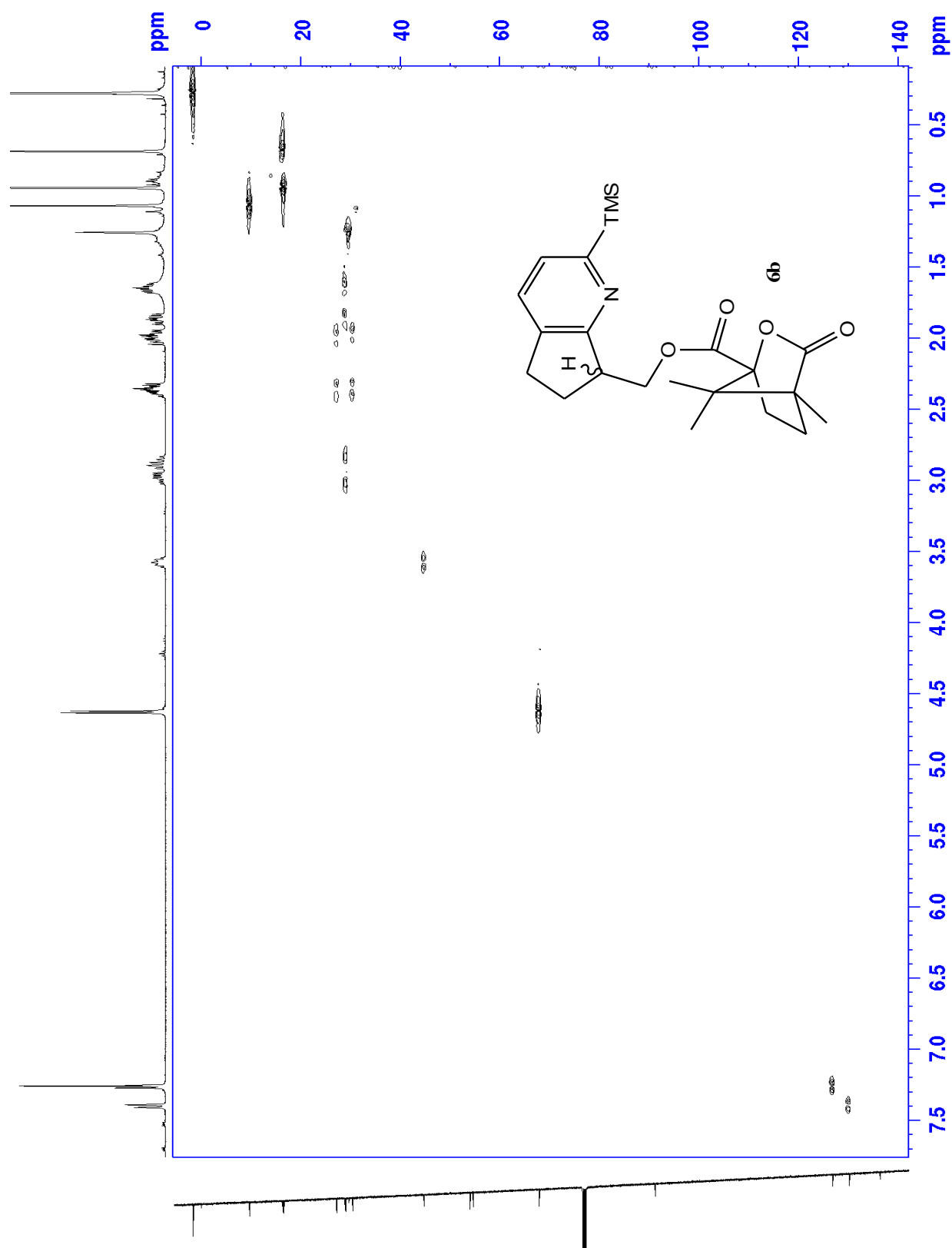
P.5 HMBC of 6b (frac 1)



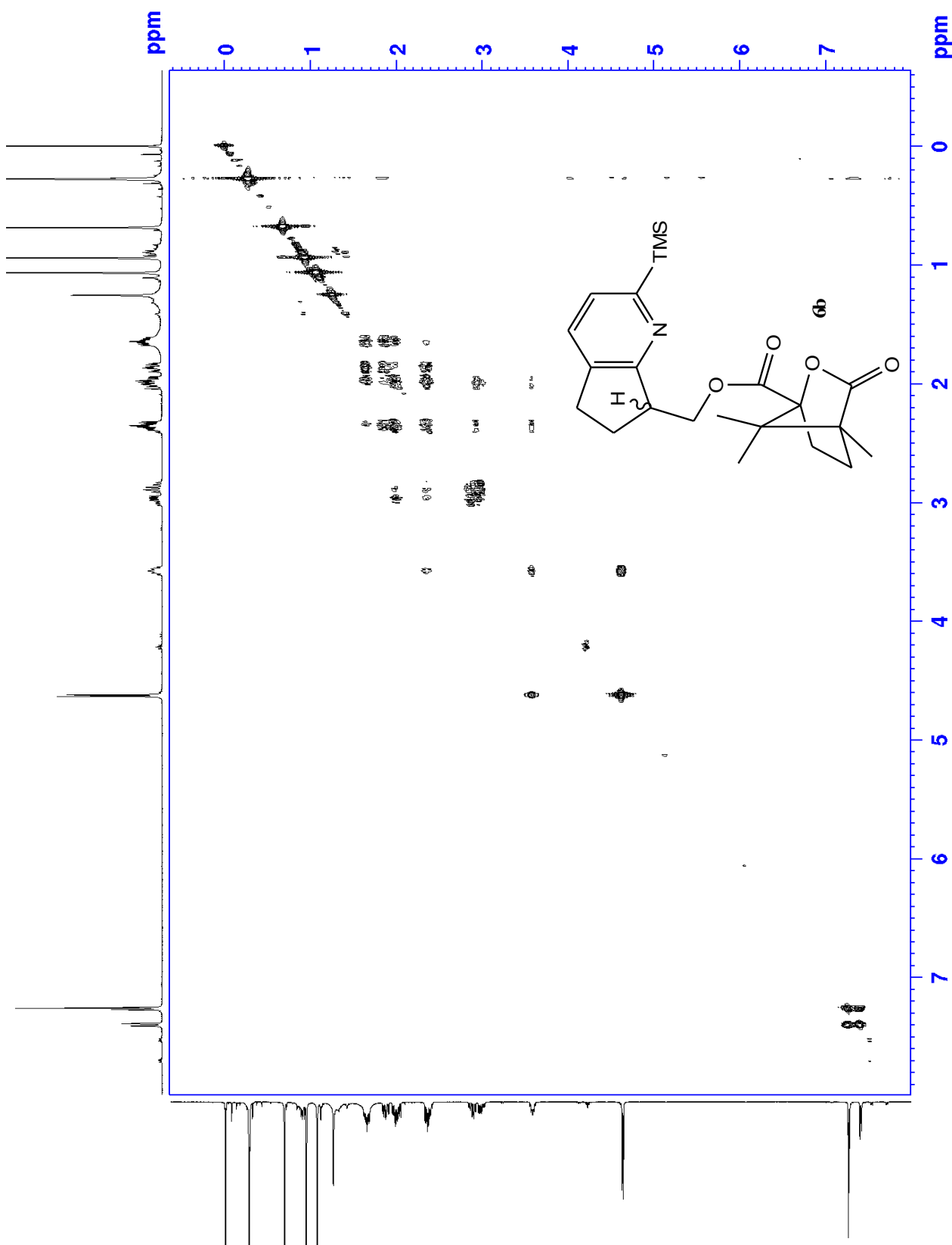
Q.2 Carbon of 6b (frac 2)



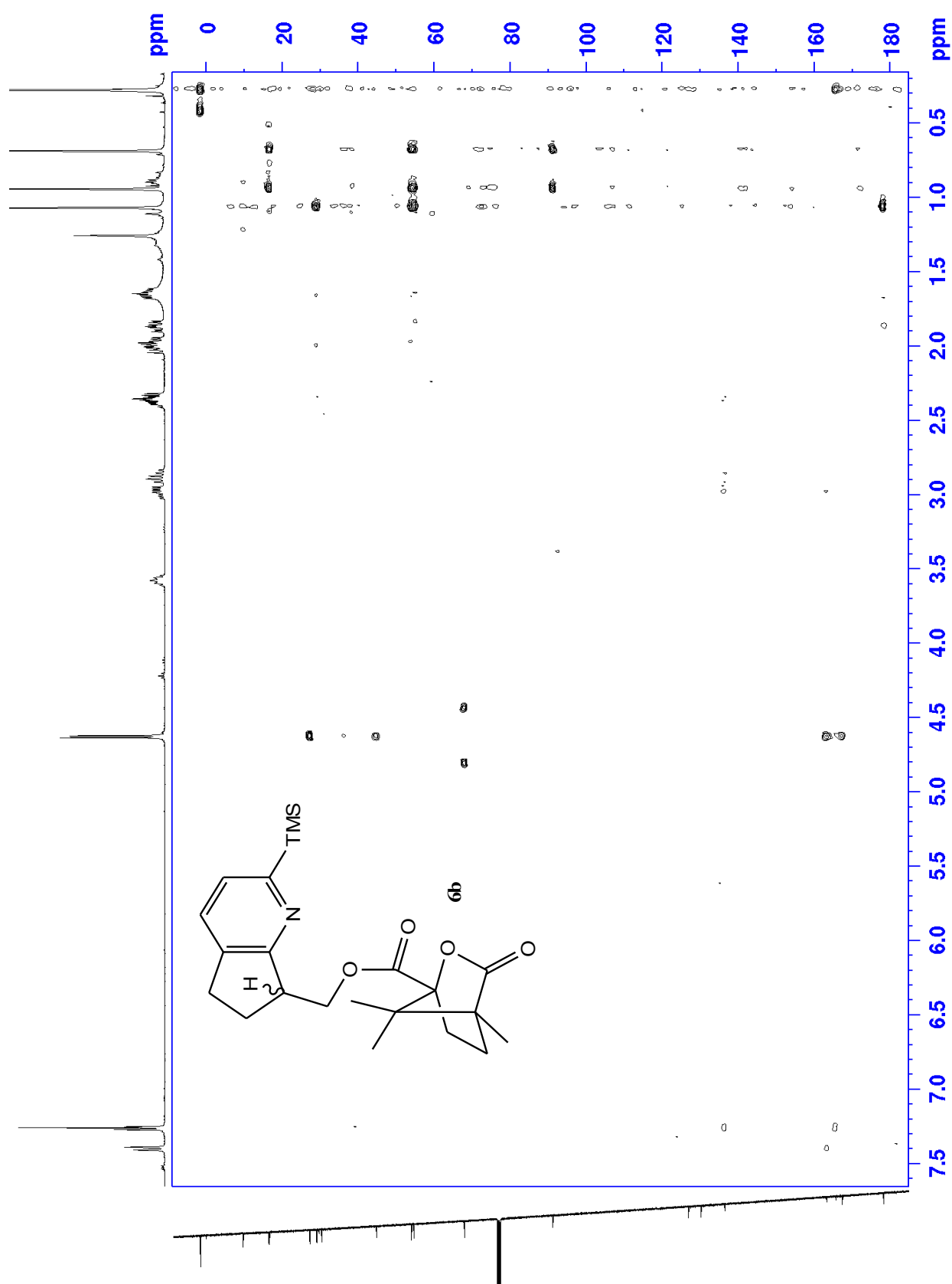
Q.3 HSQC of 6b (frac 2)



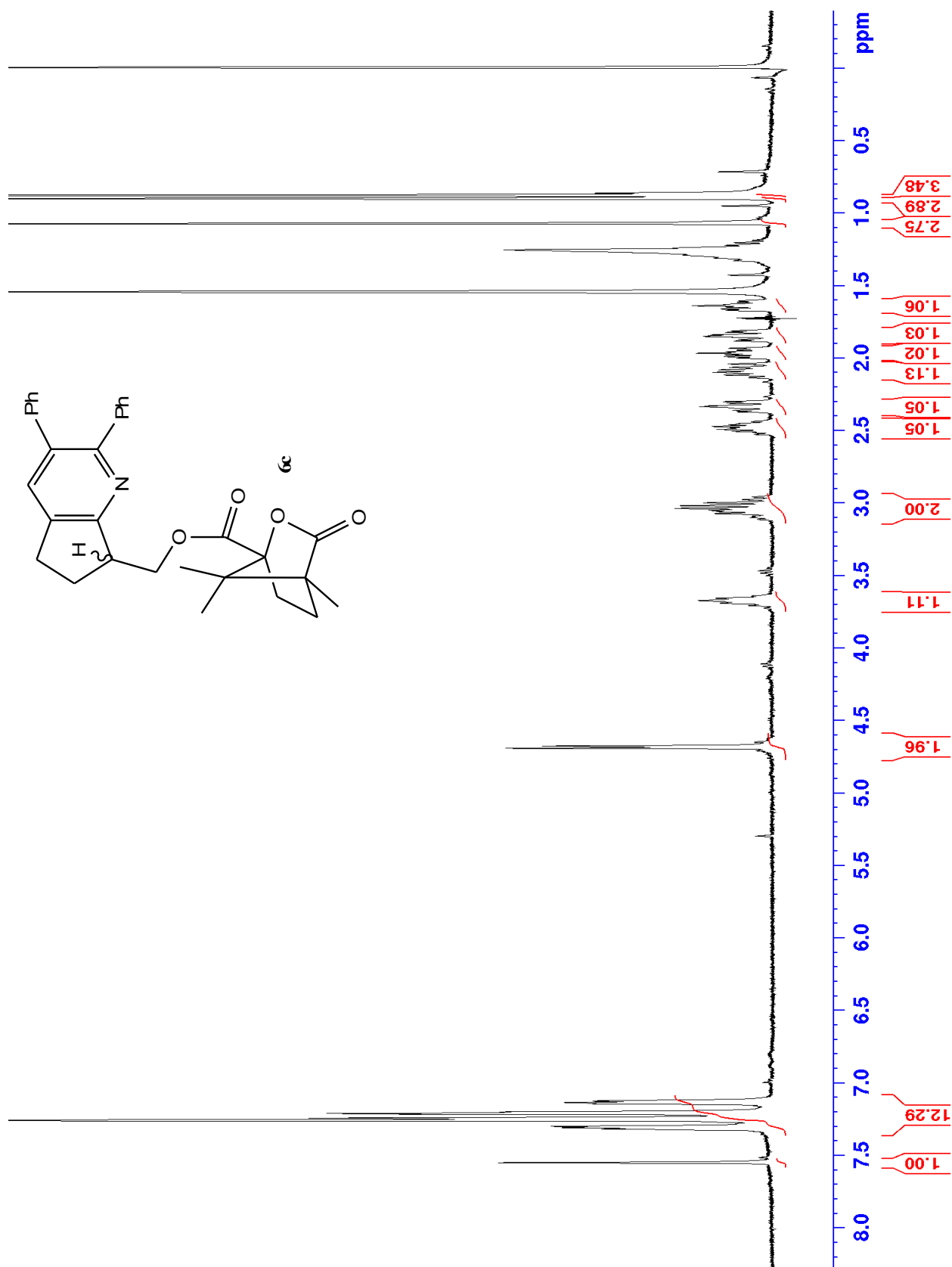
Q.4 COSY of 6b (frac 2)



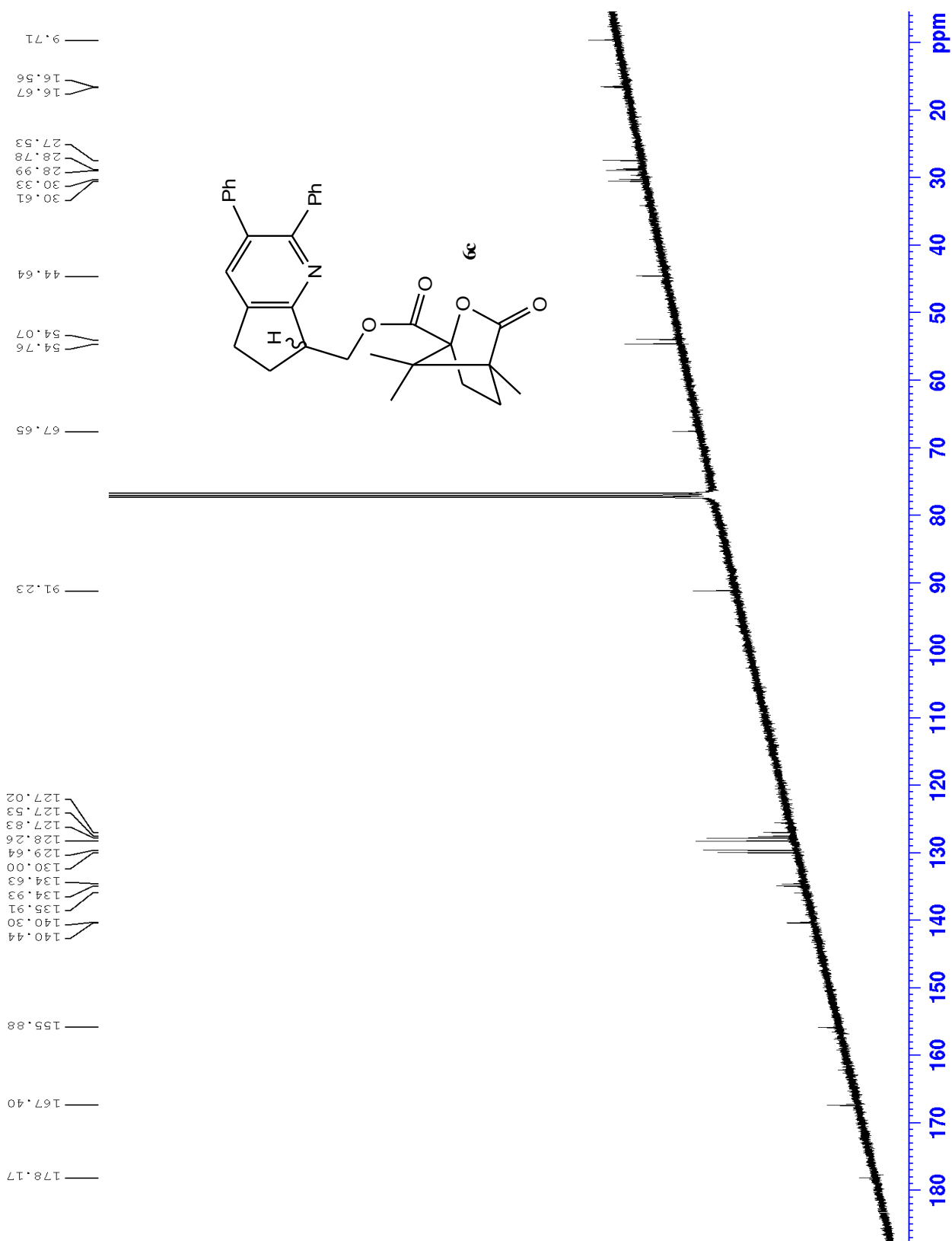
Q.5 HMBC of 6b (frac 2)



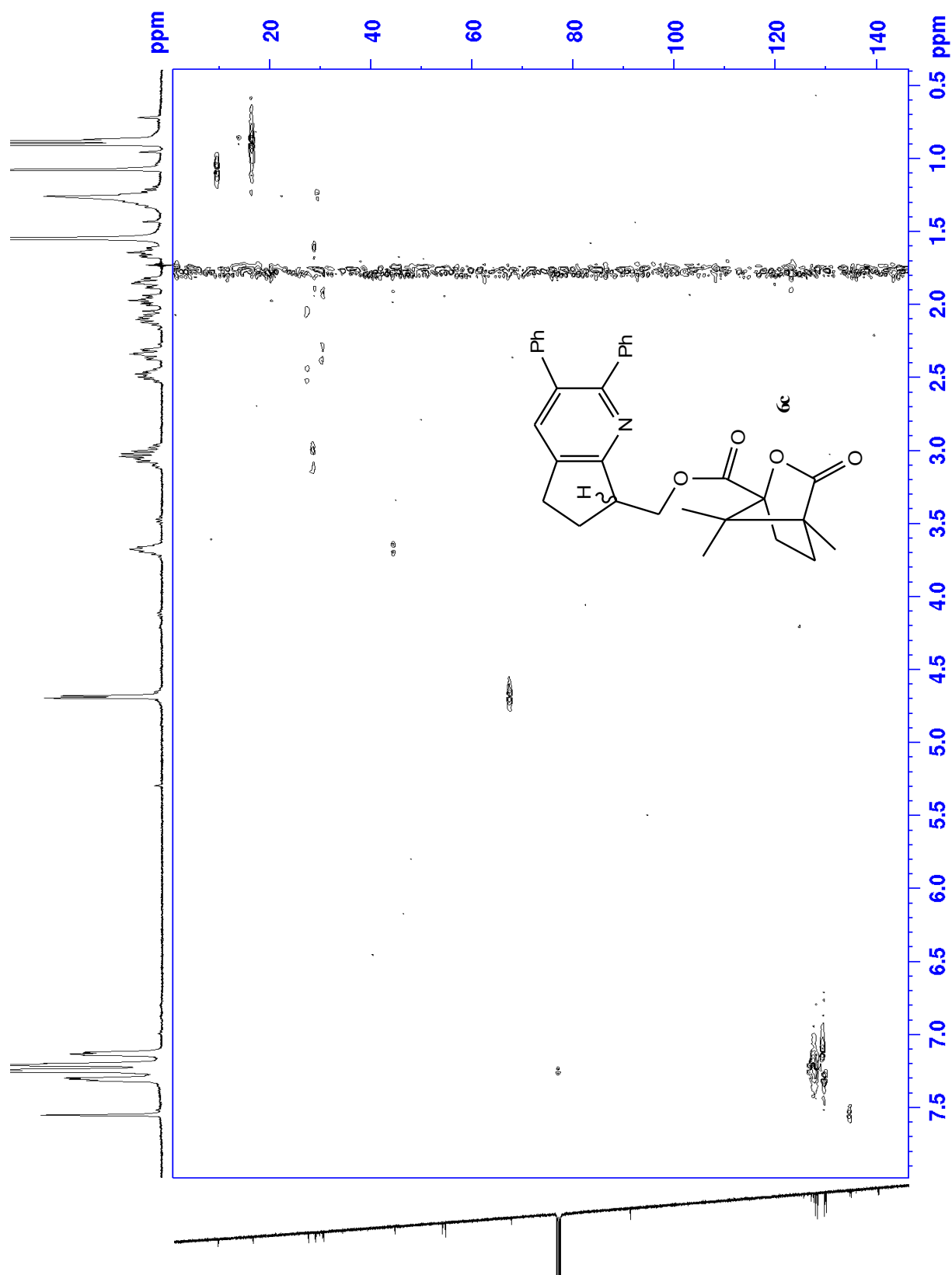
R.1 Proton of 6c (frac 1)



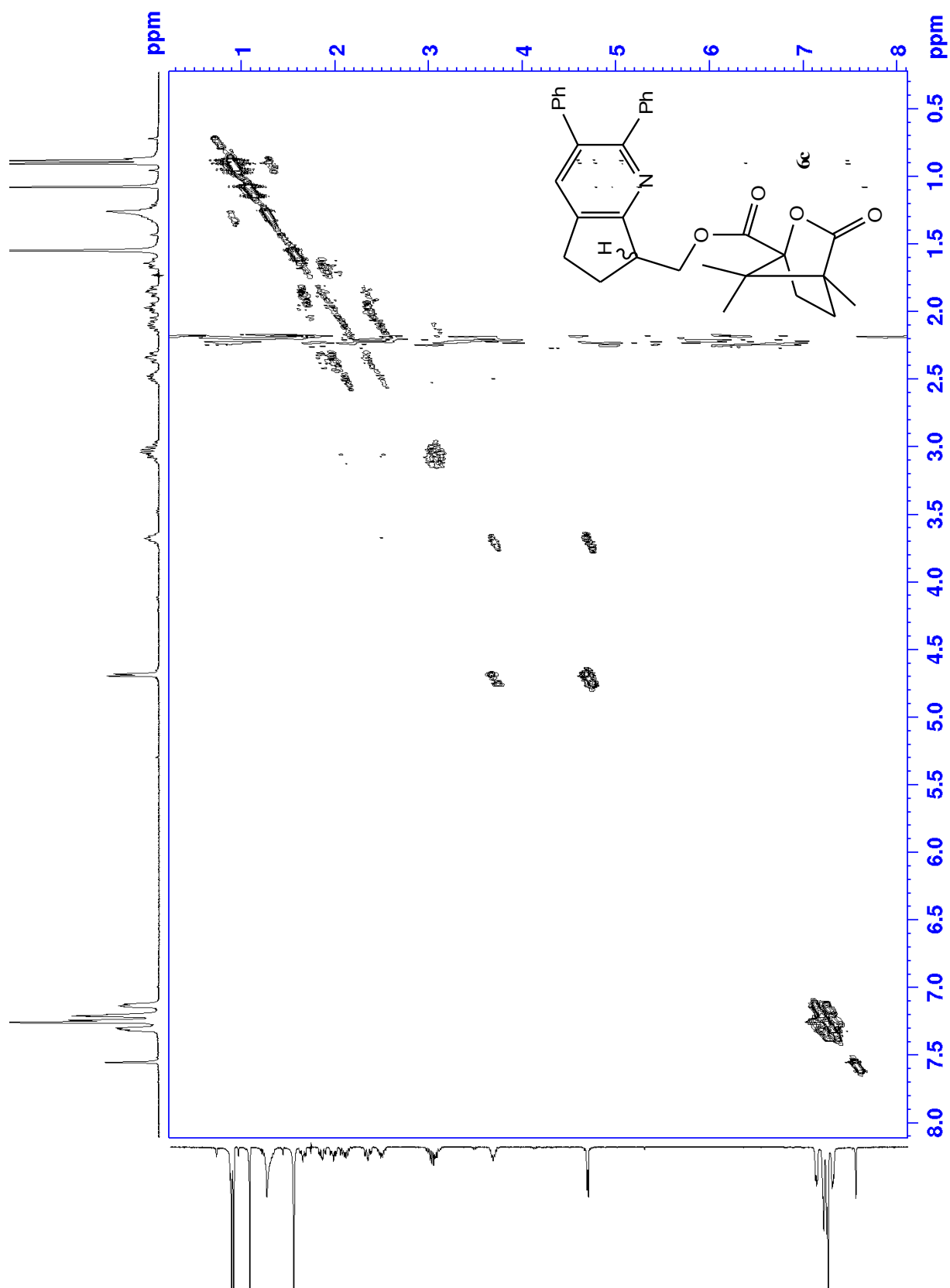
R.2 Carbon of 6c (frac 1)



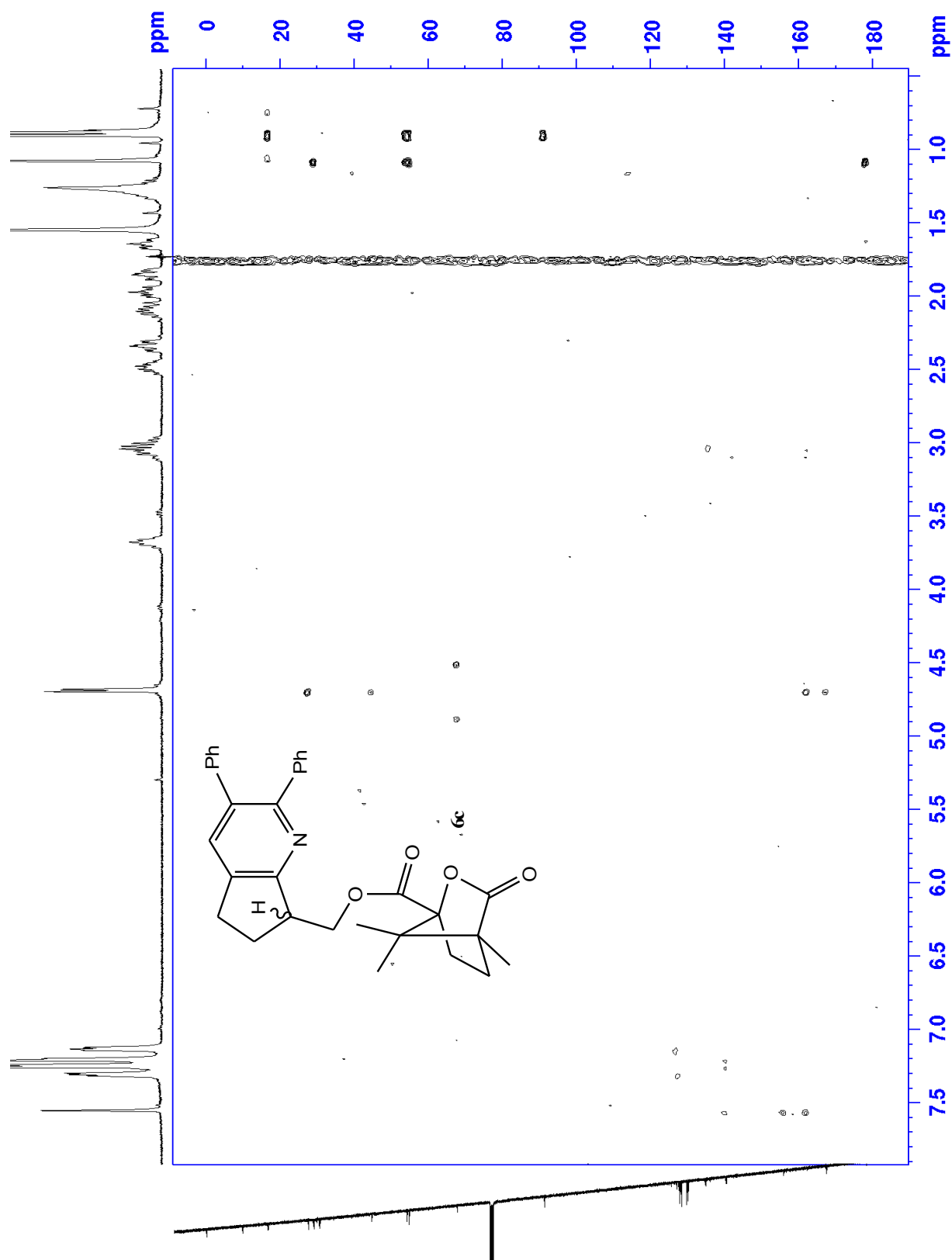
R.3 HSQC of 6c (frac 1)



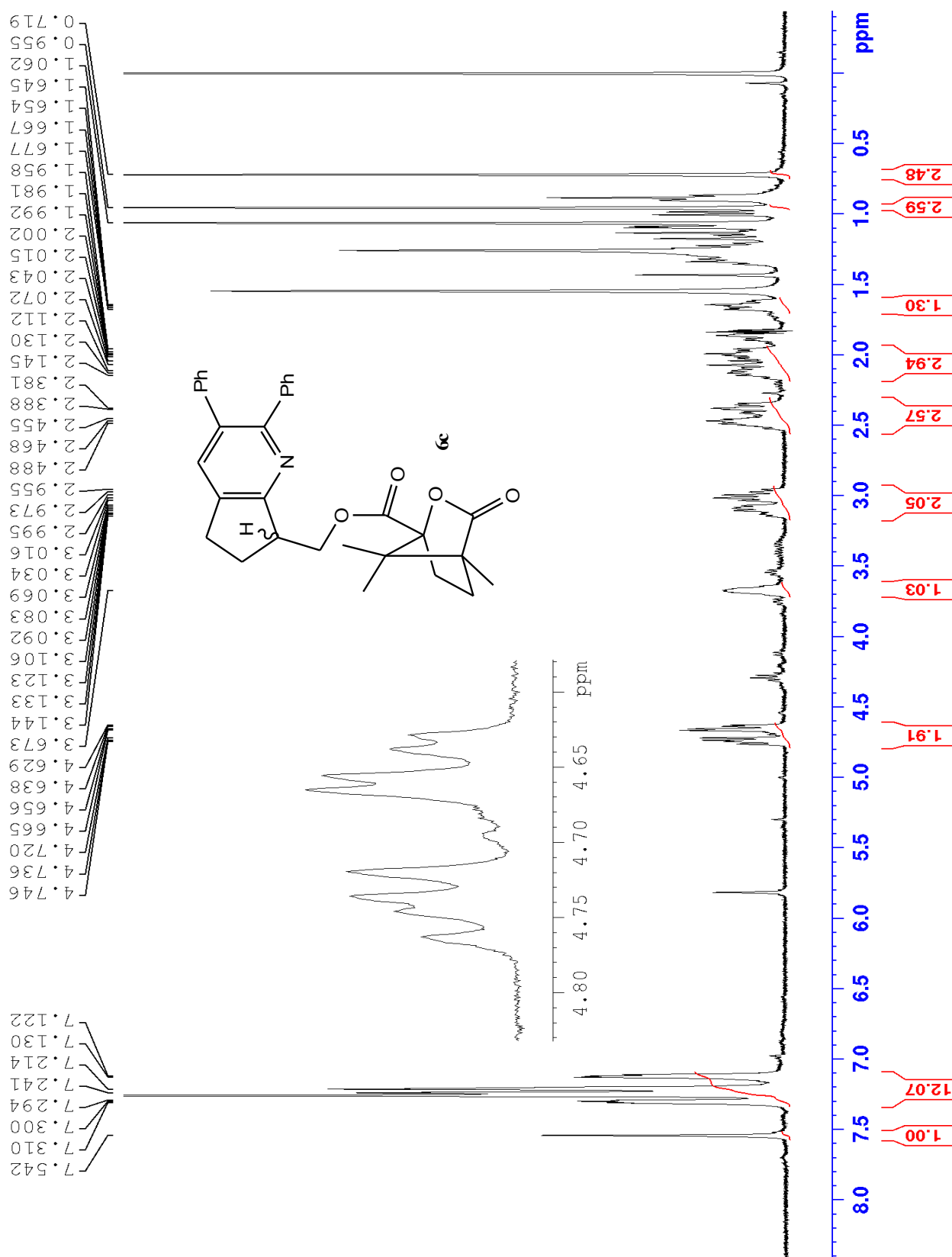
R.4 COSY of 6c (frac 1)



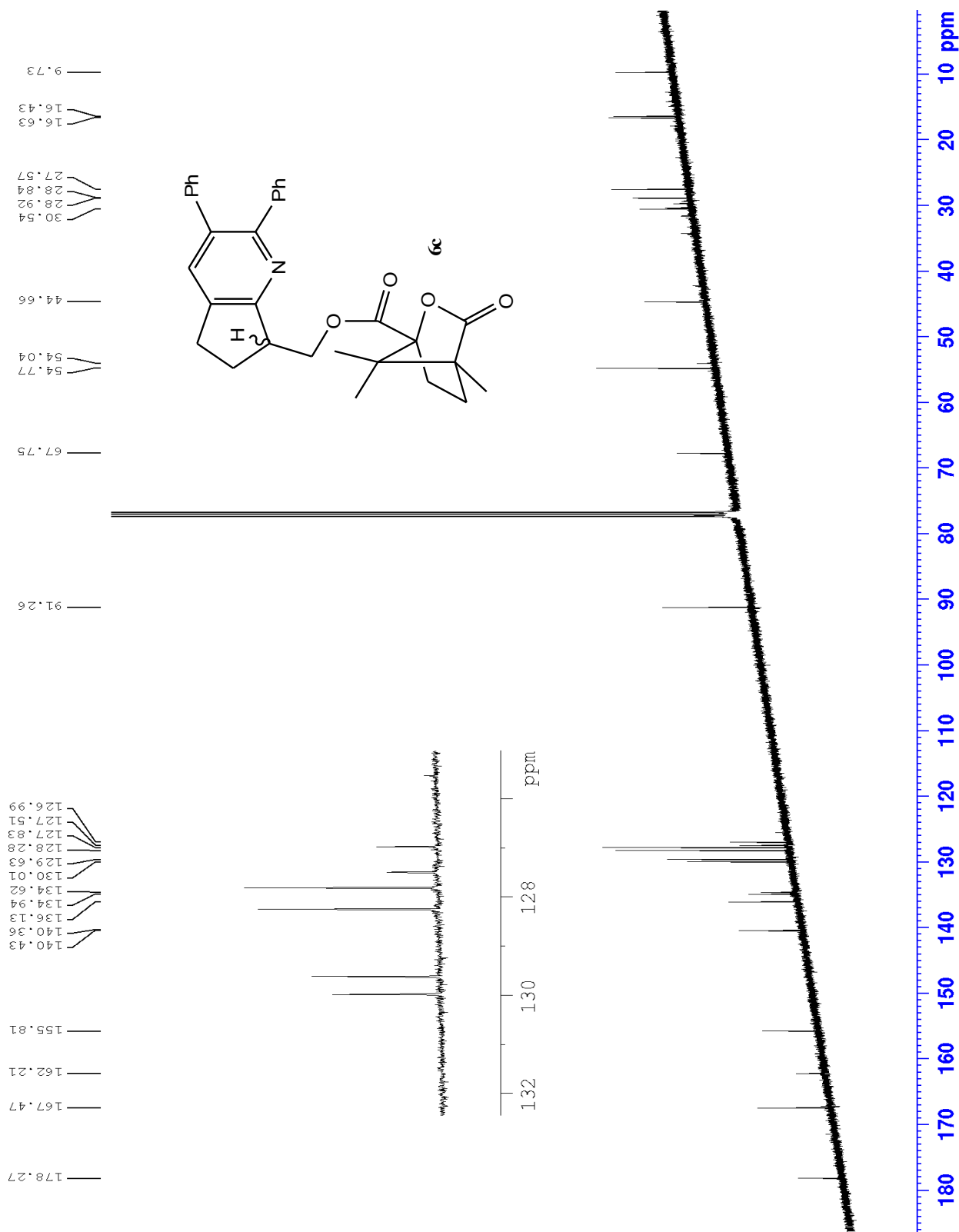
R.5 HMBC of 6c (frac 1)



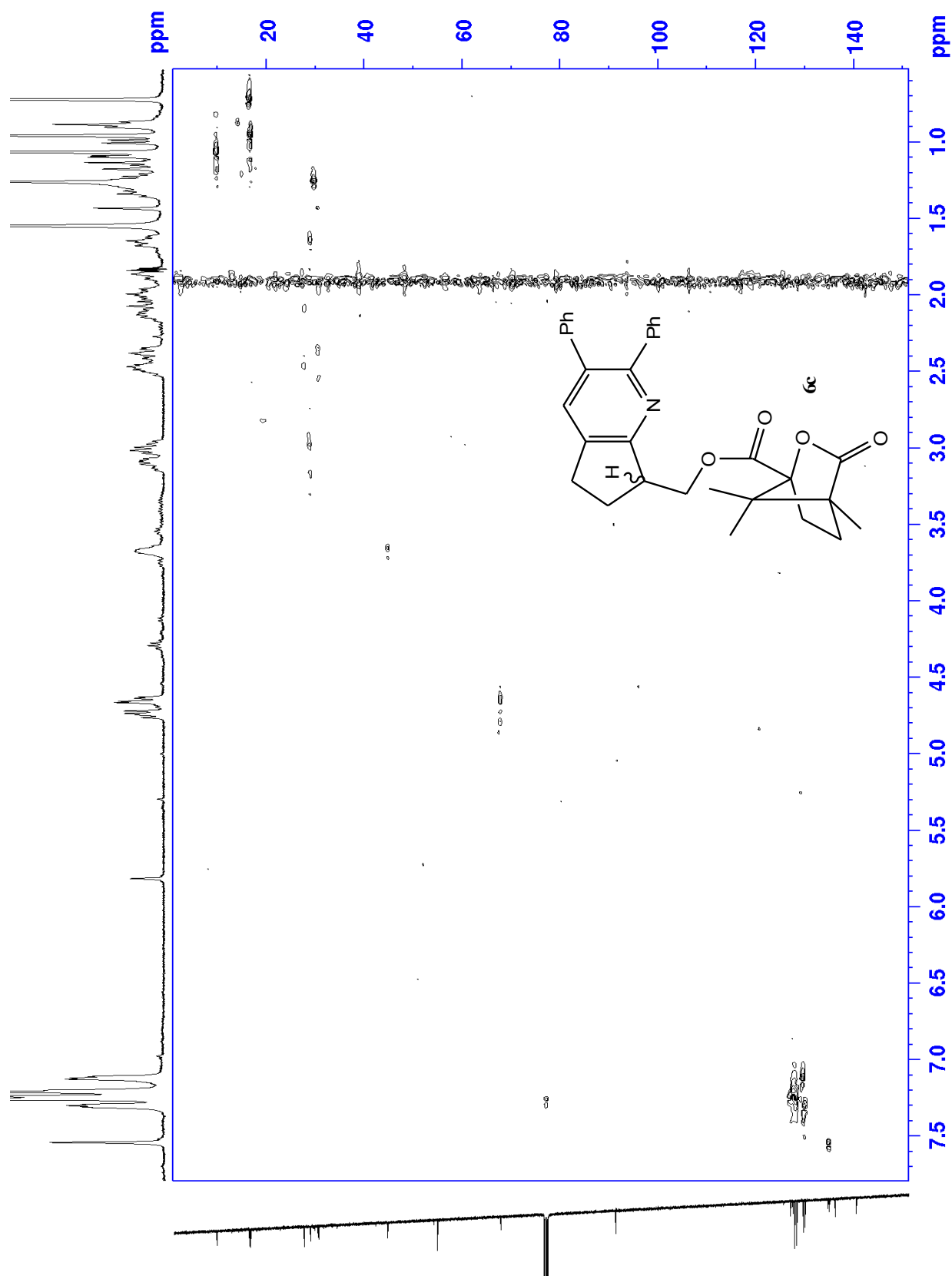
S.1 Proton of 6c (frac 2)



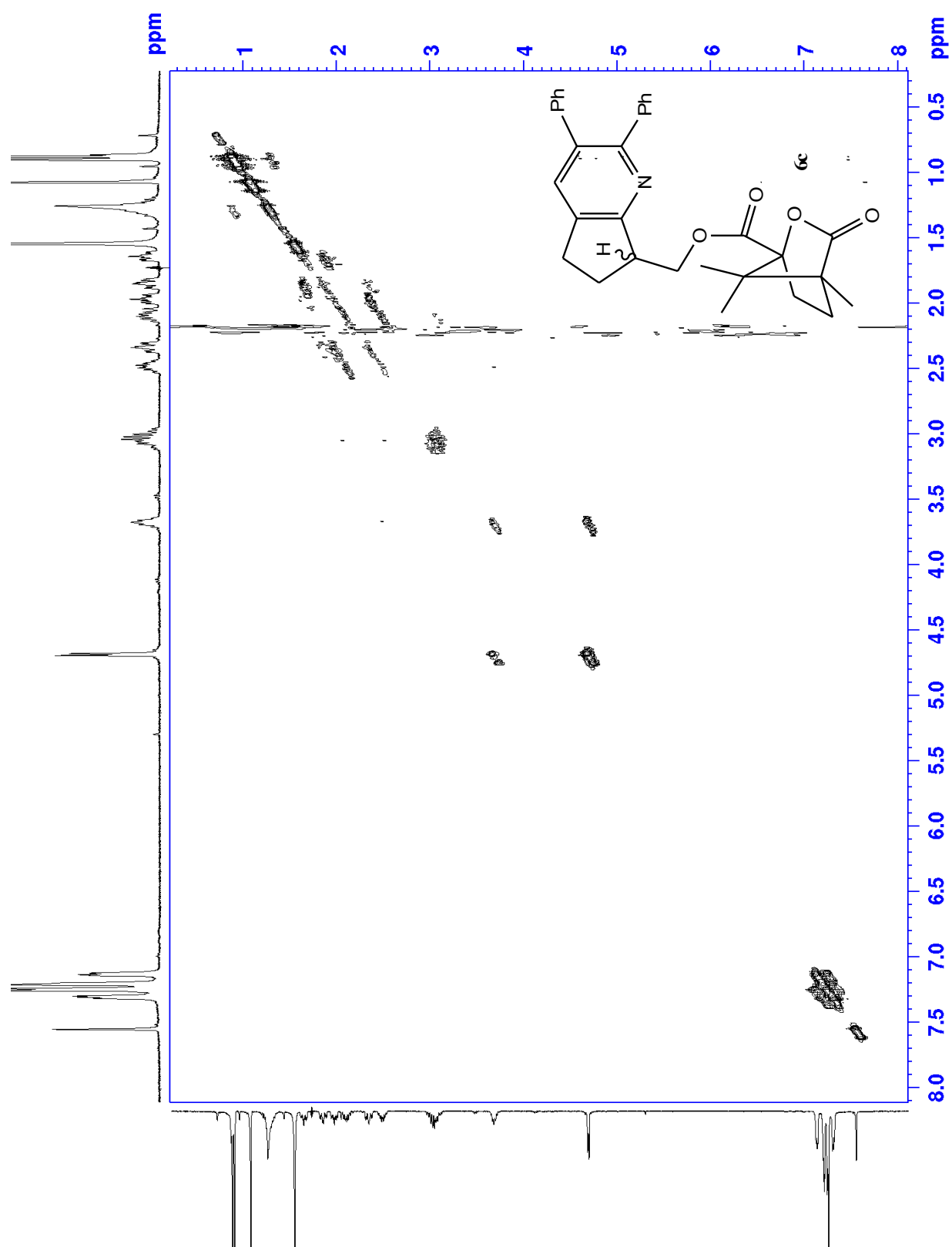
S.2 Carbon of 6c (frac 2)



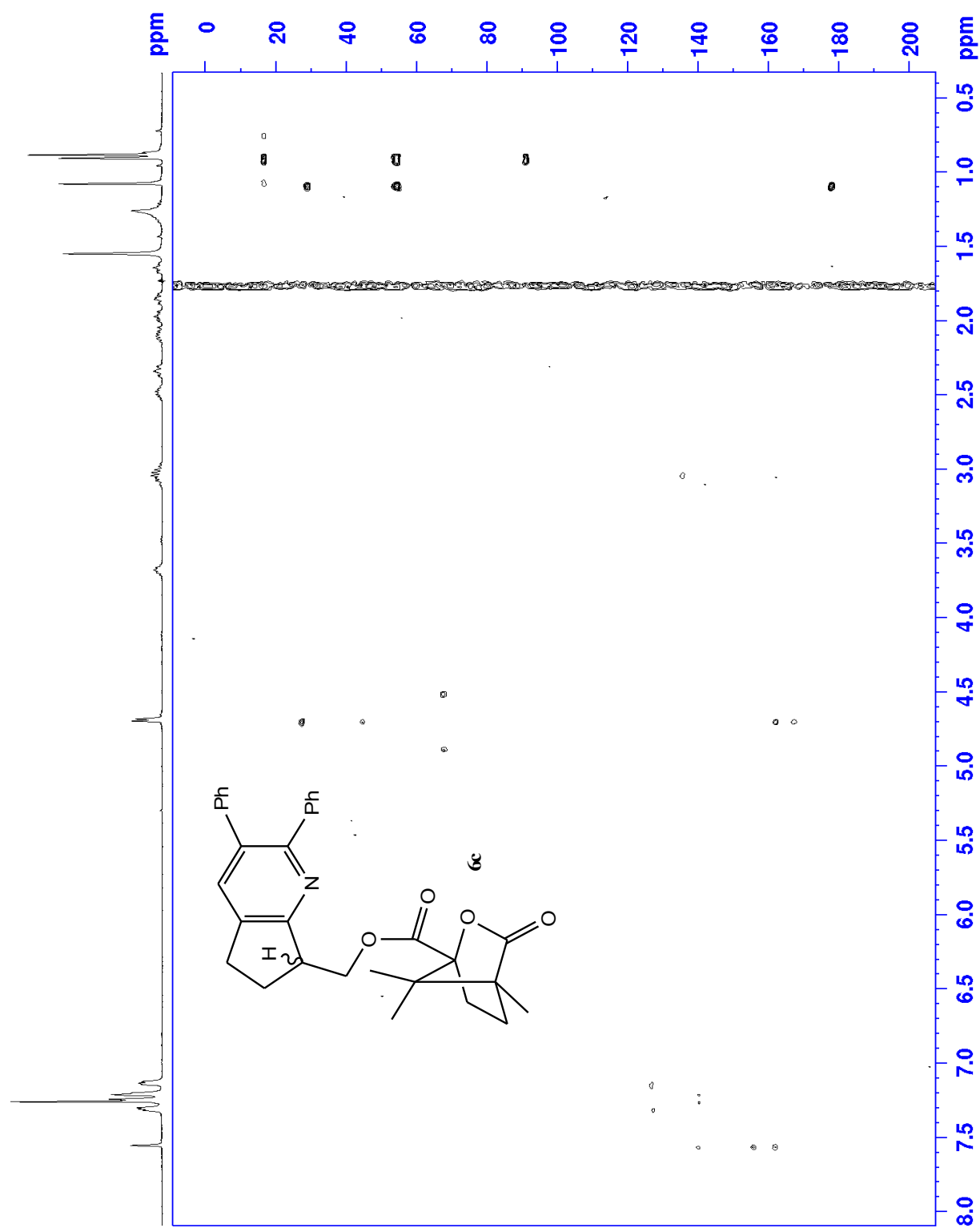
S.3 HSQC of 6c (frac 2)



S.4 COSY of 6c (frac 2)



S.5 HMBC of 6c (frac 2)



T.1 MS of 4a

Page 1

Elemental Composition Report

Single Mass Analysis

Tolerance = 2.0 PPM / DBE: min = -1.5, max = 50.0

Element prediction: Off

Number of isotope peaks used for i-FIT = 3

Monoisotopic Mass, Even Electron Ions

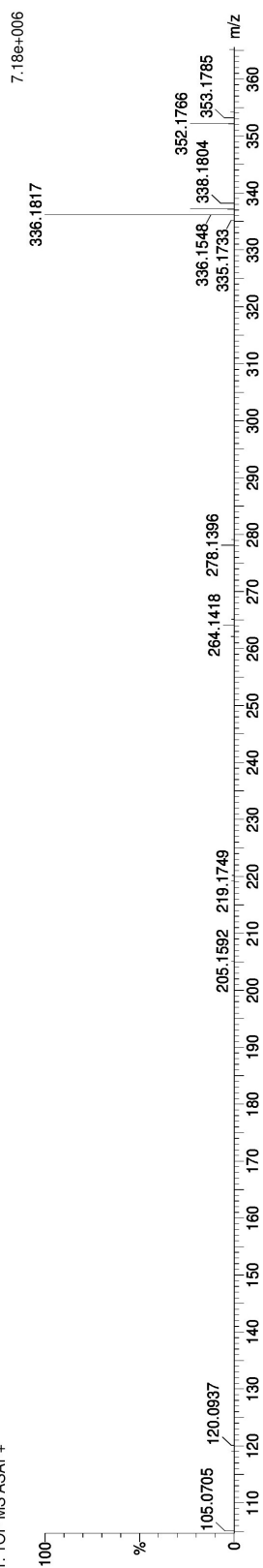
2775 formula(e) evaluated with 6 results within limits (all results (up to 1000) for each mass)

Elements Used:

C: 0-500 H: 0-1000 N: 0-200 O: 0-200 Si: 0-4

2013-48.47 (0.930) AM2 (Ar:350000.0,0.00,0.00); Cm (2:47)

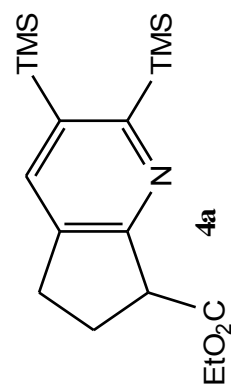
1: TOF MS ASAP+



Minimum: -1.5
Maximum: 50.0

Mass	Calc. Mass	mDa	PPM	DBE	i-FIT	Norm	Conf.(%)	Formula
336.1817	336.1816	0.1	0.3	2.5	83.4	0.219	80.35	C10 H26 N7 O4 Si1
336.1816	0.1	0.3	-0.5	95.1	11.915	0.00		C3 H22 N13 O6
336.1815	0.2	0.6	5.5	85.1	1.921	14.64		C17 H30 N O2 Si2
336.1820	-0.3	-0.9	1.5	86.7	3.442	3.20		C9 H30 N7 O Si3
336.1820	-0.3	-0.9	-1.5	87.2	4.019	1.80		C2 H26 N13 O3 Si2
336.1811	0.6	1.8	6.5	92.4	9.183	0.01		C18 H26 N O5

ION OBSERVED [M+H]⁺



T.2 MS of 4b

Page 1

Elemental Composition Report

Single Mass Analysis

Tolerance = 2.0 PPM / DBE: min = -1.5, max = 50.0

Element prediction: Off

Number of isotope peaks used for i-FIT = 3

Monoisotopic Mass, Even Electron Ions

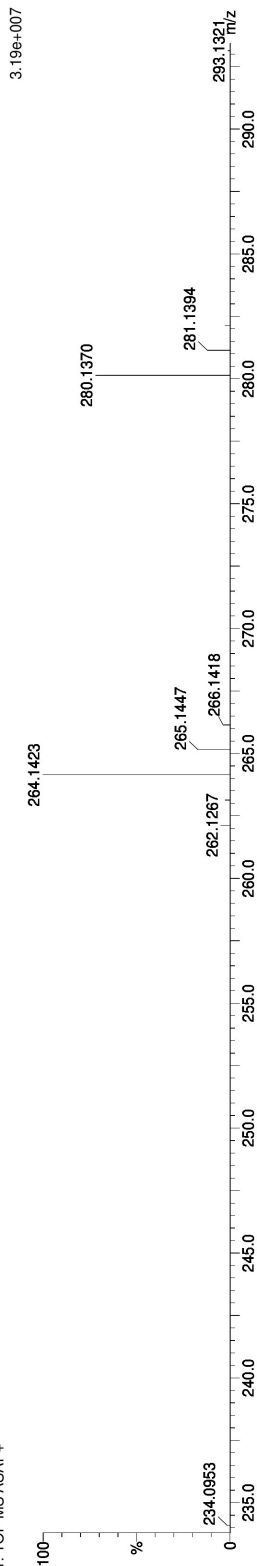
1383 formula(e) evaluated with 3 results within limits (all results (up to 1000) for each mass)

Elements Used:

C: 0-500 H: 0-1000 N: 0-200 O: 0-200 Si: 0-4

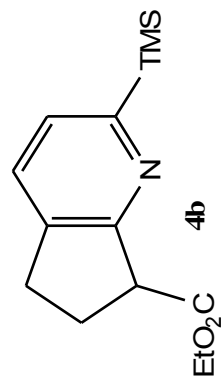
2013-75.5 (0.121) AM2 (Ar:350000.0,0.00,0.00); Cm (2:40)

1: TOF-MS ASAP+



Minimum: -1.5
Maximum: 50.0

Mass	Calc. Mass	mDa	PPM	DBE	i-FIT	Norm	Conf (%)	Formula	ION OBSERVED
264.1423	264.1424	-0.1	-0.4	1.5	44.2	6.490	0.15	C6 H22 N7 O Si2	[M+H] ⁺
264.1420	0.3	1.1	1.1	5.5	37.7	0.002	99.84	C14 H22 N O2 Si	
264.1420	0.3	1.1	1.1	2.5	46.8	9.111	0.01	C7 H18 N7 O4	



T.3 MS of 4c

Page 1

Elemental Composition Report

Single Mass Analysis

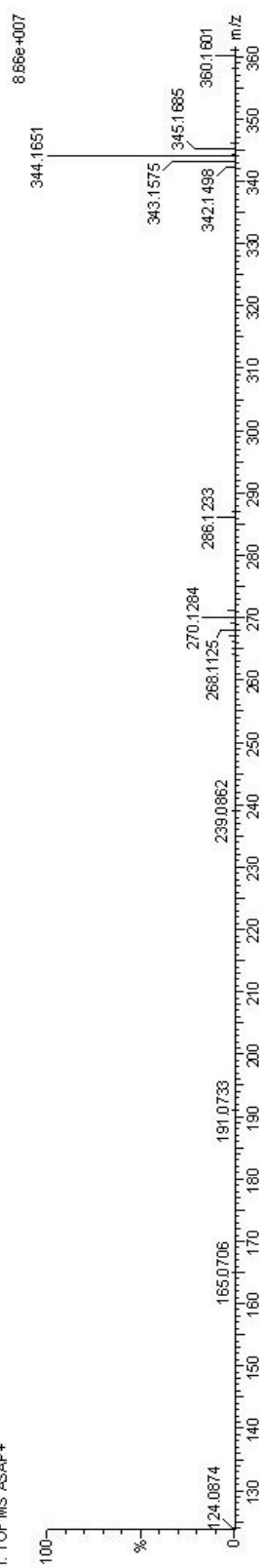
Tolerance = 2.0 PPM / DBE: min = -1.5, max = 50.0
 Element prediction: Off
 Number of isotope peaks used for i-FIT = 3

Monoisotopic Mass, Even Electron Ions

831 formula(e) evaluated with 2 results within limits (all results within limits (up to 1000) for each mass)

Elements Used:

C: 0-5000 H: 0-10000 N: 0-2000 O: 0-2000
 2013-88223 (4.341) AM2 (Ar, 350000.00,0.00,0.00), Cm (2.238)
 1: TOF MS ASAP+



Mini num
 Maxi num

-1.5
 50.0

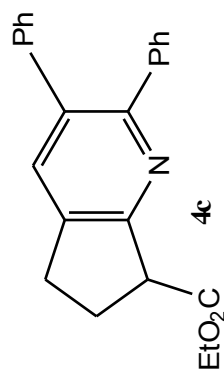
5.0 2.0

Mini num
 Maxi num

-1.5
 50.0

5.0 2.0

Mass	Calc. Mass	mda	PPM	DBE	i-FIT	Norm	Conf(%)	Formula
344.1651	344.1651	0.0	0.0	13.5	66.2	0.000	99.97	C23 H12 N O2
344.1656	344.1656	-0.5	-1.5	6.5	74.5	8.289	0.03	C8 H18 N1.3 O6



T.4 MS of 4d

Page 1

Elemental Composition Report

Single Mass Analysis

Tolerance = 2.0 PPM / DBE: min = -1.5, max = 50.0

Element prediction: Off

Number of isotope peaks used for i-FIT = 3

Monoisotopic Mass, Even Electron Ions

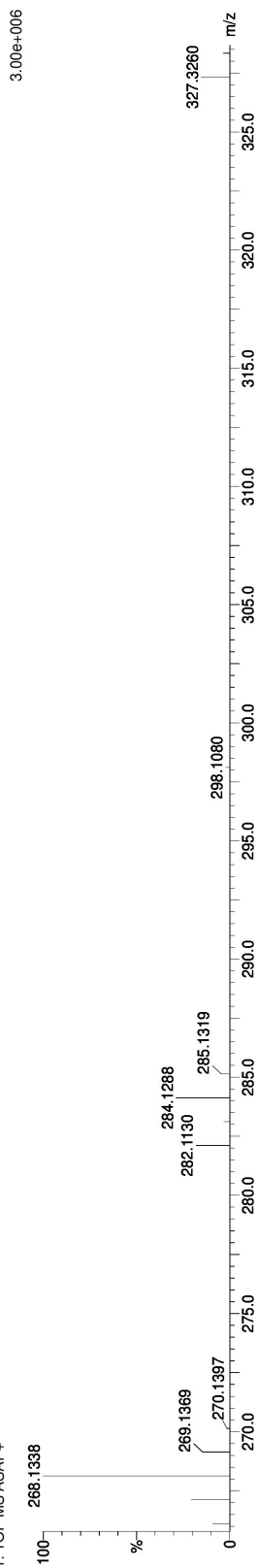
1312 formula(e) evaluated with 2 results within limits (all results (up to 1000) for each mass)

Elements Used:

C: 0-500 H: 0-1000 N: 0-200 O: 0-200 S: 0-6

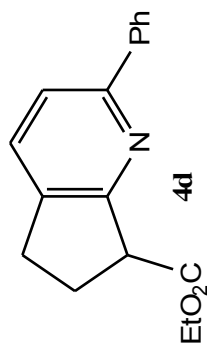
2013-69 97 (1.914) AM2 (Ar:35000.0,0.00,0.00); Cm (2:97)

1: TOF MS ASAP+



Minimum: -1.5
Maximum: 50.0

Mass	Calc. Mass	mDa	PPM	DBE	i-FIT	Norm	Conf (%)	Formula	ION OBSERVED
268.1338	268.1338	0.0	0.0	9.5	27.1	0.000	100.00	C17 H18 N O2	[M+H] ⁺
268.1343	268.1343	-0.5	-1.9	2.5	38.6	11.520	0.00	C2 H14 N13 O3	



T.5 MS of 4c

Elemental Composition Report

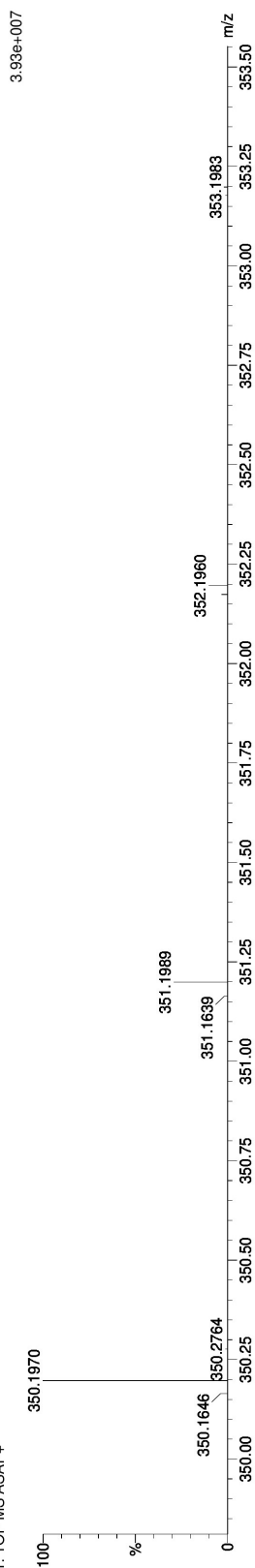
Single Mass Analysis

Tolerance = 2.0 PPM / DBE: min = -1.5, max = 50.0
 Element prediction: Off
 Number of isotope peaks used for i-FIT = 3

Monoisotopic Mass, Even Electron Ions
 5173 formula(e) evaluated with 6 results within limits (all results (up to 1000) for each mass)
 Elements Used:

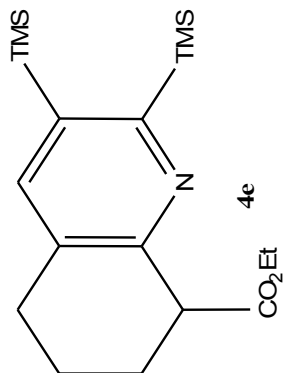
C: 0-200 H: 0-1000 N: 0-200 O: 0-200 Br: 0-3 Si: 0-4

2013-171 133 (2.602) AM2 (Ar:350000.0.00.0.00); Cm (69:134)
 1: TOF MS ASAP+



Minimum: -1.5
 Maximum: 50.0

Mass	Calc. Mass	mDa	PPM	DBE	i-FIT	Norm	Conf (%)	Formula	ion observed [M+H] ⁺
350.1970	350.1972	-0.2	-0.6	5.5	116.1	0.026	97.43	C18 H32 N O2 Si2	
350.1972	-0.2	-0.6	2.5	122.4	6.312	0.18		C11 H28 N ⁺ O4 Si	
350.1967	0.3	0.9	6.5	130.7	14.646	0.00		C19 H28 N O5	
350.1973	-0.3	-0.9	-0.5	132.2	16.077	0.00		C4 H24 N13 O6	
350.1976	-0.6	-1.7	1.5	119.8	3.743	2.37		C10 H32 N7 O Si3	
350.1977	-0.7	-2.0	-1.5	124.6	8.504	0.02		C3 H28 N13 O3 Si2	



T.6 MS of 4f

Elemental Composition Report

Single Mass Analysis

Tolerance = 2.0 PPM / DBE: min = -1.5, max = 50.0
 Element prediction: Off
 Number of isotope peaks used for i-FIT = 3

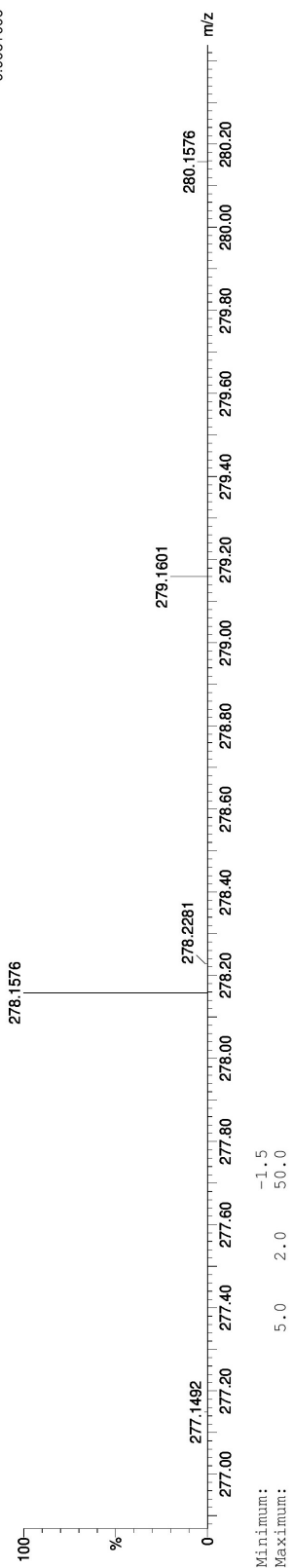
Monoisotopic Mass: Even Electron Ions
 1595 formula(e) evaluated with 4 results within limits (all results (up to 1000) for each mass)

Elements Used:

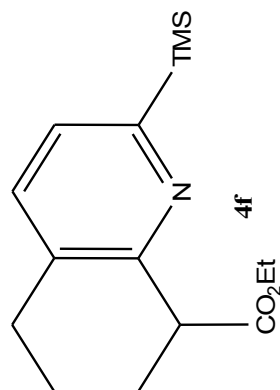
C: 0-200 H: 0-1000 N: 0-200 O: 0-200 Si: 0-4
 2013-167.53 (1.051) AM2 (Ar:35000.0,0.00,0.00); Cm (48.73)

I: TOF MS ASAP+

9.90e+006



Mass	Calc. Mass	mDa	PPM	DBE	i-FIT	Norm	Conf(%)	Formula	ion observed
278.1576	0.0	0.0	5.5	52.2	0.000	99.99	C15 H24 N O2 Si	[M+H] ⁺	
278.1577	-0.1	-0.4	2.5	67.6	15.343	0.00	C8 H20 N7 O4		
278.1581	-0.5	-1.8	1.5	62.0	9.812	0.01	C7 H24 N7 O Si2		
278.1581	-0.5	-1.8	-1.5	66.3	14.054	0.00	H20 N13 O3 Si		



T.7 MS of 4g

Page 1

Elemental Composition Report

Single Mass Analysis

Tolerance = 2.0 PPM / DBE: min = -1.5, max = 50.0

Element prediction: Off

Number of isotope peaks used for i-FIT = 3

Monoisotopic Mass: Even Electron Ions

920 formula(e) evaluated with 2 results within limits (all results (up to 1000) for each mass)

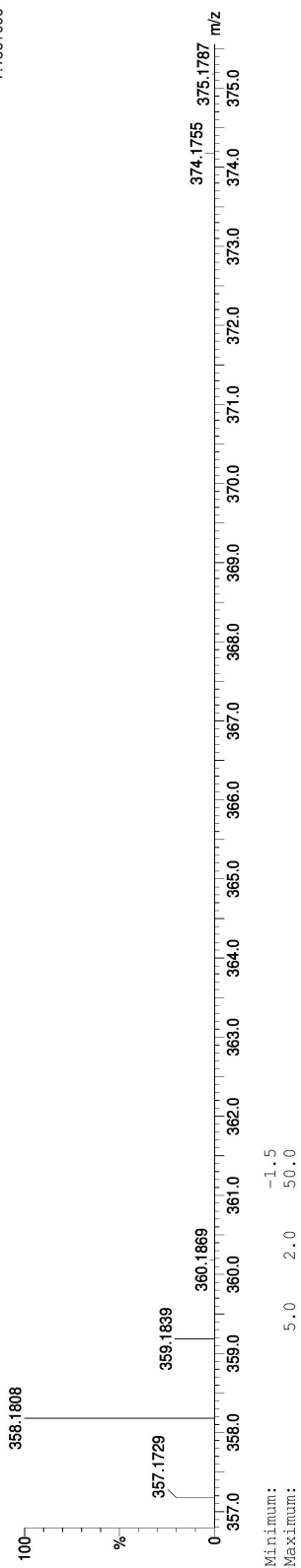
Elements Used:

C: 0-500 H: 0-1000 N: 0-200 O: 0-200

2013-46 175 (3.411) AM2 (Ar:350000.0.00.0.00); Cm (88:176)

1: TOF MS ASAP+

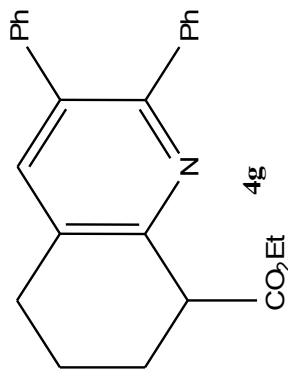
7.15e+006



Minimum: 5.0 2.0 -1.5
Maximum: 50.0

Mass	Calc. Mass	mDa	PPM	DBE	i-FIT	Norm	Conf (%)	Formula
358.1808	358.1807	0.1	0.3	13.5	31.7	0.002	99.81	C24 H24 N O2
358.1812	-0.4	-1.1	6.5	38.0	6.243	0.19		C9 H20 N13 O3

ION OBSERVED [M+H]⁺



T.8 MS of 4h

Elemental Composition Report

Single Mass Analysis

Tolerance = 2.0 PPM / DBE: min = -1.5, max = 50.0
 Element prediction: Off
 Number of isotope peaks used for i-FIT = 3

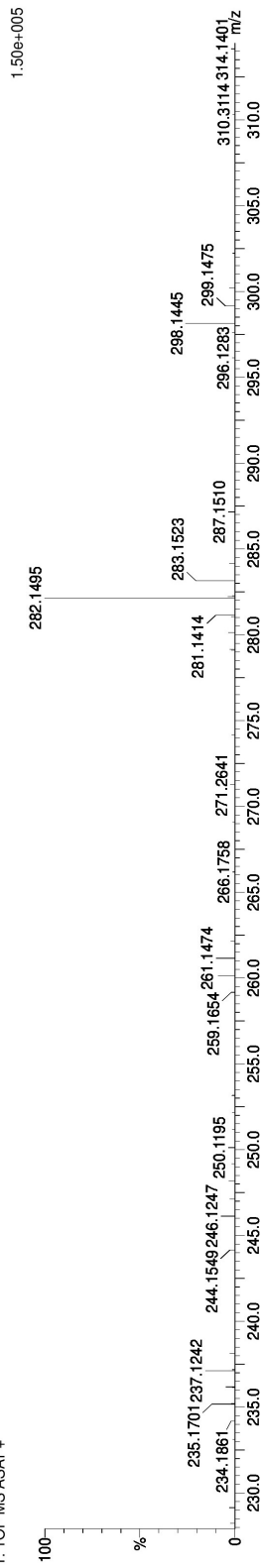
Monoisotopic Mass, Even Electron Ions
 504 formulae evaluated with 2 results within limits (all results (up to 1000) for each mass)

Elements Used:

C: 0-500 H: 0-1000 N: 0-200 O: 0-200

2013-76-42 (0.846) AM2 (Ar:350000.0,0.00,0.00); Cm (2:64)

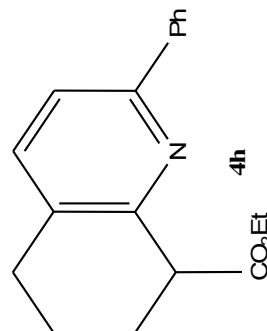
1: TOF MS ASAP+



Minimum: 5.0 2.0 -1.5
 Maximum: 50.0

Mass	Calc. Mass	mDa	PPM	DBE	i-FIT	Norm	Conf(%)	Formula
282.1495	282.1494	0.1	0.4	9.5	46.2	0.000	100.00	C18 H20 N O2
282.1499	-0.4	-1.4	2.5	63.1	16.830	0.00		C3 H16 N13 O3

ION OBSERVED [M+H]⁺



T.9 MS of 5b

Page 1

Elemental Composition Report

Single Mass Analysis

Tolerance = 2.0 PPM / DBE: min = -1.5, max = 50.0

Element prediction: Off

Number of isotope peaks used for i-FIT = 3

Monoisotopic Mass, Even Electron Ions

824 formula(e) evaluated with 3 results within limits (all results (up to 1000) for each mass)

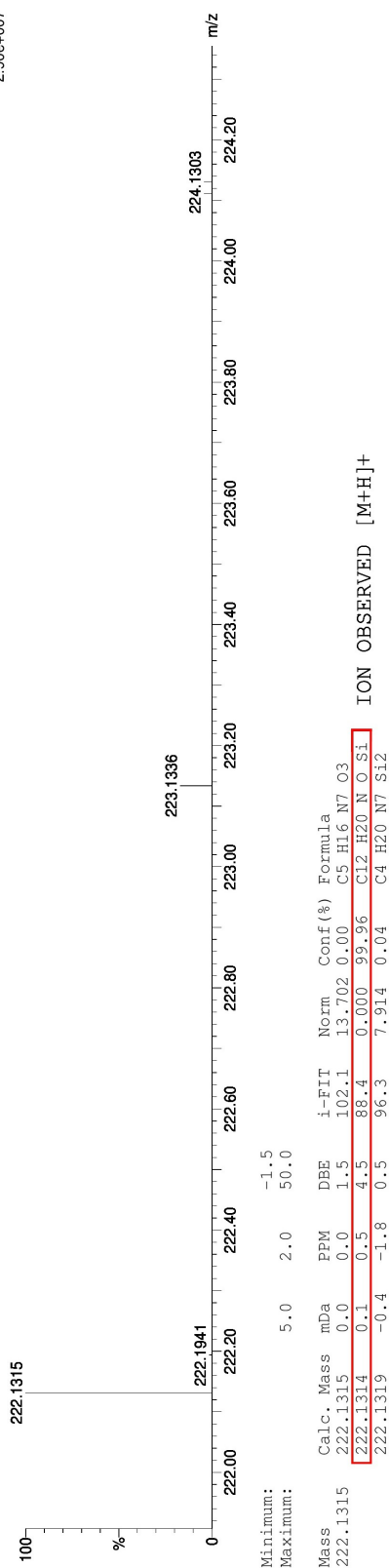
Elements Used:

C: 0-200 H: 0-1000 N: 0-200 O: 0-200 Si: 0-4

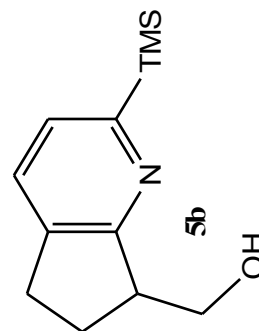
2013-164.4 (0.104) AM2 (Ar.35000.0,0.0,0.00); Cm (2:49)

1: TOF MS ASAP+

2.90e+007

Minimum:
Maximum:-1.5
50.0Mass
222.1315

Calc. Mass	mDa	PPM	DBE	i-FIT	Norm	Conf (%)	Formula
222.1315	0.0	0.0	1.5	102.1	13.702	0.00	C5 H16 N7 O3
222.1314	0.1	0.5	4.5	88.4	0.000	99.96	C12 H20 N O Si
222.1319	-0.4	-1.8	0.5	96.3	7.914	0.04	C4 H20 N7 Si2

ION OBSERVED [M+H]⁺

T.10 MS of 5c

Page 1

Elemental Composition Report

Single Mass Analysis

Tolerance = 2.0 PPM / DBE: min = -1.5, max = 50.0

Element prediction: Off

Number of isotope peaks used for i-FIT = 3

Monoisotopic Mass, Even Electron Ions

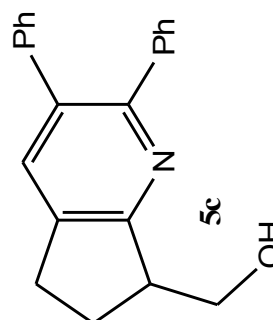
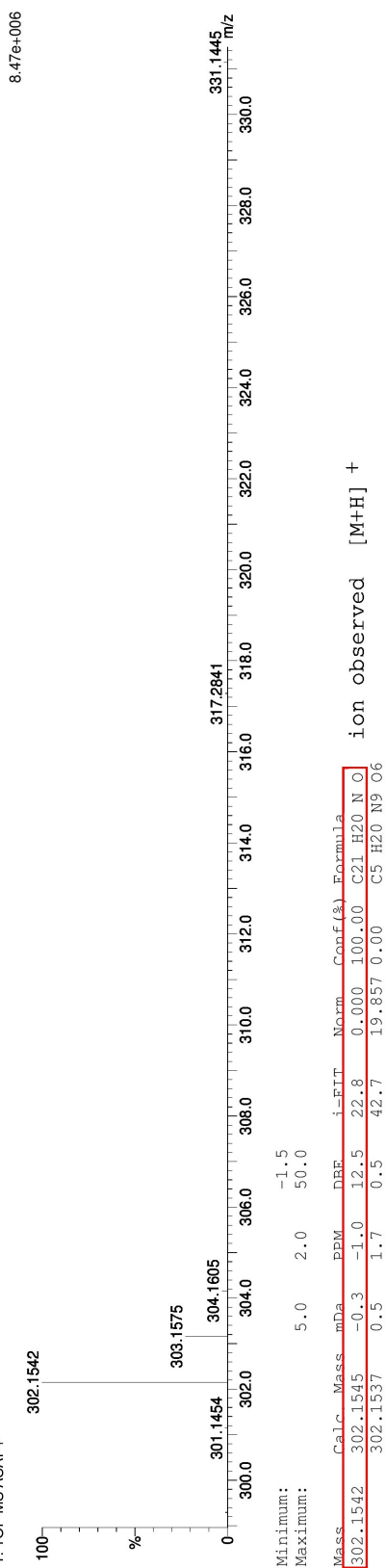
593 formula(e) evaluated with 2 results within limits (all results (up to 1000) for each mass)

Elements Used:

C: 0-200 H: 0-1000 N: 0-200 O: 0-200

2013-128.83 (1.636) AM2 (Ar:35000.0,0.00,0.00); Cm (48:116)

1: TOF MS ASAP+



T.11 MS of 6b

Page 1

Elemental Composition Report

Single Mass Analysis

Tolerance = 2.0 PPM / DBE: min = -1.5, max = 50.0
 Element prediction: Off
 Number of isotope peaks used for i-FIT = 3

Monoisotopic Mass, Even Electron Ions

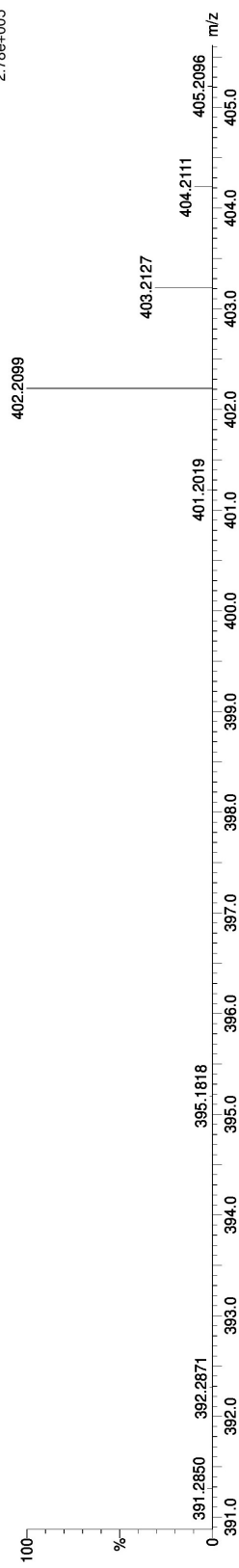
4643 formula(e) evaluated with 8 results within limits (all results within limits (up to 1000) for each mass)

Elements Used:

C: 0-200 H: 0-1000 N: 0-200 O: 0-200 Si: 0-4

2013-185.41 (0.829) AM2 (A_r:35000.0:0.00:0.00); Cm (25:45)

1: TOF MS ASAP+

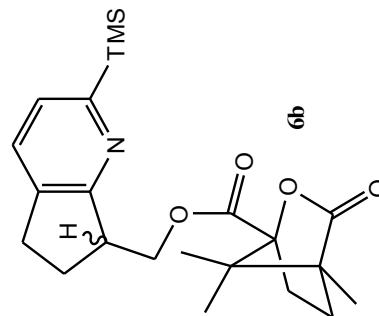


Minimum:
Maximum:

-1.5
50.0

Mass	Calc. Mass	MDA	PPM	DBE	i-FIT	Norm	Conf (%)	Formula
402.2099	402.2101	-0.2	-0.5	5.5	33.6	14.203	0.00	C15 H28 N7 O6
	402.2101	-0.2	-0.5	8.5	19.4	0.007	99.30	C22 H32 N O4 Si
	402.2096	0.3	0.7	-1.5	32.4	13.045	0.00	C12 H40 N3 O4 Si4
	402.2105	-0.6	-1.5	7.5	28.2	8.866	0.01	C21 H36 N O Si3
	402.2105	-0.6	-1.5	4.5	24.4	5.048	0.64	C14 H32 N7 O3 Si2
	402.2106	-0.7	-1.7	-1.5	37.6	18.258	0.00	H24 N19 O7
	402.2092	0.7	1.7	-0.5	27.2	7.786	0.04	C13 H36 N3 O7 Si2
	402.2106	-0.7	-1.7	1.5	30.6	11.234	0.00	C7 H28 N13 O5 Si

ION OBSERVED [M+H]⁺



T.12 MS of 6c

Page 1

Elemental Composition Report

Single Mass Analysis

Tolerance = 2.0 PPM / DBE: min = -1.5, max = 50.0

Element prediction: Off

Number of isotope peaks used for i-FIT = 3

Monoisotopic Mass, Even Electron Ions

2015 formula(e) evaluated with 3 results within limits (all results (up to 1000) for each mass)

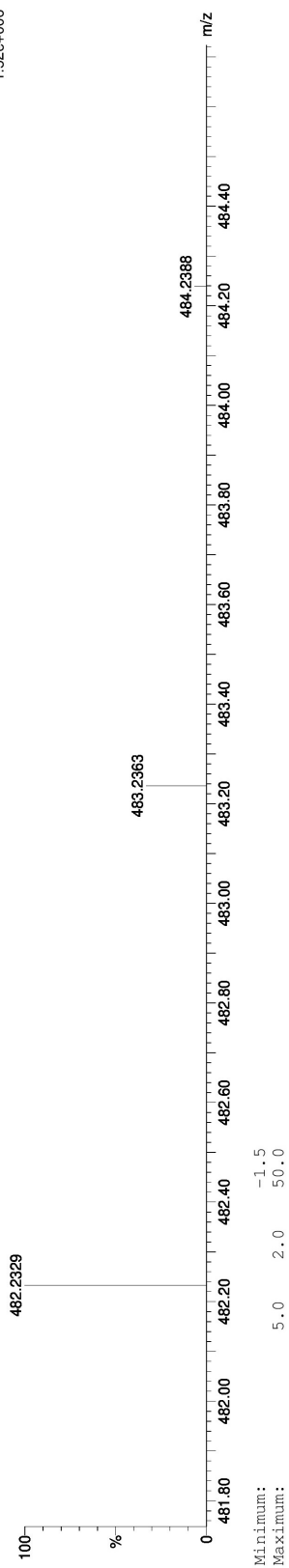
Elements Used:

C: 0-200 H: 0-1000 N: 0-200 O: 0-200

2013-184 201 (3.930) AM2 (Ar:350000.0,0.0,0.000); Cm (191:214)

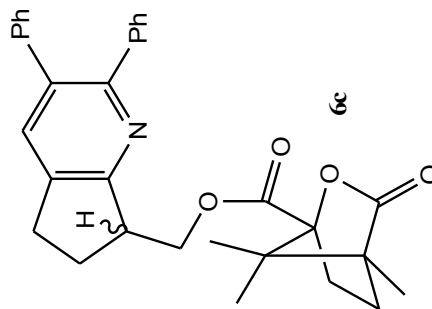
1: TOF MS ASAP+

1.52e+006

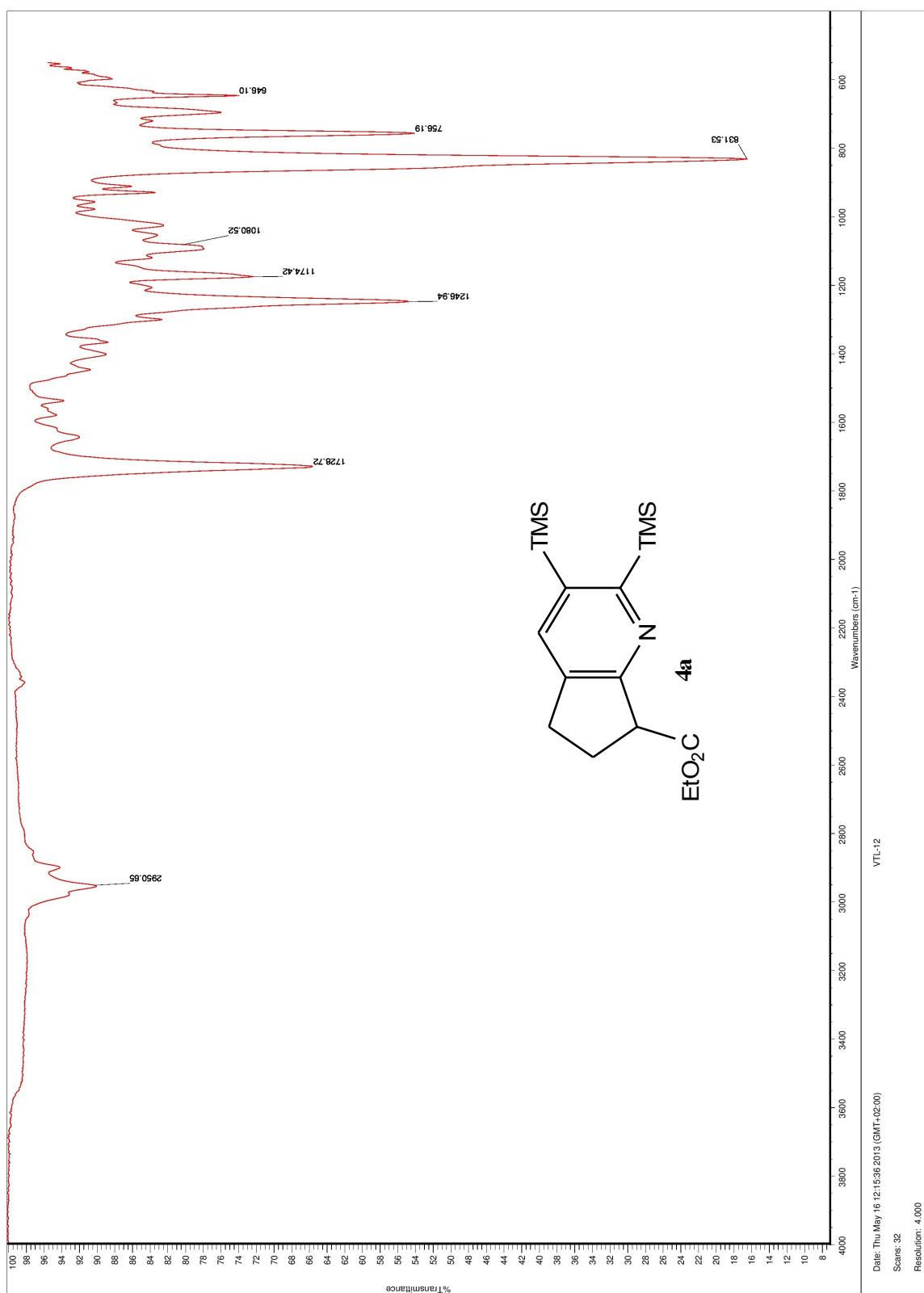


Minimum: -1.5
Maximum: 50.0

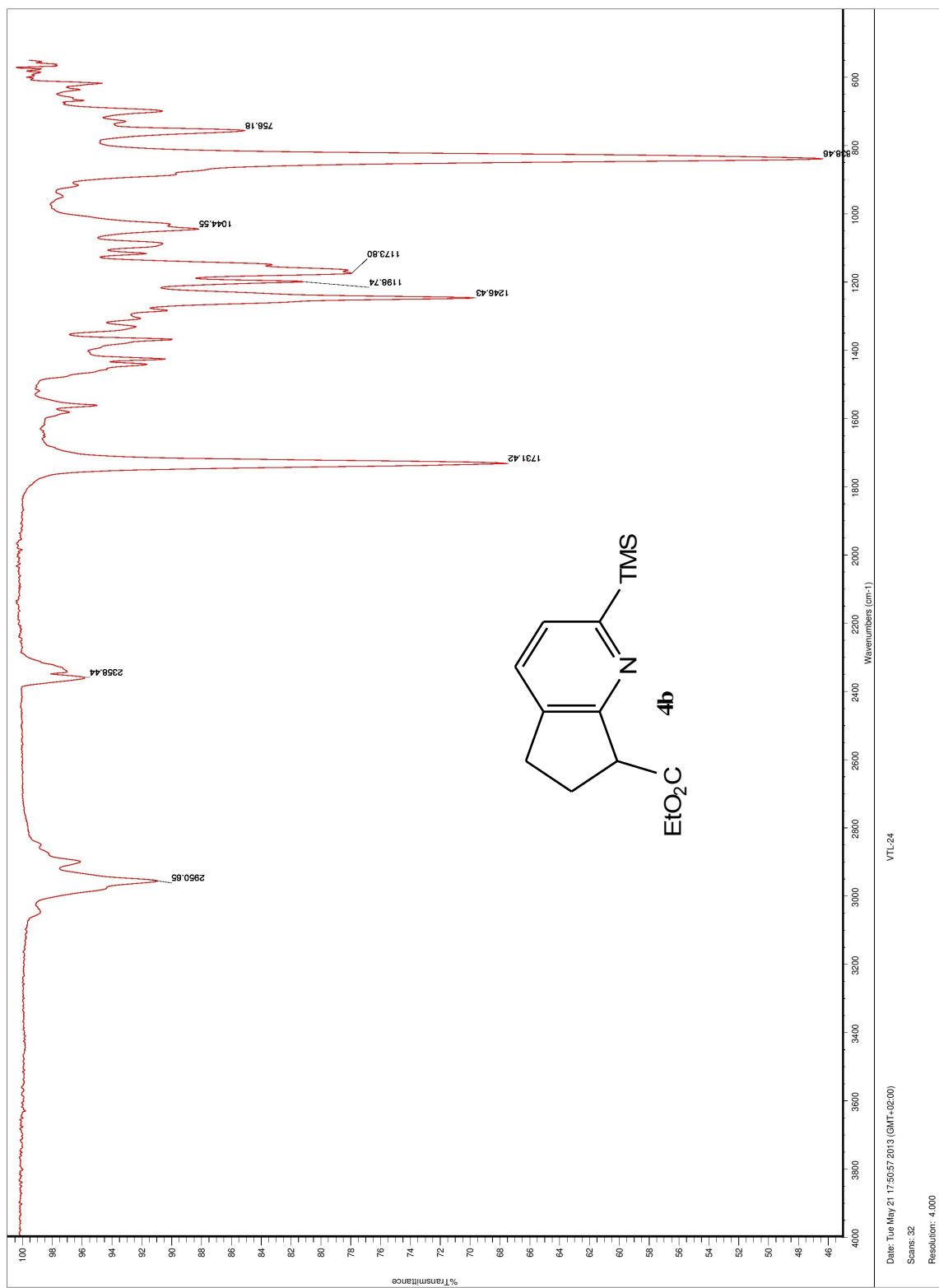
Mass	Calc. Mass	mDa	PPM	DBE	i-FIT	Norm	Conf(%)	Formula	ION OBSERVED [M+H] ⁺
482.2329	482.2331	-0.2	-0.4	16.5	21.2	0.000	100.00	C31 H32 N O4	
482.2323	0.6	1.2	4.5	34.7	13.566	0.00	C15 H32 N9 O9		
482.2336	-0.7	-1.5	9.5	33.5	12.279	0.00	C16 H28 N13 O5		



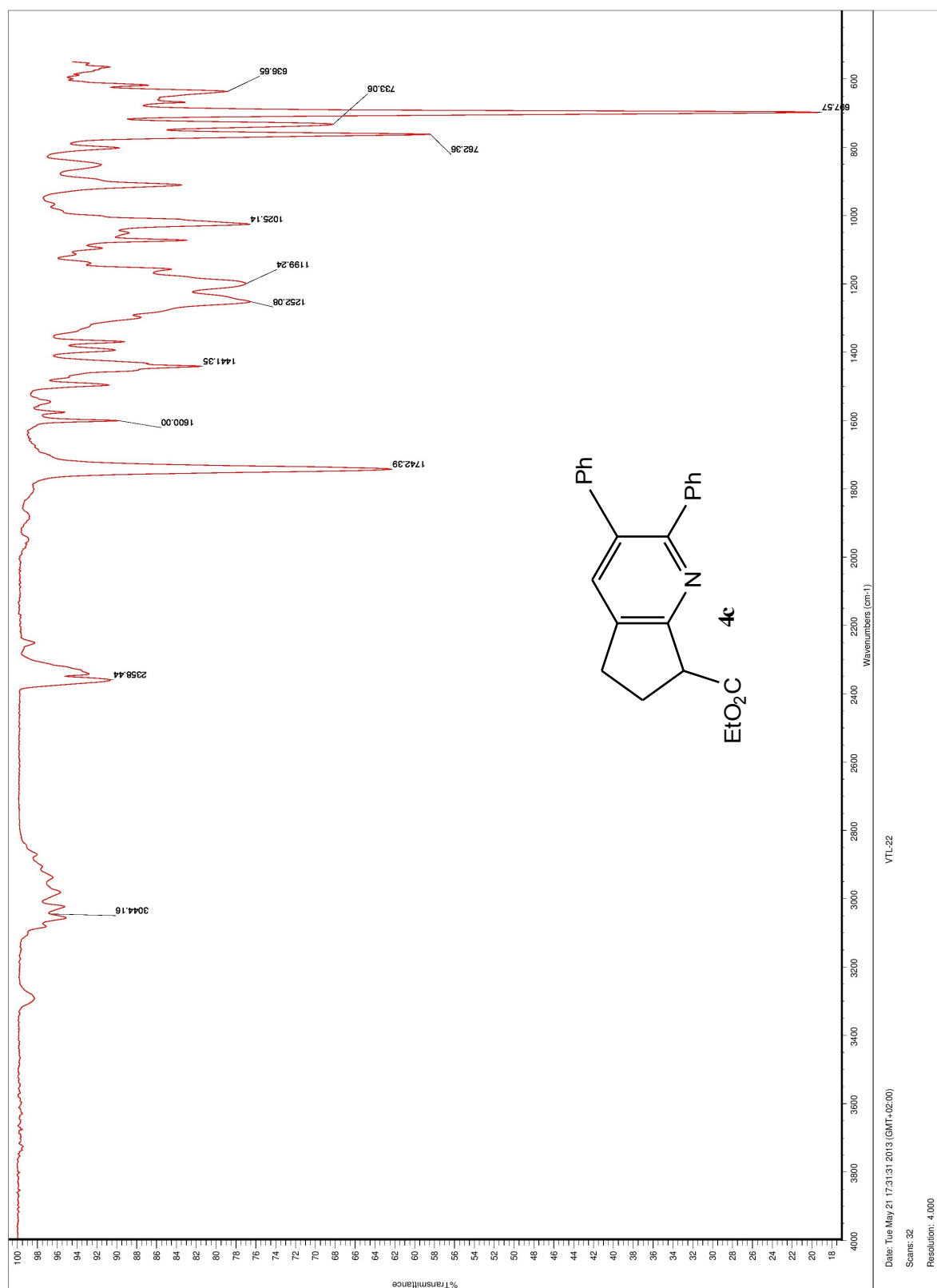
U.1 IR of 4a



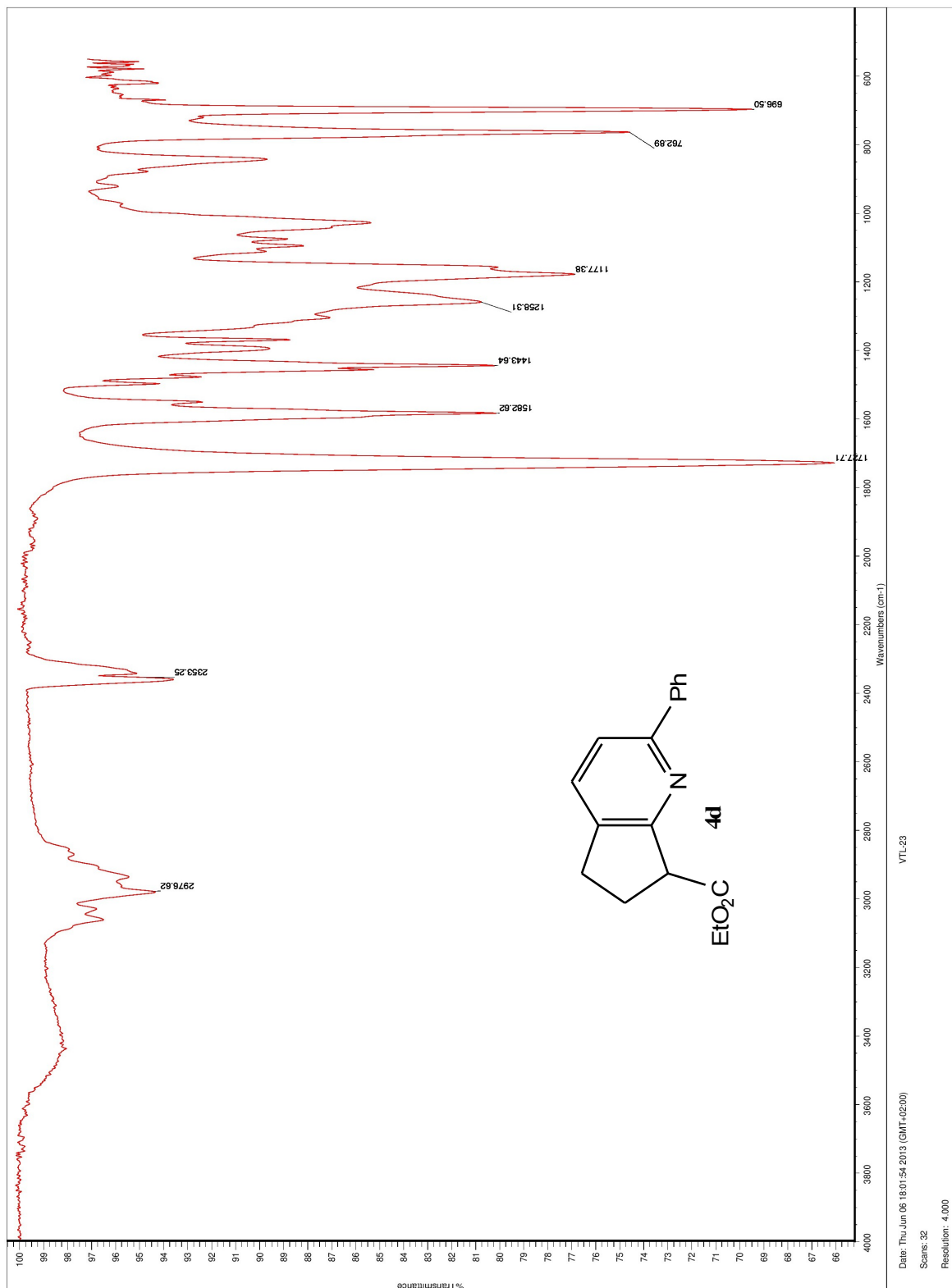
U.2 IR of 4b



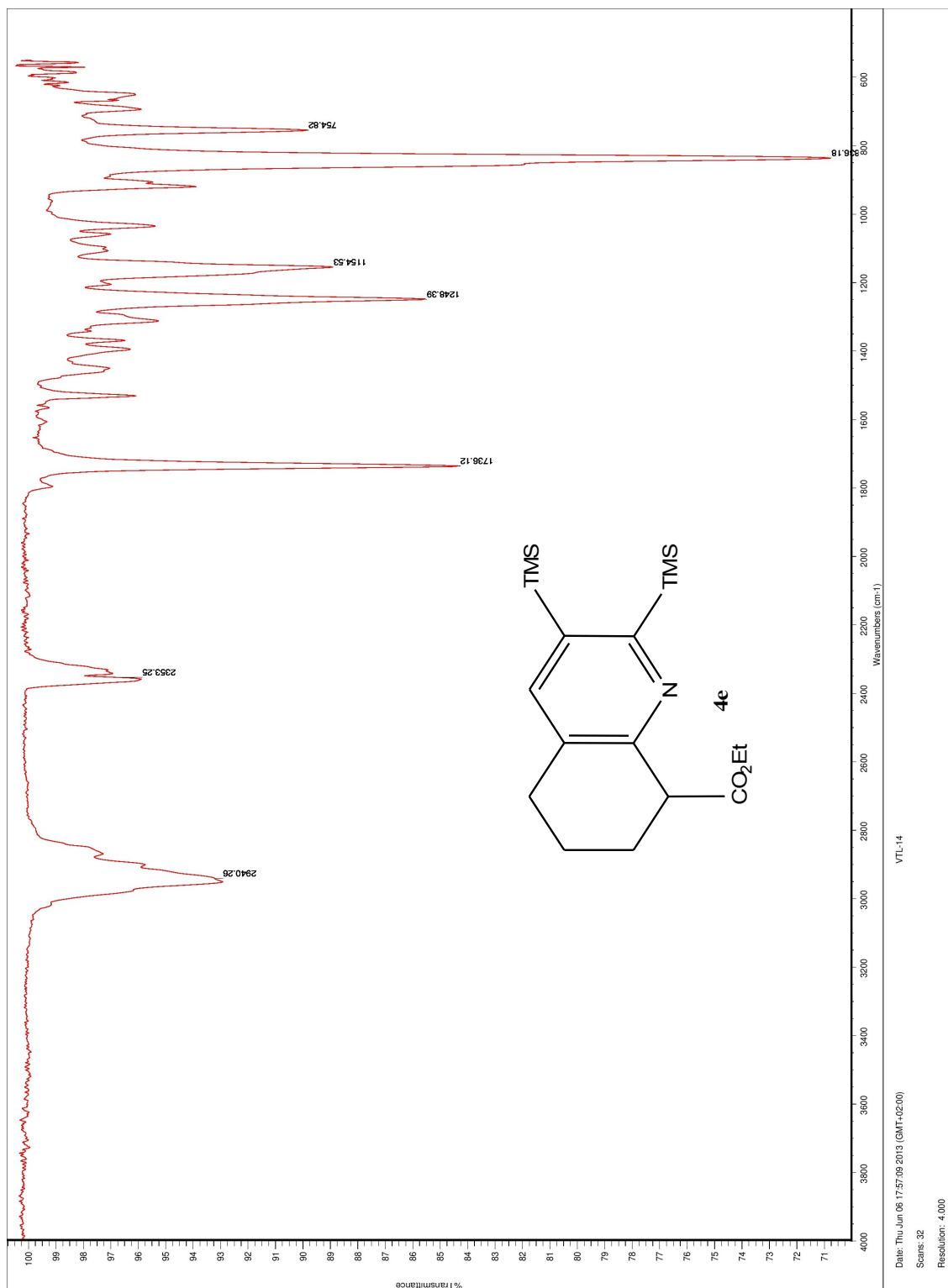
U.3 IR of 4c



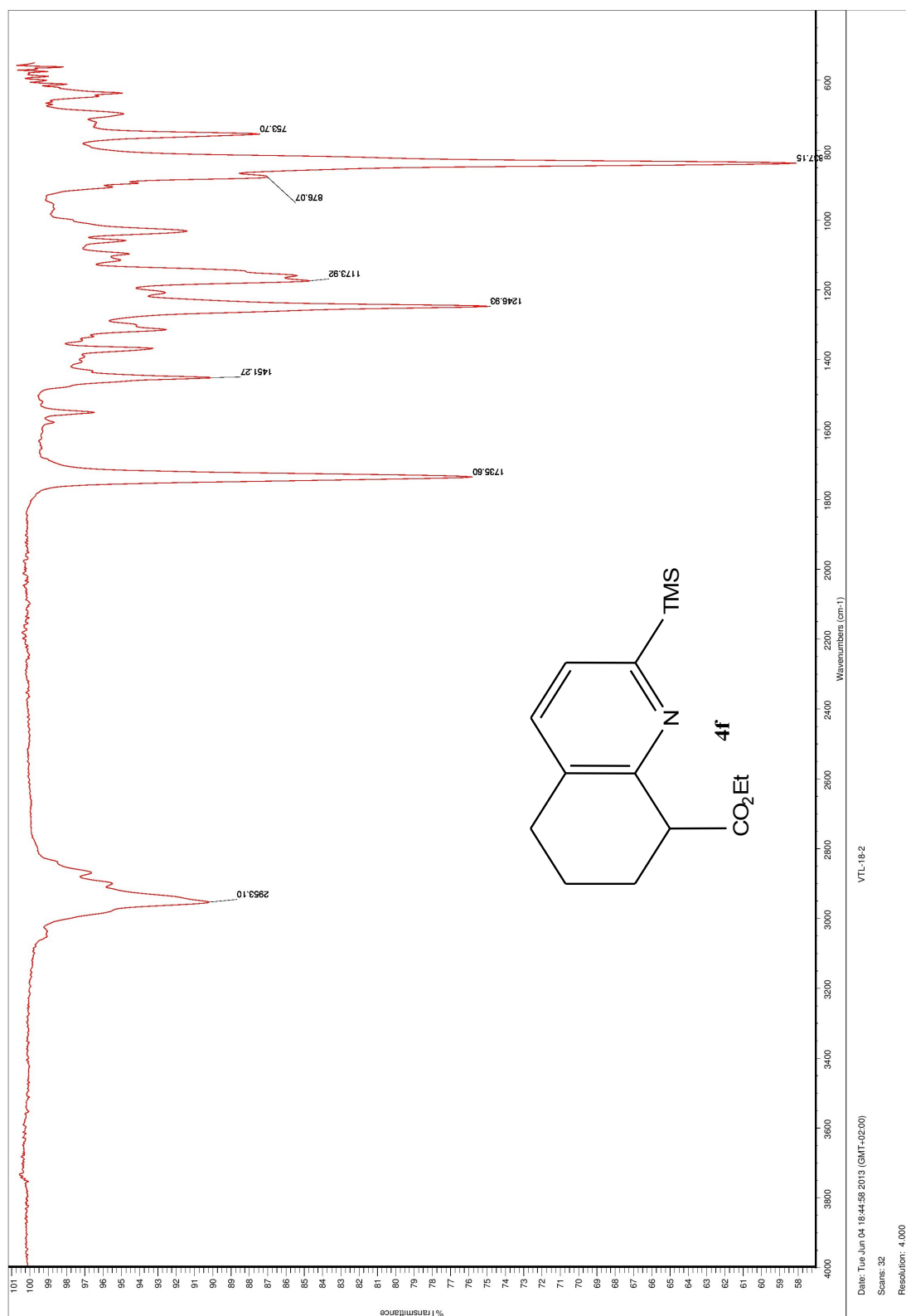
U.4 IR of 4d



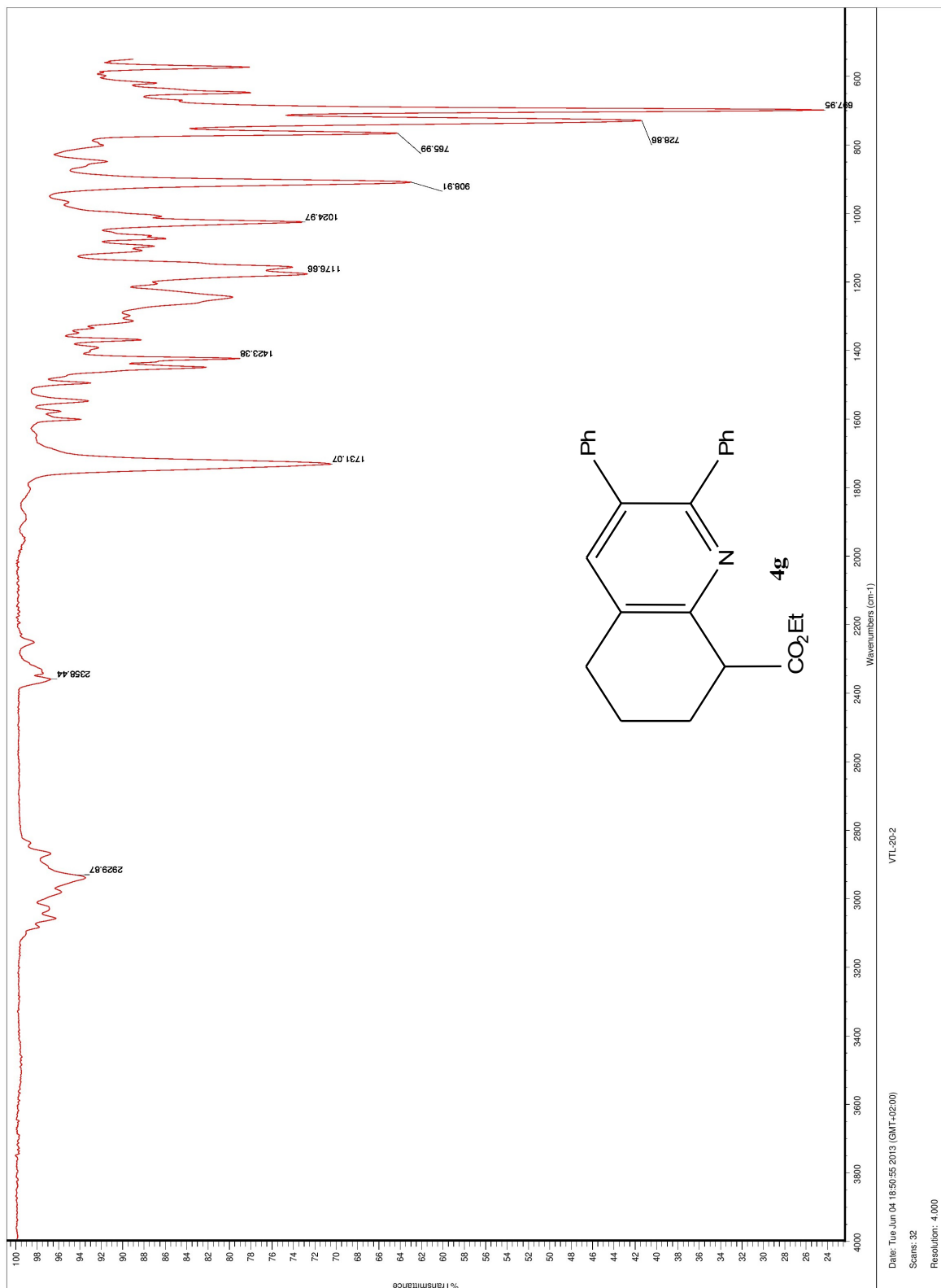
U.5 IR of 4e



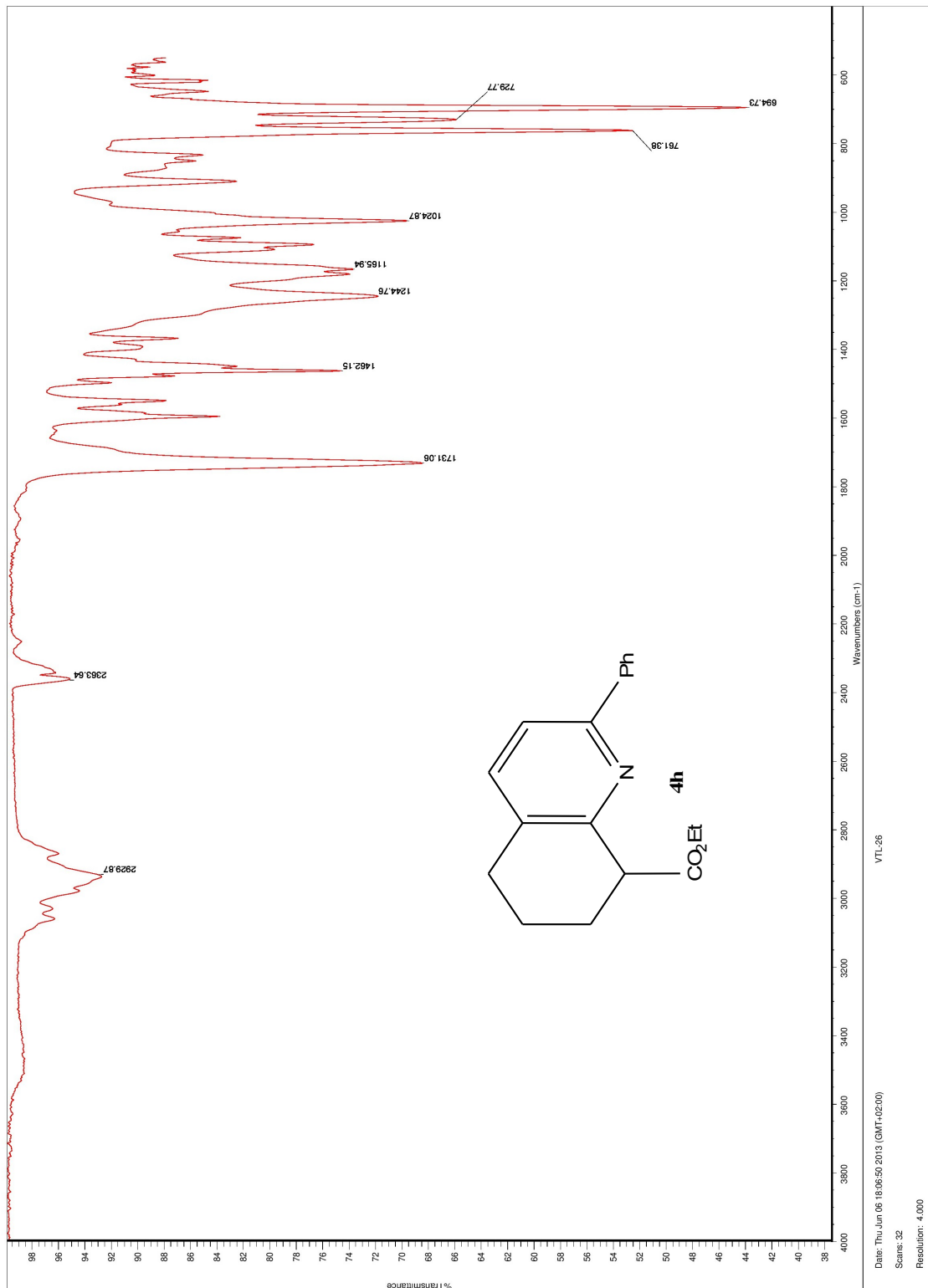
U.6 IR of 4f



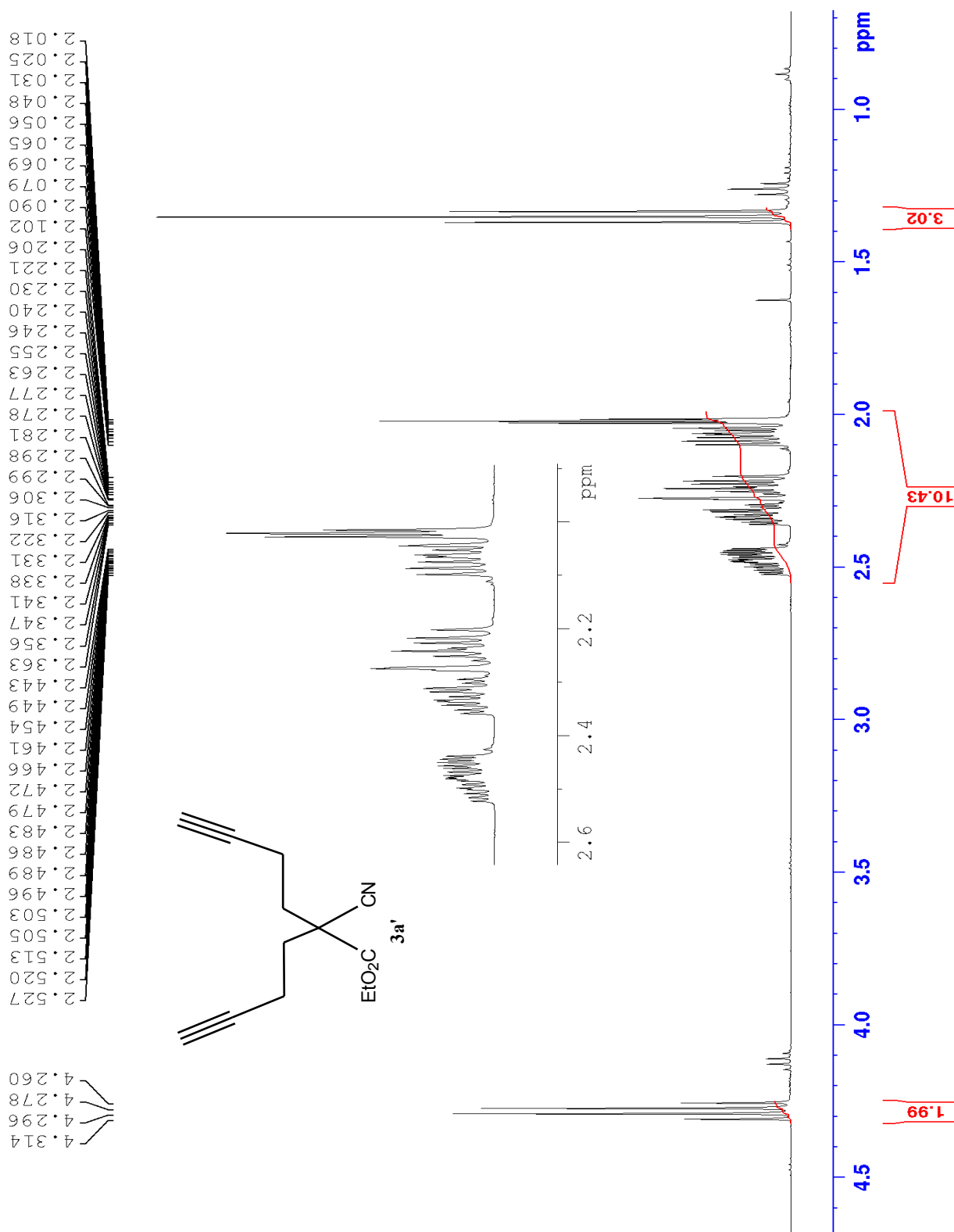
U.7 IR of 4g



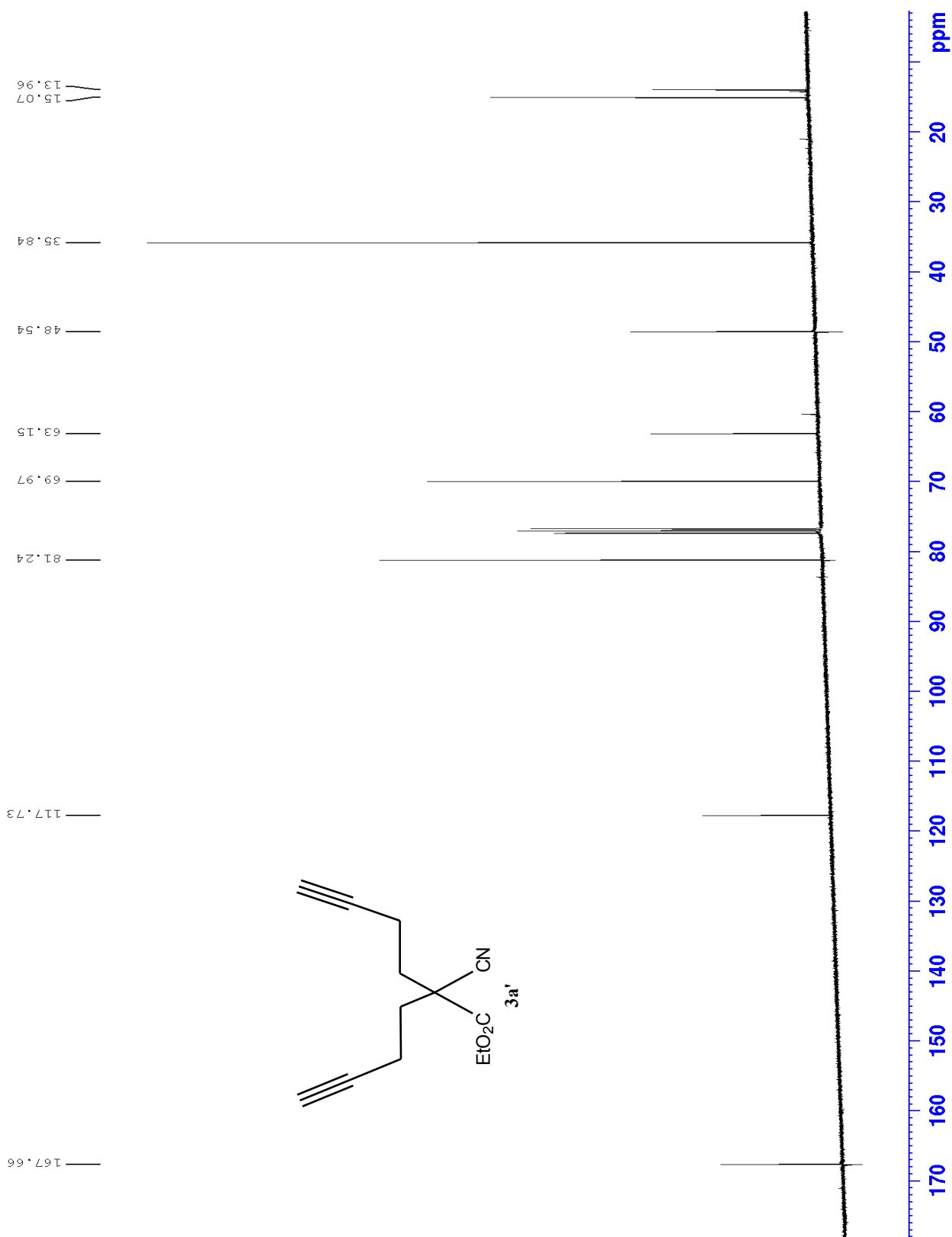
U.8 IR of 4h



V.1 Proton of 3a'



V.2 Carbon of 3a'



V.3 MS of 3a'

Page 1

Elemental Composition Report

Single Mass Analysis

Tolerance = 3.0 PPM / DBE: min = -1.5, max = 50.0

Element prediction: Off

Number of isotope peaks used for i-FIT = 3

Monoisotopic Mass: Even Electron Ions

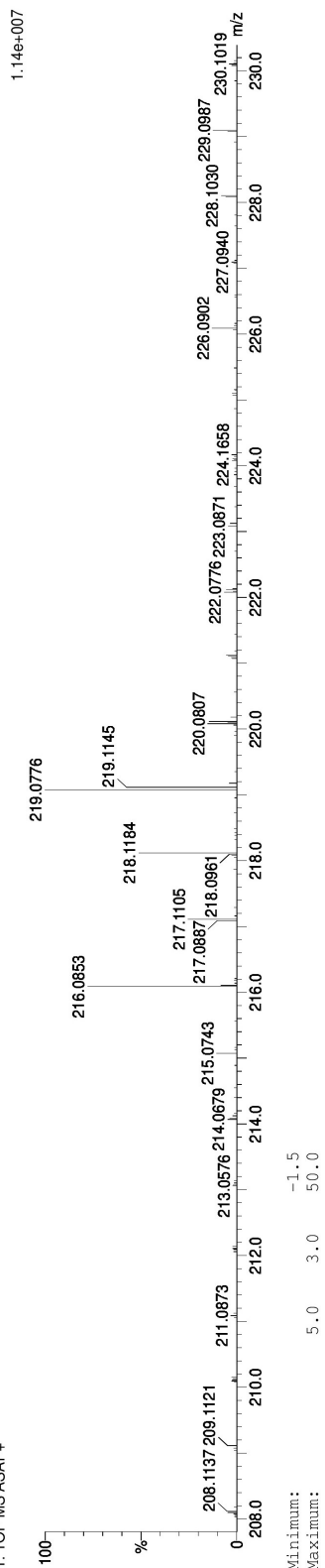
266 formula(e) evaluated with 1 results within limits (all results (up to 1000) for each mass)

Elements Used:

C: 0-200 H: 0-1000 N: 0-200 O: 0-200

2013-160 215 (4:186) AM2 (Ar:35000.0,0.0,0.00); Cm (140:215)

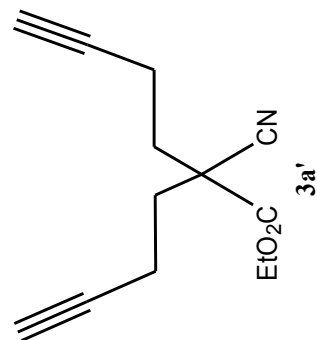
1: TOF MS ASAP+



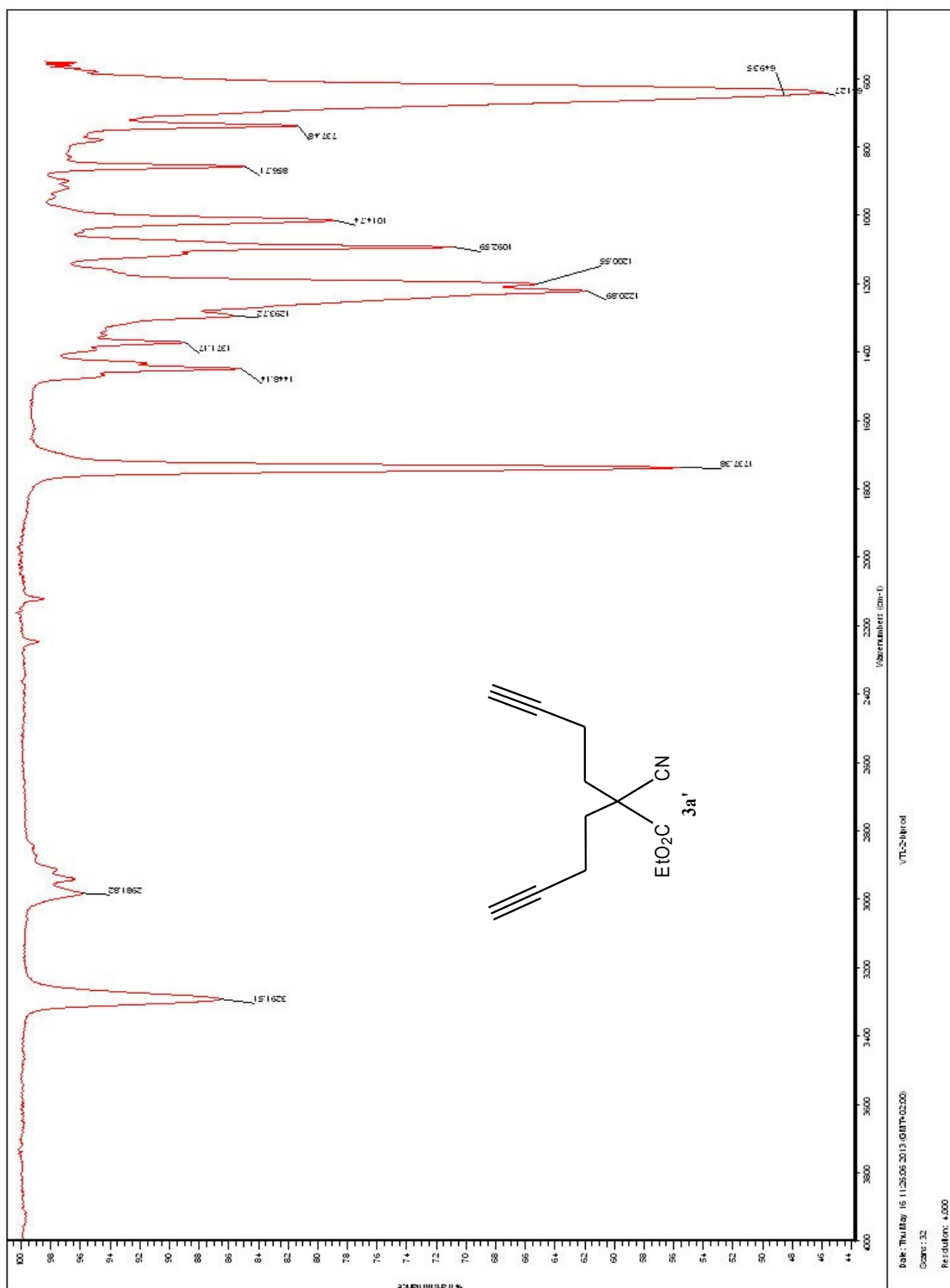
Minimum: -1.5

Maximum: 50.0

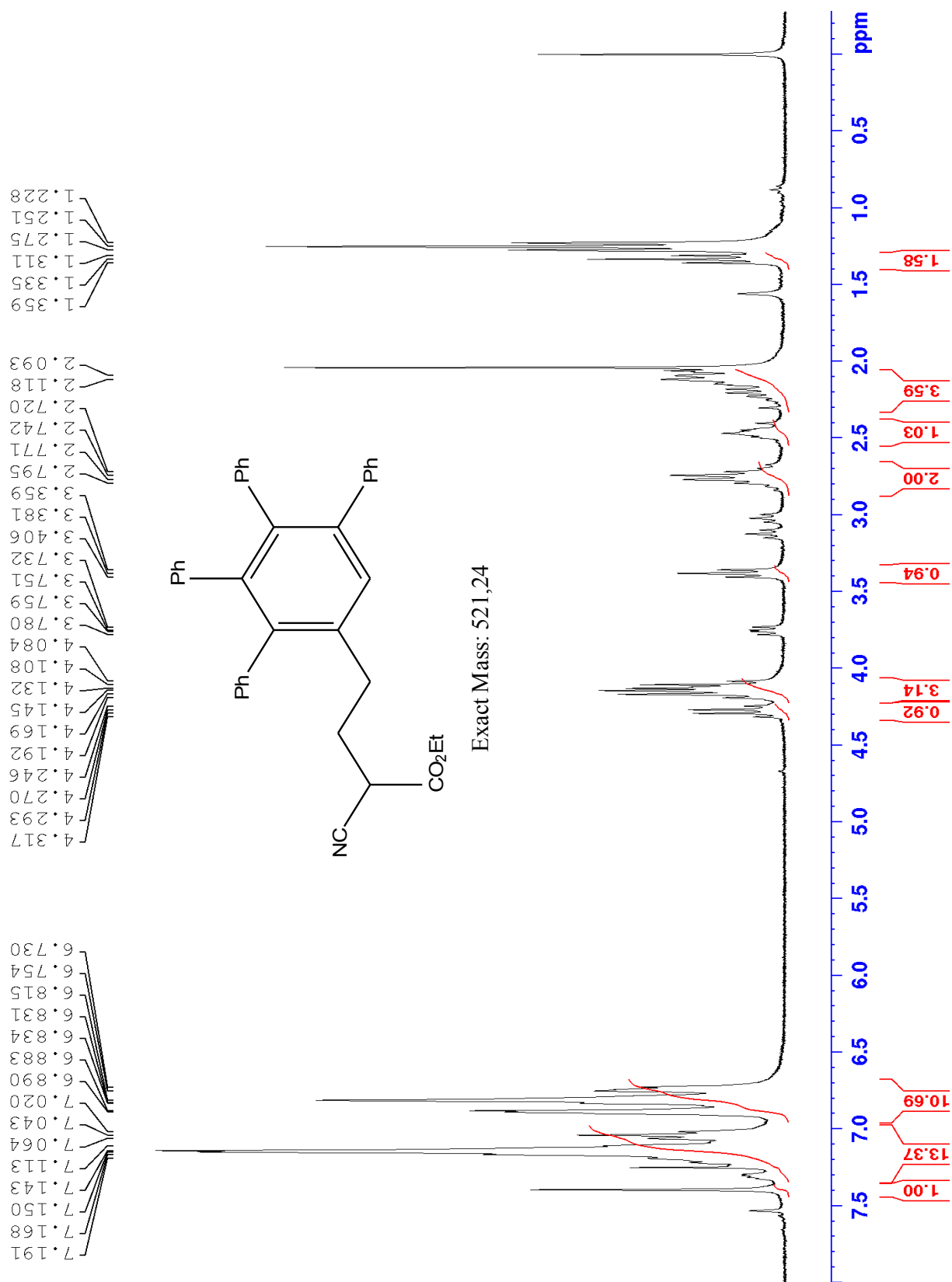
Mass	Calc. Mass	mDa	PPM	DBE	i-FIT	Norm	Conf (%)	Formula	ion observed
218.1184	218.1181	0.3	1.4	6.5	451.6	n/a	n/a	C13 H16 N O2	[M+H] ⁺



V.4 IR of 3a'



W.1 Proton of side-product from cyclotrimerization



W.2 MS of side-product from cyclotrimerization

Elemental Composition Report

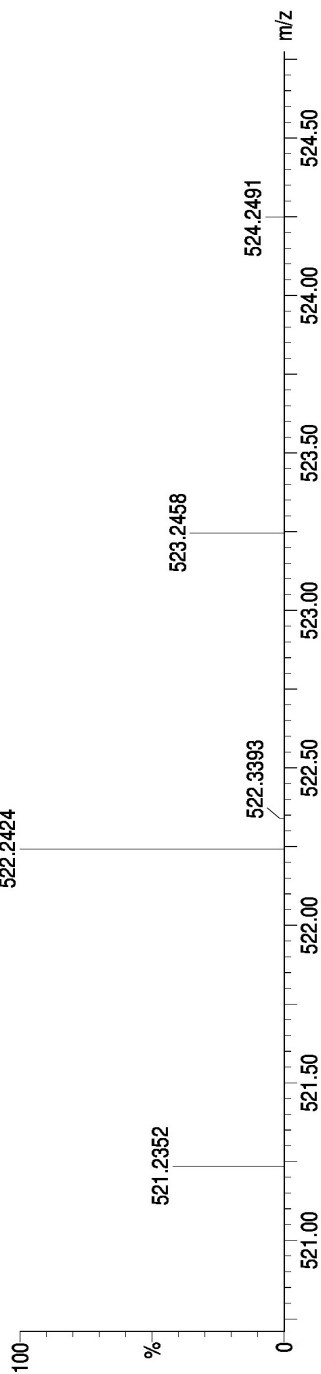
Page 1

Single Mass Analysis

Tolerance = 2.0 PPM / DBE: min = -1.5, max = 50.0
 Element prediction: Off
 Number of isotope peaks used for i-FIT = 3

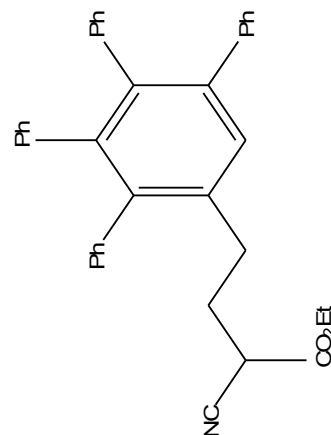
Monoisotopic Mass, Odd Electron Ions
 2537 formula(e) evaluated with 4 results within limits (all results (up to 1000) for each mass)
 Elements Used:
 C: 0-200 H: 0-1000 N: 0-200 O: 0-200
 2013-198 196 (3.825) AM2 (Ar:35000.0,0.00,0.00); Cm (168.246)
 1: TOF MS ASAP+

2.55e+007



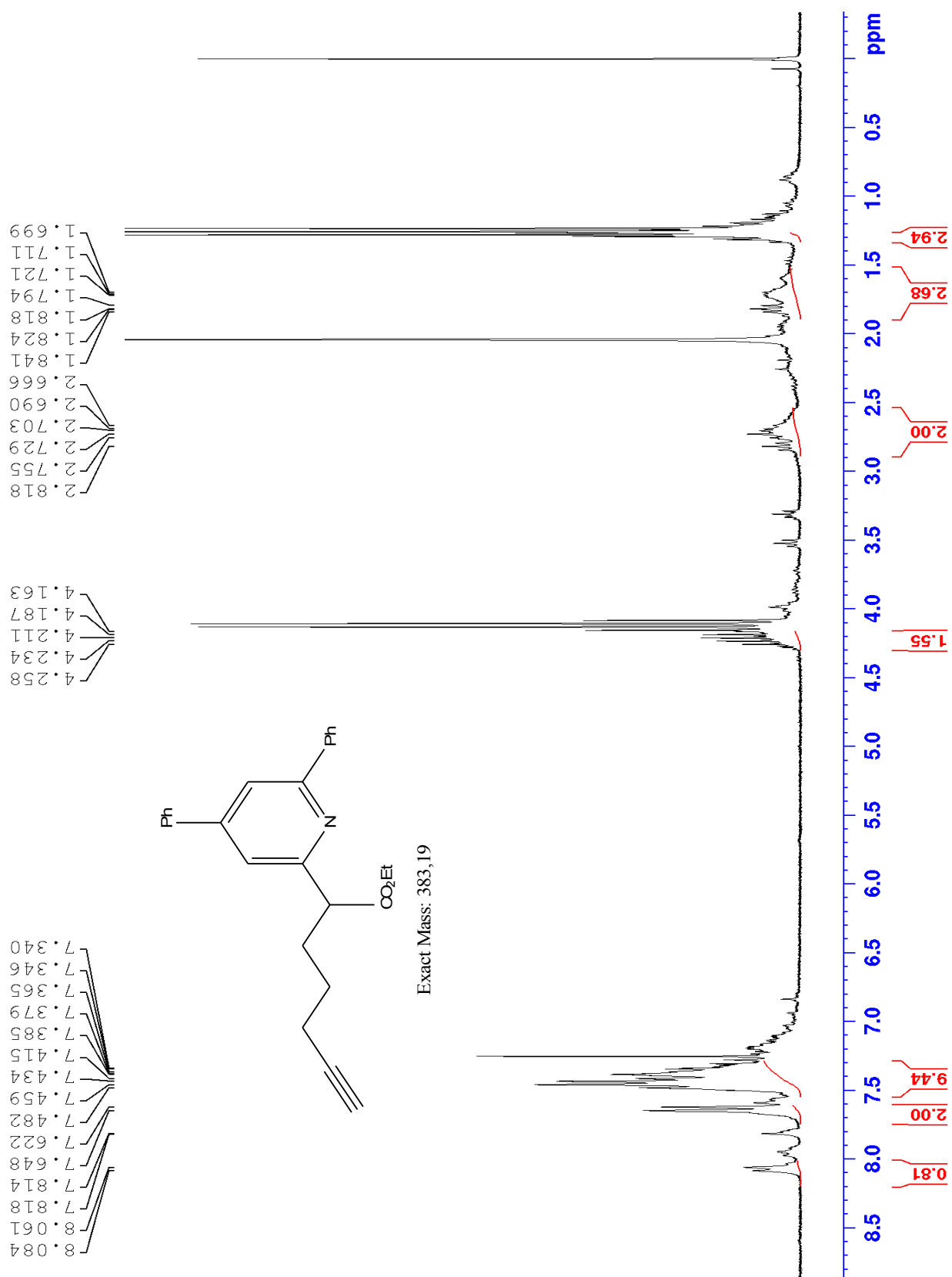
Minimum: -1.5
 Maximum: 50.0

Mass	Calc. Mass	mDa	PPM	DBE	i-FIT	Norm	Conf (%)	Formula
521.2352	521.2351	0.1	0.2	4.0	82.6	3.848	2.13	C6 H27 N21 O8
	521.2355	-0.3	-0.6	23.0	79.1	0.332	71.75	C37 H31 N O2
	521.2346	0.6	1.2	11.0	81.0	2.217	10.89	C21 H31 N9 O7
	521.2360	-0.8	-1.5	16.0	80.6	1.882	15.23	C22 H27 N13 O3



Exact Mass: 521.24

X.1 Proton of side-product from cyclotrimerization



X.2 MS of side-product from cyclotrimerization

Elemental Composition Report

Page 1

Single Mass Analysis

Tolerance = 2.0 PPM / DBE: min = -1.5, max = 50.0
 Element prediction: Off
 Number of isotope peaks used for i-FIT = 3

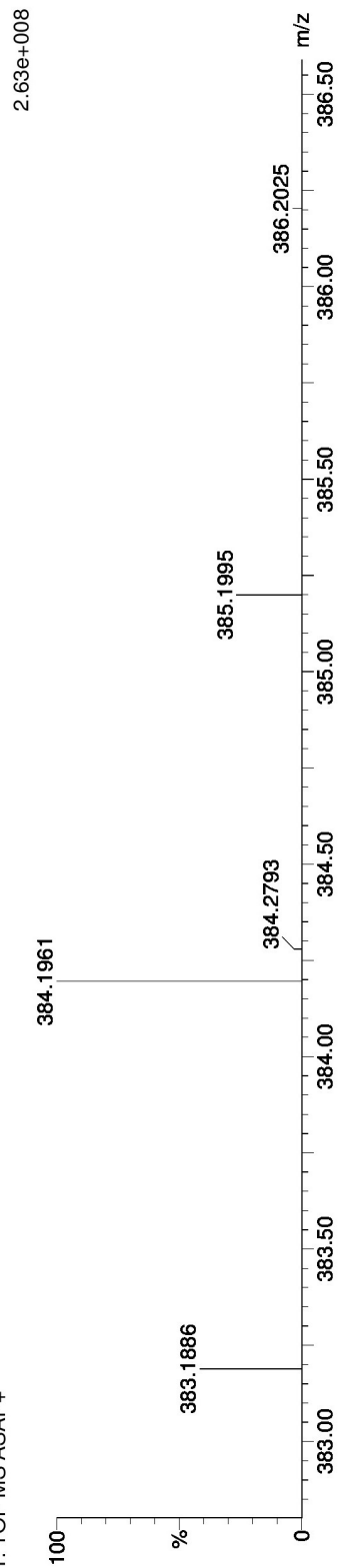
Monoisotopic Mass, Odd Electron Ions

1130 formula(e) evaluated with 2 results within limits (all results (up to 1000) for each mass)

Elements Used:

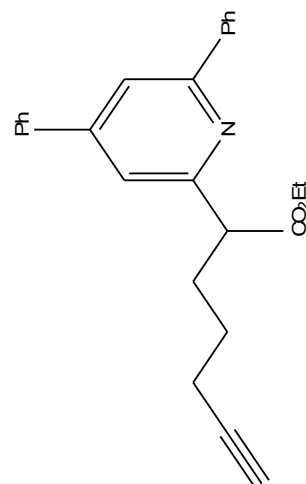
C: 0-200 H: 0-1000 N: 0-200 O: 0-200

2013-199 269 (5.237) AM2 (A1,35000.0,0.00,0.00); Cm (225:324)
 1: TOF MS ASAP+



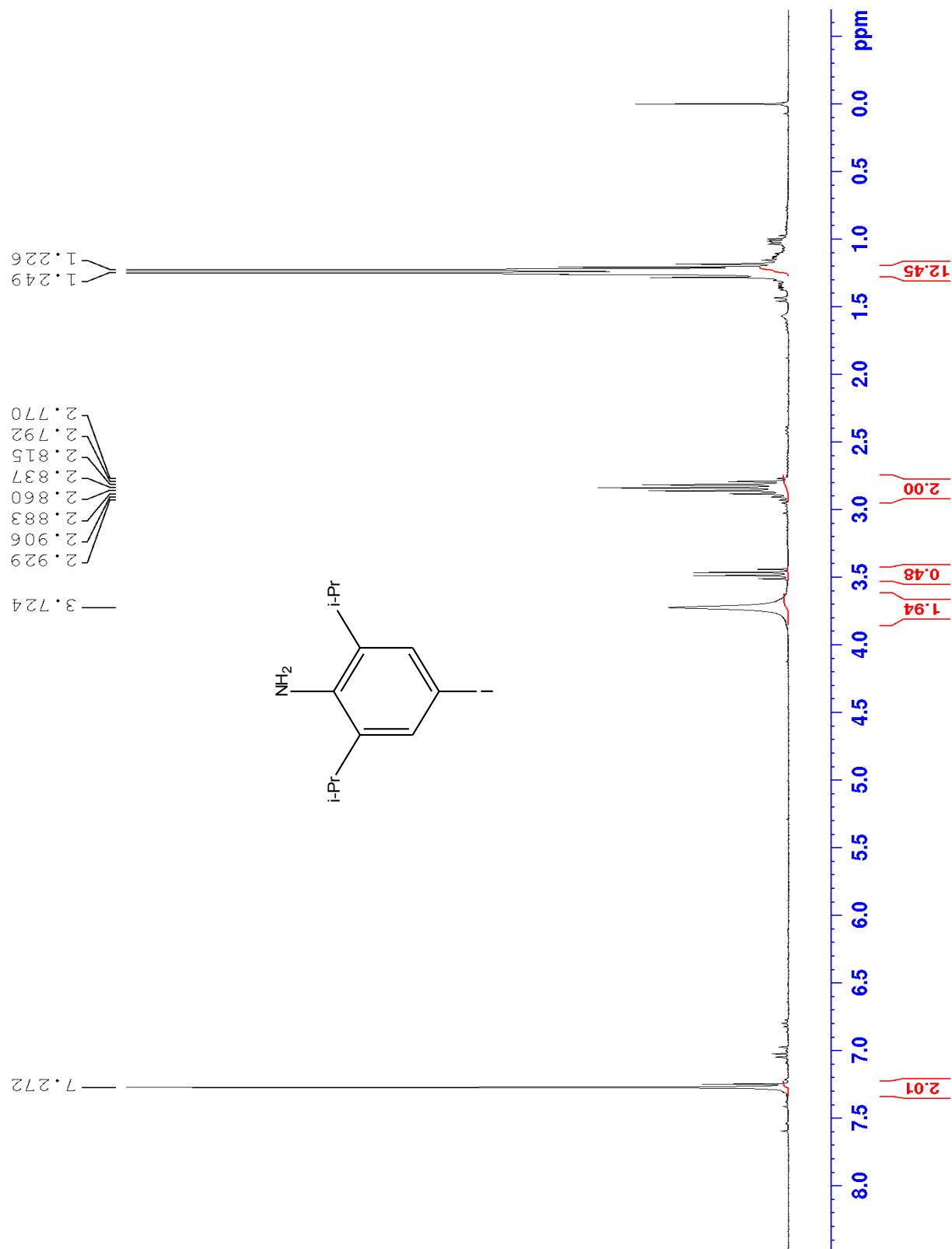
Minimum: -1.5
 Maximum: 50.0

Mass	Calc. Mass	mDa	PPM	DBE	i-FIT	Norm	Conf (%)	Formula
383.1886	383.1885	0.1	0.3	15.0	93.2	0.137	87.18	C26 H25 N O2
383.1890	383.1890	-0.4	-1.0	8.0	95.1	2.054	12.82	C11 H21 N13 O3

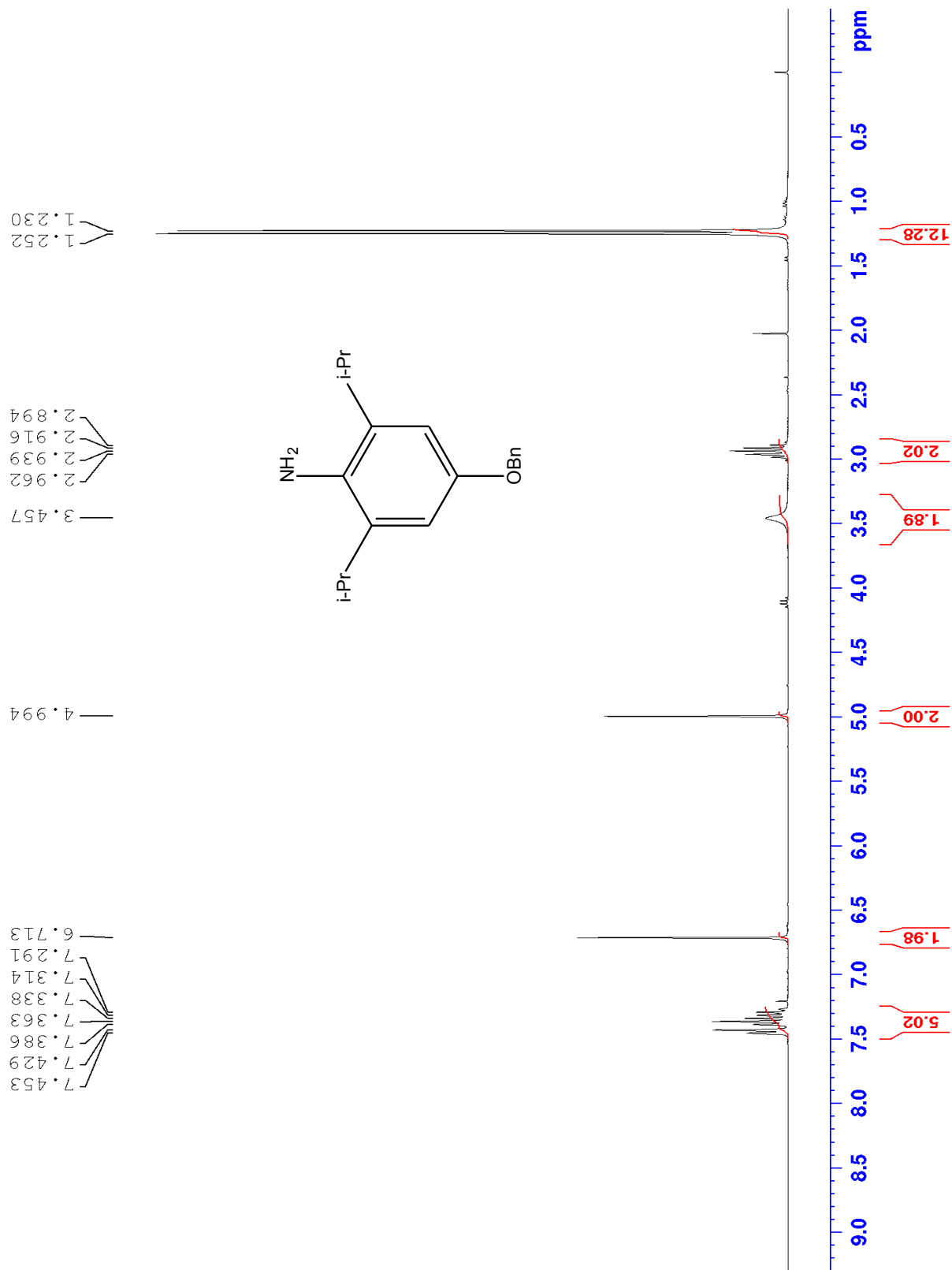


Exact Mass: 383.19

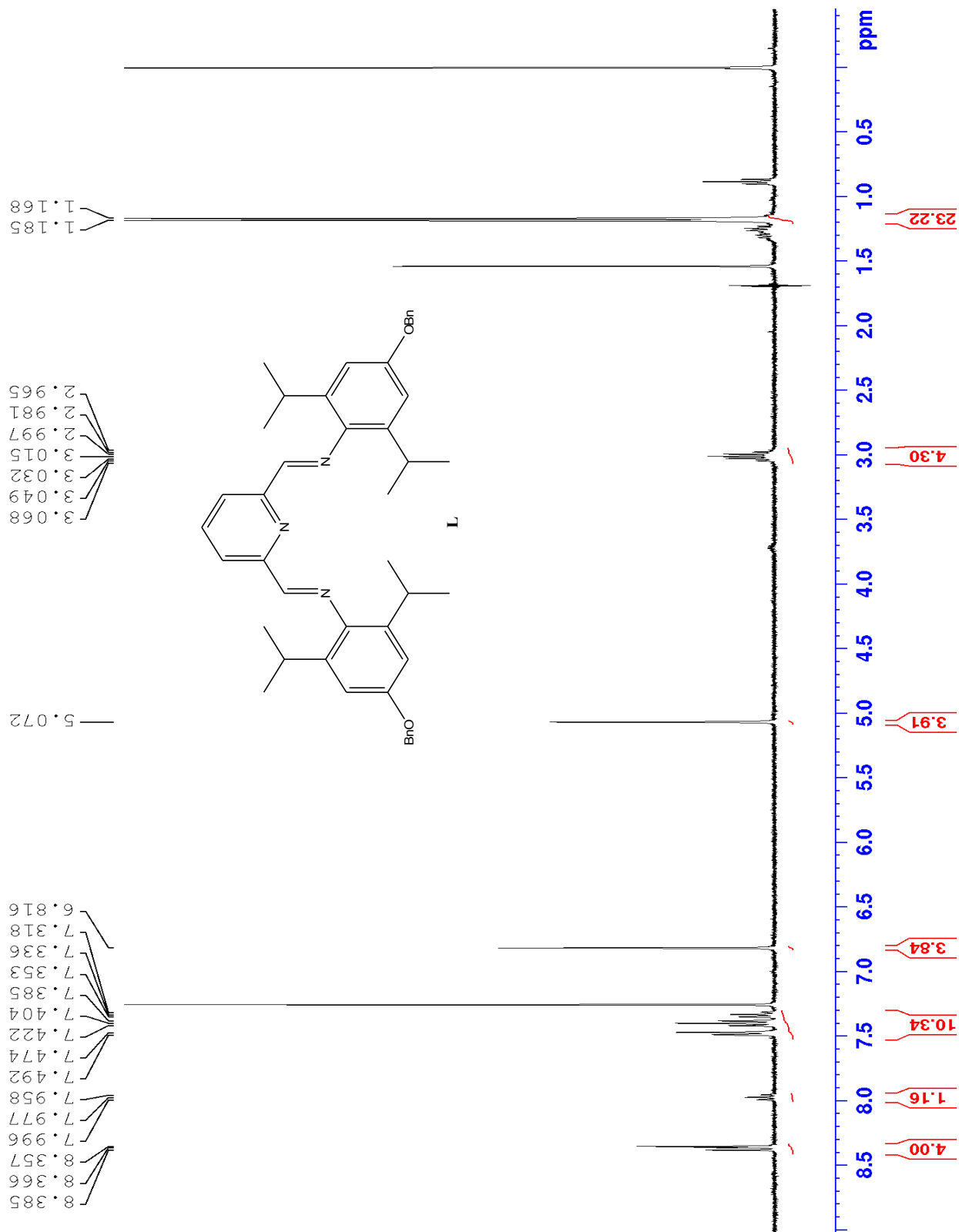
Y.1 Proton of 4-Iodo-2,6-diisopropylaniline



Y.2 Proton of 4-Benzyloxy-2,6-diisopropylaniline



Y.3 Proton of (N,N'E,N,N'E)-N,N'-(pyridine-2,6-diylbis(methanylylidene))bis(4-(benzyloxy)-2,6-diisopropylaniline) (L)



Z Proton of 5b'

